Regulation of mesenteric resistance artery diameter by pharmacological modulators of K_{Ca} channels

by

Stephanie E. Lunn

A thesis submitted in partial fulfillment of the requirements for the degree of

Doctor of Philosophy

Department of Pharmacology
University of Alberta

Abstract

Background: The diameter of resistance arteries, and thus, tissue perfusion and blood pressure, is tightly regulated through the integrated activity of endothelial and smooth muscle cells, and sympathetic nerves. The endothelium regulates the contractility of smooth muscle cells by releasing diffusible factors such as nitric oxide (NO) and via gap junction-mediated electrical coupling; opening of endothelial Ca^{2+}-activated K^+ (K_{Ca}) channels causes hyperpolarization which spreads to underlying smooth muscle cells to reduce opening of voltage-dependent Ca^{2+} channels, decrease Ca^{2+} influx and so limit contraction. The bioavailability and therefore, biological activity, of NO is determined by its interaction with the free radical superoxide anion (O_2^-), elevated levels of which are associated with risk factors for cardiovascular disease.

Traditionally, NO and endothelium-dependent smooth muscle hyperpolarization have been regarded as two separate mechanisms for regulation of arterial diameter. However, several lines of recent evidence support the proposal that NO bioavailability and K_{Ca} channel activity may be linked: *1.* Exposure of endothelial cells to shear stress results in activation of both small conductance K_{Ca} channels and increased NO production. *2.* Agonist-evoked NO production and NO-mediated relaxations can be inhibited by blockers of endothelial K_{Ca} channels. *3.* Activators of endothelial K_{Ca} channels can evoke NO-mediated relaxation. *4.* Stimulation of smooth muscle cells by α_1-adrenoceptor agonists engages both endothelial intermediate conductance K_{Ca} channels and NO production via a process termed myoendothelial feedback. *5.* O_2^- production by voltage-sensitive NADPH oxidase is reduced by membrane hyperpolarization which may lead to increased bioavailability of NO.

Thus, my over-arching goal is to further explore the relationship between endothelial K_{Ca} channels and NO in regulating resistance artery diameter by testing three hypotheses:

1. *Activation of small conductance K_{Ca} channels can enhance NO-mediated inhibition of sympathetic vasoconstriction evoked by increases in shear stress.*

2. *Intermediate conductance K_{Ca} channel-mediated myoendothelial feedback plays a role in NO-dependent modulation of sympathetic vasoconstriction.*

3. *Pharmacological activators of endothelial K_{Ca} channels can reduce vascular O_2^- production and enhance NO-mediated modulation of vasoconstriction*

To test these hypotheses, I have addressed two major aims:

1. **To investigate the role of endothelial K_{Ca} channels in NO-mediated modulation of nerve-evoked vasoconstriction in the perfused mesenteric bed.**

2. **To investigate whether pharmacological activators of endothelial K_{Ca} channels can modulate vascular O_2^- production and vasoconstriction stimulated by the α_1-adrenoceptor agonist phenylephrine.**

Methods: To address these aims I have used a combination of functional and biochemical techniques to investigate the effects of modulators of endothelial K_{Ca} channels on diameter and O_2^- production in rat mesenteric resistance arteries.

Results/Discussion: My data show that although myoendothelial feedback limits contractile responses to phenylephrine in isolated arteries, this pathway does not appear to contribute to endothelial modulation of sympathetic vasoconstriction at the level of the intact bed. Instead, shear stress-induced activation of small conductance K_{Ca} channels and release of NO provides the dominant mechanism for engagement of the endothelium to inhibit sympathetic vasoconstriction. Furthermore, activators of endothelial K_{Ca} channels can significantly limit nerve-evoked

vasoconstriction. CyPPA (N-cyclohexyl-N-[2-(3,5-dimethyl-pyrazol-1-yl)-6-methyl-4-pyrimidinamine), an activator of small conductance K_{Ca} channels, enhances NO-dependent, shear stress-mediated inhibition of sympathetic vasoconstriction whereas SKA-31 (naphtho[1,2-d]thiazol-2-ylamine), an activator of intermediate conductance K_{Ca} channels, can directly inhibit release of noradrenaline from perivascular sympathetic nerves. Both CyPPA and SKA-31 can significantly reduce acute increases in O_2^- production stimulated by phenylephrine in isolated arteries but this effect is not associated with enhancement of NO-mediated endothelial modulation of vasoconstriction.

Conclusion: To conclude, I have demonstrated that small and intermediate conductance K_{Ca} channels play different functional roles in modulation of nerve-evoked vasoconstriction; endothelial small conductance K_{Ca} channels mediate shear stress-induced, NO-dependent inhibition of vasoconstriction whereas the activity of neuronal IK_{Ca} channels can directly inhibit release of noradrenaline from sympathetic nerves. These functional roles reflect the differing locations of the channels within endothelial cells and the artery wall. Pharmacological activators of K_{Ca} channels can limit vascular O_2^- production supporting the proposal that the endothelial cell membrane potential may play a key role in vascular health and that targeting these channels could provide a novel approach to reducing O_2^- levels in disease states.

<u>Dedication</u>

To my parents, Phil and Christina Lunn, for their
unconditional love and support

And to Paul Czarnietzki, my rock,
who stayed calm through it all

Acknowledgements

Table of Contents

Chapter 1: Introduction

Chapter 2: Activation of SK_{Ca} channels enhances shear stress-mediated inhibition of sympathetic vasoconstriction in the perfused mesenteric bed

Chapter 5: Activators of SK_{Ca} and IK_{Ca} channels limit O_2^- production in isolated arteries

Chapter 6: General discussion and future directions

References

Appendix: Drugs and Chemicals

List of Tables

List of Figures

Chapter 3: Activation of IK$_{Ca}$ channels directly inhibits sympathetic vasoconstriction in the perfused mesenteric bed

Chapter 4: Activators of SK$_{Ca}$ and IK$_{Ca}$ channels limit agonist-induced O$_2^-$ production and vasoconstriction in isolated mesenteric arteries: functional studies

<u>Chapter 5:</u> Activators of SK_{Ca} and IK_{Ca} channels limit agonist-induced O_2^- production in isolated mesenteric arteries: biochemical studies

Abbreviations

ATP: adenosine triphosphate
BH$_4$: 5,6,7,8-tetrahydro-l-biopterin
BK$_{Ca}$ channels: large conductance Ca^{2+}-activated K^+ channels
CyPPA: *N*-cyclohexyl-*N*-[2-(3,5-dimethyl-pyrazol-1-yl)-6-methyl-4-pyrimidinamine
DAPI: 4′,6-Diamidino-2-phenylindole dihydrochloride
DCEBIO: 5,6-dichloro- 1-ethyl-1,3-dihydro-2H-benzimidazol-2-one
DHE: dihydroethidium
DMSO: dimethyl sulfoxide
DNA: deoxyribonucleic acid
EOH: 2-hydroxyethidium
EBIO: 1-ethyl-2-benzimidazolinone
FAD: flavin adenine dinucleotide
FMN: flavin mononucleotide
UPLC: ultra-performance liquid chromatography
IbTX: iberiotoxin
IK$_{Ca}$ channels: intermediate conductance Ca^{2+}-activated K^+ channels
IP$_3$: inositol 1,4,5 trisphosphate
K$_{ATP}$ channels: adenosine triphosphate sensitive K^+ channels
K$_{Ca}$ channels: Ca^{2+}-activated K^+ channels
LC: light chain
L-NAME: N^G-nitro-L-arginine methyl ester hydrochloride
MEGJ: myoendothelial gap junction
NADPH: nicotinamide-adenine-dinucleotide phosphate
NO: nitric oxide
NOS: nitric oxide synthase
NS 309: 6,7- dichloro-1H-indole-2,3-dione 3-oxime
NS 6180: 4-[[3-(Trifluoromethyl)phenyl]methyl]-2*H*-1,4-benzothiazin-3(4*H*)-one
NS 11021: *N*'-[3,5-Bis(trifluoromethyl)phenyl]-*N*-[4-bromo-2-(2*H*-tetrazol-5-yl-phenyl]thiourea
O$_2^-$: superoxide anion
ODQ: 1*H*-[1,2,4]Oxadiazolo[4,3-*a*]quinoxalin-1-one
OH$^-$: hydroxyl radical
ONOO$^-$: peroxynitrite
RNS: reactive nitrogen species
ROS: reactive oxygen species
SK$_{Ca}$ channels: small conductance Ca^{2+}-activated K^+ channels
SKA-31: Naphtho[1,2-*d*]thiazol-2-ylamine
STIM: stromal interaction molecule
SOD: superoxide dismutase
SOD-PEG: superoxide dismutase-polyethylene glycol
Tempol: 1-oxyl-2,2,6,6-tetramethyl-4-hydroxypiperidine
TRP channels: transient receptor potential channels
TRPC3 channels: canonical 3 transient receptor potential channels
TRPV4 channels: vanilloid 4 transient receptor potential channels
VOCC: voltage-operated Ca^{2+} channels

Ethics Approval

All animal care and experimental procedures were approved by the Animal Care and Use Committee (ACUC HS1; AUP 312) of the Faculty of Medicine and Dentistry at the University of Alberta, and performed in accordance with Canadian Council on Animal Care guidelines, and the principles and regulations as described by Grundy[1].

Animal Care and Use

Male Sprague-Dawley rats (250-300g; from Science Animal Support Services, University of Alberta) were housed in an enriched environment maintained on a 12:12 h light–dark cycle at ~23°C with fresh tap water and standard chow available ad libitum. Rats were euthanized by inhalation of isoflurane followed by decapitation. The mesenteric bed and aorta were removed and placed in cold Krebs buffer containing (mM): NaCl 119.0, NaHCO$_3$ 25.0, KCl 4.7, MgSO$_4$ 1.2, KH$_2$PO$_4$ 1.18, glucose 11, and CaCl$_2$ 2.5.

Chapter 1: Introduction

According to the World Health Organization, cardiovascular diseases, such as atherosclerosis, hypertension and diabetes, are the number one cause of death worldwide[2]. In 2015, approximately 17.7 million people died from cardiovascular diseases, around 31% of the total deaths globally[2]. There are currently a wide range of treatments for patients suffering from cardiovascular diseases (e.g. drugs, diet and/or lifestyle modifications). But, due to the high mortality and morbidity rates, new therapies are essential in order to improve our ability to treat cardiovascular disease in the future, with the development of new therapeutic approaches requiring a better understanding of blood vessel function and identification of potential targets for new drugs.

In the body, it is the diameter of small resistance arteries (20 to 400 μm in lumen diameter) that is a major determinant of vascular resistance and thus, blood flow and blood pressure[3]. Resistance artery diameter is determined by the contractile state of the smooth muscle cells, that make up the artery wall (**Figure 1.1**), which in turn is the result of the integrated response to the actions of chemical mediators, released from nerves and endothelial cells, and physical stimuli, such as increases in pressure. Changes in both resistance artery structure and function contribute to the clinical manifestations of cardiovascular disease, such as high blood pressure and strokes.
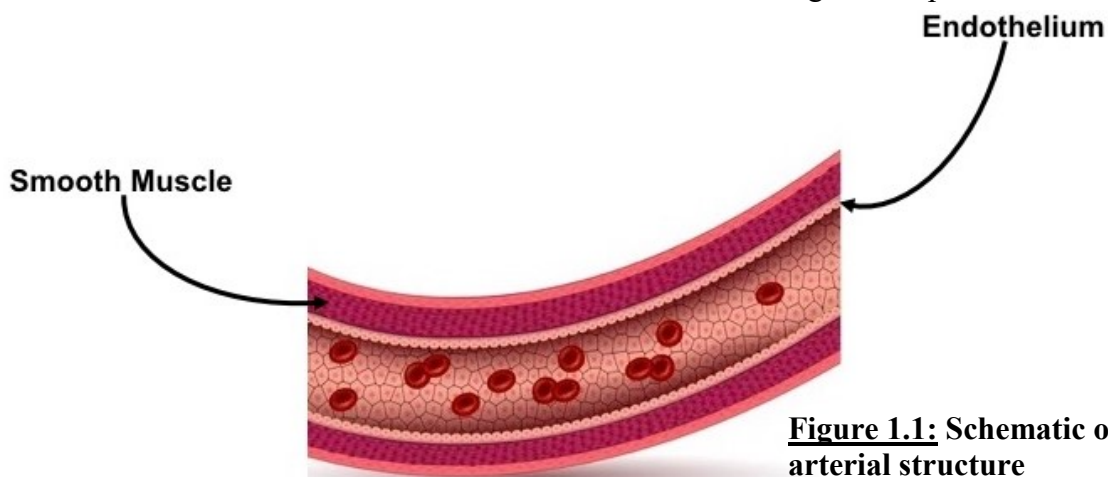
Figure 1.1: **Schematic of arterial structure**

1.1: Contraction of vascular smooth muscle cells

As in all muscle cells, vascular smooth muscle contraction requires adenosine triphosphate (ATP) and an increase in intracellular Ca^{2+} concentration[4,5], via release from intracellular stores and/or entry through Ca^{2+} channels in the cell membrane. Ca^{2+} binds to calmodulin to form a Ca^{2+}-calmodulin complex which activates myosin light chain kinase[6–8]. Myosin light chain kinase is bound via its N-terminus to actin filaments and activation allows it to phosphorylate nearby myosin molecules[9]. Myosin filaments are composed of hexameric myosin molecules, each made up of two heavy chains and two pairs of light chains (LC_{17} and LC_{20})[10–12]. Activated myosin light chain kinase phosphorylates LC_{20} to induce a conformational change that allows interaction between actin and myosin, and subsequently, an increase in the actin-activated MgATPase activity of myosin[13]. Energy generated through hydrolysis of ATP then drives cross-bridge cycling and the contraction of the muscle cell (reviewed by Saddouk et al. 2017[12]). Myosin light chain kinase is inactivated by dissociation of Ca^{2+} from calmodulin and block of the active site of myosin light chain kinase by an auto-inhibitory domain. Dephosphorylation of LC_{20} is then mediated by myosin light chain phosphatase, resulting in disruption of myosin and actin binding and thus, muscle relaxation[14–16] (reviewed by Brozovich et al. 2016; **Figure 1.2**[15]).

1.1.1: Sources of Ca^{2+} for smooth muscle contraction

Release of Ca^{2+} from intracellular stores: Ca^{2+} stored in the sarcoplasmic reticulum can be released via activation of both inositol 1,4,5-trisphosphate (IP_3) and ryanodine receptors[8,17–20,17,21,22]. IP_3 receptors are Ca^{2+} release channels consisting of four membrane-spanning subunits, each of six transmembrane domains, surrounding a pore[23]. Agonists, such as noradrenaline, act on $G_{q/11}$-protein coupled receptors to increase IP_3 through cleavage of membrane bound

phosphatidylinositol 4,5-bisphosphate by phospholipase C (reviewed by Berridge et al. 2008[24])

and so elicit IP_3-mediated Ca^{2+} release.
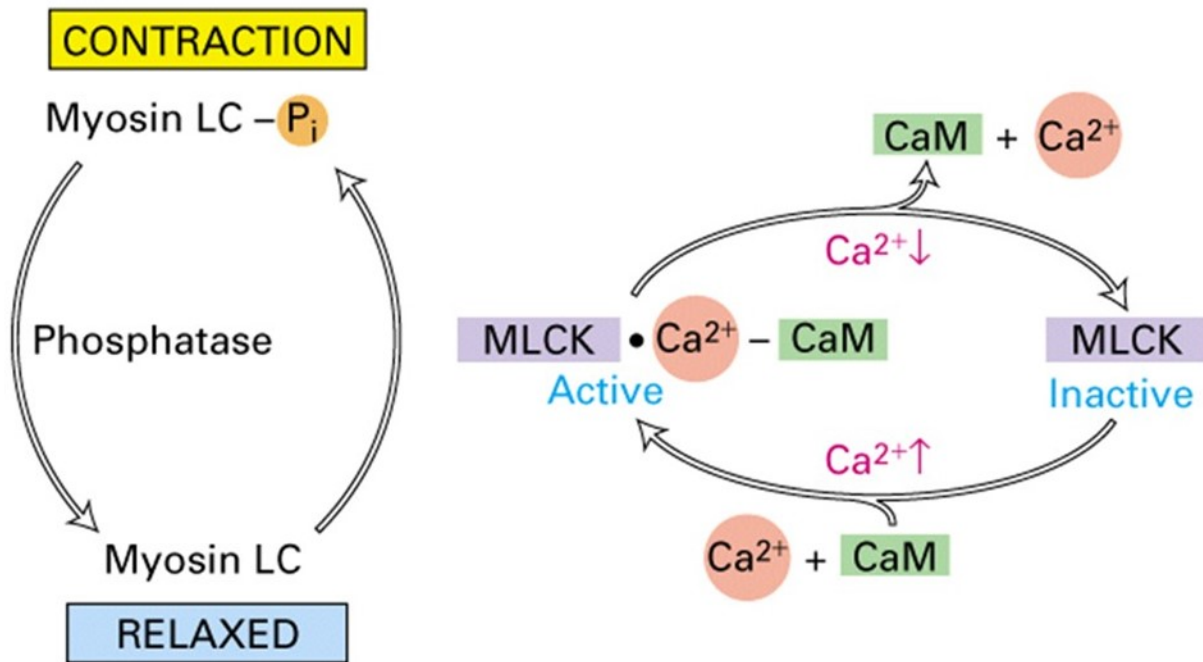
Figure 1.2: Mechanism of smooth muscle contraction. Schematic of the mechanisms underlying smooth muscle contraction elicited by a stimulus that increases Ca^{2+} levels within smooth muscle cells. An increase in Ca^{2+} leads to Ca^{2+} binding to calmodulin which activates myosin light chain kinase (MLCK). MLCK phosphorylates LC_{20} to increase the activity of the myosin ATPase which drives the cycling of actin-myosin cross-bridges to create muscle tension[15].

Like IP_3 receptors, ryanodine receptors are channels that mediate Ca^{2+} release from the sarcoplasmic reticulum but whereas IP_3-mediated Ca^{2+} release is associated with smooth muscle contraction, discrete increases in Ca^{2+} caused by release from ryanodine receptors, termed Ca^{2+} sparks, play an important role in modulating smooth muscle cell contraction due to the proximity of ryanodine receptors to plasma membrane ion channels (reviewed by Amberg and Navedo, 2013[25]). Ca^{2+} sparks activate large conductance Ca^{2+}-activated K^+ (BK_{Ca}; see below) channels to promote hyperpolarization and oppose vasoconstriction[26–32]. Modulation of sparks may contribute

to the actions of some vasodilator and vasoconstrictor agents, as protein kinase G and protein kinase C can act on ryanodine receptors to stimulate and inhibit Ca^{2+} sparks activity, respectively[31,33]. Activation of BK_{Ca} channels by Ca^{2+} sparks can be recorded in isolated cerebral arterial smooth muscle cells as spontaneous transient outward currents, the frequency and amplitude of which are linked to depolarization and driven by Ca^{2+}sparks[27,34].

Ca^{2+} influx pathways: Store-operated Ca^{2+} entry. Stromal interaction molecule (STIM) proteins are single-transmembrane domain proteins located in the sarcoplasmic reticulum that sense alterations in luminal Ca^{2+} via their N-terminal domains[35]. Depletion of Ca^{2+} stores leads to dissociation of Ca^{2+} from these domains, allowing STIM proteins to interact with Orai channels which mediate Ca^{2+} influx[36]. In addition to Orai channels, transient receptor potential (TRP; see below) channels can also be activated by STIM after store depletion[37] but their contribution to store-operated Ca^{2+} entry appears to be variable[38].

Voltage-dependent Ca^{2+}entry. Many stimuli elicit depolarization of the membrane potential of vascular smooth muscle cells and so increase the open probability of voltage-operated Ca^{2+} channels (VOCCs). VOCCs are encoded by pore-forming α_1 subunits, (Cav1.x, 2.x and 3.x); with the $Ca_V1.2$ channel (L-type) predominantly responsible for mediating vascular smooth muscle contraction (reviewed by Catterall 2011[39] and Zamponi et al. 2015[39]). Each channel is comprised of four α-subunits, each with six transmembrane domains (S1-S6), with S4 conferring voltage sensitivity[40]. The α-subunits co-localize with β-, α2δ-, and γ- subunits[41–43], which modulate their voltage sensitivity, conductance and level of expression[41,44–46] (**Figure 1.3[47]**).

L-type VOCCs are slow to activate and inactivate[48–50], and have a conductance of around 25 pS[48]. Membrane depolarization to potentials positive of -30 mV lead to increased opening of L-type VOCCs and global influx of Ca^{2+} into smooth muscle cells to cause contraction[49]. Evidence

for the functional role of L-type VOCCs in regulation of arterial diameter has come from the observations that dihydropyridine antagonists (e.g. nifedipine) that selectively inhibit α_{1c} activity abolish myogenic reactivity in isolated rat cerebral arteries, whereas dihydropyridine agonists that stimulate the activity of L-type VOCCs enhance the myogenic response in rabbit ear arteries[51,52].
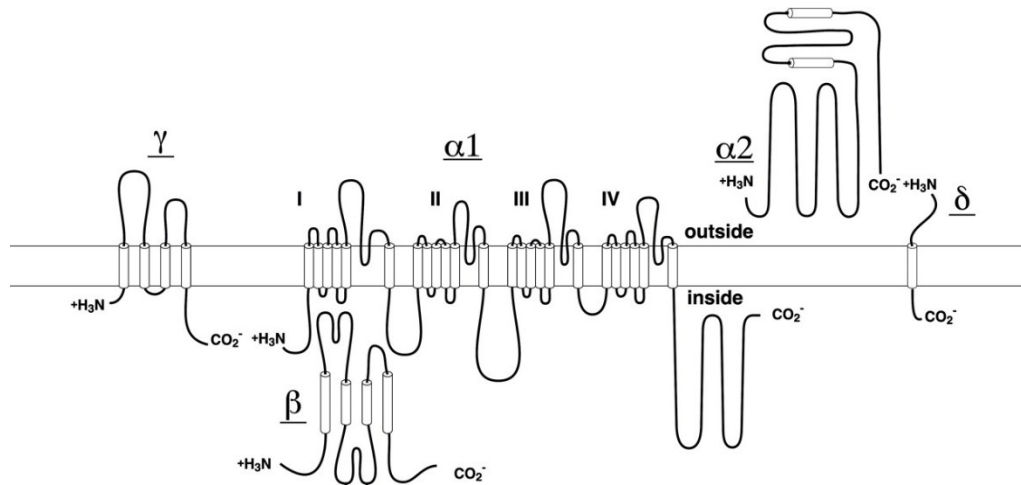
Figure 1.3: Schematic of L-type VOCC Ca^{2+} channel with α- and accessory β-,γ- and $α_2$δ-subunits. Each α-subunit is comprised of six transmembrane domains (S1-S6) with S4 conferring voltage sensitivity and co-localize with a β-,γ- and/or $α_2$δ- subunit, which modulate voltage sensitivity, conductance and level of expression[47].

The activity of L-type VOCCs can be regulated by protein kinases C, A and G. Protein kinase C-mediated phosphorylation of L-type VOCCs has been shown to enhance channel activity in ventricular myocytes from a range of species[53,54] whereas phosphorylation by protein kinase G inhibits the channel in cultured rat mesenteric arterial[55] and aortic[56,57] smooth muscle cells, chick ventricular myocytes[58] and guinea pig papillary muscle cells[59]. The effect of protein kinase A-mediated phosphorylation is not as clearly defined with both stimulatory and inhibitory effects reported. For example, in chick embryonic ventricular myocytes[58], guinea pig papillary muscle cells[59] and rat mesenteric arterial smooth muscle cells[55], protein kinase A enhanced VOCC activity but was found to have an inhibitory action in cultured rat aortic smooth muscle cells[56].

The majority of research on VOCCs in vascular smooth muscle cells has focused on L-type channels but recent evidence indicates that T-type VOCCs (Cav3.x)[60,61] can also contribute to smooth muscle contraction. T-type VOCCs have a conductance of about 8 pS[48] and are activated at more hyperpolarized potentials (positive to -45 mV[49]) as compared to L-type VOCC currents (positive to $\sim$-30 mV[62]). They are also quick to activate and inactivate[48–50]. Transcript and protein for Cav3.1 and Cav3.2 channels have been found in vascular smooth muscle cells from rat cerebral resistance arteries[63,64], and Cav3.3 channels has also been identified in human cerebral artery cells[65]. Electrophysiological recordings have identified Cav3.1 and Cav3.2 channels as being responsible for the nifedipine-insensitive component of Ca^{2+} current in rat cerebral vascular smooth muscle cells[64], as T-type VOCCs have been shown to be insensitive to dihydropyridines, such as nifedipine and nitrendipine[49,50], which block L-type VOCCs[49,50]. The functional role of T-type VOCCs in regulation of arterial diameter has largely been explored using the blocker, mibefradil[63].

Ca^{2+}-sensitization: An increase in Ca^{2+} is obligatory for the initiation of force generation within vascular smooth muscle cells. However, decreases in myosin light chain phosphatase activity following protein kinase phosphorylation can enhance contractile force without further changes in Ca^{2+} levels via a process termed Ca^{2+} sensitization[66,67]. Sensitization evoked by agonists acting at G-protein coupled receptors is thought to be due to activation of Rho-associated kinase[68,69]. Agonist-induced activation of the small GTPase RhoA, via the $G_{12/13}$ family of heterotrimeric G-proteins and a guanine nucleotide-exchange factor, leads to activation of Rho-associated kinase which inhibits myosin light chain phosphatase activity by phosphorylation of myosin phosphatase target subunit-1[68]. Protein kinases, such as Rho-associated kinase and protein kinase C[11,14,70,71], can also phosphorylate C-kinase potentiated protein phosphate-1 inhibitor[72], an

endogenous inhibitor of myosin light chain phosphatase, which when phosphorylated, binds the catalytic site of myosin light chain phosphatase (reviewed by El-Yazbi et al. 2016[73]).

1.1.2: Modulation of vascular smooth muscle contraction by K$^+$ channels

K^+ currents are the major ionic conductance in the plasma membrane of vascular smooth muscle cells and thus, set and regulate membrane potential[74–76]. In physiological conditions (3–5 mM K^+ outside of the cell and 140 mM K^+ inside), the driving force for K^+ is outward and so opening of a K^+ conducting channel leads to membrane hyperpolarization[77]. As membrane resistance is high, opening of a few K^+ channels can have a large impact on smooth muscle membrane potential and thus, the open probability of VOCCs and contractility. Vascular smooth muscle cells express a wide range of different types of K^+ channels: BK_{Ca} channels, voltage-gated K^+ channels, ATP-sensitive K^+ (K_{ATP}) channels, inward-rectifier K^+ channels, and members of the two-pore K^+ channel family (recently reviewed by Jackson, 2017[78])[27,29,79–92]. However, for the purposes of this thesis, I will focus on the structure and function of BK_{Ca} channels and their role in regulating smooth muscle contractility and therefore, arterial diameter in resistance arteries.

BK_{Ca} channels (encoded by *KCNMA1*) are composed of homotetramers of pore-forming α-subunits together with regulatory β- and γ– subunits[91–95] **(Figure 1.4[78])**. The α-subunit is composed of 7 transmembrane domains with the pore region between S5 and S6[96]. Two regulator of K^+ conductance domains (1 and 2) located in the C-terminus contain Ca^{2+} binding sites while positively charged residues in S2-4 serve as voltage sensors[77,96–98]. These channels have a large single channel conductance (150-270 pS)[97,99,100] and exhibit voltage-dependent gating for which binding of Ca^{2+} increases the apparent sensitivity to voltage[92–94]. Under physiological conditions, BK_{Ca} channels require both depolarization of the membrane potential and a rise in intracellular Ca^{2+} to occur simultaneously in order to open[81,92,97,101].

There are four β-subunits (*KCNMβ1–4*) with β1 the dominant form in vascular smooth muscle cells[82,91,102]. The β-subunits alter channel gating, sensitivity to Ca^{2+} and voltage, while the γ-subunit is associated with increasing channel sensitivity to voltage[91,95,103–105].

BK_{Ca} channels are widely expressed in a variety of tissues (**Table 1.1**). They are highly expressed in all vascular smooth muscle cells[27,29,79–92], but are not present in freshly isolated endothelial cells[76,106–108]. BK_{Ca} channels are of particular importance in the central nervous system where they regulate the excitability of neurons[97,109,110] and have been localized to the inner membrane of mitochondria in cardiac myocytes where they've been proposed as potential targets for preventing cardiac ischemia-reperfusion injury[89,110–112].
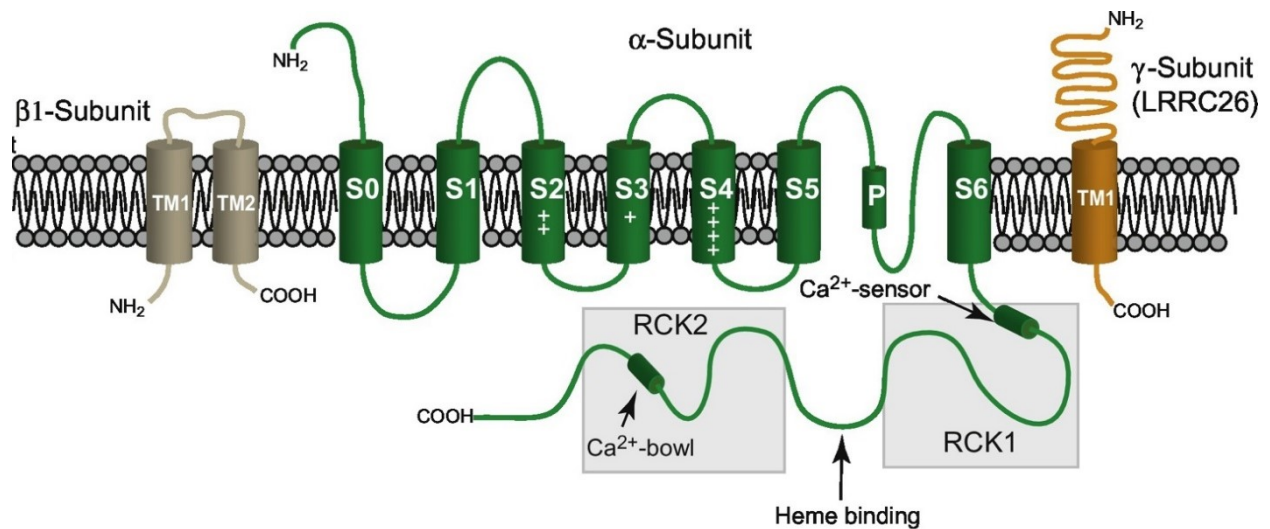
Figure 1.4: Schematic of structure of BK$_{Ca}$ channels. BK_{Ca} channels are composed of pore-forming α-, and modulatory ß1- and γ- subunits. The α-subunit is made up of 7 transmembrane domains, S2-4 being the voltage sensor and the pore region located between S5 and S6, and 4 cytoplasmic domains within the C-terminus tail. Two regulator of K^+ conductance domains (RCK1 and RCK2) located in the cytoplasmic C-terminus contain the channel's Ca^{2+} binding sites. The auxiliary subunits ß1- and γ- subunits consist of two transmembrane domains and one transmembrane domain, respectively[78].

Channel Type	Location
BK$_{Ca}$	▪ Vascular smooth muscle[27,29,79–92] ▪ Urinary smooth muscle[102] ▪ Adrenal chromaffin cells[113] ▪ Inner mitochondrial membrane of cardiac myocytes[89,110–112] ▪ Neurons[97,109,110] ▪ Inner mitochondrial membrane of neurons[114] ▪ B-lymphocytes[115] ▪ Platelets[115]
SK$_{Ca}$	▪ Vascular endothelium[26,80,84,85,116–133] ▪ Cardiac myocytes[134–136] ▪ Inner mitochondrial membrane of cardiac myocytes[137,138] ▪ Neurons[139–143] ▪ Inner mitochondrial membrane of neurons[144,145] ▪ Platelets[115,146,147] ▪ B-lymphocytes[115]
IK$_{Ca}$	▪ Vascular endothelium[80,84,100,116,118–122,124–126,128,130,131,148–151] ▪ Neurons[152–156] ▪ T-lymphocytes[157] ▪ Erythrocytes[158] ▪ Platelets [115,146,147,159] ▪ Pancreas[100,160] ▪ Intestinal epithelia[161,162] ▪ Surface epithelia (skin, oral and vaginal mucosas, oesophageal lining)[160] ▪ Ducts of fluid-secreting glands (salivary glands, lacrimal glands)[160]

Table 1.1: Cellular location of BK$_{Ca}$, SK$_{Ca}$ and IK$_{Ca}$ channels.

As mentioned earlier, activation of BK$_{Ca}$ channels by ryanodine receptor-dependent Ca^{2+} sparks regulates diameter in cerebral resistance arteries (reviewed by Jackson 2017[78]). In other vessels, such as hamster cremaster arterioles, Ca^{2+} entry through L-type VOCCs may contribute to BK$_{Ca}$ channel activation[163]. BK$_{Ca}$ channels can be targeted by vasodilators, either directly or through modification of Ca^{2+} spark activity. For example, nitrosylation via nitric oxide (NO)[79,164]

or phosphorylation via protein kinase G[165–168], enhances the open probability of BK_{Ca} channels by shifting voltage-sensitivity of the channels to more hyperpolarized membrane potentials. In contrast, protein kinase C-mediated phosphorylation of BK_{Ca} channels enhances vasoconstriction by shifting BK_{Ca} channel voltage-sensitivity towards more depolarized membrane potentials thus, limiting their ability to inhibit VOCC-mediated Ca^{2+} entry[169–172]. The importance of smooth muscle BK_{Ca} channels in limiting resistance artery vasoconstriction is shown by the observation that in pressurized rat mesenteric and cerebral arteries, BK_{Ca} channel inhibition leads to enhanced vasoconstriction and membrane depolarization[21,26], and mice deficient in BK_{Ca} channels were found to have significantly enhanced arterial blood pressure[173].

I will now discuss how resistance artery diameter is modulated by two of the most physiological important influences, sympathetic nerve activity, and chemical and electrical signals from endothelial cells.

1.2: **Modulation of resistance artery diameter by perivascular sympathetic nerves**

The sympathetic nervous system plays a major role in controlling total peripheral vascular resistance and is a key regulator of resistance artery diameter[174]. In contrast to structurally well-defined neuromuscular junctions in skeletal muscle, perivascular nerve fibres do not penetrate into the smooth muscle layers[174]. Perivascular nerves appear as a network of axon bundles, with swollen areas, called varicosities, that release neurotransmitters in a manner similar to paracrine secretion[175]. Sensory and nitrergic (that release NO) perivascular nerves have been identified[176,177] but for the purposes of this thesis, I will focus on sympathetic innervation as this accounts for the majority of nerves in resistance arteries (reviewed by Westcott and Segal[174]).

Stimulation of perivascular sympathetic nerves evokes release of noradrenaline and co-transmitters, ATP and neuropeptide Y[175–188]. Noradrenaline acts primarily on post-synaptic α_1-

adrenoceptors to cause vasoconstriction via a number of mechanisms, including IP_3-mediated release of Ca^{2+} from stores, membrane depolarization to increase Ca^{2+} influx through VOCCs and Ca^{2+}-sensitization[189,190]. ATP activates post-synaptic P_{2X} receptors to cause an influx of Na^+ and Ca^{2+} ions that excites the smooth muscle and creates an excitatory junction potential[176–179,181,184–188,191], although the relative contribution of ATP to sympathetic vasoconstriction varies between arteries and species[187,188,192]. Neuropeptide Y binds to post-synaptic Y1 or Y2 receptors[193], but its role appears to be to potentiate noradrenaline-evoked responses rather than to evoke direct vasoconstriction[182,194].

1.3: **Modulation of resistance artery diameter by the endothelium**

In 1980, Furchgott and Zawadzki made the seminal discovery that removal of the endothelial layer of rabbit aortic rings impaired vasorelaxation to acetylcholine and so provided the first example of endothelium-dependent vasodilation[195]. This finding was fundamental to our understanding of blood vessel function and opened up a wide field of research, which has led to our current view that the endothelium is a complex endocrine organ that plays a vital role in the regulation of blood pressure and flow, hemostasis, inflammation, vascular growth and remodeling in the cardiovascular system[196].

We now know that the endothelium releases a wide range of diffusible factors (e.g. NO and cyclooxygenase products, such as prostacyclin) that can alter the contractility of the surrounding smooth muscle cells, and that stimulation of the endothelium by agonists acting at G-protein coupled receptors[117,197], or physiological stimuli, such as increases in shear stress[198–201], also result in activation of endothelial Ca^{2+}-activated K^+ (K_{Ca}) channels[80,84,85,100,116–131,148–151,196,197,202–208]. Opening of these channels causes hyperpolarization of the endothelial cell

membrane potential which spreads to the underlying smooth muscle cells via myoendothelial gap junctions (MEGJs) to reduce opening of VOCCs, decreasing Ca^{2+} influx and causing relaxation.

For the purposes of this thesis, I will briefly discuss endothelial Ca^{2+} signaling, and then focus on two of the main pathways for endothelial modulation of smooth muscle contractility, NO and endothelial K_{Ca} channels, and their role in regulating smooth muscle contractility in resistance arteries.

1.3.1: Endothelial Ca^{2+} signaling

Endothelium-dependent mechanisms for regulation of smooth muscle contractility share a common feature in that they are dependent on a rise in Ca^{2+} levels within endothelial cells[202,209–214]. This increase in Ca^{2+} can be elicited through release from endoplasmic reticulum stores and/or via Ca^{2+} influx through TRP channels, with the contribution of these two mechanisms showing stimulus-dependent variation. It is notable that there are no VOCCs in native endothelial cells[215].

Agonists acting on endothelial $G_{q/11}$-protein coupled receptors stimulate IP_3-mediated release of Ca^{2+} stores which, as described above for smooth muscle cells, leads to store-operated Ca^{2+} entry through Orai1 and/or TRP channels[216–218]. The rise in endothelial Ca^{2+} activates Ca^{2+}-dependent enzymes, such as nitric oxide synthase (NOS), as well as K_{Ca} channels to elicit endothelial hyperpolarization[219]. The identity of the TRP channel mediating receptor-linked Ca^{2+} entry most likely varies between stimuli, arteries and species. TRP vanilloid 4 (TRPV4) channels have been implicated in acetylcholine-evoked Ca^{2+} entry in mouse mesenteric[220] and carotid[221] arteries, whereas TRP canonical 3 (TRPC3) and 4 (TRPC4) have been associated with the same responses in aorta from knockout mouse models[222,223].

In vivo increases in the shear stress across the endothelial cell surface is a major stimulus for activation of endothelium-dependent vasodilator pathways[198–201]. The mechanism underlying

shear stress-induced increases in endothelial Ca^{2+} have not been greatly studied but recent reports indicate a role for mechanosensitive TRP channels, and in particular TRPV4 channels, in shear stress induced increases in Ca^{2+}, NO production and activation of endothelial K_{Ca} channels[132,224]. Limited evidence has also been provided that shear stress-induced increases in endothelial Ca^{2+} are mediated by the release of acetylcholine from endothelial cells. Briefly, Wilson et al. have suggested that acetylcholine produced by endothelial cells is released into the vascular lumen in response to increased shear stress[225]. Acetylcholine then activates endothelial muscarinic receptors, leading to the generation of IP_3 which increases endothelial Ca^{2+} to stimulate NO production and activate K_{Ca} channels[225].

Endothelial TRP channels. As mentioned above, TRP channels have emerged as the most likely mediators of endothelial Ca^{2+} influx[226,227]. The TRP channel super family consists of six subfamilies: TRPV, TRPC, TRPM (melastatin), TRPML (mucolipin), TRPP (polycystin) and TRPA (ankyrin)[226,228]. These channels are all tetramers (either homo- or hetero- mers) with six transmembrane domains and a pore generated by a pore forming loop between S5 and S6[226,228]. All TRP channels are permeable to Ca^{2+}, with the exception of TRPM4 and TRPM5, which are Ca^{2+} activated, but not Ca^{2+} permeable[229–231]. TRP channels are not gated by voltage, but can respond to a wide range of different stimuli: TRPV1-V4 and TRPM3 channels are activated by high temperatures whereas TRPM8, TRPA1, and TRPC5 channels are activated by low temperatures[232,233], TRPC channels are activated either directly by diaglycerol (TRPC2, TRPC3, TRPC6, and TRPC7 channels), or indirectly through a diacylglycerol-dependent mechanism (TRPC1, TRPC4, and TRPC5 channels[234–236]) and TRPM4, TRPM5, TRPM2, and TRPA1 channels are activated by rises in Ca^{2+}[237–240].

Though many of these subfamilies are located on both the endothelium and smooth muscle of the vasculature, two TRP channels in particular, TRPC3 and TRPV4 channels, have been identified as potential mediators of Ca^{2+} influx underlying endothelium-dependent responses to shear stress and/or agonists.

TRPV4 channels are expressed on the endothelium and smooth muscle of many arteries, can be activated by shear stress[241,242] and IP_3[243], and have been linked to both NO production and opening of endothelial K_{Ca} channels[220,241–248]. Mesenteric arteries from mice lacking TRPV4 channels have reduced endothelium-dependent relaxation to acetylcholine in comparison to their wildtype counterparts[220] and in rat carotid and gracilis arteries, shear stress-evoked vasodilation is inhibited in the presence of a TRPV4 channel inhibitor[241]. However, there is also evidence that TRPV4 channels are not involved in endothelium-dependent vasodilation. For example, Pankey et al.[246] found GSK-21939874, a TRPV4 channel inhibitor, did not alter acetylcholine-evoked reductions in pulmonary and systemic arterial pressures. And in mice, global knockout of TRPV4 channels does not alter systolic or diastolic blood pressure[243], heart rate[243] or carotid artery dilation to acetylcholine [247].

TRPC3 channels have also been localized to the vascular endothelium[197,249,250] but not to the smooth muscle cells, and are activated by diacylglycerol, a product of the cleavage of phosphatidylinositol 4,5-biphosphates by phospholipase C stimulated by $G_{q/11}$-protein coupled receptor activation[249,251–255]. Also, it has been reported, by our lab and others, that TRPC3 channels are involved in endothelium-dependent hyperpolarization via the activation of K_{Ca} channels[256,257].

1.3.2: Nitric oxide (NO)

NO is produced by NOS, which converts L-arginine to citrulline and NO[213,258–262]. Oxygen and reduced nicotinamide-adenine-dinucleotide phosphate (NADPH) are co-substrates and flavin

adenine dinucleotide (FAD), flavin mononucleotide (FMN), and 5,6,7,8-tetrahydro-l-biopterin (BH$_4$) are cofactors for this reaction[213,258–265]. The biological half-life of NO and therefore, its activity, is determined by its interaction with superoxide anion (O$_2^-$) which reacts with NO to form the highly reactive intermediate peroxynitrite (ONOO$^-$): **O$_2^-$ + NO → ONOO$^-$**.

In cardiovascular disease states, enhanced oxidative stress leads to increased inactivation of NOS by O$_2^-$ and to uncoupling of NOS; uncoupled NOS produces O$_2^-$ rather than NO[266–270]. Potential mechanisms underlying this change include: oxidation of BH$_4$ and depletion of L-arginine[268,271].

There are three subtypes of NOS: neuronal, endothelial and inducible[213,260,272,273]. Endothelial NOS and neuronal NOS are constitutively active enzymes that produce NO in response to rises in intracellular Ca^{2+} [210–213]. Their activity is also regulated via phosphorylation by a number of different protein kinases[266,274]. The activity of inducible NOS is regulated by its expression level, which is up-regulated in response to cytokines and/or oxidative stress[272,275]. For the purposes of this thesis, I will focus on endothelial NOS located in the vascular endothelium.

The NOS enzyme has two domains, an N-terminal oxygenase domain which binds BH$_4$, oxygen, L-arginine and heme and a C-terminal reductase domain that binds NADPH, FAD and FMN[263–265]. The two domains are linked via a calmodulin-recognition site which is essential for the linkage between the reductase and oxygenase domains and allows dimerization[211,213,263–265]. NO synthesis occurs when electrons are transferred from NADPH via the flavins, FAD and FMN, in the C-terminal reductase domain, to the heme in the N-terminal oxygenase domain[276]. At the heme site, the electrons are used to reduce and activate oxygen and to oxidize L-arginine to L-citrulline and NO[277,278]. Binding of BH$_4$ at the dimer interface is required for the stabilization of

the NOS dimer and 'coupled' NOS activity. As mentioned above, in the absence of BH4, the NOS domains become uncoupled, leading to the production of O_2^- rather than NO[266–270].

The binding of Ca^{2+}-calmodulin is essential for NO production as it enhances the rate of electron transfer from NADPH to flavins in the C-terminus region[211,279,280] but several other proteins also interact with NOS to regulate its activity. For example, the molecular chaperone, heat shock protein 90, acts as an allosteric modulator to increase NOS production of NO[281]. It has also been suggested to inhibit uncoupling of NOS to prevent O_2^- production[282]. This would suggest that there is an intrinsic cellular mechanism regulating the uncoupling of NOS and thus, regulating the balance of NO and O_2^- production[282]. The caveolae coat protein, caveolin-1, is a tonic inhibitor of NOS activity, with recruitment of Ca^{2+}-calmodulin and heat shock protein 90 to NOS displacing caveolin-1 from the enzyme to activate it[283,284]. Furthermore, phosphorylation of serine1177 of NOS in response to prolonged increases in shear stress can stimulate NO production in a Ca^{2+}-independent manner, with phosphatidylinositol-3 kinase/AKT being implicated as the possible mediators of this phosphorylation[266,274,285].

Once released from endothelial cells, NO causes relaxation of smooth muscle cells via activation of soluble guanylyl cyclase[286] to increase production of cyclic guanosine monophosphate, which subsequently activates protein kinase G[287,288]. Protein kinase G interacts with a number of different protein targets to limit vasoconstriction and cause vasodilation. For example, protein kinase G can phosphorylate phospholipase C to inhibit IP3 production and thus, decrease IP3-mediated Ca^{2+} release required for smooth muscle vasoconstriction[166,251,289], and protein kinase G-mediated phosphorylation increases activity of BK_{Ca} channels[165–168]. NO itself can also directly nitrosylate BK_{Ca} channels to increase their open probability[79,290,291,164]. The subsequent smooth muscle hyperpolarization due to the opening of BK_{Ca} channels[292] decreases the

activity of VOCCs and reduces Ca^{2+} entry and vasoconstriction[26]. Additionally, protein kinase G-mediated phosphorylation of L-type VOCCs can inhibit their activity[55–59], to further reduce Ca^{2+} entry. See **Figure 1.5**[293] for a schematic of NO-mediated effects on vascular smooth muscle contractility.

The role of NO in regulating arterial diameter, blood flow and pressure was facilitated by the discovery that structural analogues of L-arginine, such as L-N^G-nitro arginine (L-NOARG) and N^G-nitro-L-arginine methyl ester hydrochloride (L-NAME) act as selective, competitive inhibitors of NOS[294,295]. For example, administration of L-NAME causes hypertension in rats and L-NOARG inhibits endothelium-dependent relaxation in isolated rat aorta[296,297]. The demonstration that deletion of NOS leads to hypertension in mice was also an advance in demonstrating the physiological importance of this molecule[298].
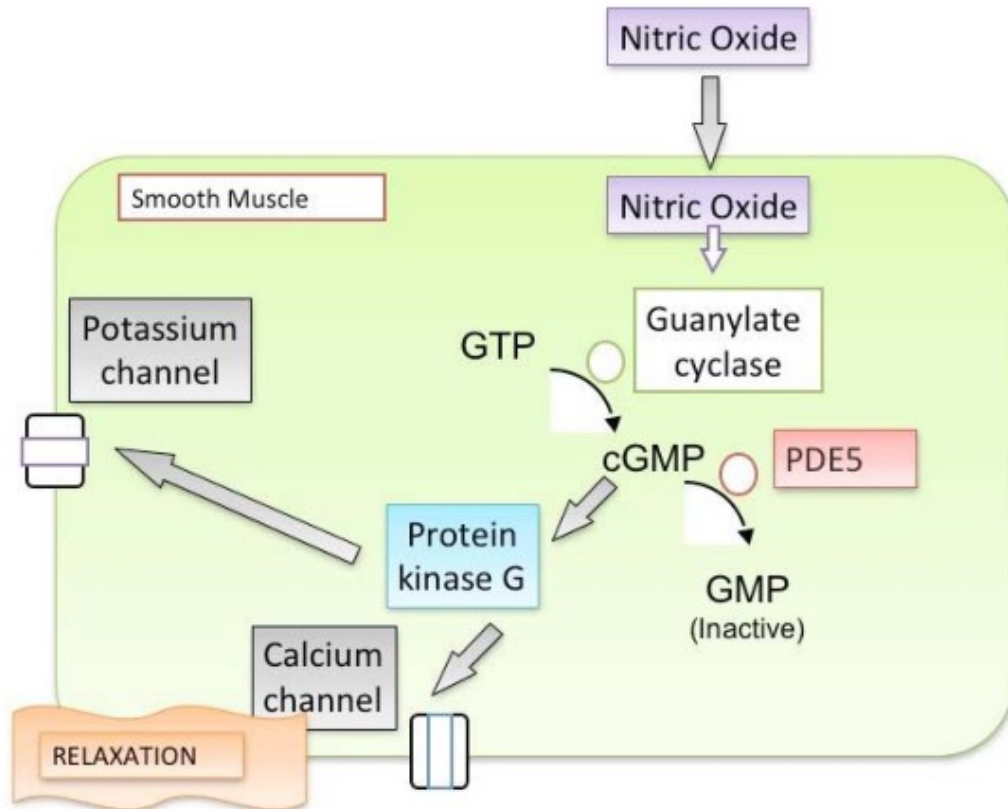
Figure 1.5: NO-mediated relaxation of vascular smooth muscle. NO is produced in endothelial cells by endothelial NOS and diffuses to the smooth muscle to activate guanylyl cyclase to produce cyclic guanosine monophosphate which stimulates protein kinase G to phosphorylate a number of targets to induce vasodilation. For example, protein kinase G phosphorylates VOCCs to decrease opening probability, and phosphorylates BK_{Ca} channels to increase opening probability[293].

1.3.3: Endothelium-dependent hyperpolarization

Opening of endothelial small (SK_{Ca}) and intermediate (IK_{Ca}) conductance Ca^{2+}-activated K^+ channels causes hyperpolarization of the endothelial cell membrane potential which spreads to underlying smooth muscle cells via MEGJs to reduce opening of VOCCs, leading to a decrease in Ca^{2+} influx and thus, relaxation[80,117,125,202,299]. The defining characteristic of hyperpolarization-mediated vasodilation is that it persists in the presence of inhibitors of NOS and cyclooxygenase and, under these conditions, is abolished by blockers of endothelial SK_{Ca} and IK_{Ca} channels, apamin and 1-[(2-Chlorophenyl)diphenylmethyl]-1*H*-pyrazole (TRAM-34) or charybdotoxin,

respectively (reviewed by Ledoux et al. 2006[103]). The physiological importance of endothelial K_{Ca} channels *in vivo* is highlighted by increased vascular reactivity and raised arterial blood pressure recorded in mice lacking one or both of the channels[127,300].

Endothelium-dependent hyperpolarization plays a more prominent role in endothelium-dependent dilation of resistance arteries than in large vessels and so it is an important determinant of local tissue perfusion[301–303]. Initially, it was thought that endothelium-dependent hyperpolarization of vascular smooth muscle was mediated by a diffusible factor, but current consensus it is due to direct electrical coupling of endothelial and smooth muscle cells via MEGJs[303].

1.3.4: Endothelial Ca^{2+}-activated K$^+$ (K$_{Ca}$) channels

There are three types of K_{Ca} channels: BK_{Ca}, SK_{Ca} and IK_{Ca} channels. Whereas BK_{Ca} channels are solely located on smooth muscle[27,29,79–92], SK_{Ca} and IK_{Ca} channels are not found on smooth muscle cells but are located on the endothelium[80,84,85,100,116–131,148–151,197,202] (See **Table 1.1**).

Endothelial SK_{Ca} and IK_{Ca} channels are voltage-independent K$^+$ channels that are activated by increases in intracellular Ca^{2+} [117,202]. There are three SK_{Ca} channel subtypes (SK1, 2 and 3), which are encoded by the genes *KCNN1-3*[117,120,139], and one IK_{Ca} channel subtype (SK4), encoded by *KCNN4*[120,202,304]. In the vascular endothelium, SK3, rather than SK1 and 2, has been shown to be the primary subtype present[117], and thus, when SK_{Ca} channel is referenced in this work it is denoting the SK3 subtype[117].

SK_{Ca} and IK_{Ca} channels are tetramers consisting of α-subunits that have six transmembrane domains (S1-S6), with the pore domain encompassed by S5-S6 and a calmodulin binding domain on the C-terminus directly after S6[140]. Calmodulin is constitutively bound to the C-terminus of

SK_{Ca} and IK_{Ca} channels and confers their Ca^{2+} sensitivity (values for half-maximal activation ranging from 95 nM to 0.3 μM[100,140]), as the channels themselves do not possess any Ca^{2+} binding sites[140]. Thus, SK_{Ca} and IK_{Ca} channels will remain closed until Ca^{2+} binds to each of the bound calmodulin as Ca^{2+}-calmodulin complexes stabilize the channel's open state[103]. See **Figure 1.6** for a schematic of SK_{Ca}/IK_{Ca} channel subunit structure[103].
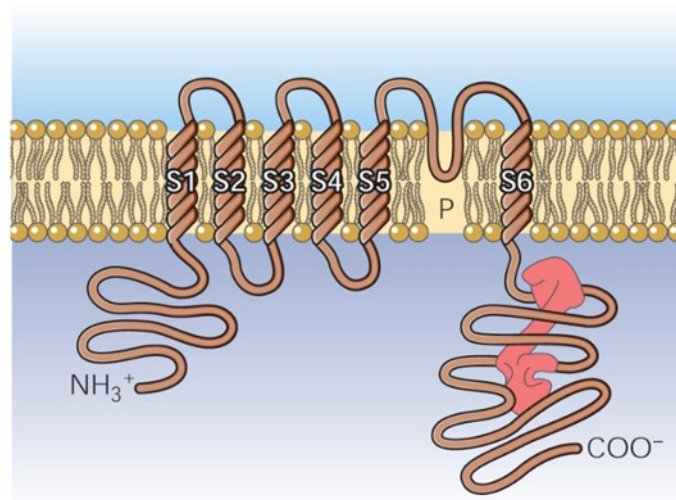
Figure 1.6. **Schematic of a SK_Ca/IK_Ca channel subunit**. Each subunit consists of six transmembrane domains with a pore region (P) between S5 and S6. Calmodulin interacts with the intracellular C-terminus[103].

SK_{Ca} and IK_{Ca} channel activity is modulated by associated proteins. Constitutively bound casein kinase 2 and protein phosphatase 2A have been shown to alter SK_{Ca} channel Ca^{2+} sensitivity through phosphorylation or dephosphorylation of the bound calmodulin[103,305,306]. Casein kinase 2-mediated phosphorylation occurs at threonine80 on the constitutively bound calmodulin and decreases the Ca^{2+} sensitivity (from sub-micromolar ranges to micromolar ranges[306]), reducing the opening probability of the channel[305]. Dephosphorylation mediated by protein phosphatase 2A removes the inhibitory phosphorylation caused by casein kinase 2[305,306].

As their name suggests, opening of SK_{Ca} channels allows for a small K^+ current (10-20 pS[100,202,307]) to move out of the endothelial cells, causing hyperpolarization of the endothelial membrane potential. Alternatively, IK_{Ca} channels have a conductance of about 30-80 pS[100,202]. K_{Ca} channel-mediated endothelial hyperpolarization has been recorded in intact porcine coronary arteries[117], internal carotid arteries of guinea pigs[80], rat mesenteric[122,123,150] and hepatic arteries[299], rat aortas[119], and freshly isolated endothelial cells from porcine coronary arteries[117,122,202], rat mesenteric arteries[150] and canine mesenteric arteries[124], and human umbilical vein endothelial cells[131]. This hyperpolarization spreads through the MEGJs to induce hyperpolarization of the smooth muscle membrane potential, limiting constriction by decreasing the open probability of VOCCs[49,214,299].

Compared to other ion channels, SK_{Ca} and IK_{Ca} channels have a well-developed pharmacology which has aided investigation of their physiological functions[308]. For example apamin, isolated from bee venom, is a selective inhibitor of rat SK2 and SK3 (IC_{50} 70 pM and 2.6 µM, respectively) but does not block rat SK1 channels[309]. Apamin is an allosteric modulator, binding to the outside of SK_{Ca} channels and causing a conformational change in the channel's pore that blocks the movement of K^+[309,310]. TRAM-34 and 4-[[3-(Trifluoromethyl)phenyl]methyl]-2*H*-1,4-benzothiazin-3(4*H*)-one (NS 6180) are both selective inhibitors of IK_{Ca} channels that bind to threonine250 and valine275 in the inner pore. Up to a concentration of 1 µM NS 6180 and 5 µM TRAM-34, these two chemicals are highly selective IK_{Ca} channel blockers that show no effect on T-lymphocyte Ca^{2+} entry or voltage-gated K^+, sodium and TRP channels[121,311,312].

There are also positive modulators selective for both SK_{Ca} and IK_{Ca} channels, such as 1-ethyl-2-benzimidazolinone (EBIO) and 6,7-dichloro-1H-indole-2,3-dione 3-oxime (NS 309), which have been shown to bind to the interface of where the α-subunits of these channels bind to

calmodulin, increasing their Ca^{2+} sensitivity[308]. Newer compounds that are selective for either channel have also been developed. For example, *N*-cyclohexyl-*N*-[2-(3,5-dimethyl-pyrazol-1-yl)-6-methyl-4-pyrimidinamine (CyPPA), was based on NS 309, and as such, is a positive modulator selective for SK2 and SK3 channels (EC_{50} value for human SK2 and SK3 channels is 14 μM and 5.6 μM, respectively) but has no effect on human IK_{Ca} channels[313]. It has been shown to enhance the Ca^{2+} sensitivity of human SK3 channels by improving the Ca^{2+} sensitivity of the channel from 429 nM to 59 nM[313]. As it is structurally similar to NS 309, it is likely that it also binds to the interface of the α-subunit and calmodulin binding site on SK_{Ca} channels to elicit its effects[308,313].

Naphtho[1,2-*d*]thiazol-2-ylamine (SKA-31) is another positive modulator but it is 7- to 10-fold more selective for IK_{Ca} (EC_{50} value of 260 nM) over SK_{Ca} channels (SK3 EC_{50} value of 2.9 μM)[121]. SKA-31 does not interact significantly with other channels when used at concentrations under 25 μM[121]. SKA-31 has been used in the literature as a positive modulator of both SK_{Ca} and IK_{Ca} channels[121,124,148,314,315] and as a selective positive modulator for IK_{Ca} channels alone[204,316]. However, Sankaranarayanan et al. found that the enhancement of acetylcholine-mediated dilation of mice carotid arteries and reduction of mean arterial pressure *in vivo* caused by SKA-31 was entirely through its actions on IK_{Ca} channels[121].

While SK_{Ca} and IK_{Ca} channels share significant similarities in their structures and regulation, their discrete cellular locations within endothelial cells may correspond to differences in how they regulate vascular tone in response to various stimuli[125,317]. SK_{Ca} are located at endothelial junctions on the luminal surface and co-localize in caveolae with TRPV4 channels[318] where they are able to respond to local Ca^{2+} increases evoked by increases in shear stress-induced activation of TRPV4 channels[319]. In contrast, IK_{Ca} channels are located on the abluminal side of

endothelial cells at MEGJs, the sites of contact between endothelial and smooth muscle cells (**Figure 1.7**).
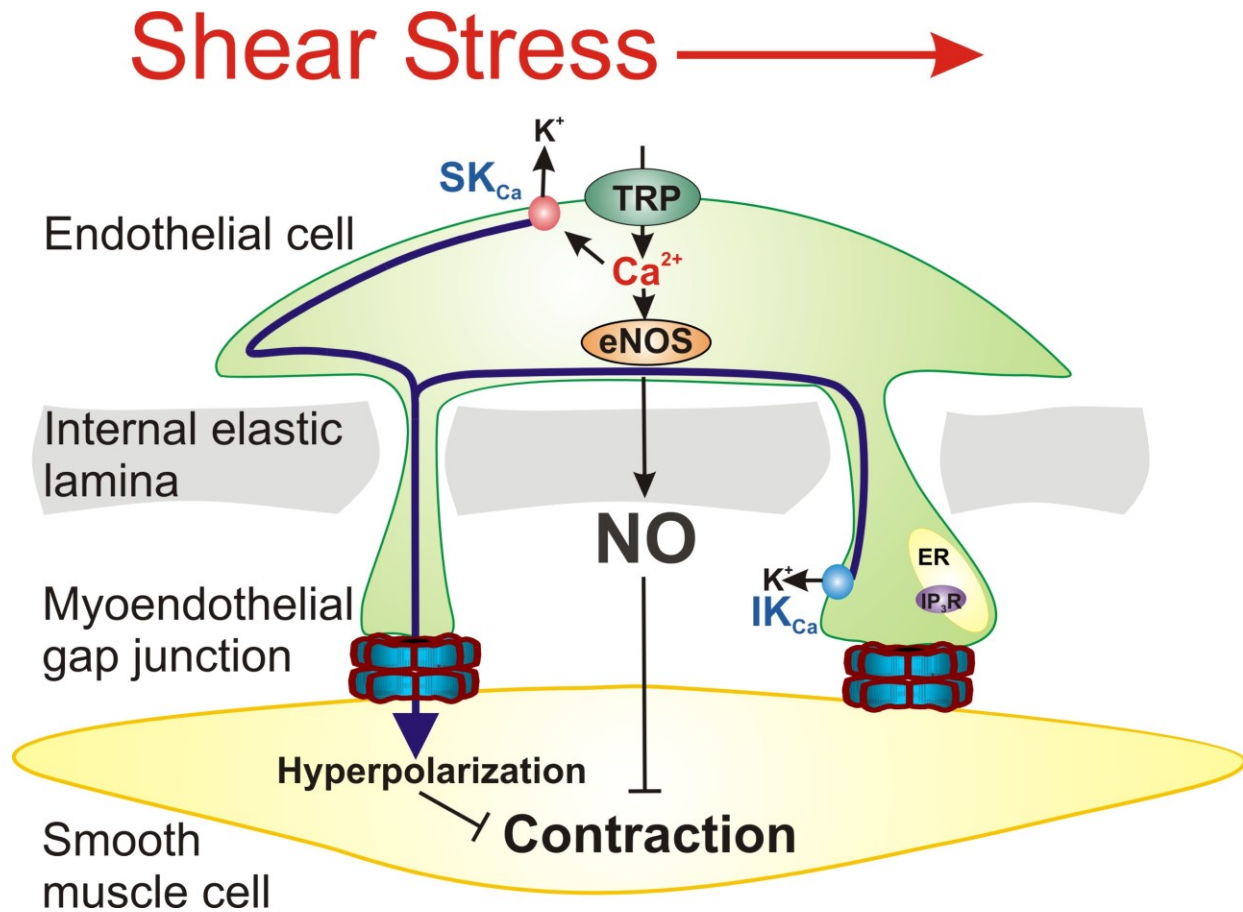
Figure 1.7: **Schematic showing the cellular locations of SK$_{Ca}$ and IK$_{Ca}$ channels within endothelial cells.** SK$_{Ca}$ channels have been localized to the endothelial luminal membrane while IK$_{Ca}$ channels have been localized to the MEGJs. Their differing locations are proposed to confer them different functional roles in terms of regulating vascular tone. SK$_{Ca}$, small conductance Ca^{2+}-activated K$^+$; IK$_{Ca}$, intermediate conductance Ca^{2+}-activated K$^+$; ER, endoplasmic reticulum; NSCC, non-selective calcium channel (most likely a TRPV4 channel); IP$_3$, inositol triphosphate.

Recent work from our lab and others, has demonstrated that the localization of IK$_{Ca}$ channels at MEGJs enables them to mediate myoendothelial feedback, a mechanism by which contractile activation of smooth muscle cells is limited by the endothelium (**Figure 1.8**[197]). Briefly, IP$_3$, produced in smooth muscle cells by the activation of α_1-adrenoceptors[8,17–20,251–255,320], diffuses

through the MEGJs to activate endothelial IP$_3$ receptors to cause localized increases in Ca^{2+}, close to the MEGJs[28,197,321]. This rise in endothelial Ca^{2+} activates the IK$_{Ca}$ channels localized to the MEGJs[118,125,130,151,197], leading to activation of NOS[224] and endothelial hyperpolarization which spreads back to the smooth muscle to limit further contraction. A population of NOS has recently been shown to be located close to MEGJs and its activity is regulated by local IP$_3$-mediated Ca^{2+} release in response to agonist-induced vasoconstriction[322]. Additionally, we showed that production of NO is limited by inhibition of IK$_{Ca}$ channels and TRPC3 channels[197], which may indicate IK$_{Ca}$ channels play a role in tuning endothelial Ca^{2+} signaling[323], and support the notion that rather than being distinct pathways, there is a link between NO and K$_{Ca}$ channel activity.
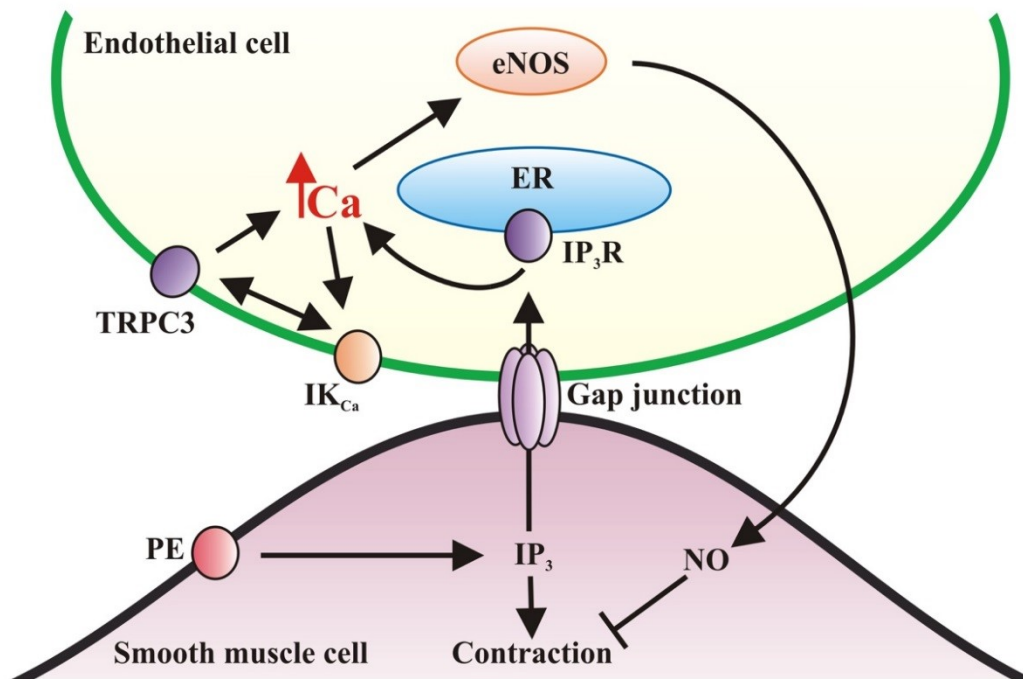
Figure 1.8: Myoendothelial feedback. Contractile agonists increase IP$_3$ levels within smooth muscle cells. Flux of IP$_3$ through MEGJs gives rise to localized increases in Ca^{2+} and subsequent activation of a discrete pool of IK$_{Ca}$ channels and NOS localized within spatially restricted myoendothelial projections. The resulting hyperpolarization and/or NO feeds back to the surrounding smooth muscle cells to attenuate agonist-induced depolarization and contraction[197].

It has been suggested that endothelial K_{Ca} channel-mediated hyperpolarization of the membrane potential maintains the driving force for Ca^{2+} influx to endothelial cells necessary for activation of NOS. But, the ability of hyperpolarization to regulate Ca^{2+} entry by increasing the electrical driving force is controversial, particularly as there is a large concentration gradient of ~20,000-fold from outside to inside of endothelial cells[324,325]. However, recent studies of isolated endothelial tubes have demonstrated that Ca^{2+} influx in the presence of acetylcholine is enhanced by K_{Ca} channel-mediated membrane potential hyperpolarization and reduced by membrane potential depolarization[326]. In human umbilical vein endothelial cells, inhibition of SK_{Ca} and IK_{Ca} channels blocked Ca^{2+} influx and NO production in response to G protein-coupled receptor activation[131], and both SK_{Ca} and IK_{Ca} channels have been shown to influence endothelial Ca^{2+} dynamics in intact mouse mesenteric arteries[323]. Furthermore, in rat cremaster arterioles, NS 309 and 5,6-dichloro- 1-ethyl-1,3-dihydro-2H-benzimidazol-2-one (DCEBIO), activators of SK_{Ca}/IK_{Ca} channels, enhanced ATP-induced hyperpolarization, cytosolic Ca^{2+} concentration and NO synthesis[128,131]. Thus, these findings indicate that opening of endothelial SK_{Ca} and IK_{Ca} channels may enhance NO bioavailability[80,84,85,100,116–131,148–151,197,202–205].

1.4: Endothelial dysfunction

Endothelium-derived NO elicits relaxation of surrounding smooth muscle cells to cause vasodilation, regulates local cell growth and protects blood vessels from the deleterious consequences of platelet aggregation and activation of inflammatory responses[327]. Endothelial dysfunction is associated with risk factors for cardiovascular diseases, such as diabetes, hypertension and atherosclerosis, is characterized by increased production of O_2^- and decreased NO bioavailability[268,328–336] leading to enhanced vasoconstriction, clot formation and inflammation within the vasculature (**Figure 1.9**[116]).
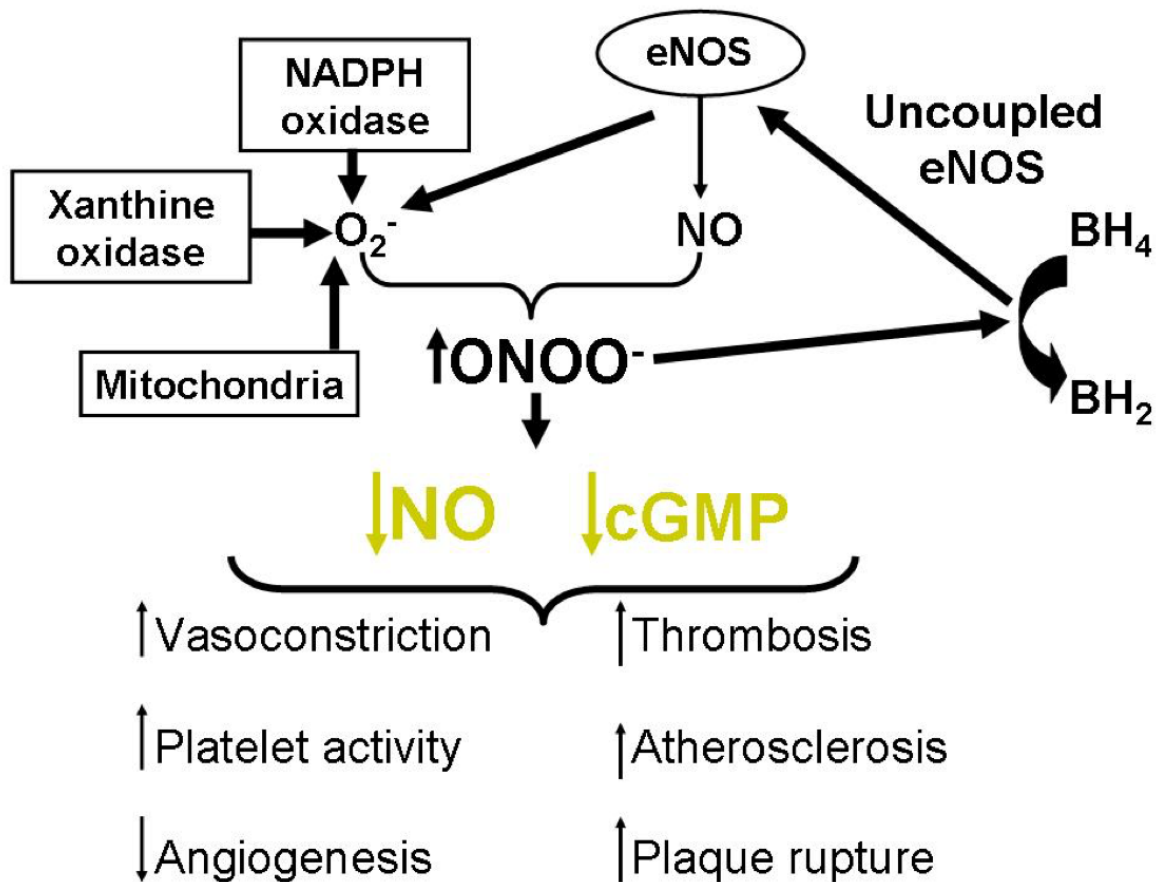
Figure 1.9: Schematic showing the deleterious consequences of decreased NO and increased O_2^- levels on the vasculature. Enhanced O_2^- production leads to increased $ONOO^-$ and reduced bioavailability of NO leading to increased vasoconstriction, platelet activity, thrombosis, atherosclerosis and plaque rupture and diminished angiogenesis. eNOS, endothelial nitric oxide; NO, nitric oxide; O_2^-, superoxide anion; $ONOO^-$, peroxynitrite; BH_4, tetrahydrobiopterin; cGMP, cyclic guanine monophosphate[116].

Attempts to reduce vascular O_2^- levels through the use of dietary anti-oxidants, such as vitamins B, C and E, have been unsuccessful in clinical trials[337–342] and so there is the need to identify new targets for therapeutic approaches to reduce O_2^- levels and enhance NO bioavailability in pathological settings.

1.4.1: Vascular O_2^- production

Reactive oxygen or nitrogen species (ROS or RNS, respectively) are highly reactive compounds involved in a variety of different cellular processes under both physiological and

pathophysiological conditions[328,329,343]. Whether ROS/RNS cause cellular damage or not, is usually determined by their cellular concentrations, with low levels of ROS and RNS necessary for normal cellular processes and high concentrations leading to dysfunction[329,343–346]. For example, vasoconstriction of rat mesenteric resistance arteries evoked by α_1-adrenoceptor agonists is dependent on production of O_2^- by NADPH oxidase and vascular smooth muscle mitochondria[347–349] whereas deleterious high levels of O_2^- production leads to endothelial dysfunction associated with increased risk of cardiovascular disease[268,328–336]. Some examples of ROS and RNS are O_2^-, hydroxyl radical (OH^-), NO, $ONOO^-$ and hydrogen peroxide (H_2O_2) but for the purposes of this thesis, I will be focusing on O_2^-.

O_2^- is produced through the addition of an electron to molecular oxygen[350]. In the vasculature, this is primarily mediated by NADPH oxidase enzymes[351–356], and to a lesser extent by xanthine oxidase, the mitochondrial electron transport chain, cyclooxygenase enzymes and uncoupled endothelial NOS[268,329,343,344]. In hypoxic conditions, xanthine dehydrogenase can undergo oxidation or Ca^{2+}-induced proteolysis to form xanthine oxidase which produces O_2^{-}[357,358]. The electron transport chain on the mitochondrial membrane consistently produces low levels of O_2^- from Complex I, II and III, but in neurons and cardiac myocytes, this is significantly enhanced in conditions of ischemia-reperfusion[89,111,144,359–364]. Additionally, although the primary function of endothelial NOS is production of NO, under conditions of oxidative stress, oxidation of the endothelial NOS co-factor BH_4 leads to uncoupling of endothelial NOS[266–270]. Uncoupled endothelial NOS produces O_2^- instead of NO, which directly increases O_2^- levels and decreases the amount of NO available to scavenge O_2^{-} [267,268,365,366].

NADPH oxidase enzymes are comprised of catalytic NOX proteins which form a complex, with p22[phox], p47[phox], p67[phox], p40[phox] and a small G protein called Rac1, the latter thought to be

involved in regulating NADPH oxidase activity through its association and dissociation with the complex[355,367–372] (**Figure 1.10**[373]). The NOX protein and p22[phox] form the flavocytochrome b_{558} reductase to which NADPH, the electron donor, binds on the cytosolic side of the membrane[371,374,375]. Oxygen is then reduced across the endothelial membrane to produce O_2^- intracellularly[375]. Thus, NADPH oxidase catalyzes the production of O_2^- and $NADP^+$ by transferring an electron from NADPH to oxygen[368,372]. Vascular NADPH oxidase produce about 90-99%[371,374] less O_2^- than their phagocytic counterparts and do so constantly.
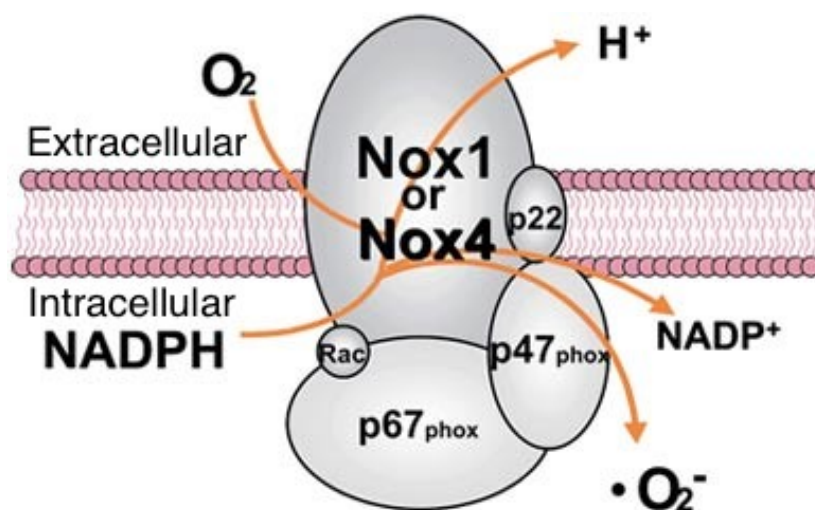
Figure 1.10: Schematic of an NADPH oxidase complex. NADPH oxidase enzymes are comprised of a NOX protein plus p22[phox], p47[phox], p67[phox], p40[phox] and a small G protein, Rac1. The NOX protein and p22[phox] form the flavocytochrome b_{558} reductase to which NADPH, the electron donor, binds on the cytosolic side of the membrane. NADPH, nicotinamide adenine dinucleotide phosphate; FAD, flavin adenine dinucleotide[376].

The NOX catalytic subunits are transmembrane proteins with six α-helices, which include five conserved histidine residues capable of binding two hemes[375,377]. There are seven homologues of the NOX catalytic subunit of NADPH oxidase enzymes: NOX1, NOX2, NOX3, NOX4, NOX5, DUOX1 and DUOX2[377,378]. The NOX2 subtype was the first to be identified due to its crucial role

in phagocytic O_2^- production in macrophages[379,380]. NOX1, NOX2, NOX4 and NOX5 NADPH oxidase subtypes have all been shown to be expressed in the vasculature[368,370,381]. NOX2 and NOX4, and possibly NOX1 (depending on the arterial subtype), have been localized to endothelial cell membranes[356,368,369,381,382], whereas NOX1 and NOX4 can be found on smooth muscle cells[332–336,346,383]. NOX4 in particular, appears to be the dominant NADPH oxidase type present in arterial endothelial cells, with its expression significantly higher than the other NOX homologues[368,381]. Furthermore, increased activity of the NOX1 subtype on smooth muscle cells has been linked to the development of cardiovascular diseases[332–336,383].

NADPH oxidase enzymes found in the vasculature are constitutively active[371,374] and their activity can be enhanced under certain conditions. For example, oxidized low-level lipoproteins have been shown to increase both the expression and activity of endothelial NADPH oxidase[374]. Additionally, elevated NADPH levels have been shown to stimulate NADPH oxidase[351–353,384,385]. And finally, and of particular importance for this thesis, it has been shown that cell membrane potential regulates the activity of NADPH oxidase in the vasculature[126,367,386–388]. Depolarization of the endothelial membrane potential stimulates endothelial NADPH oxidase enzymes to produce more O_2^- in both intact arteries and cultured endothelial cells[126,367,386,387], while hyperpolarization of the membrane potential of cultured endothelial cells was found to reduce O_2^- production[388]. Pharmacological activation of human endothelial umbilical vein K_{ATP} channels decreased NADPH oxidase activity by hyperpolarizing the endothelial membrane potential[367]. Inhibition of SK_{Ca} and IK_{Ca} channels has been shown to increase NADPH oxidase production of O_2^- in rat perfused mesenteric beds and lead to increased phosphorylation of endothelial NOS and a reduction in NO production[126]. The membrane potential sensitivity of NADPH oxidase has been suggested to be

conferred by the binding of Rac1 to the complex, which has been shown to occur as a result of its phosphorylation induced by endothelial membrane depolarization[367].

O_2^-, as a radical, has the ability to oxidize proteins, such as lipoproteins[374] and BH_4, the endothelial NOS co-factor[13,171,185,335]. O_2^- has also been shown to evoke phosphorylation of endothelial NOS at threonine495, leading to a reduction in NO production[126].

Under physiological conditions, O_2^- is quickly reduced to H_2O_2 by the superoxide dismutase (SOD) enzymes. Thus, many of the cellular effects of O_2^- occur indirectly through H_2O_2. O_2^- also interacts with NO to produce $ONOO^-$, at a rate three times faster than O_2^- undergoes dismutation via SOD[389,390]. Therefore, increases in O_2^- levels significantly impact the amount of free NO available to induce vasodilation and other protective effects by regulating both NO production and bioavailability.

There are three subtypes of SOD found in the vasculature: SOD1 (cytosolic copper/zinc SOD), SOD2 (manganese SOD) and SOD3 (extracellular copper/zinc SOD)[364,391–394]. The copper/zinc SOD types have been shown to be the predominant subtype in the vascular endothelium and their loss or inhibition results in a significant enhancement of O_2^- production and a reduction in NO bioavailability leading to vascular dysfunction[390,394]. The product of O_2^- dismutation by SOD enzymes is H_2O_2, which itself is an active regulator of vascular tone that can cause both vasodilation[395,396] and vasoconstriction[397–400], depending on the vascular bed, concentration of H_2O_2 and the overall health status of the vasculature [397].

The production of $ONOO^-$ from the combination of NO and O_2^- is necessary for normal cellular function. Under physiological conditions, this interaction between NO and O_2^- regulates both the amount of NO and O_2^- in the vasculature[344] and has been suggested as a way in which NO regulates its own production. $ONOO^-$ also has important roles in vasodilation when present at

normal levels[344,401,402]. $ONOO^-$ has been shown to enhance sarcoendoplasmic reticulum Ca^{2+} ATPase activity, via S-glutathiolation[401], thus, increasing the rate of smooth muscle intracellular Ca^{2+} removal to facilitate vasodilation. Additionally, $ONOO^-$ has been shown to stimulate guanylyl cyclase, in a similar manner to NO, to induce vasodilation[403]. Finally, upon interaction with glutathione, $ONOO^-$ is returned back to NO, which becomes free to induce vasodilation[403], making $ONOO^-$ an endogenous NO donor.

However, in pathological conditions, such as atherosclerosis[328,329], O_2^- levels are significantly enhanced and high levels of $ONOO^-$ result in deleterious effects. Arguably the most important result of $ONOO^-$ production is that the conjugation of NO with O_2^- leads to a decrease in the amount of NO available to induce vasodilation as well as to regulate platelet adhesion and aggregation, angiogenesis and vascular smooth muscle cell proliferation[298,328,404–406]. Additionally, $ONOO^-$ can oxidize BH_4, leading to the uncoupling of endothelial NOS and the production of O_2^- instead of NO, further reducing NO levels[269,270]. Thus, increased production of $ONOO^-$ initiates a positive feedback loop for O_2^- production; more O_2^- produced from uncoupled endothelial NOS further enhances $ONOO^-$ levels and subsequently, additional endothelial NOS complexes become uncoupled and produce even more O_2^-[407]. $ONOO^-$ has also been shown to detrimentally oxidize proteins and lipids, such as low-density lipoproteins[344].

Glutathione is the most common low-weight molecular peptide in cells[408,409] and is essential for the regulation of ROS levels within cells; it scavenges free radicals, such as O_2^-, and reduces RNS, such as $ONOO^-$[407], through its thiol moiety[408,410]. This thiol moiety also enables glutathione to reversibly modify the cysteine residues of proteins, such as BK_{Ca} channels through S-glutathiolation, leading to alterations in protein function[79,400].

Glutathione is comprised of three amino acids, glutamine, cysteine and glycine, and is

produced in two steps; γ-glutanylcysteine synthetase catalyzes the first and rate-limiting step, to generate γ-glutanylcysteine from glutamate and cysteine, and then glutathione synthetase is responsible for the addition of the glycine molecule to produce γ-glutanylcysteinylglycine or glutathione [407,408].

When glutathione undergoes oxidation after interacting with ROS or RNS, glutathione disulfide is formed from two oxidized glutathione molecules[408,411]. Glutathione disulfide is also capable of S-glutathiolation protein modifications of sulfhydryl groups[125] and is converted into two glutathione molecules by glutathione reductase, which requires NADPH as a co-factor and electron donor[408,411]. The generation of glutathione from glutathione disulfide thus, results in the production of $NADP^+$ from NADPH (**Figure 1.11**).

Glutathione plays a crucial role in regulating the reduction-oxidation potential of cells, including the vascular endothelial and smooth muscle cells[412], through its scavenging of O_2^{-}[408,410]. The ratio of glutathione to glutathione disulfide can be an indicator of the reduction-oxidation status of cells, as under physiological conditions, glutathione levels are static and significantly higher than glutathione disulfide (in canine pancreatic microsomes this ratio has been shown to range from 30:1 to 100:1)[409]. However, under pathophysiological conditions characterized by oxidative stress, NADPH levels become depleted as glutathione reductase activity is drastically enhanced and glutathione disulfide accumulates. Glutathione disulfide accumulation leads to abnormal, and possibly detrimental, S-gutathionylation of proteins and/or excretion from the cell[407,413], further reducing glutathione levels.

NO has also been shown to be involved in regulating the levels of glutathione[410]. NO, or its downstream effectors, can increase expression of γ-glutanylcysteine synthetase [407], the enzyme responsible for catalyzing the rate-limiting step in the production of glutathione[407,408,414], and so by increasing glutathione levels, NO indirectly enhances its own bioavailability, as more glutathione will be available to scavenge O_2^-[410].
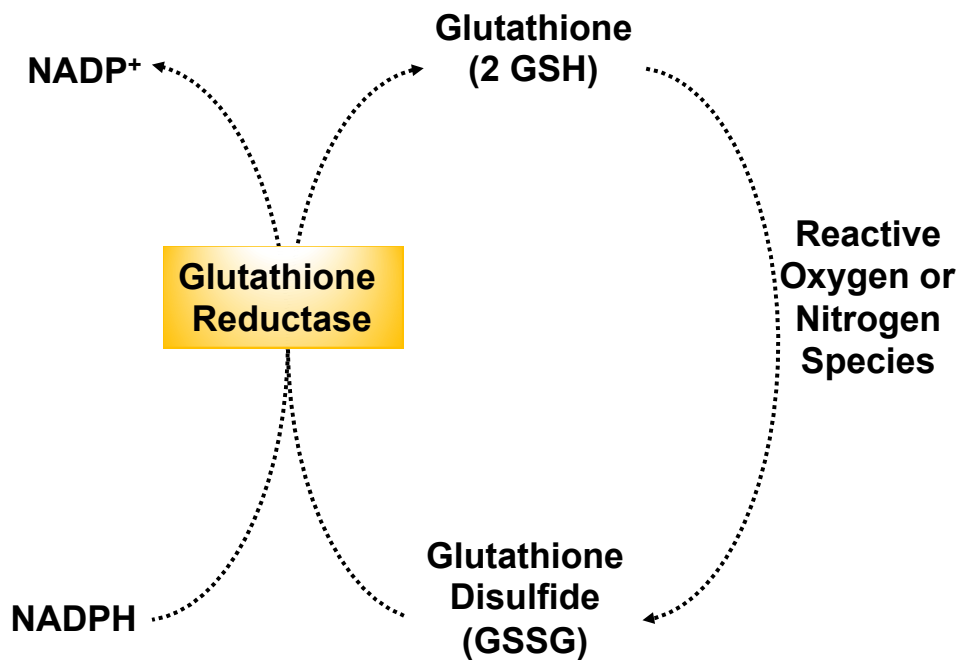
Figure 1.11: The glutathione pathway. Glutathione is oxidized through interactions with ROS or RNS. Two oxidized glutathione (GSH) molecules will combine to form glutathione disulfide (GSSG) which is converted back into two glutathione molecules by glutathione reductase. Glutathione reductase requires the electron donor, NADPH, to catalyze this reaction. NADPH, nicotinamide adenine dinucleotide phosphate.

Glutathione levels are regulated by its synthesis, the levels of ROS and the rate at which it is converted back from glutathione disulfide by glutathione reductase, the activity of which is dependent on cellular NADPH levels[408,411,415–417]. Additionally, both glutathione and glutathione disulfide, due to their ability to reversibly modify proteins via S-glutathiolation, can have a role in regulating vascular tone through altering the function of proteins, such as ion channels. In HEK293

cells, glutathione disulfide can inhibit K_{ATP} channels[400] and in guinea-pig smooth muscle cells, glutathione increases the open probability of BK_{Ca} channels by shifting their voltage sensitivity to more hyperpolarized membrane potentials[79].

To conclude, the vascular endothelium plays a crucial role in regulating resistance artery diameter and thus, blood flow and pressure. This is accomplished through release of NO and endothelial K_{Ca} channel-mediated hyperpolarization which spreads to smooth muscle cells via MEGJs. Although long thought of as distinct mechanisms for vasodilation, recent evidence suggests that there may be a link between these two pathways; for example, IK_{Ca} channel-mediated myoendothelial feedback leads to release of NO[197], and block of K_{Ca} channels can inhibit NO-mediated vasorelaxation[203,418].

Endothelial dysfunction is associated with increased cardiovascular risk[328,329] and characterized by an increase in O_2^- production and a decrease in NO bioavailability[268,328–336]. Therefore, the development of new drugs which possess indirect antioxidant properties mediated by the stimulation of NO production and simultaneous inhibition of O_2^- production is an attractive proposition for cardiovascular disease prevention and therapy. I propose that drugs which activate SK_{Ca} and IK_{Ca} channels may fall into this category.

These channels mediate vasodilation through spread of membrane hyperpolarization from endothelial to smooth muscle cells[80,84,85,100,116–131,148–151,197,202], and have recently been suggested to also be involved with enhancing NO bioavailability[116,126,128,131,203–205]. Furthermore, it has been shown that NADPH oxidase enzymatic activity in the vasculature is regulated by membrane potential; with depolarization stimulating NADPH oxidase production of O_2^- and hyperpolarization inhibiting NADPH oxidase production of O_2^- [126,367,386–388]. Therefore, increasing

the opening of endothelial K_{Ca} channels to elicit hyperpolarization could lead to vasodilation, decreased O_2^- production and increased NO bioavailability.

1.5: Hypothesis and aims

My over-arching goal is to further explore the relationship between endothelial K_{Ca} channels and NO in regulating resistance artery diameter by testing three hypotheses:

1. *Activation of SK_{Ca} channels can enhance NO-mediated inhibition of sympathetic vasoconstriction evoked by increases in shear stress.*

2. *IK_{Ca} channel-mediated myoendothelial feedback plays a role in NO-dependent modulation of sympathetic vasoconstriction.*

3. *Pharmacological activators of endothelial K_{Ca} channels can reduce vascular O_2^- production and enhance NO-mediated modulation of vasoconstriction*

To test these hypotheses, I have addressed two major aims:

1. **To investigate the role of endothelial K_{Ca} channels in NO-mediated modulation of nerve-evoked vasoconstriction in the perfused mesenteric bed.**

2. **To investigate whether pharmacological activators of endothelial K_{Ca} channels can modulate vascular O_2^- production and vasoconstriction stimulated by the α_1-adrenoceptor agonist phenylephrine.**

Chapter 2: Activation of SK_{Ca} channels enhances shear stress-mediated inhibition of sympathetic vasoconstriction in the perfused mesenteric bed

2.1: Introduction

As described in **Chapter 1**, endothelial and vascular smooth muscle cells work together to regulate resistance artery diameter through a variety of mechanisms, such as release of NO, cyclooxygenase-derived mediators and changes in membrane potential. *In vivo*, endothelial sensing of increases in shear stress, the frictional force exerted by flow of blood across the cell surface, plays an important role in regulating tissue perfusion by limiting vasoconstriction[198–201]. Measurement of acute responses to increases in shear stress is the most widely used method to test endothelial function in clinical studies[419] and attenuation of shear stress-induced dilation is associated with the early stages of cardiovascular diseases[419,420]. However, despite its obvious physiological importance, the mechanisms underlying shear stress-induced increases in arterial diameter and thus, blood flow are still a topic of debate.

Studies of cultured endothelial cells and isolated arteries have shown that acute increases in shear stress cause a rise in the intracellular Ca^{2+} concentration in endothelial cells leading to both release of NO and membrane hyperpolarization mediated by opening of SK_{Ca} channels[206,318,421–424]. Data from *in vivo* and clinical studies have demonstrated an important role for NO in acute responses to increases in shear stress[425,426] and also support the contribution of endothelial hyperpolarization[427–431]. However, whether release of NO and activation of SK_{Ca} channels are distinct pathways for shear stress-induced modulation of arterial diameter, or two facets of the same mechanism is still unclear.

As described in **Chapter 1**, SK_{Ca} channels are located on the luminal membrane of endothelial cells in rat mesenteric arteries[118,122,125,130] , porcine coronary arteries[122], mouse and bovine coronary endothelial cells[132,133] and human microvascular endothelial cells[132,133], an ideal

location for activation by localized increases in Ca^{2+} elicited by enhanced shear stress[118,122,130]. The subsequent hyperpolarization of the endothelial membrane potential then spreads to the surrounding smooth muscle cells via MEGJs to limit vasoconstriction[80,84,85,100,116–131,148–151,197,202]. The identity of the endothelial mechanosensor activated by increases in shear stress has yet to be defined but recent evidence supports a role for the mechanosensitive TRPV4 channels in mediating shear stress-induced Ca^{2+} entry to endothelial cells in isolated arteries[132,133,220,241–248,432,433]. TRPV4 channels co-localize with both SK_{Ca} channels and endothelial NOS to caveolae on the luminal surface of human microvascular and bovine coronary endothelial cells[132,133]. Additionally, acute exposure of bovine coronary endothelial cells to shear stress resulted in the activation of both SK_{Ca} and TRPV4 channels and increased NO production supporting a potential link between SK_{Ca} channel activity and NO[133]. In rat carotid arteries and gracilis muscle arterioles, shear stress-mediated vasodilation was blocked by TRPV4 channel inhibition[241]. Thus, these findings support a functional relationship between SK_{Ca} channels, TRPV4 channels and NO.

A link between endothelial K_{Ca} channel activity and NO production is also supported by previous work from our lab and others. In cultured endothelial cells, NO production is regulated by K_{Ca} channel-mediated changes in membrane potential[131] and in rat basilar arteries and cultured endothelial cells, agonist-evoked endothelium-dependent relaxations mediated by NO are inhibited by K_{Ca} channel blockers[203,418]. However, the possibility of a link between NO and SK_{Ca} channel activity in endothelial responses to shear stress has not been investigated.

In vivo, sympathetic nerve activity is the primary regulator of resistance artery diameter, and therefore, peripheral vascular resistance[434,435], with the endothelium playing a key role in limiting the vasoconstriction caused by neurotransmitters released from perivascular sympathetic nerves. However, the majority of studies examining the contribution of NO and SK_{Ca} channels to

endothelium-dependent modulation of arterial diameter have focused on their role in vasorelaxation, i.e. the ability of endothelial stimuli to reverse agonist-induced tone rather than modulation of vasoconstriction. Thus, given the importance of both the endothelial response to shear stress and sympathetic nerve activity in controlling arterial diameter, blood flow and blood pressure, the goal of the experiments described in this chapter was to explore the functional link between NO and SK_{Ca} channel activity in shear stress-induced modulation of sympathetic vasoconstriction and to test the hypothesis that *activation of SK_{Ca} channels will enhance NO-mediated inhibition of sympathetic vasoconstriction evoked by increases in shear stress.*

To test this hypothesis I have used the rat mesenteric bed perfused at a constant luminal flow so vasoconstriction leads to increases in shear stress; decreases in arterial diameter augment shear stress because of its inverse relationship to the third power of the internal vessel diameter[436]. Under these experimental conditions, stimulation of sympathetic perivascular nerves leads to vasoconstriction (recorded as increases in perfusion pressure) that is limited by stimulation of the endothelium by acute increases in shear stress. Pharmacological tools were applied to investigate the contribution of NO and endothelial K_{Ca} channels to shear stress-induced modulation of sympathetic vasoconstriction and CyPPA, a small molecule activator of SK_{Ca} channels that enhances the channels sensitivity to Ca^{2+} [313,437], was used to examine if increased activation of SK_{Ca} channels could enhance the NO-mediated component of the response to shear stress.

2.2: Methods and materials

See **Appendix: Drugs and chemicals** for a list of the drugs and chemicals used.

2.2.1: Perfused mesenteric vascular bed

The mesenteric bed was perfused via the superior mesenteric artery as previously described[438]. Briefly, the mesenteric vascular bed was separated from the intestine and the superior

mesenteric artery cleaned of connective tissue, cannulated with a blunted hypodermic needle (20 G), secured with 5-0 surgical silk (Ethicon) and flushed with Krebs buffer to remove blood. In some experiments the endothelium was removed by flushing the bed with 0.5% Triton X-100 in water for 30 seconds followed by rapid washout with Krebs. The vascular bed was placed on a wire mesh in a warm chamber and perfused with oxygenated Krebs buffer at a constant flow rate of 5 mlmin^{-1} (37°C, bubbled with 95% O_2/5% CO_2). Changes in perfusion pressure were monitored via an in-line pressure transducer (AD instruments, Colorado) and recorded via a PowerLab data acquisition system using Chart 5.0 software (AD Instruments, Colorado). In experiments conducted with endothelium-denuded preparations, endothelial function was assessed as the response to acetylcholine (1 µM) following vasoconstriction with methoxamine (1 µM); tissues in which acetylcholine failed to evoke a response were deemed to be endothelium-denuded.

2.2.1.1: Responses to stimulation of perivascular nerves. Electrodes were attached to the cannulating needle and to the wire mesh to allow electrical field stimulation using a Grass SD9 stimulator (Grass Technologies, USA). Following an equilibration period of 30 minutes, a single stimulation (30 Hz, 90 V, pulse width 1 millisecond, 30 seconds) was applied to assess the viability of the preparation. After a further 10 minutes, a frequency-response curve was constructed by stimulating the preparation at 1-40 Hz (90 V, pulse width 1 millisecond, 30 seconds) at 10 minute intervals[188]. The effects of agents on nerve-evoked vasoconstriction were assessed by perfusing the drugs through the lumen of the preparation for 20 minutes prior to constructing a second frequency-response curve. In some experiments a third frequency-response curve was constructed following washout.

Nerve-evoked responses recorded in the perfused mesenteric vascular bed are shown as normalized values. Changes in perfusion pressure were normalized to the maximum control

response (%) as is convention in these types of experiments. For all frequency response curves, electrical stimulation caused frequency-dependent increases in perfusion pressure ($p<0.05$).

2.2.2: Wire myography

Third order mesenteric arteries were cleaned of adhering tissue and cut into segments (~2 mm in length). Arterial segments were mounted between two gold-plated tungsten wires (20 µm diameter) in a Mulvany-Halpern myograph (model 400A, J.P. Trading, Denmark) as previously described[438]. Changes in isometric tension were recorded via a PowerLab using Chart 5.0 or 8.0 software (AD Instruments, Colorado, USA). Tissues were maintained in Krebs' buffer gassed with 95% O_2/5% CO_2 at 37°C (pH 7.4) and set to a pre-determined optimal resting tension of 5 mN for mesenteric arteries (this was previously determined from active length-tension curves). In some experiments, the endothelium was removed by flushing of the mesenteric bed with 0.5% Triton X-100 (20 µl of Triton X-100 in 40 ml water) for 30 seconds followed by rapid washout with Krebs. After an equilibration period of 30 minutes, endothelial function was assessed as % relaxation to acetylcholine (3 µM) following pre-stimulation with phenylephrine (3 µM; 75% of maximal tone). Arteries in which acetylcholine induced >90% reversal of agonist-induced tone were designated as endothelium-intact and tissues in which the response to acetylcholine was <10% were deemed to be endothelium-denuded. Arteries in which the % reversal of agonist-induced tone elicited by acetylcholine fell between these values were discarded.

2.2.2.1: Concentration-response curves.
Cumulative concentration-response curves to CyPPA (0.001-30 µM) were constructed in arteries in which tone was raised with phenylephrine (3 µM). For all CyPPA concentration-response curves, CyPPA caused relaxation in a concentration-dependent manner ($p<0.05$). In endothelium-intact arterial segments, concentration-response curves to CyPPA were constructed in the absence and presence of apamin (50 nM) or L-NAME

(100 μM). Cumulative concentration-response curves to CyPPA (0.001-30 μM) were also constructed in endothelium-denuded mesenteric arteries. In all experiments, the level of phenylephrine -induced tone was matched in the absence and presence of inhibitors and relaxations to CyPPA were expressed as % relaxation as is the convention in this type of experiment.

Cumulative concentration-response curves to phenylephrine (0.001-100 μM) were constructed in the absence and presence of CyPPA (5 μM) without and with apamin (50 nM) or L-NAME (100 μM) in endothelium -intact and -denuded isolated mesenteric arteries. Results were expressed as % maximal response as is convention for this type of experiment. Phenylephrine increased tone in a concentration-dependent manner ($p<0.05$).

2.2.3: Analysis of noradrenaline levels in perfusate from the mesenteric vascular bed

The mesenteric vascular bed was placed on a wire mesh and placed in a plastic dish on a hot plate (Model HP-A1915B-13, Thermolyne) and maintained at 37°C. The flow rate was 2 mlmin^{-1} and the mesenteric bed was stimulated at 30 Hz for 60 seconds. Perfusate was collected for 60 seconds prior to the stimulation and during the stimulation. Samples were immediately frozen in liquid nitrogen and stored at -80°C prior to analysis by Ultra-performance liquid chromatography (UPLC).

2.2.3.1: Measurement of noradrenaline outflow from the perfused mesenteric bed by UPLC. Noradrenaline levels in perfusate samples were analyzed using a Waters Acquity UPLC System (H Class) consisting of a binary solvent manager, sample manager, column manager and fluorescence detector. Pre-column derivatization of samples with benzylamine and 1,2-diphenylethyleendiamine was conducted[439]. Separation of noradrenaline was achieved by gradient elution using a mixture of acetonitrile and 15 mM acetate buffer (pH 4.5) containing 1 mM octanesulfonic acid (sodium salt) on a Waters Acquity UPLC BEH Shield reversed phase column

(C18, 2.1 mm ID 100 mm, 1.7 μm). The column temperature was 60°C, flow rate 0.7 ml/min and the run time was 8 minutes. Excitation and emission wavelength were set at 345 and 480 nm, respectively. All data was acquired and analyzed by means of Waters Empower 3 software. Noradrenaline and acetonitrile were purchased from Sigma-Aldrich. All chemicals and solvents were of analytical grade. All solutions were prepared in ultrapure milliQ water (Millipore MilliQm Germany) and filtered over a 0.22 μm filter (Millipore, Bedford, USA). A standard curve for noradrenaline was obtained each day prior to collection and injection of samples. Analysis was done with the operator blinded to sample identity. The lowest detectable level of noradrenaline was 4 fmol/50 μl sample. The concentration of noradrenaline in the perfusate samples are shown as normalized values due to variation in control values for noradrenaline overflow between different preparations.

2.2.4: Statistics

All data are expressed as mean ± SEM, *n* rats used. For repeated measures, two-way ANOVA followed by either a Tukey's multiple comparison post-hoc test (used when there were more than two experimental groups) or Šídák method post-hoc test (used when there was two experimental groups) was performed. A paired *t*-test was used in **Figure 2.10b**. $p<0.05$ was considered statistically significant in all cases.

2.3: Results

2.3.1: Characterization of nerve-evoked vasoconstriction in the rat perfused mesenteric vascular bed

As shown in the representative trace in **Figure 2.1a**, stimulation of perivascular nerves evoked frequency-dependent increases in perfusion pressure in the endothelium-intact perfused mesenteric vascular bed. The mean maximal increase in perfusion pressure at a frequency of 30 Hz in endothelium-intact mesenteric beds was 97.8 ± 16.2 mmHg (n=4). Three repeated

frequency-response curves could be constructed at 30 minute intervals without a significant change in amplitude of responses and sensitivity ($p>0.05$; **Figure 2.1b**).

Tetrodotoxin (0.5 µM), a voltage-gated sodium channel inhibitor, abolished responses to electrical stimulation, confirming that the frequency-dependent changes in perfusion pressure are due to the release of neurotransmitters from nerves and not caused by direct electrical stimulation of muscle cells (n=4). In the presence of prazosin (0.1 µM), an α_1-adrenoreceptor antagonist, nerve-evoked vasoconstriction was significantly inhibited ($p<0.05$, **Figure 2.1c**). Thus, under my experimental conditions, nerve-evoked responses in the mesenteric bed can be largely accounted for by noradrenaline acting on α_1-adrenoceptors.
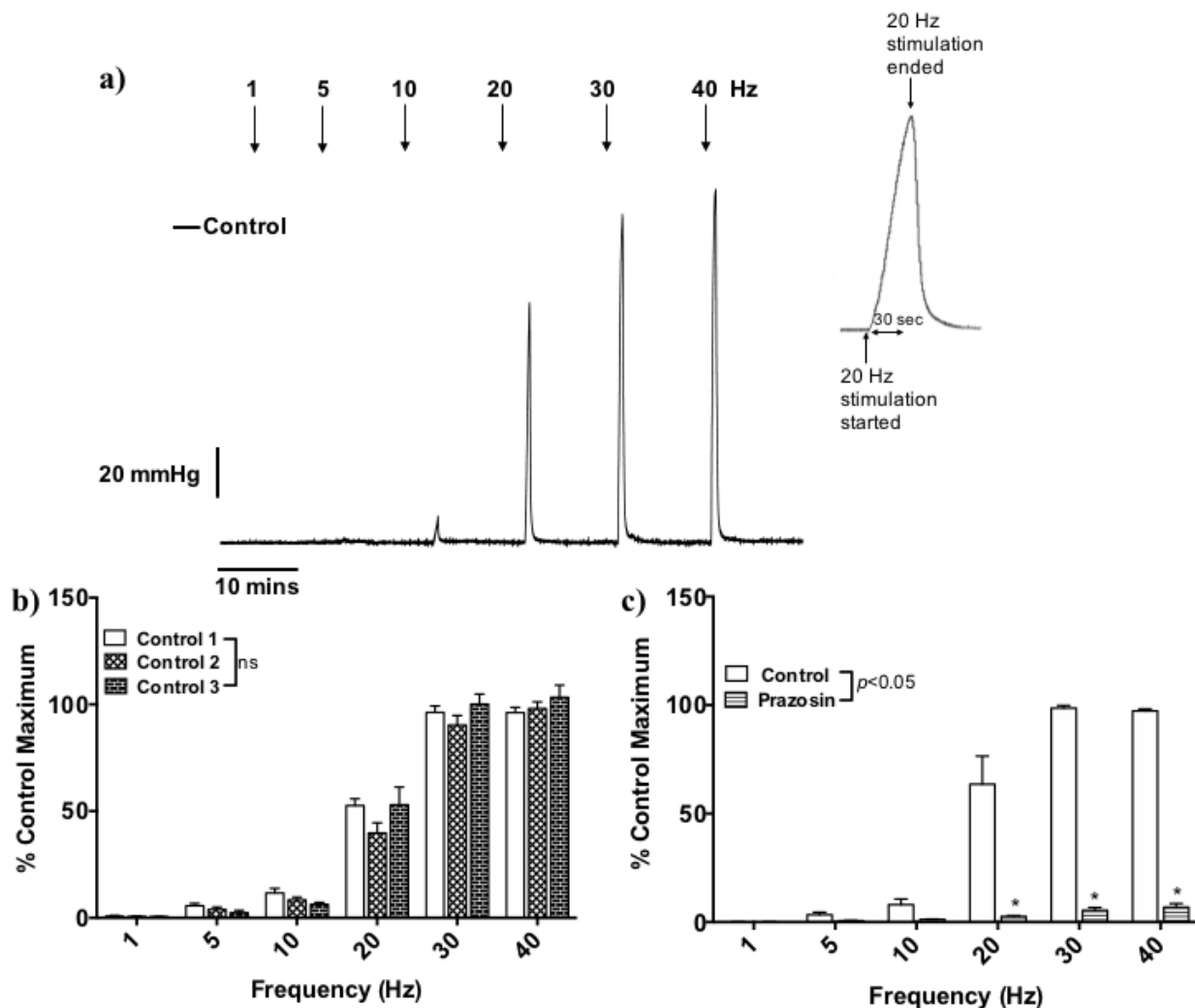
Figure 2.1: **Vasoconstriction elicited by stimulation of perivascular nerves is frequency-dependent, time-independent and mediated by the release of noradrenaline from perivascular nerves. a)** Representative trace of a frequency-response relationship obtained from an endothelium-intact perfused mesenteric bed perfused at a constant flow rate. Mean frequency-response relationships in endothelium-intact perfused mesenteric beds **b)** time controls, values are presented as mean ± SEM, n=6; two-way repeated-measures ANOVA, and **c)** in the absence and presence of prazosin (0.1 μM), values are presented as mean ± SEM, n=4. * denotes $p<0.05$ from control; two-way repeated-measures ANOVA.

Both voltage-dependent and -independent mechanisms can mediate contraction of vascular smooth muscle. Perivascular nerves in rat mesenteric arteries do not express L-type VOCCs but rather express N-, P- and Q-type VOCCs[440]. Therefore, the contribution of voltage-dependent influx of Ca^{2+} through L-type VOCCs to nerve-evoked vasoconstriction in the perfused mesenteric

vascular bed was investigated using the selective inhibitor nifedipine. Nifedipine limited nerve-evoked vasoconstriction in a concentration-dependent manner in endothelium-intact perfused mesenteric beds ($p<0.05$, **Figure 2.2a**); the effect of 10 μM nifedipine was significantly different from that of 1 μM nifedipine at frequencies from 20 through 40 Hz ($p<0.05$, **Figure 2.2a**). In endothelium-denuded mesenteric beds, nifedipine (10 μM) also significantly reduced nerve-evoked vasoconstriction ($p<0.05$; **Figure 2.2b**). Thus, both voltage -dependent and -independent mechanisms appear to contribute to nerve-evoked responses in the rat mesenteric bed, and in line with the lack of evidence for VOCC on endothelial cells in the published literature, the effect of nifedipine is endothelium-independent.
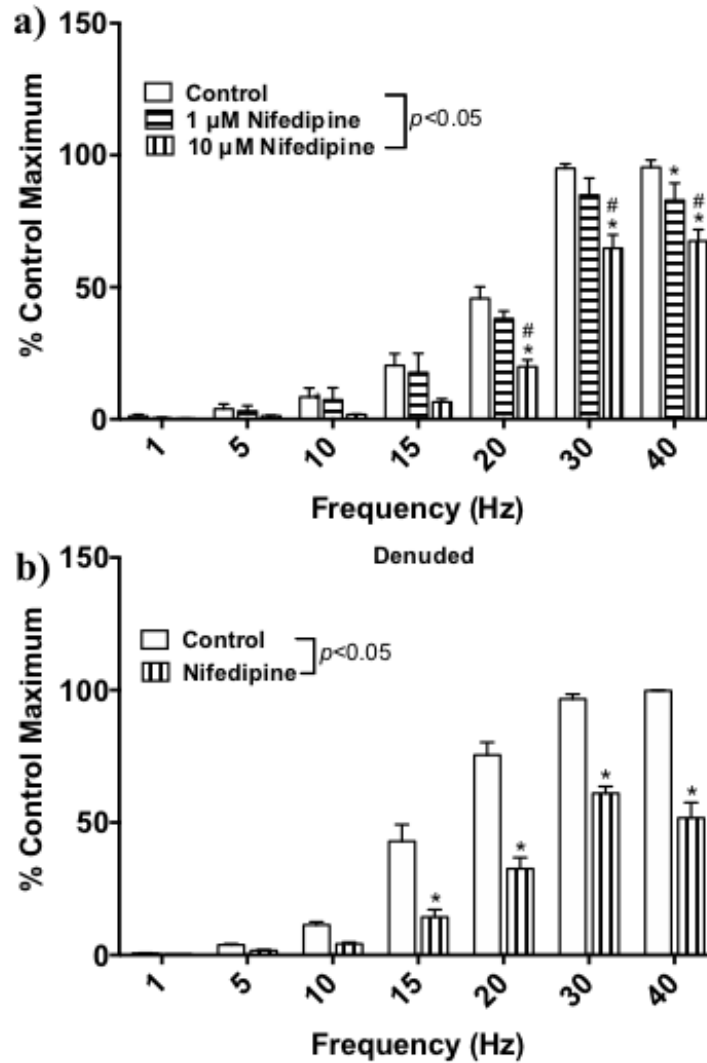
Figure 2.2: Nerve-evoked vasoconstriction is partially dependent on L-type VOCCs. a) Mean frequency-response relationships obtained from endothelium-intact perfused mesenteric beds in the absence and presence of nifedipine (1 and 10 μM). Values are presented as mean ± SEM, n=4-10. * denotes $p<0.05$ from control and # denotes $p<0.05$ from nifedipine (1 μM); two-way repeated-measures ANOVA. **b)** Mean frequency-response relationships obtained from endothelium-denuded perfused mesenteric beds in the absence and presence of nifedipine (10 μM). Values are presented as mean ± SEM, n=4. * denotes $p<0.05$ from control; two-way repeated-measures ANOVA.

2.3.2: Modulation of nerve-evoked vasoconstriction by increases in shear stress in the rat perfused mesenteric bed

Both NO and endothelial SK_{Ca} channels have been suggested to mediate the effects of shear stress on arterial diameter. Thus, I investigated the contribution of these effectors to shear-stress-induced, endothelium-dependent modulation of sympathetic vasoconstriction in the perfused rat mesenteric bed.

The role of NO in modulating nerve-evoked vasoconstriction was investigated by perfusing preparations with L-NAME, a selective inhibitor of NOS. L-NAME (100 μM) significantly enhanced nerve-evoked vasoconstriction at stimulation frequencies from 20 to 40 Hz ($p<0.05$, **Figure 2.3a**). Additionally, 1H-[1,2,4]oxadiazolo[4,3-a]quinoxalin-1-one (ODQ; 10 μM)), an inhibitor of guanylyl cyclase, the downstream target of NO, significantly enhanced nerve-evoked vasoconstriction ($p<0.05$) at stimulation frequencies from 15 to 40 Hz ($p<0.05$, **Figure 2.3c**).

Removal of the endothelium did not alter the frequency-response relationship (**Figure 2.3d**) or the magnitude of responses evoked by stimulation of perivascular nerves; the mean response ± SEM to a stimulation of 30 Hz in endothelium-intact and denuded arteries was 97.8 ± 16.2 and 99.6 ± 8.7 mmHg (n=4; $p>0.05$), respectively. L-NAME was without effect in endothelium-denuded mesenteric beds ($p>0.05$, **Figure 2.3d**), indicating its actions in potentiating nerve-evoked vasoconstriction were most likely due to inhibition of endothelial NOS rather than neuronal NOS.
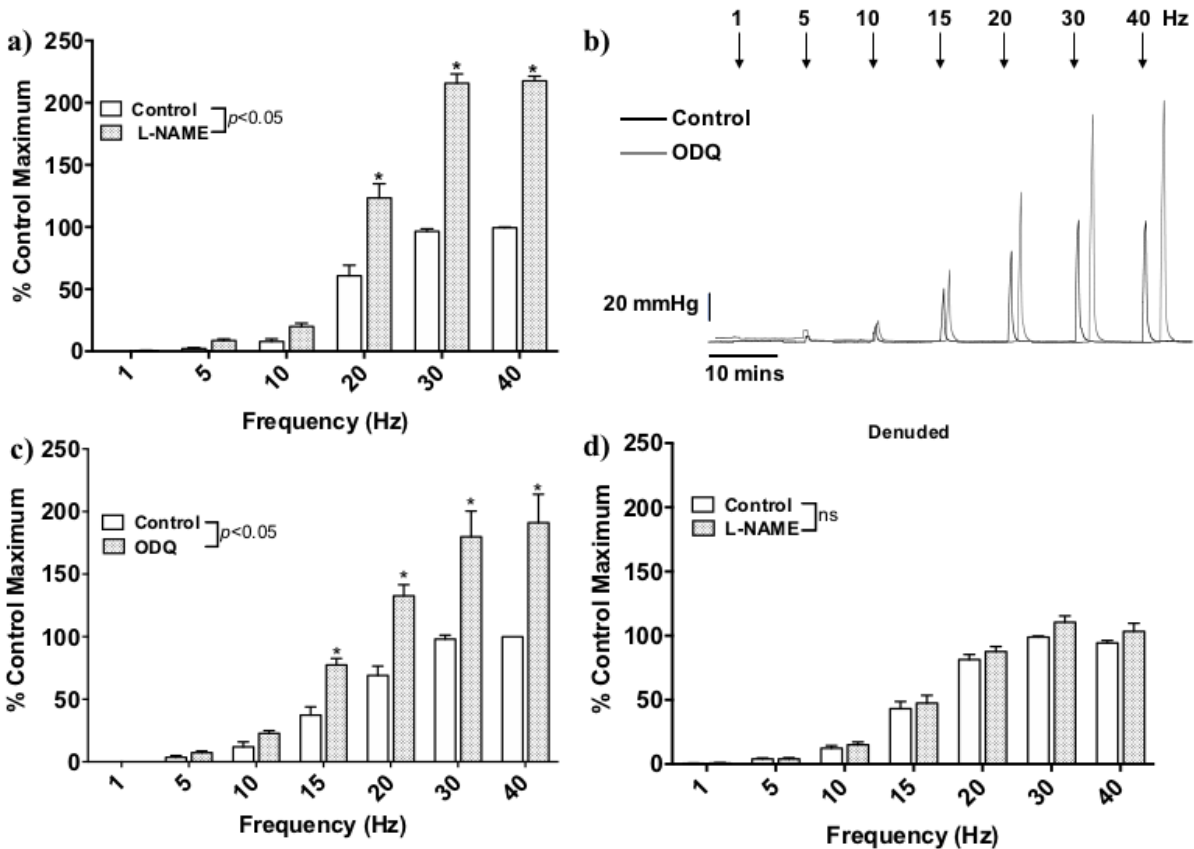
Figure 2.3: Nerve-evoked vasoconstriction is modulated by the release of NO from the endothelium. a) Mean frequency-response relationships obtained from endothelium-intact perfused mesenteric beds in the absence and presence of L-NAME (100 μM). Values are presented as mean ± SEM, n=4. * denotes $p<0.05$ from control; two-way repeated-measures ANOVA. **b)** Representative trace showing a frequency-response relationship obtained from an endothelium-intact perfused mesenteric bed in the absence and presence of ODQ (10 μM). **c)** Mean frequency-response relationships obtained from endothelium-intact perfused mesenteric beds in the absence and presence of ODQ (10 μM). Values are presented as mean ± SEM, n=4. * denotes $p<0.05$ from control; two-way repeated-measures ANOVA. **d)** Mean frequency-response relationships obtained from endothelium-denuded perfused mesenteric beds in the absence and presence of L-NAME (100 μM). Values are presented as mean ± SEM, n=6; two-way repeated-measures ANOVA.

The functional role of SK_{Ca} channels in endothelium-dependent modulation of nerve-evoked vasoconstriction in the perfused mesenteric vascular bed was investigated using apamin, a selective inhibitor of SK_{Ca} channels. In endothelium-intact mesenteric beds, apamin (50 nM) significantly enhanced nerve-evoked vasoconstriction ($p<0.05$) at frequencies from 10 to 40 Hz ($p<0.05$, **Figure 2.4b)**, but was without effect in endothelium-denuded tissues ($p>0.05$, **Figure 2.4c**). In contrast, inhibition of endothelial IK_{Ca} channels with NS 6180 (1 μM) was without effect on nerve-evoked responses (p>0.05; **Figure 2.4d**). Furthermore, the effect of apamin was not additive with that of L-NAME (100 μM), suggesting a link between SK_{Ca} channels and endothelium-derived NO (**Figure 2.5**). Thus, while SK_{Ca} channels play a significant role in limiting nerve-evoked vasoconstriction in the mesenteric bed, IK_{Ca} channels do not. This difference in their functional importance is likely due to their differing locations within the endothelium, as SK_{Ca} channels are located on the endothelial luminal membrane[118,122,125,130,132,133] while IK_{Ca} channels are located within the MEGJs[118,125,130,151,197].
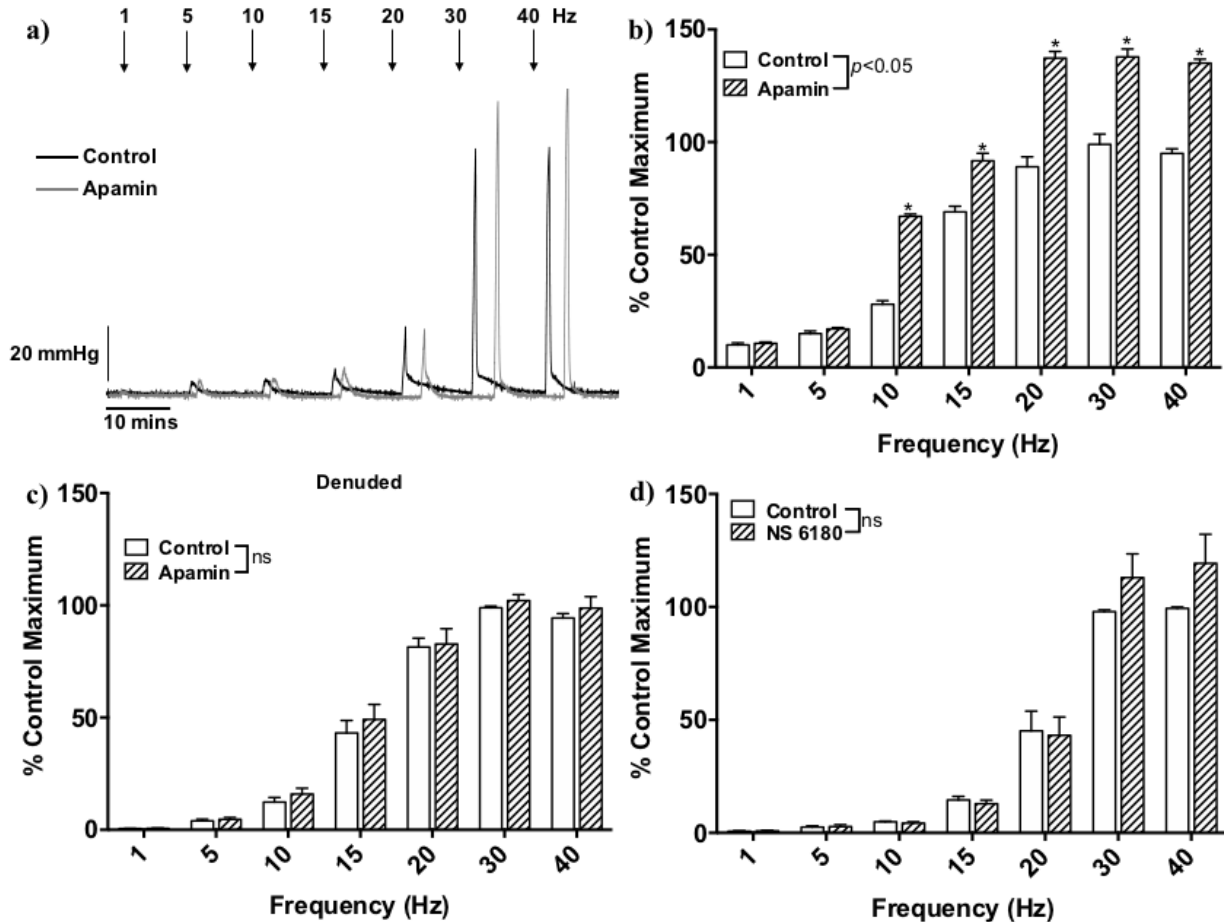
Figure 2.4: Inhibition of SK$_{Ca}$ channels potentiates nerve-evoked vasoconstriction in the endothelium-intact perfused mesenteric bed. a) Representative trace showing a frequency-response relationship obtained from an endothelium-intact perfused mesenteric bed in the absence and presence of apamin (50 nM). **b)** Mean frequency-response relationships obtained from endothelium-intact perfused mesenteric beds in the absence and presence of apamin (50 nM). Values are presented as mean ± SEM, n=4. * denotes $p<0.05$ from control; two-way repeated-measures ANOVA. **c)** Mean frequency-response relationships obtained from endothelium-denuded perfused mesenteric beds in the absence and presence of apamin (50 nM). Values are presented as mean ± SEM, n=6; two-way repeated-measures ANOVA. **d)** Mean frequency-response relationships obtained from endothelium-intact perfused mesenteric beds in the absence and presence of NS 6180 (1 μM). Values are presented as mean ± SEM, n=5; two-way repeated-measures ANOVA.

50

Figure 2.5: Inhibition of SK_Ca channels and NOS potentiates nerve-evoked vasoconstriction in a non-additive manner in the endothelium-intact perfused mesenteric bed. Mean frequency-response relationships obtained from endothelium-intact perfused mesenteric beds in the absence and presence of apamin (50 nM), L-NAME (100 μM) and apamin (50 nM) with L-NAME (100 μM). Values are presented as mean ± SEM, n=5. * denotes $p<0.05$ from control and # denotes $p<0.05$ from apamin (50 nM) and ^ denotes $p<0.05$ from L-NAME (100 μM); two-way repeated-measures ANOVA.

As shown above (**Figure 2.2**), both voltage -dependent and -independent mechanisms underlie nerve-evoked vasoconstriction in the perfused mesenteric bed. Opening of endothelial K_{Ca} channels leads to hyperpolarization of the membrane potential which spreads to surrounding smooth muscle cells to reduce influx of Ca^{2+} through VOCCs and so is more effective in reversing depolarization-mediated smooth muscle contraction than contraction elicited via voltage-independent mechanisms (i.e. release of Ca^{2+} from intracellular stores and Ca^{2+} sensitization). In contrast, NO can inhibit smooth muscle contractility through both voltage -dependent (e.g. activation of BK_{Ca} channels to hyperpolarize the membrane potential to reduce Ca^{2+} influx though VOCCs[55–59,79,290,291,164–168]) and -independent signaling pathways (e.g. phospholamban phosphorylation and phospholipase C[166,251,289,441,442]). Thus, in the next set of experiments L-NAME was applied in combination with nifedipine. The rationale for these experiments was that in the presence of nifedipine, the remaining nerve-evoked vasoconstriction occurs independently of L-type VOCC activity thus, hyperpolarization would not be expected to be an effective inhibitory mechanism. As shown above, L-NAME (100 µM) significantly potentiated nerve-evoked vasoconstriction in endothelium-intact mesenteric beds ($p<0.05$, **Figure 2.3a**) and was also able to do so in the presence of nifedipine (10 µM; $p<0.05$; **Figure 2.6**). However, the size of responses in the presence of L-NAME and nifedipine was significantly less than with L-NAME alone ($p<0.05$) indicating that endothelium-derived NO limit both the voltage -dependent and -independent components of nerve-evoked vasoconstriction.
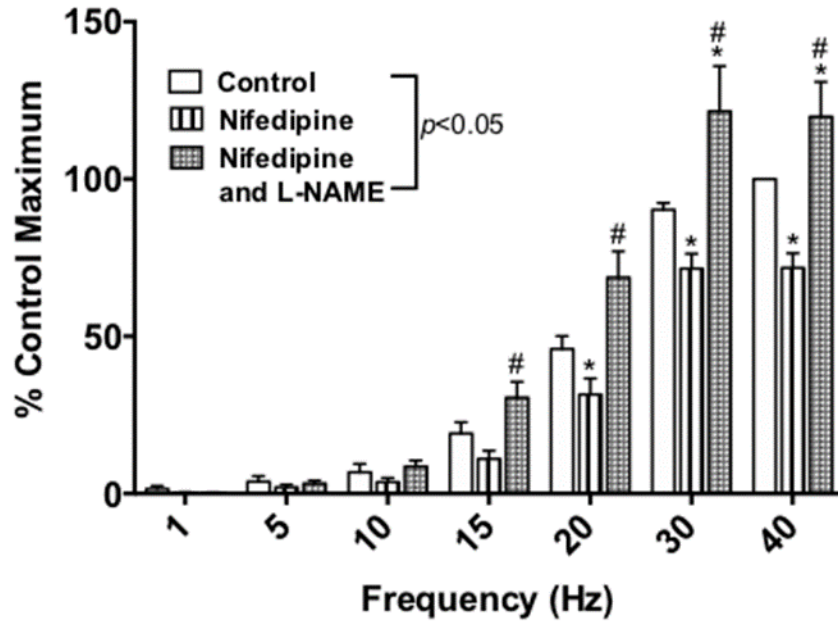
Figure 2.6: **Block of NO signaling is able to enhance the nifedipine-insensitive component of nerve-evoked vasoconstriction.** Mean frequency-response relationships obtained from endothelium-intact perfused mesenteric beds in the absence and presence of nifedipine (10 µM) without and with L-NAME (100 µM). Values are presented as mean ± SEM, n=4. * denotes $p<0.05$ from control and # denotes $p<0.05$ from nifedipine (10 µM); two-way repeated-measures ANOVA.

2.3.3: Effect of CyPPA on phenylephrine-induced tone in isolated mesenteric arteries mounted in a wire myograph

The effects of the SK_{Ca} channel activator CyPPA on vascular tone in rat mesenteric arteries have not previously been reported. Therefore, before examining its ability to enhance shear stress-mediated inhibition of nerve-evoked vasoconstriction in the perfused bed, I characterized the effects of CyPPA on agonist-evoked increases in tone in arteries mounted under isometric conditions in a wire myograph. In these experiments, phenylephrine was used to induce tone as it is a selective α_1-adrenoceptor agonist whereas noradrenaline can act at multiple adrenoceptors.

Concentration-relaxation curves to CyPPA (0.001-30 μM) were constructed in endothelium -intact and -denuded arterial segments in which tone was raised with phenylephrine (3 μM). In endothelium-intact arterial segments, CyPPA-evoked relaxations were significantly reduced by the presence of apamin (50 nM) or L-NAME (100 μM; $p<0.05$, **Figure 2.7**). In endothelium-denuded arteries, responses to CyPPA were significantly reduced compared to endothelium-intact tissues such that relaxation was only observed at the highest concentration of 30 μM ($p<0.05$, **Figure 2.7**). Thus, CyPPA-evoked relaxation of phenylephrine-induced tone is endothelium-dependent and reliant on both SK_{Ca} channel activation and NO.
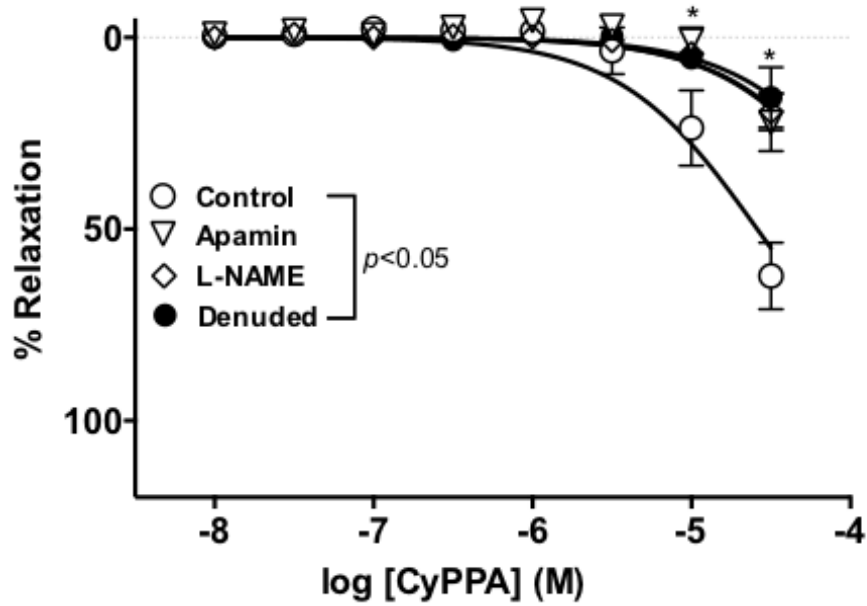
Figure 2.7: CyPPA-mediates endothelium-dependent relaxation through SK$_{Ca}$ channel activation and NO. Third order mesenteric arteries were mounted in a wire myograph. Mean data showing CyPPA-induced relaxation in endothelium-intact isolated rat mesenteric artery segments mounted in a wire myograph in the absence (control n=9) and presence of apamin (50 nM; n=9) or L-NAME (100 μM; n=9) and in endothelium-denuded (n=4) isolated rat mesenteric artery segments. Values are presented as mean ± SEM. * denotes $p<0.05$ from control; two-way repeated-measures ANOVA.

The effect of CyPPA (5 µM) on phenylephrine-evoked increases in tone was then examined in arteries mounted in a wire myograph. This concentration of CyPPA was selected as it evoked relaxation which was endothelium-dependent and sensitive to apamin, the inhibitor of SK_{Ca} channels. Concentration-response curves to phenylephrine (phenylephrine denoted as PE in **Figure 2.8a and b**; 0.001- 100 µM) were constructed in the absence and presence of CyPPA. In endothelium-intact arteries, CyPPA did not affect resting tone but significantly reduced increases in tone elicited by phenylephrine at concentration of 1-10 µM ($p<0.05$; **Figure 2.8a**) causing a rightward shift in the concentration-response curve. This effect was blocked by apamin (50 nM) or L-NAME (100 µM) (**Figure 2.8a**). In contrast, in endothelium-denuded arteries, CyPPA did not significantly affect phenylephrine-induced increases in tone ($p>0.05$; **Figure 2.8b**).
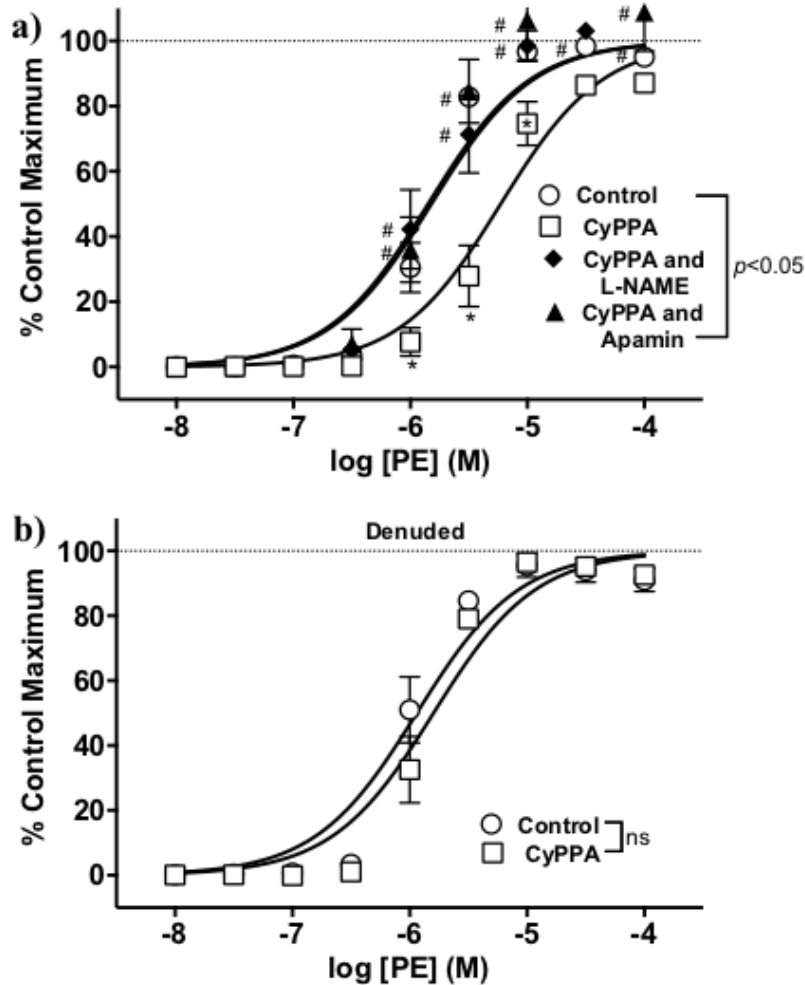
Figure 2.8: CyPPA limits phenylephrine-induced increases in tone in an endothelium-dependent manner. Third order mesenteric arteries were mounted in a wire myograph. **a)** Mean data showing phenylephrine-induced increases in tone in the absence (control n=14) and presence of CyPPA (5 μM; n=14) in endothelium-intact without and with L-NAME (100 μM; n=4) or apamin (50 nM; n=4). * denotes $p<0.05$ from control and # denotes $p<0.05$ from CyPPA (5 μM); two-way repeated-measures ANOVA. **b)** Mean data showing phenylephrine-induced increases in tone in the absence and presence of CyPPA (5 μM) in endothelium-denuded isolated rat mesenteric artery segments. Values are presented as mean ± SEM, n=5; two-way repeated-measures ANOVA.

2.3.4: CyPPA enhances shear stress-induced modulation of nerve-evoked vasoconstriction in the rat perfused mesenteric bed

Having demonstrated that SK_{Ca} channels play a key role in shear stress-induced modulation of sympathetic vasoconstriction in the perfused mesenteric bed (**Figure 2.4**), I then examined whether CyPPA can enhance the effects of shear stress on sympathetic vasoconstriction in the perfused mesenteric bed. CyPPA (5 and 10 µM) had no effect on basal perfusion pressure but significantly limited nerve-evoked vasoconstriction in endothelium-intact mesenteric beds in a concentration-dependent manner ($p < 0.05$, **Figure 2.9**). For the remaining experiments I used CyPPA at a concentration of 5 µM as at this concentration, CyPPA had little direct relaxant effect (**Figure 2.7**).

In contrast, in endothelium-denuded mesenteric beds, CyPPA (5 µM) had no significant effect on nerve-evoked vasoconstriction ($p > 0.05$, **Figure 2.10a**). This is in line with functional and histochemical studies demonstrating that SK_{Ca} channels are expressed on endothelial but not smooth muscle cells in mesenteric arteries[125,197]. However, whether SK_{Ca} channels are located on nerves has not been investigated. Rat mesenteric arteries are densely innervated[176,185], with sufficient amounts of noradrenaline released as can be measured as overflow in the perfusate[438] and so the ability of CyPPA to inhibit the release of noradrenaline from perivascular nerves was investigated. Perfusate was collected before and during a 30 Hz stimulation in the absence and presence of CyPPA. Noradrenaline overflow was undetectable in the 60 seconds prior to the 30 Hz stimulation but increased significantly during nerve stimulation, a response which was not altered by CyPPA ($p > 0.05$, **Figure 2.10b**), indicating that reductions in nerve-evoked increases in perfusion pressure caused by this agent are not due to an action on perivascular nerves.
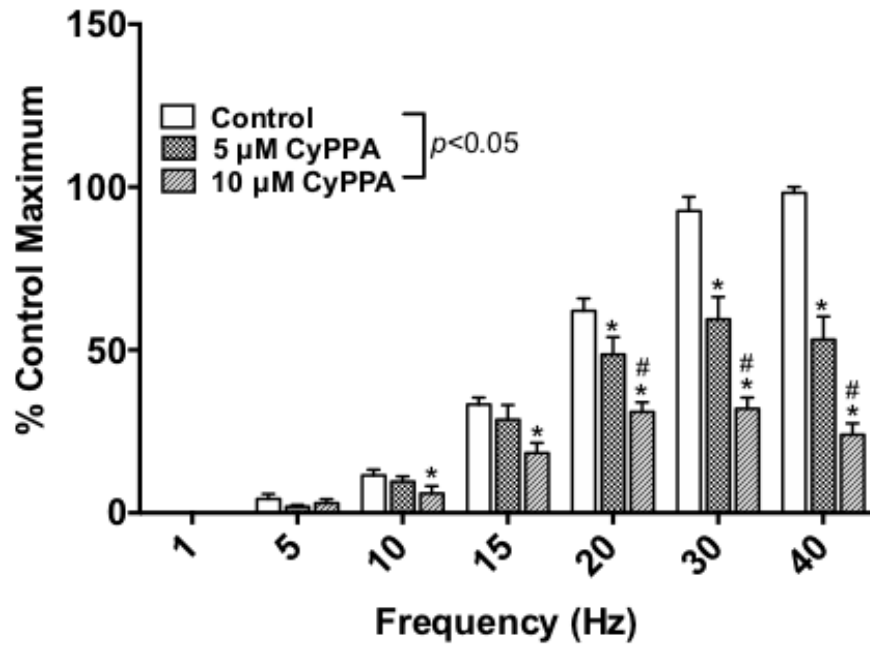
Figure 2.9: CyPPA enhances shear stress-mediated inhibition of nerve-evoked vasoconstriction in the endothelium-intact perfused mesenteric bed. Mean frequency-response relationships obtained from endothelium-intact perfused mesenteric beds in the absence and presence of CyPPA (5 and 10 µM). Values are presented as mean ± SEM, n=4. * denotes $p<0.05$ from control, # denotes $p<0.05$ from 5 µM CyPPA; two-way repeated-measures ANOVA.
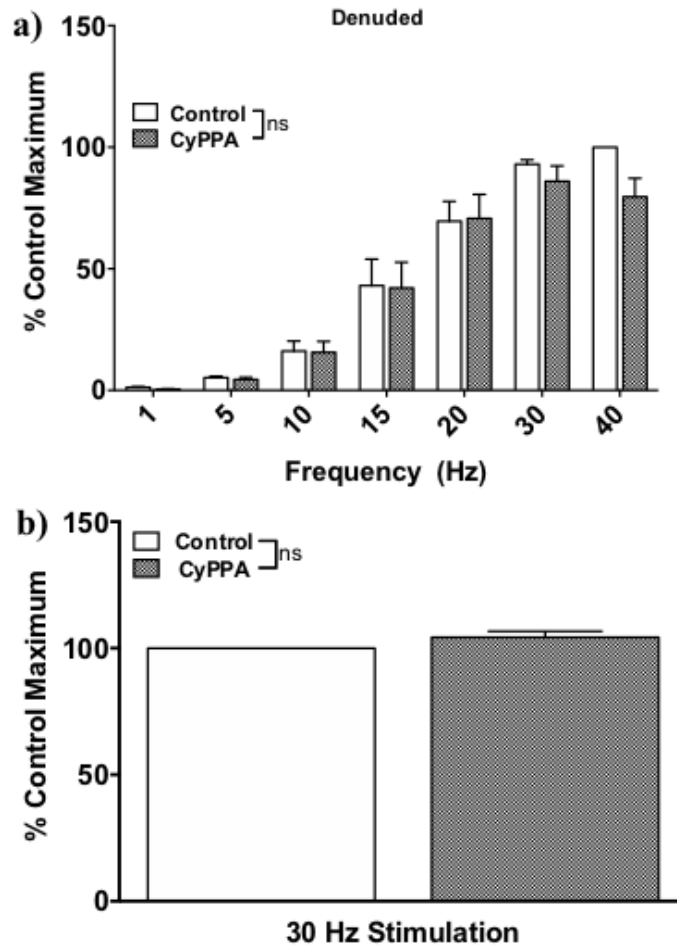
Figure 2.10: CyPPA enhances shear stress-mediated inhibition of nerve-evoked vasoconstriction in an endothelium-dependent manner. a) Mean frequency-response relationships obtained from endothelium-denuded mesenteric beds in the absence and presence of CyPPA (5 µM). Values are presented as mean ± SEM, n=4; two-way repeated measures ANOVA. **b)** Mean data showing release of noradrenaline (as measured by UPLC) in the absence and presence of CyPPA (5 µM) in endothelium-intact perfused mesenteric vascular beds. Values are presented as mean ± SEM, n=4; paired *t*-test.

To confirm the actions of CyPPA were indeed due to activation of SK_{Ca} channels, I used apamin, the selective SK_{Ca} channel inhibitor. Apamin (50 nM) significantly enhanced nerve-evoked vasoconstriction when applied alone (as shown in **Figure 2.4**) and blocked the effect of CyPPA ($p<0.05$, **Figure 2.11**); responses in the presence of apamin alone in comparison to apamin with CyPPA were not significantly different ($p>0.05$, **Figure 2.11**). Therefore, the actions of CyPPA can be attributed to activation of endothelial SK_{Ca} channels.
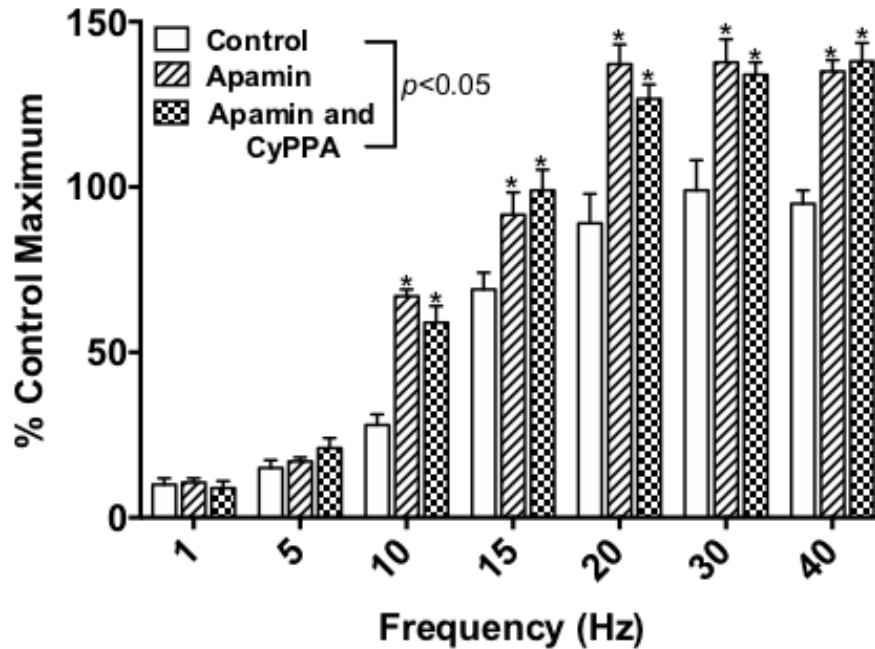
Figure 2.11: CyPPA enhances shear stress mediated inhibition of nerve-evoked vasoconstriction through activation of SK_{Ca} channels. Mean frequency-response relationships obtained from endothelium-intact perfused mesenteric beds in the absence and presence of apamin (50 nM) without and with CyPPA (5 µM). Values are presented as mean ± SEM, n=4. * denotes $p < 0.05$ from control; two-way repeated-measures ANOVA.

The contribution of NO to the actions of CyPPA was investigated using the NOS inhibitor, L-NAME, and the soluble guanylyl cyclase inhibitor, ODQ. L-NAME (100 μM) significantly enhanced nerve-evoked vasoconstriction when applied alone (as shown above **Figure 2.3**) and inhibited the effects of CyPPA ($p<0.05$, **Figure 2.12a**); responses in the presence of L-NAME alone in comparison to L-NAME plus CyPPA were not significantly different ($p>0.05$, **Figure 2.12a**). Similarly, ODQ (10 μM) significantly enhanced nerve-evoked vasoconstrictions at frequencies from 15 to 40 Hz ($p<0.05$, **Figure 2.12b**) and inhibited the effects of CyPPA; responses in the presence of ODQ alone in comparison to ODQ plus CyPPA were not significantly different ($p>0.05$, **Figure 2.12b**). Thus, it appears that the ability of CyPPA to inhibit nerve-evoked vasoconstriction in the perfused mesenteric bed is due to activation of SK_{Ca} channels and is largely dependent on NO.

As described above, smooth muscle hyperpolarization is more effective at reversing increases in tone caused by depolarization, whereas NO is effective against voltage -dependent and -independent smooth muscle contraction[55–59,79,290,291,164–168,251,443]. In my experiments the actions of CyPPA are dependent on both SK_{Ca} channel activity and NO, thus the importance of CyPPA-mediated smooth muscle hyperpolarization to inhibit nerve-evoked vasoconstriction was investigated by conducting experiments in the presence of nifedipine. Nifedipine (10 μM) alone significantly reduced nerve-evoked vasoconstriction (as shown above **Figure 2.2**) and in the presence of nifedipine, CyPPA was able to significantly reduce the nifedipine-independent vasoconstriction ($p<0.05$, **Figure 2.13**) indicating that it can inhibit voltage-independent smooth muscle contraction, an unexpected finding if CyPPA were acting via hyperpolarization alone.
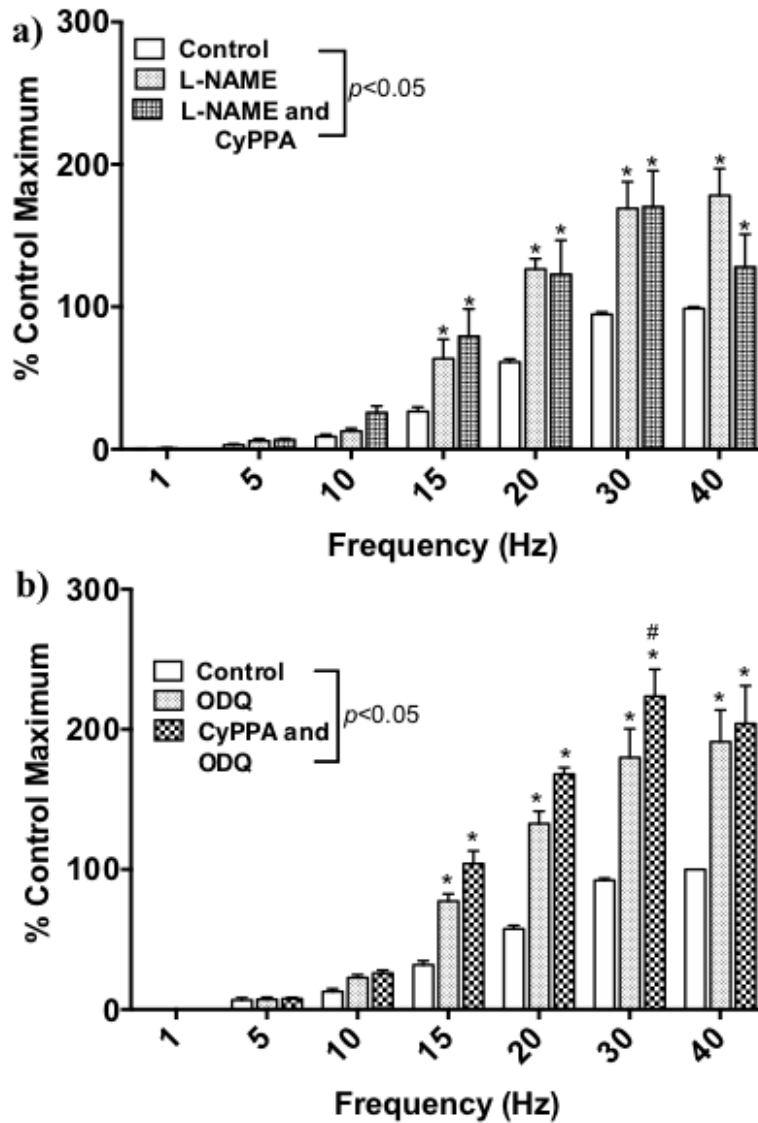
Figure 2.12: The effect of CyPPA on nerve-evoked vasoconstriction is dependent on NO.
a) Mean frequency-response relationships obtained from endothelium-intact perfused mesenteric beds in the absence and presence of L-NAME (100 μM) without and with CyPPA (5 μM). Values are presented as mean ± SEM, n=4. * denotes $p<0.05$ from control; two-way repeated-measures ANOVA. **b)** Mean frequency-response relationships obtained from endothelium-intact perfused mesenteric beds in the absence and presence of ODQ (10 μM) without and with CyPPA (5 μM). Values are presented as mean ± SEM, n=4. * denotes $p<0.05$ from control and # denotes $p<0.05$ from ODQ (10 μM); two-way repeated-measures ANOVA.
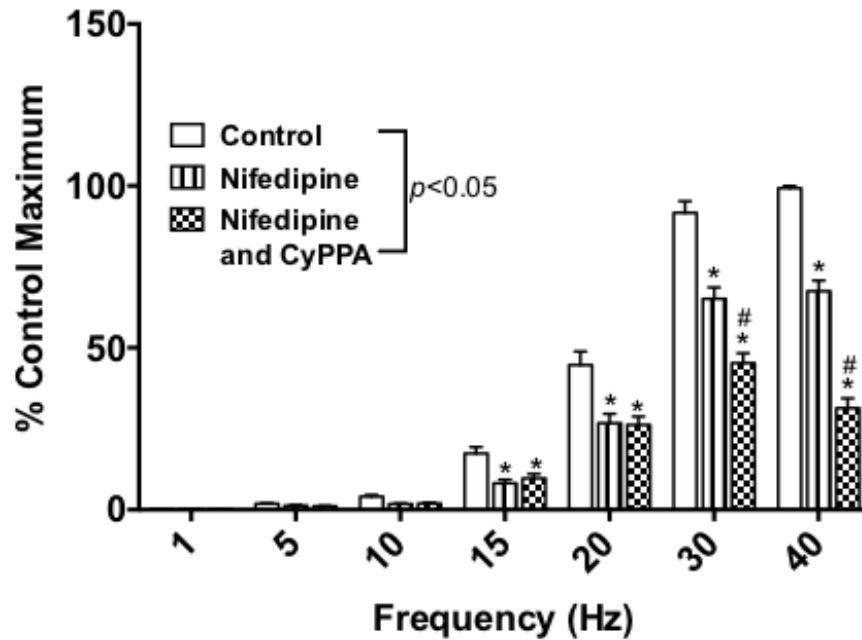
Figure 2.13: **The ability of CyPPA to inhibit nerve-evoked vasoconstriction is partially dependent on L-type VOCCs.** Mean frequency-response relationships obtained from endothelium-intact perfused mesenteric beds in the absence and presence of nifedipine (10 µM) without and with CyPPA (5 µM). Values are presented as mean ± SEM, n=4. * denotes $p<0.05$ from control and # denotes $p<0.05$ from nifedipine (10 µM); two-way repeated-measures ANOVA.

2.4: Discussion

Increases in shear stress stimulate an influx of Ca^{2+} into endothelial cells which leads to the production of NO and hyperpolarization of the endothelial cell membrane potential via opening of SK_{Ca} channels[206,318,421–424]. My data show that in the perfused mesenteric bed, shear stress-induced inhibition of sympathetic vasoconstriction is mediated by both NO and SK_{Ca} channels. Additionally, I found that CyPPA, a small molecule activator of SK_{Ca} channels that increases the channels sensitivity to Ca^{2+} [313,437], can enhance the response to shear stress in this preparation. This enhancement of shear stress-induced vasodilation by CyPPA occurred at a concentration that caused minimal direct vasorelaxation and via a mechanism dependent on endothelium-derived NO. These findings indicate that opening of SK_{Ca} channels in response to acute increases in shear stress may enhance NO bioavailability and support the proposal that activators of these channels may have therapeutic potential in enhancing shear stress-induced NO bioavailability in cardiovascular disease states[420].

In the experiments described in this chapter, the rat mesenteric bed was perfused at a constant luminal flow and the perivascular nerves were stimulated, resulting in vasoconstriction that was recorded as increases in perfusion pressure. Stimulation of the sympathetic nerves leads to the release of noradrenaline and the co-transmitter ATP, which act on arterial α_1-adrenoceptors and P_{2X} receptors, respectively[176–179,181,184–188]. In my experiments, nerve-evoked increases in perfusion pressure were abolished by the α_1-adrenoceptor antagonist prazosin indicating that these responses are mediated by noradrenaline acting on α_1-adrenoceptors with little contribution from ATP. This is in line with previous studies in which the relative importance of ATP as a functional sympathetic neurotransmitter in the rat and porcine mesenteric beds was revealed only when the level of preexisting vascular tone or pressure was increased[187,188]. Furthermore, the removal of the

endothelium had no effect on nerve-evoked vasoconstriction, indicating that both vasoconstrictors and vasodilators released from the endothelium are modulating these responses.

Activation of smooth muscle α_1-adrenoceptors by noradrenaline results in phospholipase C-mediated increases in diacylglycerol and IP_3[249,251–255] and membrane depolarization, which enhances Ca^{2+}-influx through L-type VOCCs[21,51,444]. The relative contribution of these voltage-dependent (VOCC-mediated Ca^{2+} influx) and -independent (mediated by IP_3 and diacylglycerol) mechanisms to α_1-adrenoceptor-mediated contraction has been shown to vary depending on experimental conditions. In isolated hamster skeletal muscle arteries, bath application of the α_1-adrenoceptor agonist phenylephrine (0.1 µM), evoked sustained constrictions largely dependent on Ca^{2+} influx through L-type VOCCs, whereas focal application of a high dose (1 mM) of phenylephrine in the same preparation generated a local constriction that was independent of changes in smooth muscle membrane potential and entirely dependent on IP_3[445]. Additionally, the ability of phenylephrine to cause vasoconstriction in the hind limb vascular bed *in vivo* was reduced by 50% in mice lacking nifedipine-sensitive $Ca_V1.2$ as compared to wild-type mice[444] and nifedipine reduced phenylephrine-mediated vasoconstriction by 35-45% in rat pulmonary arteries mounted in an organ bath[8]. However, these previous studies utilized exogenous α_1-adrenoceptor agonists and the contribution of voltage-dependent and -independent mechanisms to noradrenaline-mediated sympathetic vasoconstriction in resistance arteries has not been widely studied.

In my experiments, inhibition of L-type VOCCs with nifedipine reduced sympathetic vasoconstriction at all frequencies. However, >50% of the response remained, indicating that voltage-independent mechanisms of smooth muscle contraction are a major contributor to nerve-evoked vasoconstriction in the rat mesenteric bed. In perfused preparations of the rabbit isolated

ileocolic, saphenous and ear arteries, constriction induced by sympathetic nerve stimulation (frequencies above 5 Hz) was also found to occur via primarily voltage-independent pathways[446,447] In addition to nifedipine-sensitive L-type VOCCs, nifedipine-insensitive T-type VOCCs have also been identified on vascular smooth muscle cells[48–50,61] but, T-type channels have a small conductance (~8 pS[48]) and show low levels of expression in rat mesenteric artery smooth muscle cells[60].

The physiological significance of nerve-evoked vasoconstriction being mediated by voltage-independent mechanisms is not clear. Depolarization-mediated smooth muscle contraction is limited by opening of smooth muscle voltage-gated K^+ channels and BK_{Ca} channels, both of which hyperpolarize the membrane potential[26–29,76,448,449] to limit contraction, whereas voltage-independent contraction does not engage similar "braking" mechanisms. Therefore, the reliance of nerve-evoked vasoconstriction on voltage-independent mechanisms of constriction may allow for a greater range of response than would be possible if smooth muscle depolarization was the only active mechanism for smooth muscle contraction.

The role of both NO and endothelial K_{Ca} channels in mediating endothelium-dependent vasodilation to agonists, such as acetylcholine, has been well described in many arteries from different species[120,149,195,222,450–452]. However, while the primary stimulus for *in vivo* endothelial modulation of arterial diameter is increases in shear stress the underlying mechanisms of shear stress-induced vasodilation have received less attention. In cultured endothelial cells and isolated arterial segments, acute increases in shear stress lead to both the release of NO and the opening of SK_{Ca} channels[206,318,421–424,453] but there appears to be variation between vessels, species and sex in terms of the relative contribution of NO and hyperpolarization to the response. For example, matching of rat skeletal muscle blood flow to contractile activity depends on the release of NO

from the endothelium of feed arteries in response to elevated shear stress caused by dilation of downstream arterioles[454]. In contrast, in hamster cremaster, and rat and mouse mesenteric arteries, dilation to acute increases in shear stress are mediated by both NO and endothelial hyperpolarization[224,455] and shear stress-induced dilation is impaired in carotid arteries from mice lacking SK3 channels[204]. In rat gracilis muscle arterioles, flow-induced dilation is predominantly NO-dependent and greater in arterioles from female rats in comparison to male rats[456], likely due to estrogen-mediated NO production[285,456].

The extent to which shear stress-induced vasodilation is dependent on NO in humans is controversial[425]. Early clinical investigations ascribed a major role for NO in flow-mediated dilation[457–459] but more recent studies have demonstrated that NO does not fully account for shear stress-induced dilation of human brachial and radial arteries[460,461] and that in patients with hypertension or coronary artery disease, NO bioavailability is diminished[462,463] and shear stress-mediated vasodilation may rely more on endothelial hyperpolarization[429,430]. This reliance on endothelial-dependent hyperpolarization as the dominant flow-induced dilation mechanism in the absence of NO has also been shown in rats and sex differences were also discovered during the course of these experiments[456,464,465]. In gracilis muscle arterioles from female and male rats lacking eNOS, endothelial-dependent hyperpolarization was the main contributor of flow-induced dilation in arteries from females whereas in arteries from male animals, flow-induced dilation was mediated by increased release of prostaglandins[456,464,465]. In humans, it has also been shown that estrogen enhances endothelial NOS expression[466] and flow-mediated NO-dependent vasodilation is significantly impaired in post-menopausal women in comparison to pre-menopausal women[467,468].

Nevertheless, while the contribution of NO and SK_{Ca} channel activation to shear stress-induced vasodilation may be impacted by a variety of factors, none of these previous studies have examined the possibility that there is a link between the NO and SK_{Ca} channels. In my experiments, the NOS inhibitor, L-NAME, and the soluble guanylyl cyclase inhibitor, ODQ, each had no effect on basal perfusion pressure but significantly enhanced nerve-evoked vasoconstriction in the perfused mesenteric bed, indicating that NO does play an important role in the acute response to shear stress but does not regulate basal perfusion pressure in this preparation. This lack of effect may be due to the low experimental basal perfusion pressure (on average 5-15 mmHg) in comparison to *in vivo* conditions, where basal mesenteric conductance has been shown to be reduced by L-NAME[469]. Nitrergic nerves also innervate rat mesenteric arteries[176,177,180,470] and L-NAME does not distinguish between NOS isoforms[471], but the lack of effect of L-NAME on nerve-evoked responses in endothelium-denuded preparations indicates that the endothelium is the only source of NO modulating nerve-evoked vasoconstriction[470].

The selective SK_{Ca} channel inhibitor, apamin, significantly enhanced nerve-evoked vasoconstriction in an endothelium-dependent manner, indicating that these channels play an important role in the response to shear stress in the rat mesenteric bed. SK_{Ca} channels[118,122,125,130,132,133], together with TRPV4 channels[132,133,432,433], are localized to the luminal membrane of endothelial cells in rat mesenteric arteries[125], an ideal location for activation by the localized increases in Ca^{2+} stimulated by increases in shear stress[118,122,130]. SK_{Ca} channel-mediated hyperpolarization of the endothelial membrane potential can spread to the surrounding smooth muscle cells via MEGJs to limit vasoconstriction. SK_{Ca} channels have also been suggested to play a role in the regulation of sympathetic neurotransmission in canine pulmonary arteries[472]. However, as the effect of apamin and CyPPA on nerve-evoked vasoconstriction was endothelium-

dependent, and activation of SK_{Ca} channels by CyPPA did not affect noradrenaline outflow, this is unlikely to be the case in the rat mesenteric bed.

Inhibition of SK_{Ca} channels with apamin did not enhance phenylephrine-induced tone in endothelium-intact arteries mounted under isometric conditions in the wire myograph (i.e. in the absence of flow). This finding supports previous work from our lab that has shown that IK_{Ca}, but not SK_{Ca}, channels mediate endothelial modulation of vascular tone to contractile agonists in isolated arteries under static conditions via myoendothelial feedback[197]. As described in **Chapter 1**, flux of IP_3 from smooth muscle cells to endothelial cells via MEGJs elicits localized increases in Ca^{2+} [28,197,321,445] leading to the activation of IK_{Ca} channels, located at the MEGJs[118,125,130,151,197], and the production of NO. As SK_{Ca} channels are present at the endothelial luminal membrane, and not at MEGJs[118,122,125,130,132,133], they do not play a role in myoendothelial feedback. In contrast, inhibition of IK_{Ca} channels had no effect on sympathetic vasoconstriction in the perfused bed, indicating that IK_{Ca} channel-mediated myoendothelial feedback does not play a role in modulating responses to nerve-derived noradrenaline in the intact bed. This is the first demonstration that shear stress activates endothelial SK_{Ca} channels, and not IK_{Ca} channel-dependent myoendothelial feedback, to modulate sympathetic vasoconstriction in the intact rat mesenteric bed.

The effect of apamin on nerve-evoked vasoconstriction was not additive with that of the NOS inhibitor, L-NAME, supporting the idea that there is a degree of overlap in these two pathways. Additional support for this proposal is provided by the data showing CyPPA limited nerve-evoked vasoconstriction in both an apamin- and L-NAME- sensitive manner. Importantly, at a concentration of 5 μM, CyPPA caused little direct vasorelaxation in vessels mounted static conditions yet significantly inhibited sympathetic vasoconstriction in the perfused mesenteric bed suggesting that activators of SK_{Ca} channels may be able to enhance the availability of shear stress-

induced NO without causing significant direct vasodilation. Thus, small molecule activators of SK_{Ca} channels may provide a means to maintain the coupling between physiological stimuli and changes in blood flow which is essential for appropriate regulation of tissue perfusion.

Only a few published studies have demonstrated that CyPPA elicits vascular relaxation. For example, in isolated rat uterine arteries, 30 µM CyPPA evoked a dilation that was apamin sensitive, though the NO- and endothelium- dependence of this effect was not investigated[473]. Additionally, in porcine isolated retinal arteries, CyPPA (1–100 µM) caused concentration-dependent relaxations of induced tone, with complete reversal of tone observed at 100 µM[437]. As in my experiments in rat mesenteric arteries, the responses in porcine retinal arteries were blocked by apamin, endothelial removal or inhibition of NO signaling, but only at concentrations up to 10 µM[437]. This indicates that responses to lower concentrations ($\leq$10 µM) of CyPPA are due to SK_{Ca} channel activation and release of NO, with higher concentrations of CyPPA potentially having endothelium-independent actions.

Although only a few previous studies utilized CyPPA, additional support for a link between NO and endothelial SK_{Ca} channel activity in modulating arterial diameter has come from studies showing other activators of K_{Ca} channels modulating NO release[131] and K_{Ca} channel blockers attenuating relaxation mediated by endothelium-derived NO[116,205]. NS309 and 5,6-dichloro- 1-ethyl-1,3-dihydro-2H-benzimidazol-2-one (EBIO), both activators of SK_{Ca} and IK_{Ca} channels, enhance ATP-induced hyperpolarization, increased cytosolic Ca^{2+} concentration and stimulated NO synthesis in cultured endothelial cells[128]. NS309 has also been shown to induce NO-dependent dilation that was blocked by apamin and TRAM-34 in mesenteric arteries[88]. Furthermore, inhibition of both K_{Ca} channels has been shown to block acetylcholine -mediated NO production in rat mesenteric arteries[126,203]. Also, in rat basilar and superior mesenteric arteries, where agonist-

induced endothelium-dependent vasorelaxation is primarily mediated through the release of NO, inhibition of SK_{Ca} and IK_{Ca} channels reduced smooth muscle hyperpolarization, NO release and prevented relaxation[116,418]. And finally, NO-dependent responses to shear stress and to low concentrations of acetylcholine are diminished in carotid arteries from mice lacking SK3 channels[204].

The mechanism linking activation of SK_{Ca} channels and NO production elicited by increases in shear stress is unclear. Since endothelial cells do not express VOCCs, the major route for Ca^{2+} entry is through non-selective cation channels, now identified as TRP channels. As mentioned above, recent evidence supports a structural link between TRPV4 and SK_{Ca} channels in endothelial cells[318], and activation of SK_{Ca} channels in response to both agonists and increases in shear stress may be facilitated by TRPV4 channel-mediated Ca^{2+} influx[132,133,432,433]. Furthermore, endothelial NOS has also been localized to the endothelial luminal membrane within caveolae[474–476]. Thus, the effects of CyPPA on NO bioavailability could be related to the localization of SK_{Ca} channels to the luminal surface of endothelial cells in signaling microdomains with caveolin-1, endothelial NOS and mechanosensitive TRPV4 channels[132,220,241–248,474–476]. In cultured endothelial cells, increases in shear stress led to the activation of SK_{Ca} channel currents by Ca^{2+} influx through TRPV4 channels[132]. Additionally, in mouse small pulmonary and mesenteric arteries and rat carotid arteries, TRPV4 channel activity has been linked to NO production and in rat pulmonary arteries, vasodilation to the TRPV4 channel agonist, GSK 1016790A, was shown to be mediated by NO, SK_{Ca} and IK_{Ca} channels[241,432,477]. Therefore, one possibility to explain the NO-dependence of CyPPA-mediated effects in the perfused mesenteric bed could be that CyPPA evokes SK_{Ca} channel-mediated hyperpolarization which enhances TRPV4 channel-mediated Ca^{2+} influx and subsequently, increases NO production.

Early studies using cultured endothelial cells indicated that agonist-evoked activation of K_{Ca} channels was necessary to increase the driving force for agonist-stimulated Ca^{2+} influx[478–480]. However, in rat mesenteric and porcine retinal arteries, NS309 caused relaxation and NO release without an increase in endothelial bulk Ca^{2+} concentration[437,481] and in rat cerebral arteries, dilation to 1-EBIO also occurred without a significant change in endothelial Ca^{2+} levels[482]. Furthermore, in rat mesenteric arteries, agonist-mediated increases in endothelial Ca^{2+} were not blocked by inhibition of SK_{Ca} and IK_{Ca} channels[203,451,483]. These observations, combined with the large driving force for Ca^{2+} entry under physiological conditions[131], cast doubt on the importance of endothelial membrane potential as a modulator of Ca^{2+} levels. However, the debate has recently been reopened by reports that inhibition of SK_{Ca} and IK_{Ca} channels reduces Ca^{2+} influx and subsequently, NO production, in response to G protein-coupled receptor activation in cultured endothelial cells[131], and that Ca^{2+} influx into endothelial cell tubes is enhanced by K_{Ca} channel-mediated membrane potential hyperpolarization and reduced by depolarization[326]. Additionally, as it is now apparent that endothelial cells display significant compartmentalization of ion channels, receptors and Ca^{2+} stores into specific microdomains[484], an alternative scenario is that SK_{Ca} channel-mediated membrane hyperpolarization facilitates local, spatially restricted increases in Ca^{2+} within specialized microdomains to selectively stimulate eNOS[131,326,485] activity in response to enhanced shear stress.

In my experiments, L-NAME abolished the actions of CyPPA in both isolated mesenteric arteries mounted under isometric conditions and in the perfused mesenteric bed, supporting the proposal that CyPPA's actions are NO-dependent. NO can regulate the permeability of MEGJs to facilitate the spread of hyperpolarization from endothelial to smooth muscle cells[486]. Evidence from experiments using co-cultured endothelial and smooth muscle cells show that NO can directly

enhance the permeability of MEGJs, through S-nitrosylation of connexin43 at cysteine 271, which may be important for maintaining the open state and permeability of MEGJs[486,487]. Thus, it is possible that inhibition of NO production could impede the spread of CyPPA-stimulated hyperpolarization from endothelial to smooth muscle cells. However, the observation that apamin was able to further enhance vasoconstriction in the presence of L-NAME suggests that this is likely not the case.

Another possibility is that rather than altering NO production, SK_{Ca} channel-mediated hyperpolarization could enhance NO bioavailability by modulating production of O_2^-. NO interacts with O_2^- to form $ONOO^-$ [389,488] and production of O_2^- by NADPH oxidase has been shown to be regulated by cell membrane potential[126,367,386–388]. Depolarization of the membrane potential of endothelial cells stimulates production of O_2^- by NADPH oxidase in both intact arteries and cultured endothelial cells[126,367,386–388], whereas membrane hyperpolarization reduces NADPH oxidase-mediated production of O_2^- [388]. Additionally, in cultured endothelial cells, activation of K_{ATP} channels to elicit membrane hyperpolarization decreased NADPH oxidase activity[388]. Also, inhibition of SK_{Ca} and IK_{Ca} channels increased production of O_2^- leading to reduced NO bioavailability in the rat perfused mesenteric vascular bed[126]. The membrane potential sensitivity of NADPH oxidase has been suggested to be conferred by the binding of Rac1 to the NADPH oxidase complex, which has been shown to occur as a result of its phosphorylation induced by endothelial membrane depolarization[367]. CyPPA evokes membrane potential hyperpolarization via activation of SK_{Ca} channels and so could enhance NO bioavailability by reducing production of O_2^- by NADPH oxidase. This possibility will be investigated in **Chapter 4.**

As described above, nerve-evoked vasoconstriction in the mesenteric bed is mediated by voltage -dependent and -independent contractile mechanisms. To limit voltage-dependent

contraction, NO, or its downstream effectors, can activate BK_{Ca} channels, causing membrane potential hyperpolarization to reduce the open probability of VOCCs[55–59,79,290,291,164–168] and can also elicit protein kinase G-mediated phosphorylation of VOCCs to inhibit their activity directly[55–59]. NO can also inhibit voltage-independent contractile pathways by enhancing sarcoendoplasmic reticulum Ca^{2+} ATPase pump activity to increase the rate of Ca^{2+} uptake into the sarcoplasmic reticulum via post-translational modifications of the sarcoendoplasmic reticulum Ca^{2+} ATPase protein[389,401,489] or by phosphorylating phospholamban to prevent its inhibitory effect on sarcoendoplasmic reticulum Ca^{2+} ATPase[251,441,442]. Furthermore, protein kinase G-mediated phosphorylation of phospholipase C can also lead to a decrease in IP_3 production and subsequently, IP_3-mediated Ca^{2+} release[166,251,289]. Evidence for these effects of NO has largely come from studies of isolated vascular smooth muscle cells so their relative contribution to NO-mediated inhibition of nerve-evoked vasoconstriction in intact arteries has not previously been investigated. In my experiments, the ability of L-NAME to significantly enhance nerve-evoked vasoconstriction in the absence and presence of nifedipine indicates that inhibition of sympathetic vasoconstriction by endothelium-derived NO may be mediated by effects on both the voltage -dependent and -independent components of smooth muscle contraction. In contrast to NO, smooth muscle membrane hyperpolarization is predominantly effective against contractions due to Ca^{2+} entry through VOCCs[490]. Thus, the observation that CyPPA was able to limit nerve-evoked vasoconstriction at higher frequencies in the presence of nifedipine, supports the proposal that a voltage-independent mechanism makes a major contribution to the actions of CyPPA.

A limitation of using the mesenteric bed in this study is that it does not allow for quantification of changes in shear stress. Previous studies have used isolated vessels mounted on cannulae to examine the impact of changes in flow on arterial diameter, which has the advantage

of allowing quantification of changes in shear stress[436]. However, interpretation of data obtained from this approach can be confounded by the previously described interaction between myogenic reactivity and shear stress[491]. Also, it must be acknowledged that the basal perfusion pressure of 5-15 mmHg is lower than experienced under physiological conditions and that although evoking vasoconstriction under conditions of constant flow and increasing flow through vessels both augment shear stress, they may do so via different mechanism. Such methodological differences, together with species, vessel and sex variation, could contribute to the wide range of signaling molecules and ion channels which have been implicated in the endothelial response to increases in shear stress. As all of these factors can impact vascular responses and thus, future studies are required to determine whether these findings are more broadly applicable.

To summarize, in the present study I have shown that shear stress-mediated inhibition of sympathetic vasoconstriction in the rat perfused mesenteric bed is mediated by both NO and SK_{Ca} channels. CyPPA, a small molecule activator of SK_{Ca} channels[313,437], can enhance the response to shear stress in this preparation via a mechanism which is dependent on endothelium-derived NO, suggesting a link between these two effector pathways so that opening of SK_{Ca} channels may enhance NO bioavailability. To date, these two pathways have predominantly been regarded as separate entities, working in parallel to limit vasoconstriction but my data supports the notion that this is not the case and that they may interact to modulate arterial diameter. The localization of SK_{Ca} channels to the luminal endothelial membrane[118,122,125,130,132,133] provides an ideal location for their activation by increases in shear stress; increased shear stress stimulates Ca^{2+} influx into endothelial cells (likely via TRPV4 channels[132,133,432,433]) leading to a rise in Ca^{2+} locally near the luminal endothelial membrane causing SK_{Ca} channels to open. By increasing the sensitivity of

SK_{Ca} channels to Ca^{2+}, CyPPA can selectively enhance the response of the endothelium to shear stress.

Thus, I have found that instead of myoendothelial feedback, it is shear stress-induced activation of SK_{Ca} channels and the release of NO that provides an endothelial-dependent vasodilatory response to sympathetic vasoconstriction to ensure appropriate distribution of blood flow at the level of the intact vascular bed. Together, these findings highlight the role of the endothelium in integrating responses from direct mechanical stimuli and nerves to regulate vasoconstriction, and also emphasizes the importance of context in defining the mechanisms underlying regulation of arterial diameter.

Finally, as loss of shear stress-induced dilation is associated with the development of cardiovascular diseases[420], my data supports the proposal that small molecule activators of SK_{Ca} channels may have therapeutic potential in terms of being able to enhance the bioavailability of shear stress-induced NO without causing significant direct vasodilation and so be able to maintain the coupling between physiological stimuli and changes in blood flow essential for appropriate regulation of tissue perfusion.

Chapter 3: Activation of IK_{Ca} channels directly inhibits sympathetic vasoconstriction in the perfused mesenteric bed

3.1: Introduction

In **Chapter 2**, I demonstrated that increases in shear stress activate endothelial SK_{Ca} channels to limit sympathetic vasoconstriction in the perfused mesenteric bed. The localization of SK_{Ca} channels to the luminal surface of vascular endothelial cells[118,122,125,130,132,133] places them in an ideal position for activation by localized increases in Ca^{2+} stimulated by enhanced shear stress[118,122,130]. In contrast, endothelial IK_{Ca} channels are found on the abluminal side of endothelial cells at MEGJs[118,125,130,151,197], sites of contact between endothelial cells and the surrounding smooth muscle cells. As demonstrated by our lab and others[197,445], this localization allows IK_{Ca} channels to play a pivotal role in myoendothelial feedback, the negative feedback pathway by which agonist-evoked contraction of smooth muscle cells in resistance arteries is limited by reciprocal activation of the endothelium. This work led to the current model for myoendothelial feedback in which movement of IP_3 from smooth muscle to endothelial cells via MEGJs, generates localized IP_3-dependent Ca^{2+} transients that activate IK_{Ca} channels within myoendothelial projections[130,197]. The resulting release of NO and hyperpolarization of the endothelial membrane potential then feeds back to the smooth muscle cells to limit further reductions in vessel diameter[197].

This model arose from experiments utilizing the application of α_1-adrenoceptor agonists to isolated vessels in order to elicit both smooth muscle depolarization to increase Ca^{2+} influx through L-type VOCCs, and generation of IP_3 by phospholipase C in a large number, if not all, smooth muscle cells[197,492]. However, sympathetic nerve activity, a major stimulus for vasoconstriction *in vivo,* results in the release of quanta of noradrenaline to act on clusters of α_1-adrenoceptors within spatially restricted post-synaptic regions on a limited number of smooth

muscle cells[434,435]. Furthermore, as demonstrated in **Chapter 2**, in the intact vasculature, increases in shear stress appear to play a major role in stimulating endothelial pathways to modulate vasoconstriction. Thus, whether myoendothelial feedback contributes to endothelial modulation of sympathetic vasoconstriction in the presence of flow and shear stress has not been investigated.

Furthermore, the contribution of NO and spread of hyperpolarization from endothelial to smooth muscle cells to myoendothelial feedback appears to vary. In hamster skeletal muscle feed arteries, spread of IK_{Ca} channel-mediated hyperpolarization to limit smooth muscle depolarization fully accounts for endothelium-dependent modulation of constriction to the α_1-adrenoceptor agonist, phenylephrine[492]. But in rat mesenteric and basilar arteries, IP_3/IK_{Ca} mediated myoendothelial feedback is linked to both hyperpolarization and release of NO[197]. Smooth muscle cell hyperpolarization is primarily effective against depolarization-induced contraction whereas NO can inhibit vasoconstriction through a range of mechanisms, such as decreasing the Ca^{2+} sensitivity of contractile proteins, inhibiting IP_3-induced Ca^{2+} release, and activating K^+ channels [11,165–168,251,289]. Thus, as shown previously for acetylcholine -evoked relaxations[443], the relative importance of hyperpolarization and NO to endothelial modulation of vasoconstriction may reflect variations in the contribution of electrical and non-electrical pathways to vasoconstriction.

The dependence of the effects of shear stress on endothelial SK_{Ca} channels, which are not involved in the myoendothelial feedback pathway (**Chapter 2** and previous studies[197,492,493]), and the reliance of myoendothelial feedback on IK_{Ca} channels, provides the opportunity to use selective inhibitors of these channels to dissect out the contribution of the two pathways to functional vascular responses. Thus, given the importance of both the endothelial response to shear stress and sympathetic nerve activity in control of arterial diameter, blood flow and blood pressure, the goal of the experiments described in this chapter was to explore the role of the IK_{Ca} channel-mediated

myoendothelial feedback pathway in limiting sympathetic vasoconstriction in the presence of flow and to test the hypothesis that *IK_{Ca} channel-mediated myoendothelial feedback plays a role in NO-dependent modulation of sympathetic vasoconstriction.*

In contracting skeletal muscle, sympathetic vasoconstriction is attenuated in comparison to resting muscle in order to ensure adequate blood flow, despite the elevated sympathetic drive[494]. This process, termed functional sympatholysis[495], occurs at the level of the vascular smooth muscle[496] and recent work suggests a role for myoendothelial feedback in blunting sympathetic vasoconstriction in human skeletal muscle[497]. Thus, SKA-31, a putative IK_{Ca} channel activator[121,124], was also used to determine whether activation of IK_{Ca} channels can enhance myoendothelial feedback to limit vasoconstriction in the perfused bed.

As in **Chapter 2**, I have primarily used the rat mesenteric bed perfused at a constant luminal flow such that vasoconstriction leads to increases in shear stress[436]. Pharmacological tools were applied to investigate the contribution of IK_{Ca} channels to shear stress-induced modulation of sympathetic vasoconstriction.

3.2: Methods and materials

See **Appendix: Drugs and chemicals** for a list of the drugs and chemicals used.

3.2.1: Perfused mesenteric vascular bed

The mesenteric bed was perfused via the superior mesenteric artery as previously described[438]. Briefly, the mesenteric vascular bed was separated from the intestine and the superior mesenteric artery cleaned of connective tissue, cannulated with a blunted hypodermic needle (20 G), secured with 5-0 surgical silk (Ethicon) and flushed with Krebs buffer to remove blood. In some experiments, the endothelium was removed by flushing the bed with 0.5% Triton X-100 in water for 30 seconds followed by rapid washout with Krebs. The vascular bed was placed on a

wire mesh in a warm chamber and perfused with oxygenated Krebs buffer at a constant flow rate of 5 mlmin^{-1} (37°C, bubbled with 95% O_2/5% CO_2). Changes in perfusion pressure were monitored via an in-line pressure transducer (AD instruments, Colorado) and recorded via a PowerLab data acquisition system using Chart 5.0 software (AD Instruments, Colorado). In experiments conducted with endothelium-denuded preparations, endothelial function was assessed as the response to acetylcholine (1 µM) following vasoconstriction with methoxamine (1 µM); tissues in which acetylcholine failed to reverse constriction were deemed to be denuded.

3.2.1.1: Responses to stimulation of perivascular nerves. Electrodes were attached to the cannulating needle and to the wire mesh to allow electrical field stimulation using a Grass SD9 stimulator (Grass Technologies, USA). Following an equilibration period of 30 minutes, a single stimulation (30 Hz, 90 V, pulse width 1 millisecond, 30 seconds) was applied to assess the viability of the preparation. After a further 10 minutes, a frequency-response curve was constructed by stimulating the preparation at 1-40 Hz (90 V, pulse width 1 millisecond, 30 seconds) at 10 minute intervals[188]. The effects of agents on nerve-evoked vasoconstriction were assessed by perfusing the drugs through the lumen of the preparation for 20 minutes prior to constructing a second frequency-response curve. In some experiments a third frequency-response curve was constructed following washout of the drugs or the perfusion of different drug combinations.

Nerve-evoked responses recorded in the perfused mesenteric vascular bed are shown as normalized values. Changes in perfusion pressure were normalized to the maximum control response (%) as is convention in these types of experiments. For all frequency response curves, electrical stimulation caused frequency-dependent increases in perfusion pressure ($p<0.05$).

3.2.2: Wire myography

Third order mesenteric arteries were cleaned of adhering tissue and cut into segments (~2

mm in length). Arterial segments were mounted between two gold-plated tungsten wires (20 μm diameter) in a Mulvany-Halpern myograph (model 400A, J.P. Trading, Denmark) as previously described[438]. Changes in isometric tension were recorded via a PowerLab using Chart 5.0 or 8.0 software (AD Instruments, Colorado, USA). Tissues were maintained in Krebs' buffer gassed with 95% O_2/5% CO_2 at 37°C (pH 7.4) and set to a pre-determined optimal resting tension of 5 mN for mesenteric arteries (this was previously determined from active length-tension curves). In some experiments, the endothelium was removed by flushing of the mesenteric bed with 0.5% Triton X-100 in water for 30 seconds followed by rapid washout with Krebs. After an equilibration period of 30 minutes, endothelial function was assessed as % relaxation to acetylcholine (3 μM) following pre-stimulation with phenylephrine (3 μM; 75% of maximal tone). Arteries in which acetylcholine induced >90% reversal of agonist-induced tone were designated as endothelium-intact and tissues in which the response to acetylcholine was <10% were deemed to be endothelium-denuded. Arteries in which the % reversal of agonist-induced tone elicited by acetylcholine fell between these values were discarded.

3.2.2.1: Concentration-response curves. Cumulative concentration-response curves to SKA-31 (0.001-30 μM) were constructed in arteries in which tone was raised with phenylephrine (3 μM). For all SKA-31 concentration-response curves, SKA-31 caused relaxation in a concentration-dependent manner ($p<0.05$). In endothelium-intact arterial segments, SKA-31 concentration-response curves were constructed in the absence and presence of TRAM-34 (1 μM) or L-NAME (100 μM). Cumulative concentration-response curves to SKA-31 (0.001-30 μM) were also carried out in endothelium-denuded mesenteric arteries. In all experiments, the level of phenylephrine-induced tone was matched in the absence and presence of inhibitors and relaxations to SKA-31 were expressed as % relaxation as is the convention in this type of experiment.

Cumulative concentration-response curves to phenylephrine (0.001-100 μM) were constructed in the absence and presence of SKA-31 (10 μM) without and with TRAM-34 (1 μM) or L-NAME (100 μM) in endothelium-intact isolated mesenteric arteries. Results were expressed as % maximal response as is convention for this type of experiment. Phenylephrine increased tone in a concentration-dependent manner ($p<0.05$).

3.2.3: Confocal immunohistochemistry

IK_{Ca} (IK1) channel distribution was determined using conventional confocal immunohistochemistry, performed by Dr. Shaun Sandow, University of the Sunshine Coast. Animals were perfused via the left ventricle with a clearance solution (0.1% bovine serum albumin, 10 U/ml of heparin and 0.1% $NaNO_3$ in saline), and subsequently fixed with 2% paraformaldehyde in 0.1 mM of phosphate buffered saline. To optimize the area visible in the narrow internal elastic lamina hole focal region, as potential myoendothelial microdomain signaling sites, vessel segments were cut along one lateral plane and pinned out as a flat sheet. Tissues were then incubated in phosphate buffered saline with 1% bovine serum albumin, as blocking buffer, and 0.2% Triton X-100, for 2 hours at room temperature, rinsed in phosphate buffered saline (3 × 5 minutes) and incubated with IK1 (M20 bleed; GlaxoSmithKline) and tyrosine hydroxylase (Immunostar, product number 22941) primary antibodies in blocking buffer for 18 hours at 4°C. Tissues were then rinsed in phosphate buffered saline (3 × 5 minutes) and incubated in secondary antibody (AlexaFluor 633 goat anti rabbit; Invitrogen, A21070; lot 1,120,101) diluted in 0.01% Triton X-100, for 2 hours, and rinsed in phosphate buffered saline (3 × 5 minutes), mounted uppermost in anti-fade glycerol and examined using matched settings on a confocal microscope (Nikon Eclipse Ti; Nikon, Australia). The specificity of the IK1 antibodies used here was previously characterized using tissue from mice lacking IK_{Ca} channels, transfected

cell lines, Western blotting and additional positive and negative control. The internal elastic lamina was visualized using autofluorescence at 488 nm.

3.2.4: Analysis of noradrenaline levels in perfusate from the mesenteric vascular bed

The mesenteric vascular bed was placed on a wire mesh and placed in a plastic dish on hot a plate (Model HP-A1915B-13, Thermolyne) and maintained at 37°C. The flow rate was 2 mlmin^{-1} and the mesenteric bed was stimulated at 30 Hz for 60 seconds. Perfusate was collected for the 60 seconds before and during the stimulation. Samples were immediately frozen in liquid nitrogen and stored at -80°C prior to analysis by UPLC.

3.2.4.1: Measurement of noradrenaline outflow from the perfused mesenteric bed by UPLC.

Noradrenaline levels in perfusate samples were analyzed using a Waters Acquity UPLC System (H Class) consisting of a binary solvent manager, sample manager, column manager and fluorescence detector. Pre-column derivatization with benzylamine and 1,2-diphenylethyleendiamine was conducted[439]. Separation of noradrenaline was achieved by gradient elution using a mixture of acetonitrile and 15 mM acetate buffer (pH 4.5) containing 1 mM octanesulfonic acid (sodium salt) on a Waters Acquity UPLC BEH Shield reversed phase column (C18, 2.1 mm ID 100 mm, 1.7 μm). The column temperature was 60°C, flow rate 0.7 ml/min and the run time was 8 minutes. Excitation and emission wavelength were set at 345 and 480 nm, respectively. All data was acquired and analyzed by means of Waters Empower 3 software. Noradrenaline and acetonitrile were purchased from Sigma-Aldrich. All chemicals and solvents were of analytical grade. All solutions were prepared in ultrapure milliQ water (Millipore MilliQm Germany) and filtered over a 0.22 μm filter (Millipore, Bedford, USA). A standard curve for noradrenaline was obtained each day prior to collection and injection of samples. Analysis was done with the operator blinded to sample identity. The lowest detectable level of noradrenaline

was 4 fmol/50 µl sample. The concentration of noradrenaline in the perfusate samples are shown as normalized values due to variation in control values for noradrenaline overflow between different preparations.

3.2.5: Statistics

All data are expressed as mean ± SEM, *n* rats used. For repeated measures, two-way ANOVA followed by either a Tukey's multiple comparison post-hoc test (used when there were more than two experimental groups) or a Šídák method post-hoc test (used when there was two experimental groups) was performed. Paired *t*-tests were used in **Figure 3.9**. $p<0.05$ was considered statistically significant in all cases.

3.3: Results

3.3.1: Role of IK_{Ca} channels in endothelial modulation of sympathetic vasoconstriction in the perfused mesenteric bed

In endothelium-intact mesenteric beds, infusion of noradrenaline (15 µM) caused vasoconstriction that was significantly enhanced by TRAM-34 (1 µM); in the presence of TRAM-34 the response to noradrenaline was 134.2 ± 10.5 % of control (n=5, $p<0.05$), indicating that myoendothelial feedback can occur in this preparation. In endothelium-denuded arteries, TRAM-34 was without effect on noradrenaline-evoked constriction (n=4, $p>0.05$).

The functional role of IK_{Ca} channels in endothelial-dependent modulation of nerve-evoked vasoconstriction in the perfused mesenteric bed was investigated using the selective IK_{Ca} channel inhibitors, TRAM-34 and NS 6180 (1 µM). Neither NS 6180 ($p>0.05$, **Figure 3.1a** and **b**) nor TRAM-34 (n=5) significantly affected nerve-evoked vasoconstriction. Also, TRAM-34 in combination with the SK_{Ca} channel inhibitor, apamin (50 nM), did not enhance nerve-evoked vasoconstriction more than apamin alone; nerve-evoked responses in the presence of apamin or apamin plus TRAM-34 were not significantly different ($p>0.05$, **Figure 3.1c**). Thus, IK_{Ca} channel-

mediated myoendothelial feedback does not appear to play a significant role in endothelial

modulation of nerve-evoked vasoconstriction in the intact mesenteric bed.
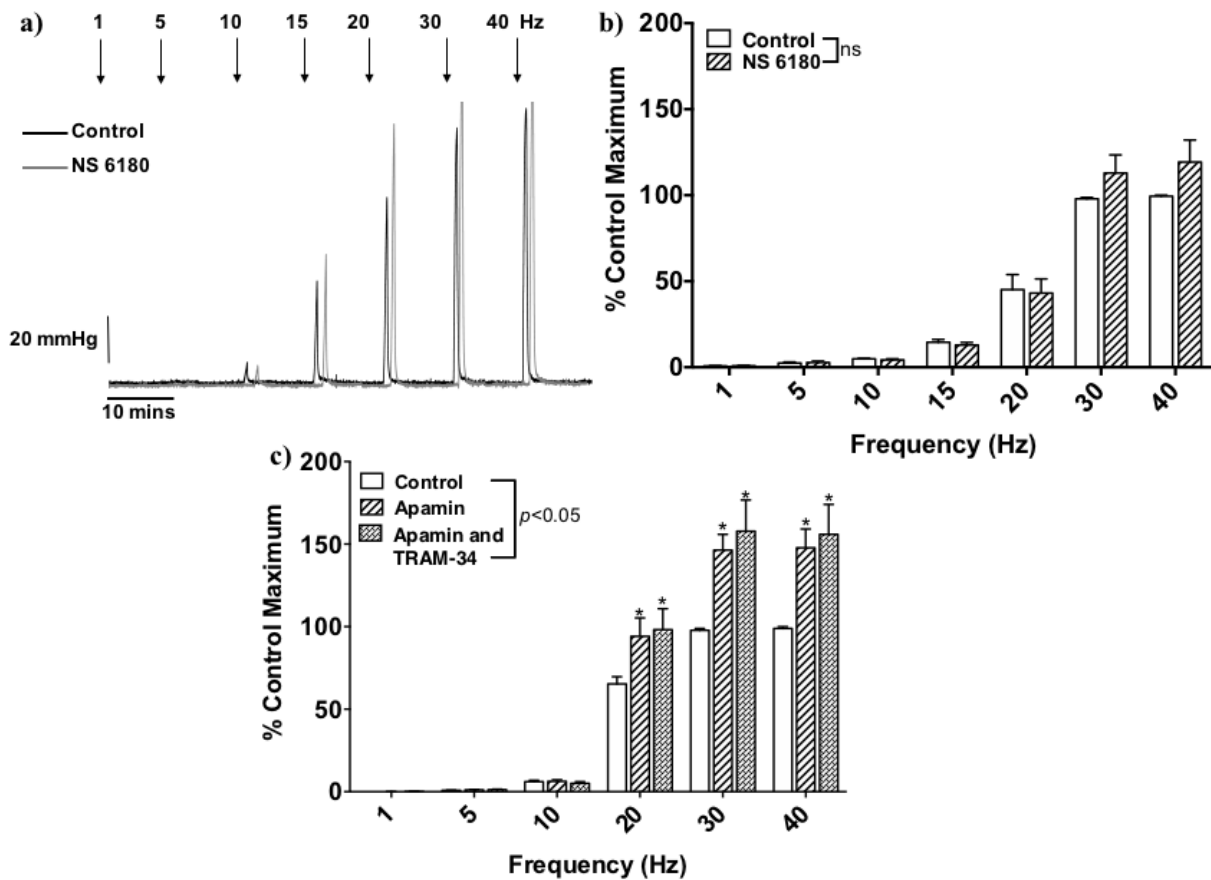
Figure 3.1: IK$_{Ca}$ channels do not play a role in nerve-evoked vasoconstriction.
a) Representative trace showing a frequency-response relationship obtained from an endothelium-intact perfused mesenteric bed in the absence and presence of NS 6180 (1 μM). **b)** Mean frequency-response relationships obtained from endothelium-intact perfused mesenteric beds in the absence and presence of NS 6180 (1 μM). Values are presented as mean ± SEM, n=5; two-way repeated-measures ANOVA. **c)** Mean frequency-response relationships obtained from endothelium-intact perfused mesenteric beds in the absence and presence of apamin (50 nM) without and with TRAM-34 (1 μM). Values are presented as mean ± SEM, n=5. * denotes $p<0.05$ from control; two-way repeated-measures ANOVA.

3.3.2: Effect of SKA-31 on phenylephrine-induced tone in isolated mesenteric arteries

In order to investigate whether activation of IK_{Ca} channels can enhance myoendothelial feedback, I used the putative IK_{Ca} channel opener, SKA-31[121,124]. As the effects on vascular tone in rat mesenteric arteries have not previously been reported, I first characterized the effect of SKA-31 on phenylephrine-induced tone in isolated arteries mounted under isometric conditions in the wire myograph.

In endothelium-intact arteries, SKA-31 (0.001- 30 µM)-evoked relaxations of phenylephrine (3 µM)-induced tone were significantly reduced by the presence of TRAM-34 (1 µM) but unaffected by the NOS inhibitor, L-NAME (100 µM). In endothelium-denuded tissues, relaxations to SKA-31 were only observed at concentrations ≥3 µM and the maximum response was significantly reduced compared to endothelium-intact arteries ($p<0.05$, **Figure 3.2**).
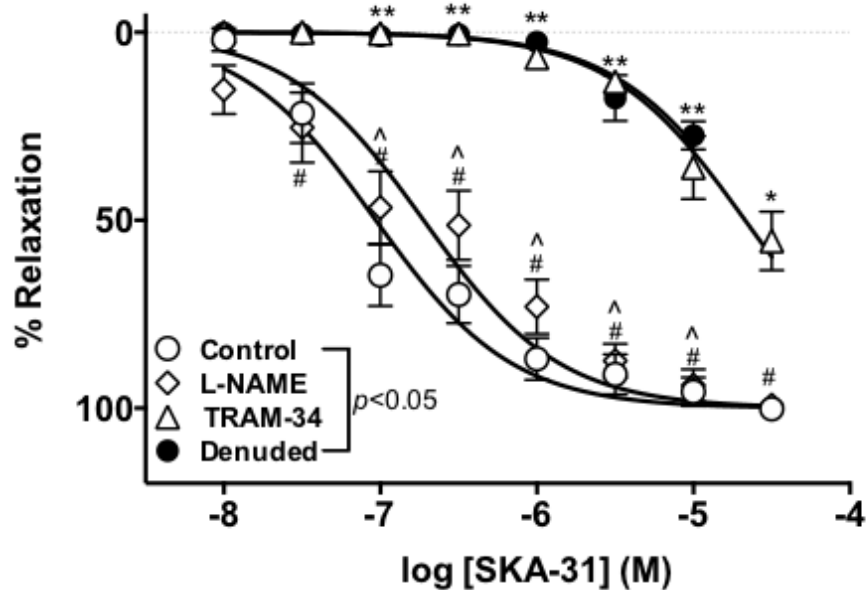
Figure 3.2: **SKA-31-mediates endothelium-dependent relaxation through IK$_{Ca}$ channel activation.** Third order mesenteric arteries were mounted in a wire myograph. Mean data showing SKA-31-induced relaxation in endothelium-intact isolated rat mesenteric artery segments mounted in a wire myograph in the absence (control n=13) and presence of TRAM-34 (1 μM; n=10) or L-NAME (100 μM; n=13) and in endothelium-denuded (n=5) isolated rat mesenteric artery segments. Values are presented as mean ± SEM. * denotes $p<0.05$ from control, # denotes $p<0.05$ from TRAM-34 (1 μM) and ^ denotes $p<0.05$ from denuded; two-way repeated-measures ANOVA.

The effect of SKA-31 (10 μM) on phenylephrine-evoked increases in tone was also examined as responses to phenylephrine are limited by IK$_{Ca}$ channel-mediated myoendothelial feedback. This concentration of SKA-31 was selected as it evoked relaxations which were predominantly endothelium-dependent and sensitive to TRAM-34. Concentration-response curves to phenylephrine (phenylephrine denoted as PE in **Figure 3.3**; 0.001- 100 μM) were constructed in the absence and presence of SKA-31. In endothelium-intact arteries, SKA-31 did not affect resting tone but significantly reduced increases in tone elicited by 1 and 3 μM phenylephrine ($p<0.05$; **Figure 3.3**) causing a rightward shift in the concentration-response curve to

phenylephrine. This effect was blocked by TRAM-34 (1 μM) but not L-NAME (100 μM) (**Figure 3.3**).
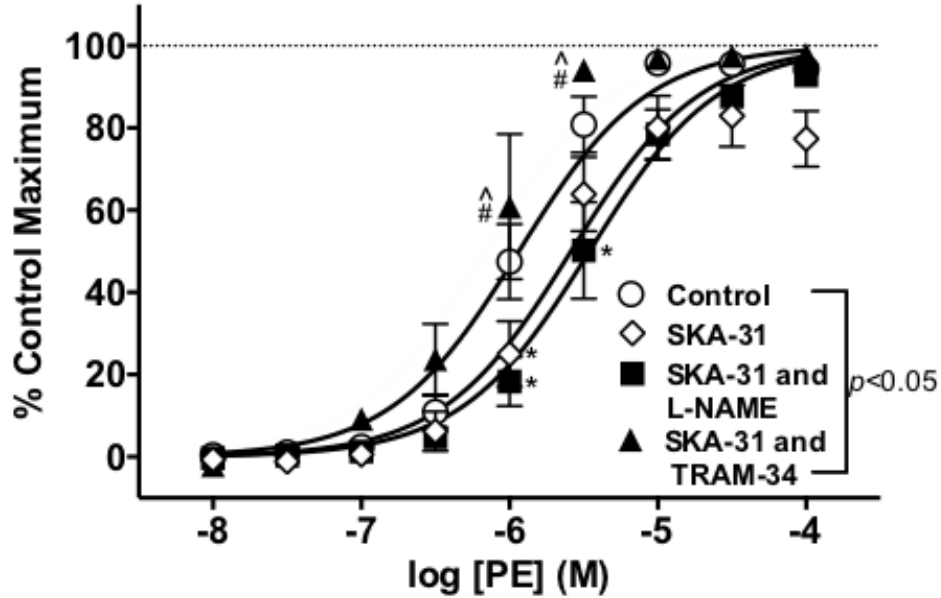
Figure 3.3: SKA-31 limits phenylephrine-induced increases in tone through IK$_{Ca}$ channel activation in a NO-independent manner. Third order mesenteric arteries were mounted in a wire myograph. Mean data showing phenylephrine-induced increases in tone in the absence (control n=13) and presence of SKA-31 (10 μM; n=13) without and with L-NAME (100 μM; n=4) or TRAM-34 (1 μM; n=4) in endothelium-intact isolated rat mesenteric artery segments. Values are presented as mean ± SEM. * denotes $p<0.05$ from control, # denotes $p<0.05$ from SKA-31 (10 μM) and ^ denotes $p<0.05$ from SKA-31(10 μM) with L-NAME (100 μM); two-way repeated-measures ANOVA.

3.3.3: Effect of SKA-31 on sympathetic vasoconstriction in the rat perfused mesenteric bed

SKA-31 (1-10 µM) had no effect on basal perfusion pressure but SKA-31 (10 µM) significantly reducing nerve-evoked vasoconstriction at frequencies from 15 to 40 Hz ($p<0.05$, **Figure 3.4b**); lower concentrations of SKA-31 (1 and 5 µM) did not affect responses ($p>0.05$, **Figure 3.4a**).

NS 6180 (1 µM), a selective IK_{Ca} channel blocker had no effect on basal perfusion pressure but prevented the effects of SKA-31 (10 µM) so that responses were not significantly different to control ($p>0.05$, **Figure 3.4c**), indicating that SKA-31 does exert its effects on nerve-evoked constriction through activation of IK_{Ca} channels.
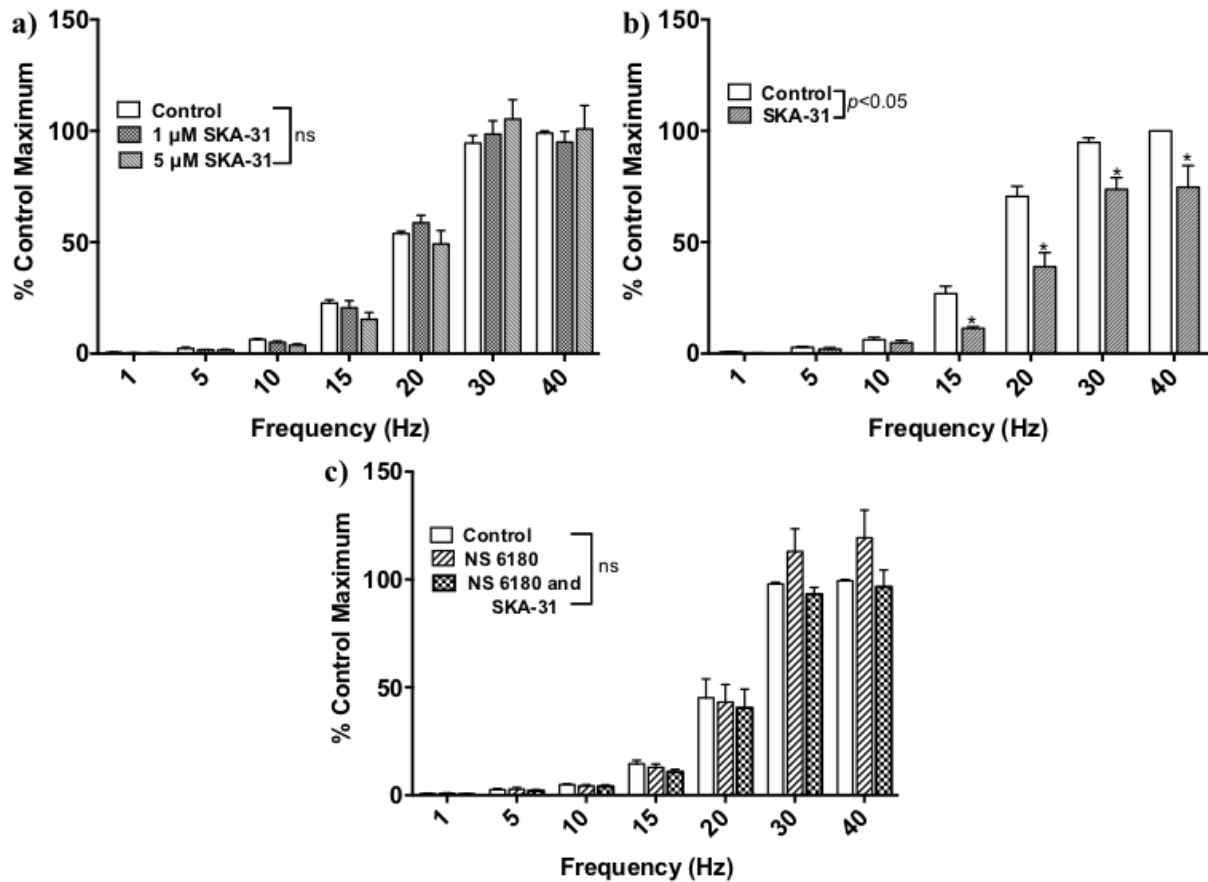
Figure 3.4: SKA-31 limits nerve-evoked vasoconstriction through IK$_{Ca}$ channel activation.
a) Mean frequency-response relationships obtained from endothelium-intact perfused mesenteric beds in the absence and presence of SKA-31 (1 and 5 μM). Values are presented as mean ± SEM, n=4; two-way repeated-measures ANOVA. **b)** Mean frequency-response relationships obtained from endothelium-intact perfused mesenteric beds in the absence and presence of SKA-31 (10 μM). Values are presented as mean ± SEM, n=4. * denotes $p<0.05$ from control; two-way repeated-measures ANOVA. **c)** Mean frequency-response relationships obtained from endothelium-intact perfused mesenteric beds in the absence and presence of NS 6180 (1 μM) without and with SKA-31 (10 μM). Values are presented as mean ± SEM, n=5; two-way repeated-measures ANOVA.

To investigate if inhibition of nerve-evoked vasoconstriction by SKA-31 was mediated by NO, SKA-31 (10 µM) was applied in the presence of L-NAME (100 µM). As shown in **Chapter 2** (**Figure 2.3**), L-NAME significantly enhanced nerve-evoked vasoconstriction in endothelium-intact mesenteric beds at frequencies from 20 to 40 Hz ($p<0.05$, **Figure 3.5**). In the presence of L-NAME, SKA-31 was still able to inhibit nerve-evoked responses at frequencies of 20 to 40 Hz ($p<0.05$, **Figure 3.5**).
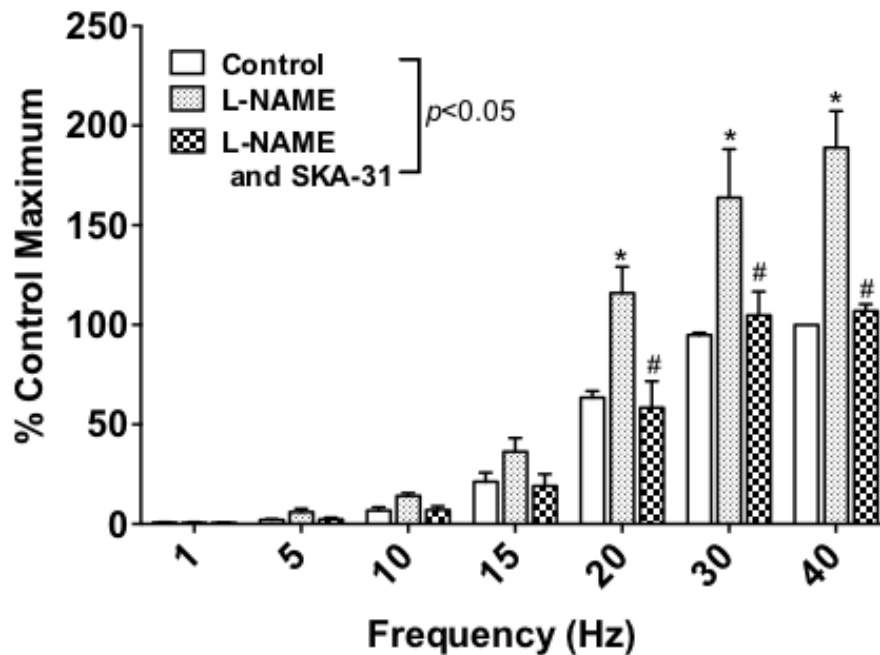
Figure 3.5: Inhibition of nerve-evoked vasoconstriction by SKA-31 is not mediated by NO. Mean frequency-response relationships obtained from endothelium-intact perfused mesenteric beds in the absence and presence of L-NAME (100 µM) without and with SKA-31 (10 µM). Values are presented as mean ± SEM, n=4. * denotes $p<0.05$ from control, # denotes $p<0.05$ from L-NAME (100 µM); two-way repeated-measures ANOVA.

As shown in **Chapter 2** (**Figure 2.2** and **2.3**), nerve-evoked vasoconstriction is mediated by both voltage -dependent and -independent pathways of smooth muscle contraction. If inhibition of nerve-evoked vasoconstriction by SKA-31 is mediated by spread of hyperpolarization from endothelial to smooth muscle cells, then it would be expected that it would be most effective against contractions due to Ca^{2+} entry through VOCCs[490] rather than voltage-independent smooth muscle mechanisms. Thus, the ability of SKA-31 to inhibit nerve-evoked vasoconstriction in the presence of the L-type VOCC inhibitor, nifedipine, was investigated. The rationale for these experiments was that in the presence of nifedipine, vasoconstriction would be due to voltage-independent mechanisms and so SKA-31 would be less effective at limiting nerve-evoked vasoconstriction. As shown in **Chapter 2** (**Figure 2.2**), nifedipine (10 μM) significantly reduced nerve-evoked vasoconstriction at 30 and 40 Hz in comparison with control ($p<0.05$, **Figure 3.6**). In the presence of nifedipine, SKA-31 (10 μM) significantly reduced responses compared to control at frequencies of 15 to 40 Hz ($p<0.05$) and compared to nifedipine alone at the 30 and 40 Hz frequencies ($p<0.05$, **Figure 3.6**).
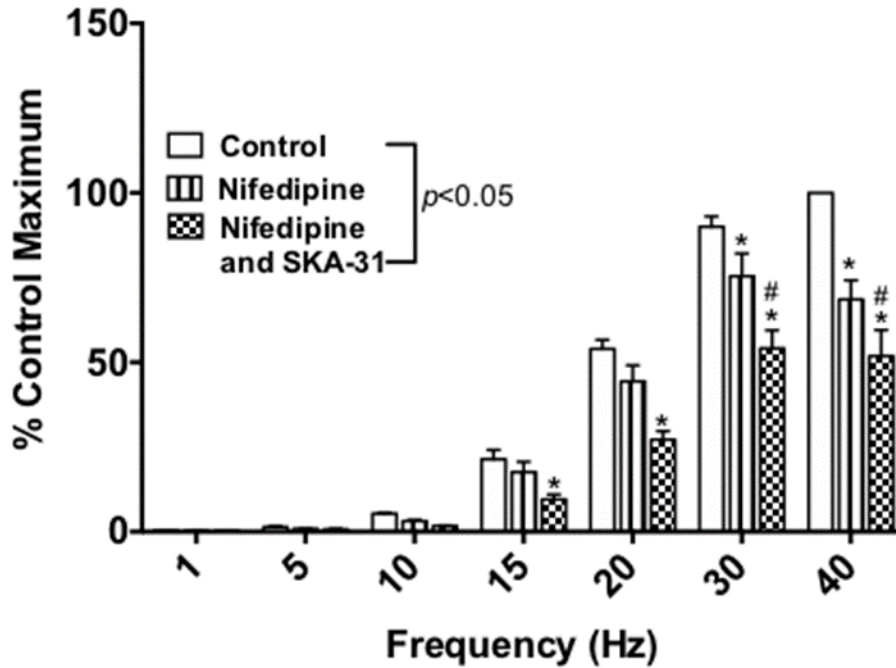
Figure 3.6: **SKA-31 inhibits the voltage-independent component of nerve-evoked vasoconstriction.** Mean frequency-response relationships obtained from endothelium-intact perfused mesenteric beds in the absence and presence of nifedipine (10 μM) without and with SKA-31 (10 μM). Values are presented as mean ± SEM, n=4. * denotes $p<0.05$ from control and # denotes $p<0.05$ from nifedipine (10 μM); two-way repeated-measures ANOVA.

The ability of SKA-31 to inhibit nerve-evoked vasoconstriction in the presence of nifedipine indicates that a mechanism other than hyperpolarization may underlie its effects on smooth muscle contractility. Thus, I investigated whether SKA-31 could influence vasoconstriction in endothelium-denuded preparations. SKA-31 (10 μM) significantly reduced nerve-evoked vasoconstriction ($p<0.05$, **Figure 3.7**) in endothelium-denuded mesenteric beds.
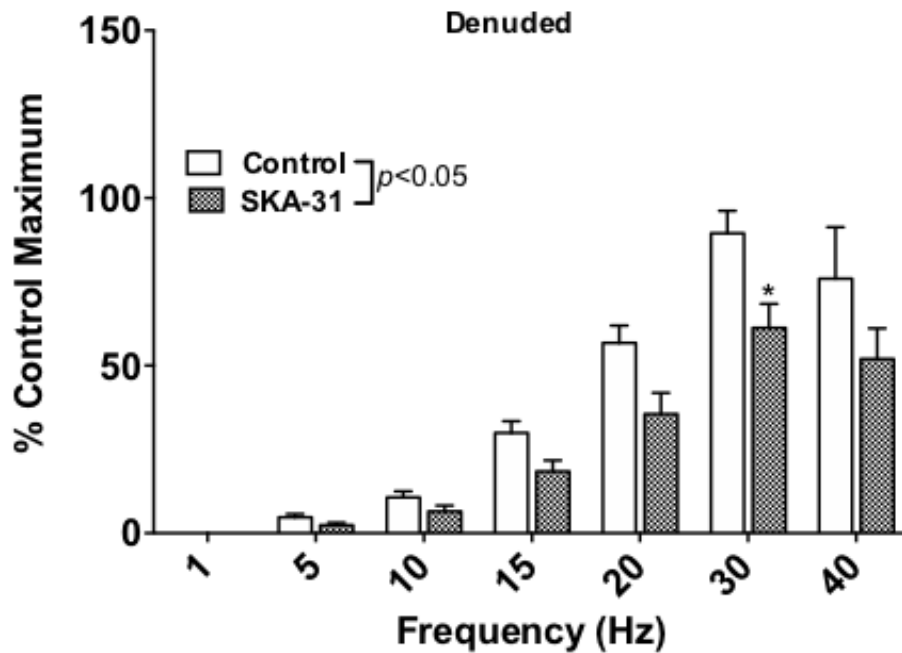
Figure 3.7: **SKA-31 limits nerve-evoked vasoconstriction in an endothelium-independent manner.** Mean frequency-response relationships obtained from endothelium-denuded mesenteric beds in the absence and presence of SKA- 31 (10 μM). Values are presented as mean ± SEM, n=4. * denotes $p<0.05$ from control; two-way repeated-measures ANOVA.

As our lab has previously demonstrated that IK_{Ca} channels are present only in endothelial cells of rat mesenteric arteries[197], I investigated whether the inhibitory effects of SKA-31 on nerve-evoked vasoconstriction in the perfused mesenteric bed were due to activation of IK_{Ca} channels located on perivascular nerves to reduce the amount of noradrenaline released during nerve stimulation. Confocal immunohistochemistry of whole vessel mounts of third order mesenteric arteries were incubated with either antibodies specific for IK1 channels or tyrosine hydroxylase, the latter being the rate-limiting enzyme in catecholamine biosynthesis and used to identify sympathetic nerves[498]. Though overlay was not possible due to technical issues, the images in **Figure 3.8** clearly demonstrate the localization of IK_{Ca} channels on sympathetic perivascular nerves.
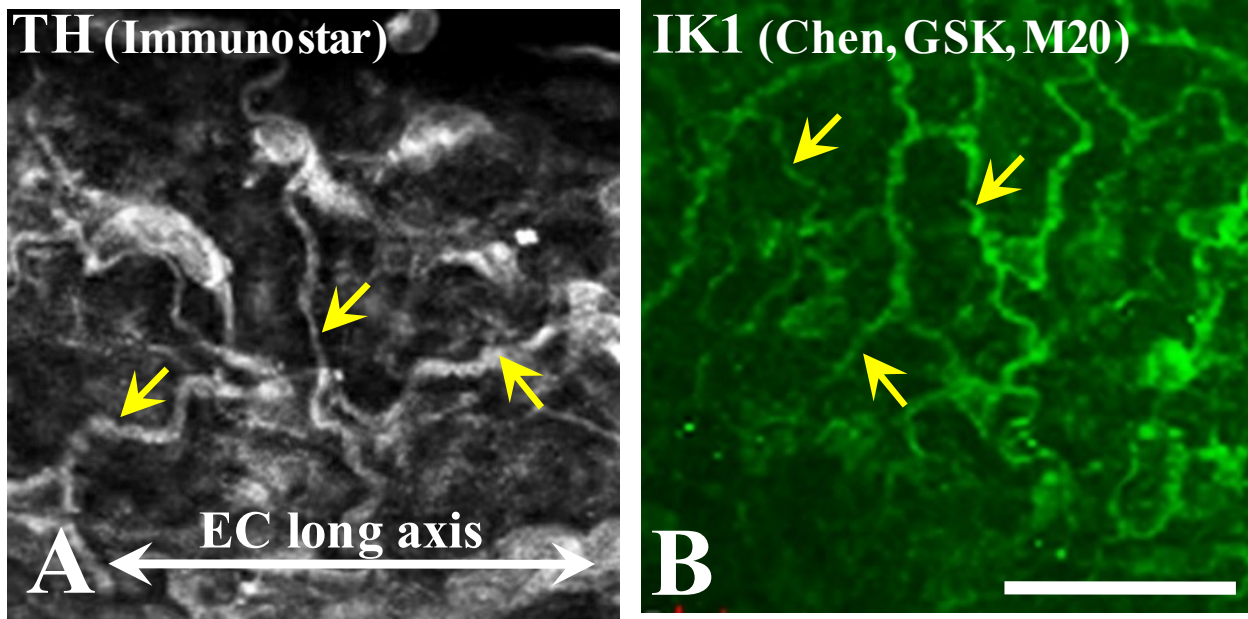
Figure 3.8: **IK$_{Ca}$ channels are localized on the rat mesenteric artery sympathetic perivascular plexus.** Confocal immunohistochemistry demonstrates **A)** tyrosine hydroxylase (TH**;** a marker for sympathetic neurons) and **B)** IK1 (IK$_{Ca}$ channels) labelling of the adventitial perivascular plexus (example fibres arrowed). n=6; bar, 50 μm. *Confocal imaging by Dr. Shaun Sandow, University of the Sunshine Coast, Australia.*

To determine if activation of IK$_{Ca}$ channels localized to perivascular sympathetic nerves could be regulating noradrenaline release, noradrenaline overflow following nerve stimulation was assessed by UPLC. Perfusate was collected before and during a 60 second 30 Hz stimulation in the absence and presence of SKA-31 (10 μM). Noradrenaline overflow was found to be undetectable in the 60 seconds prior to the 30 Hz stimulation and increased during stimulation. Noradrenaline overflow showed no significant change over three consecutive stimulations at 20 minute intervals ($p>0.05$, **Figure 3.9a**) but in the presence of SKA-31 (10 μM), noradrenaline overflow was significantly reduced ($p<0.05$, **Figure 3.9b**). Perfusate before and during a 30 Hz stimulation was also collected in the absence and presence of SKA-31 plus NS 6180 (1 μM). NS 6180 blocked the reduction in noradrenaline mediated by SKA-31 so that noradrenaline release in the presence of SKA-31 with NS 6180 was not significantly different to control ($p>0.05$, **Figure**

3.9c). Thus, the effects of SKA-31 on nerve-evoked vasoconstriction could be mediated by the activation of neuronal IK_{Ca} channels to inhibit noradrenaline release.
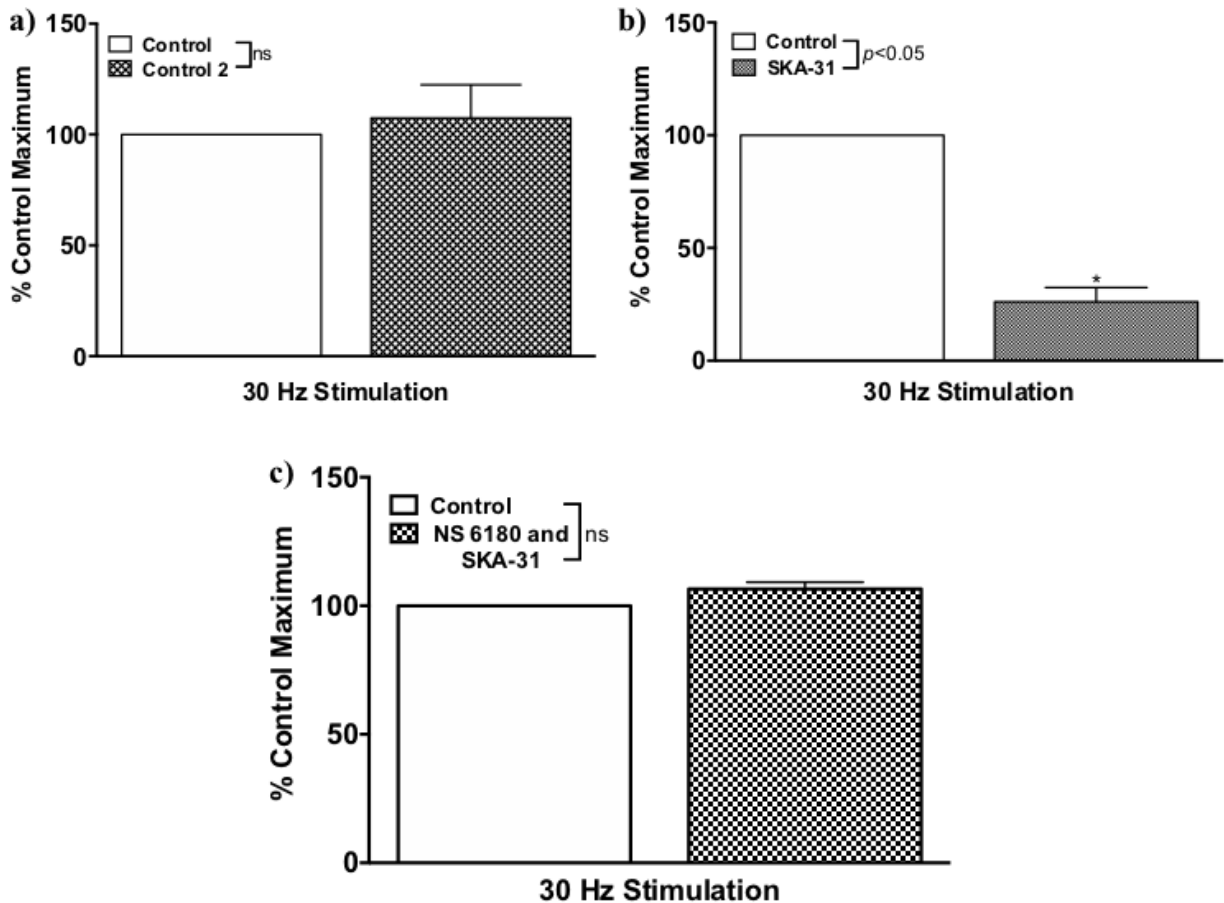
Figure 3.9: SKA-31 reduces noradrenaline release from perivascular nerves of rat mesenteric beds. a) Mean data showing release of noradrenaline (as measured by UPLC) in the absence of drugs in endothelium-intact perfused mesenteric vascular beds. Values are presented as mean ± SEM, n=6; paired *t*-test. **b)** Mean data showing release of noradrenaline (as measured by UPLC) in the absence and presence of SKA-31 (10 μM) in endothelium-intact perfused mesenteric vascular beds. Values are presented as mean ± SEM, n=5. * denotes $p<0.05$ from control; paired *t*-test. **c)** Mean data showing release of noradrenaline (as measured by UPLC) in the absence and presence of NS 6180 (1 μM) and SKA-31 (10 μM) in endothelium-intact perfused mesenteric vascular beds. Values are presented as mean ± SEM, n=5; paired *t*-test.

3.4: Discussion

Endothelial IK_{Ca} channels are located on the abluminal side of endothelial cells at MEGJs[118,125,130,151,197], the sites of contact between endothelial and surrounding smooth muscle cells, where they play a pivotal role in limiting agonist-mediated vasoconstriction via myoendothelial feedback[130,197]. Here in **Chapter 3**, I have shown that IK_{Ca} channels are not involved in shear stress-induced endothelial-dependent modulation of sympathetic vasoconstriction in the perfused mesenteric bed. SKA-31, an activator of IK_{Ca} channels, can inhibit nerve-evoked vasoconstriction in this preparation but this effect is independent of the endothelium and appears to be due to the activation of neuronal IK_{Ca} channels to reduce noradrenaline release. This is the first description of a role for IK_{Ca} channels in the release of noradrenaline from perivascular sympathetic nerves in resistance arteries and suggest that targeting these channels could provide a novel approach to reducing vasoconstriction in conditions associated with increased sympathetic drive, such as hypertension[174,499,500].

As described earlier, the reliance of myoendothelial feedback on IK_{Ca} channels and the availability of selective inhibitors for these channels, provides the opportunity to dissect the contribution of this pathway in functional vascular responses[118,125,130,151,197,493]. The inhibition of IK_{Ca} channels by TRAM-34, causes endothelium-dependent enhancement of both phenylephrine-evoked increases in tone in isolated mesenteric arteries and vasoconstriction to infusion of noradrenaline in the perfused mesenteric bed. Thus, IK_{Ca} channel-mediated myoendothelial feedback is functional in these arteries. The lack of effect of TRAM-34 and a second selective IK_{Ca} channel inhibitor, NS 6180, on nerve-evoked vasoconstriction indicates that these channels, and by extension the myoendothelial feedback pathway, are not involved in modulating sympathetic vasoconstriction in this preparation. Thus, as described in **Chapter 2**, it appears that shear stress-

induced activation of endothelial SK_{Ca} channels is the dominant mechanism for engagement of the endothelium to limit sympathetic vasoconstriction.

The reason for the differential functional roles of the two types of endothelial K_{Ca} channels may be explained by their discrete locations within endothelial cells. As described in **Chapter 2**, SK_{Ca} channels are located on the luminal membrane of endothelial cells[118,122,125,130,132,133] whereas IK_{Ca} channels are located at MEGJs[118,125,130,151,197]. Increases in shear stress lead to Ca^{2+} influx through TRPV4 channels, which are co-localized with SK_{Ca} channels and caveolin-1 in discrete signalling microdomains on the luminal endothelial cell membrane[132,220,241–248,474–476]. The location of IK_{Ca} channels at MEGJs[118,125,130,151,197] may mean that they are not exposed to shear stress-mediated localized increases in Ca^{2+} at the luminal membrane and so are unable to participate in the subsequent endothelial modulation of nerve-evoked vasoconstriction. This conclusion is supported by previous work showing that responses to increases in shear stress are unaltered in isolated carotid arteries from IK1^{-/-} mice whereas arteries from animals lacking both SK_{Ca} and IK_{Ca} channels had diminished shear stress-induced responses[204].

SKA-31 enhances the sensitivity of IK_{Ca} channels to Ca^{2+} [121,124,437] to induce TRAM-34-sensitive hyperpolarization in isolated endothelial cells from canine mesenteric and mouse carotid arteries[124,316], and to activate IK_{Ca} channel currents in isolated murine endothelial cells[121,316]. Given this mechanism of action, I proposed that although IK_{Ca} channels may not be involved in modulating nerve-evoked vasoconstriction, SKA-31 may be able enhance IK_{Ca} channel activity in order to limit nerve-evoked vasoconstriction. As the effects of SKA-31 have not been investigated in rat mesenteric arteries, I first examined its actions in isolated mesenteric arteries and showed that it evoked relaxations which are dependent on the endothelium and IK_{Ca} channels, but independent of NO. These findings are in line with previous studies showing that SKA-31 dilates

rat cerebral[314], skeletal muscle arterioles[316] and mouse mesenteric arteries[501], effects which were dependent on IK_{Ca} channels but not affected by block of NOS. Furthermore, bolus doses of SKA-31 caused NO-independent dilation of rat coronary arteries in the intact heart[502], and L-NAME did not affect vasodilation to NS309, a structurally-related SK_{Ca}/IK_{Ca} channel activator, in rat cremaster and small mesenteric arteries[128,205].

SKA-31 activates IK_{Ca} channels, with an EC_{50} value of 0.26 µM, it can also activate SK_{Ca} channels, with an EC_{50} value of 2.9 µM, showing a 10-fold lower potency for SK_{Ca} channels[316]. In canine mesenteric artery endothelial cells, SKA-31-evoked K_{Ca} currents and membrane hyperpolarization that were sensitive to both TRAM-34 and the SK_{Ca} channel inhibitor, UCL 1684[124]. SK_{Ca} channels have also been shown to contribute to the effects of SKA-31 on arterial diameter as block of SK_{Ca} channels by apamin or UCL1684, inhibited the ability of SKA-31 to dilate myogenically active rat cremaster, middle cerebral arteries[314], and pressurized mouse mesenteric arteries[501]. In the present study, SKA-31-evoked responses were abolished by TRAM-34 and NS 1680 and were shown to be endothelium-independent, the role of SK_{Ca} channels was not investigated.

Bolus doses of SKA-31 caused immediate and transient reductions in blood pressure in anesthetized pigs[503] and conscious mice and dogs[121,124,316]. This effect was also seen in mice lacking SK_{Ca} channels[204] and mouse models of hypertension[121], but was lost in mice lacking IK_{Ca} channels[121]. These effects of SKA-31 are hypothesized to be due to direct actions on blood vessels and *in vitro* studies have largely focused on its ability to cause dilation in isolated arteries. However, other than the demonstration that SKA-31 does dilate the coronary vasculature in isolated hearts[315,502], there is limited information on its effects in intact vascular beds thus, the use of the rat perfused mesenteric vascular bed in this chapter allowed for the novel investigation of

SKA-31's effects at the level of the intact mesenteric bed. This is an important gap in our knowledge as in anesthetized pigs, vascular conductance in coronary and carotid arteries was increased in response to SKA-31 but renal conductance was unaffected[503], suggesting that its effects may not be uniform across the entire vasculature.

In the perfused mesenteric bed, SKA-31 (10 µM) reduced sympathetic vasoconstriction in a TRAM-34- and NS 6180- sensitive manner but its effects were NO- and endothelium-independent. Also, inhibition of vasoconstriction was observed in the presence of nifedipine, to block the contribution of L-type VOCCs to vasoconstriction. This was an unexpected result for two reasons. First, we and others have shown that IK_{Ca} channels are localized on endothelial but not smooth muscle cells of rat mesenteric arteries[118,125,130,151,197]. IK_{Ca} channels have been shown to be present on proliferating vascular smooth muscle cells[173,504–509], with their expression upregulated by growth factors[505,510] but only two reports describe IK_{Ca} channels in vascular smooth muscle cells of intact arteries, one in human chorionic plate arteries[511] and the other in rat middle cerebral arteries[512], and neither demonstrated a functional role for these channels in mediating vasodilation. Furthermore, although NS 6180 and TRAM-34 had no effect on nerve-evoked vasoconstriction, TRAM-34 did enhance noradrenaline-evoked vasoconstriction in the perfused bed in an endothelium-dependent manner, indicating that the myoendothelial feedback pathway is functional in this vascular bed. These findings are in contrast to the human skeletal muscle vasculature where myoendothelial feedback plays a significant role in blunting sympathetic vasoconstriction[497].

Second, my data on the effects of SKA-31 on isolated arteries described above, and in the published literature[116,121,124,148,204,314,316,502,503], support the notion that SKA-31 causes vascular relaxation of isolated arteries via endothelium-dependent hyperpolarization of the surrounding

smooth muscle to inhibit L-type VOCC-mediated Ca^{2+} influx. The only report to potentially contradict this notion demonstrates that intraperitoneal injection of SKA-31 reduced mean arterial blood pressure in mice lacking connexin40[316]. This connexin is an essential component of MEGJs in a number of vessels[513,514] thus, the ability of SKA-31 to affect the vasculature in mice lacking this protein suggests that the response is independent of myoendothelial coupling (i.e. not dependent on the transfer of an electrical signal from endothelial to smooth muscle cells), although the mediator of this response was not determined[316].

A possible explanation for the endothelial-independent effects of SKA-31 on nerve-evoked vasoconstriction in the perfused bed versus its predominantly endothelium-dependent effects in isolated arteries, is that SKA-31 activates IK_{Ca} channels on sympathetic nerves to hyperpolarize neuronal membrane potential and reduce noradrenaline release. IK_{Ca} channels are localized on specific neurons in the rat, mouse, guinea-pig and human enteric nervous system[152–156] where they mediate the slow after-hyperpolarization following an action potential but to date, there are no reports of these channels on perivascular nerves. Our lab has previously demonstrated that noradrenaline released by stimulation of perivascular nerves can be measured in the perfusate of the perfused rat mesenteric bed and that those levels can be modulated by pharmacological agents which act as sympathomimetics[438]. Using this approach, I demonstrated that SKA-31 did inhibit noradrenaline overflow and that this effect was prevented by NS 6180. Furthermore, confocal immunohistochemistry using antibodies specific for IK1 channels and tyrosine hydroxylase, the rate-limiting enzyme in catecholamine biosynthesis used to identify sympathetic nerves[498], demonstrated that IK_{Ca} channels are localized to perivascular nerves in mesenteric arteries. While overlay was not possible, there is no parasympathetic innervation of rat mesenteric arteries and the sensory plexus are sparse and distinct from sympathetic nerves[176,179].

A neuronal site of action for SKA-31 or other SK_{Ca}/IK_{Ca} channel openers has not previously been considered. The lack of effect of TRAM-34 on sympathetic vasoconstriction suggests that IK_{Ca} channels do not play a role in regulating noradrenaline release under normal conditions. However, stimulation of perivascular nerves leads to depolarization of the neuronal membrane potential which causes Ca^{2+}-influx through neuronal VOCCs (N-, P- and Q-type[440]) and thus, SKA-31 may act by sensitizing neuronal IK_{Ca} channels to the increased levels of Ca^{2+}. L-type VOCCs are co-localized with BK_{Ca} channels in smooth muscle cells[152], and both with BK_{Ca} and SK_{Ca} channels in central nervous system neurons[515] but the potential for such interactions between IK_{Ca} channels and VOCCs in perivascular sympathetic nerves has yet to be investigated. Interestingly, TRPC3 channels, which have been identified as a mediator of Ca^{2+} influx for activation of SK_{Ca} and IK_{Ca} channels in endothelial cells[256,257,516,517], have also been localized to perivascular nerves in mesenteric arteries[256], Their role has not been determined but they could serve as an important Ca^{2+} source for these neuronal IK_{Ca} channels.

To conclude, in isolated mesenteric arteries, endothelial IK_{Ca} channels are crucial for engagement of the endothelium through myoendothelial feedback to limit agonist-evoked vasoconstriction but these channels do not appear to play a functional role in modulating nerve-evoked vasoconstriction in the perfused mesenteric bed. Nevertheless, activation of IK_{Ca} channels by SKA-31 does limit vasoconstriction most likely via inhibition of noradrenaline release from sympathetic nerves. Targeting IK_{Ca} channels as a novel strategy for treatment and/or prevention of cardiovascular diseases has been proposed and SKA-31, a IK_{Ca} channel activator, has been suggested as an agent which may improve endothelial function[121,148,316]. For example, SKA-31 was able to enhance acetylcholine-mediated dilations in pressurized carotid arteries from mice lacking eNOS, indicating that increased IK_{Ca} channel activity may be able to overcome impaired

endothelium-dependent vasodilation due to the absence of NO[148]. However, although SKA-31 can cause endothelium-dependent relaxation of rat isolated mesenteric arteries, in the perfused mesenteric bed, its primary action appears to be inhibition of noradrenaline release from sympathetic nerves. Thus, while IK_{Ca} channels may be a valid target to limit vasoconstriction, increased activation of these channels may involve both endothelium-dependent and -independent actions. The data presented in this chapter provides the first description of a role for IK_{Ca} channels in modulating release of noradrenaline from perivascular sympathetic nerves and indicates that targeting of these channels could provide a new approach to reducing vasoconstriction in conditions associated with increased sympathetic drive, such as hypertension[174,499,500].

Chapter 4: Effects of activators of SK_{Ca} and IK_{Ca} channels on agonist-induced O_2^- production and vasoconstriction in isolated mesenteric arteries

4.1: Introduction

As described in **Chapter 1**, endothelium-derived NO plays a vital role in regulating normal vascular function and endothelial damage associated with risk factors for cardiovascular diseases, such as diabetes, hypertension and atherosclerosis, is characterized by increased production of O_2^- and decreased NO bioavailability[268,328–336]. Attempts to reduce O_2^- levels through the use of dietary anti-oxidants, such as vitamins B, C and E,` have failed in clinical trials[337–342], most likely due to their inability to reach a high enough concentration in the vasculature and/or within endothelial cells. Therefore, there is the need to identify new targets for therapeutic approaches to reduce O_2^- levels and enhance NO bioavailability in cardiovascular disease settings.

Numerous changes have been proposed to contribute to endothelial dysfunction but a common mechanism appears to be enhanced O_2^- production leading to decreased NO bioavailability and NOS expression[518], and increased synthesis of endothelium-derived contractile factors such as thromboxanes[518–521]. Elevated O_2^- levels rapidly diminish NO bioavailability and generate excessive amounts of $ONOO^-$, an oxidant that accelerates cardiovascular disease progression by causing structural damage to vascular cells, inhibiting prostacyclin synthesis, disrupting NO signaling and increasing O_2^- production through oxidation of the endothelial NOS co-factor, BH_4; in the absence of BH_4, endothelial NOS becomes uncoupled and reduces molecular oxygen to generate O_2^- rather than NO[266–270,521].

Treatment of hypercholesteraemic and diabetic animals with statins or angiotensin receptor blockers[522,523] reduces the activity and expression of NADPH oxidase and "recouples" endothelial NOS by preventing BH_4 oxidation[524,525]. Statins and angiotensin receptor blockers have also been shown to improve endothelial function and to reduce the incidence of cardiovascular events in

patients with cardiovascular diseases[526,527]. Thus, the development of new drugs which possess indirect antioxidant properties, mediated by the enhancement of NO production and simultaneous inhibition of O_2^- generation (e.g. from NADPH oxidase), is an attractive proposition for cardiovascular disease prevention and therapy. I propose that drugs which activate SK_{Ca} and IK_{Ca} channels may fall into this category.

NO bioavailability is determined by the balance between production of NO by endothelial NOS and its interaction with O_2^-. In numerous disease models, reduced NO bioavailability is associated with upregulation of expression and activity of NADPH oxidase[332–336,383,528], a voltage-sensitive enzyme which generates O_2^- by transferring electrons from cytosolic NADPH to extracellular oxygen[126,367,368,371,372,374,386–388,529]. In isolated endothelial cells, membrane depolarization activates NADPH oxidase, either directly or via Akt[387,529]. In this setting, drugs which open K_{ATP} channels attenuate both the membrane depolarization and O_2^- production, indicating that endothelial cell membrane potential can regulate O_2^- production[387,529].

As discussed previously, opening of SK_{Ca} and IK_{Ca} channels mediates vasodilation through hyperpolarization of the endothelial membrane potential which spreads to surrounding smooth muscle cells via MEGJs[80,84,85,100,116–131,148–151,197,202]. Activators of these channels have been shown to elicit NO-mediated relaxation and to enhance NO production[116,126,128,131,203–205]. Also, in **Chapter 2**, I demonstrated that the SK_{Ca} channel opener CyPPA, elicits endothelium-mediated relaxation in isolated rat mesenteric arteries and enhances shear stress-induced inhibition of nerve-evoked vasoconstriction in the perfused mesenteric bed, both through a NO-dependent mechanism. Our lab has previously shown that endothelial depolarization inhibits agonist-evoked, NO-mediated relaxation of rat basilar arteries, an effect that was overcome by the K_{ATP} channel opener, pinacidil[418]. Furthermore, we and others, have demonstrated that the membrane potential of

endothelial cells in tail[530] and mesenteric arteries[531–533] from cardiovascular disease rat models are depolarized compared to controls. We have also shown NO-mediated relaxations are attenuated in these depolarized vessels and that these effects can be reversed by the SK_{Ca}/IK_{Ca} channel opener, 1-EBIO[534]. Thus, it is possible that the opening of endothelial K_{Ca} channels to elicit hyperpolarization could lead to a decrease in O_2^- production by voltage-sensitive NADPH oxidase and thus, an increase in NO bioavailability.

The goal of this, and the following chapter, was to further explore the relationship between endothelial K_{Ca} channels, O_2^- production and diameter in intact arteries, and to test the hypothesis that *pharmacological activators of endothelial K_{Ca} channels can reduce vascular O_2^- production and enhance NO-mediated modulation of vasoconstriction.*

To test this hypothesis, I utilized isolated endothelium-intact mesenteric resistance arteries mounted in a pressure myograph coupled to a fluorescence detection system (IonOptix) for simultaneous measurement of changes in arterial diameter and O_2^- production using dihydroethidium (DHE), a dye that interacts with O_2^- to form 2-hydroxyethidium (EOH) which fluoresces when bound to deoxyribonucleic acid (DNA)[349,535–540]. The effects of CyPPA and SKA-31 on phenylephrine-evoked O_2^- production and vasoconstriction were assessed to investigate if increased activation of endothelial K_{Ca} channels can modulate vascular O_2^- levels and endothelial modulation of arterial diameter.

I chose to use this approach as vasoconstriction of mesenteric arteries elicited by α_1-adrenoceptor agonists has been associated with increases in $O_2^{-[347-349]}$ and, as stated earlier, a primary role of the endothelium *in vivo* is to modulate vasoconstriction. Also, constriction of rat mesenteric arteries to phenylephrine is modulated by endothelium-derived NO[130,197]. Thus,

changes in O_2^- levels may lead to changes in the bioavailability of NO and subsequently, alterations in phenylephrine-evoked vasoconstrictor responses.

4.2: Methods and materials

See **Appendix: Drugs and chemicals** for a list of the drugs and chemicals used.

4.2.1: Simultaneous assessment of O_2^- production and changes in arterial diameter in intact arteries

Real-time assessment of changes in O_2^- production and diameter were carried out in mesenteric resistance arteries loaded with DHE and mounted in a pressure myograph (Danish Myo Technology (DMT) 110P model, Aarhus, Denmark) placed on an inverted microscope (AE30-31, Motic Instruments Inc. Canada) fitted with an Eiscopic-Fluorescence Attachment (EF-INV-11).

4.2.1.1: Pressure myography. Leak-free segments of third or fourth order mesenteric arteries (2-3 mm in length) were cleaned of adhering connective tissue and mounted between two glass cannulae in an arteriograph chamber (DMT 110P model, Aarhus, Denmark) under conditions of no luminal flow. The glass cannulae (borosilicate glass with OD of 1.2 mm and ID of 0.69 mm) were fabricated using a Flaming/Brown micropipette puller (Model P87; Sutter Instruments, Novato, USA) and flame polished. In some experiments, the endothelium was removed by gently rubbing the lumen of individual arteries with a hair.

The arteriograph was placed on the stage of an inverted microscope (AE30-31, Motic Instruments Inc. Canada). Vessels were maintained in Krebs buffer at 37°C (pH 7.4) continuously bubbled with 95% O_2, 5% CO_2. Intravascular pressure was maintained via a pressure controller (DMT 110P model, Aarhus, Denmark) and vessel images were captured using a CCD video camera (CFA300 Cell Framing Adapter, Ionoptix MyoCam). Vessels were loaded with DHE (see below) and upon excitation at 535 nm, fluorescence of EOH bound to DNA at 610 nm was captured

via an Eiscopic-Fluorescence Attachment (EF-INV-11) and an IonOptix Fluorescence System Interface, and recorded using IonWizard 6.2 (IonOptix, Massachusetts, USA) software.

To avoid the development of myogenic tone, arterial segments were held at an intravascular pressure of 60 mmHg (mean resting diameter at this pressure was $208.45 \pm 6.3 \mu m$, n=5) for 20 minutes before being tested for viability through the addition of phenylephrine (3 μM) to cause constriction, and acetylcholine (3 μM) to induce endothelium-dependent vasodilation; vessels in which acetylcholine elicited >90% reversal of phenylephrine-induced vasoconstriction were considered to have an intact endothelium and those that elicited <10% relaxation were deemed to be endothelium denuded. Vessels which did not meet these criteria were discarded.

<u>4.2.1.2</u>: Use of DHE to assess O_2^- production in intact mesenteric arteries. Solutions of DHE (10 mM) were freshly made in dimethyl sulfoxide (DMSO)[349,535,536] prior to each experiment in a darkened room and experiments were carried out in the same darkened room. After viability had been determined through addition of phenylephrine and acetylcholine, DHE (10 μM) was added to the tissue bath and arteries were incubated for 30 minutes[349,535,536]. Vessels were then washed and allowed to recover for 15 minutes before cumulative concentration-response curves to phenylephrine (0.01-10 μM) were constructed[347–349]. After washing, pharmacological reagents were added to the tissue bath for 15 minutes, after which time a second concentration-response curve to phenylephrine was constructed. At the end of each concentration-response curve to phenylephrine, acetylcholine (3 μM) or sodium nitroprusside (1 μM) was added to demonstrate that the vessel remained functional. For some experiments, pharmacological agents were added to the tissue bath in the absence of phenylephrine, and changes in florescence intensity were measured over a 15-30 minute time period. The viability of these vessels was then assessed by addition of phenylephrine (10 μM) followed by acetylcholine (3 μM).

For concentration-response curves to phenylephrine, vessel diameter and DHE fluorescence intensity were recorded simultaneously and expressed as a % of their respective control maximum. For experiments where basal O_2^- production was measured over a period of 15-30 minutes, raw values of fluorescence intensity were plotted as these experiments were performed in individual arteries. For all experiments, phenylephrine increased O_2^- production and vasoconstriction in a concentration-dependent manner ($p<0.05$).

4.2.2: Perfused mesenteric vascular bed

The mesenteric bed was perfused via the superior mesenteric artery as previously described[438]. Briefly, the mesenteric vascular bed was separated from the intestine and the superior mesenteric artery cleaned of connective tissue, cannulated with a blunted hypodermic needle (20 G), secured with 5-0 surgical silk (Ethicon) and flushed with Krebs buffer to remove blood. The vascular bed was placed on a wire mesh in a warm chamber and perfused with oxygenated Krebs buffer at a constant flow rate of 5 mlmin^{-1} (37°C, bubbled with 95% O_2/5% CO_2). A short length of plastic tubing was placed around the needle to ensure that it did not come into contact with the wire mesh. Changes in perfusion pressure were monitored via an in-line pressure transducer (AD instruments, Colorado) and recorded via a PowerLab data acquisition system using Chart 5.0 software (AD Instruments, Colorado).

4.2.2.1: Responses to stimulation of perivascular nerves. Electrodes were attached to the cannulating needle and to the wire mesh to allow electrical field stimulation using a Grass SD9 stimulator (Grass Technologies, USA). Following an equilibration period of 30 minutes, a single stimulation (30 Hz, 90 V, pulse width 1 millisecond, 30 seconds) was applied to assess the viability of the preparation. After a further 10 minutes, a frequency-response curve was constructed by stimulating the preparation at 20-40 Hz (90 V, pulse width 1 millisecond, 30 seconds) at 10 minute

intervals[188]. The effects of agents on nerve-evoked vasoconstriction were assessed by perfusing the drugs through the lumen of the preparation for 20 minutes prior to constructing a second frequency-response curve. A third and fourth frequency-response curve were constructed following perfusion of different drug combinations.

Nerve-evoked responses recorded in the perfused mesenteric vascular bed are shown as normalized values. Changes in perfusion pressure were normalized to the maximum control response (%) as is convention in these types of experiments. For all frequency response curves, electrical stimulation caused frequency-dependent increases in perfusion pressure ($p<0.05$).

4.2.3: Statistics

All data are expressed as mean ± SEM, n rats used. For repeated measures, two-way ANOVA followed by either a Tukey's multiple comparison post-hoc test (used when there were more than two experimental groups) or Šídák method post-hoc test (used when there was two experimental groups) was performed. An ordinary one-way ANOVA followed by a Tukey's multiple comparisons post-hoc test was performed for **Figure 4.9b** and an unpaired *t*-test was used for **Figure 4.11**. $p<0.05$ was considered statistically significant in all cases.

4.3: Results

4.3.1: Characterization of phenylephrine-induced O_2^- production and vasoconstriction in mesenteric resistance arteries

Application of the α_1-adrenoceptor agonist phenylephrine (0.01-10 μM) to mesenteric arteries resulted in concentration-dependent increases in O_2^- production and vasoconstriction ($p<0.05$); phenylephrine is denoted as PE in the figures of this chapter. The fluorescence intensity returned to baseline after arterial relaxation through acetylcholine or SNP, indicating that DHE's interaction with O_2^- is reversible. Representative traces showing changes in O_2^- and diameter in response to increasing concentrations of phenylephrine are shown in **Figure 4.1a,** and mean

diameter changes evoked by phenylephrine (0.01-10 μM) are shown as absolute values in **Figure 4.1b.** Two consecutive concentration-response curves to phenylephrine could be constructed without significant change ($p>0.05$) in either phenylephrine-induced O_2^- production or vasoconstriction (**Figure 4.2a** and **b).** Also, as many of the pharmacological agents used in this study were dissolved in DMSO, phenylephrine-evoked concentration-response curves were constructed in the absence and presence of DMSO (1 in 500 dilution). DMSO had no significant effect on phenylephrine-induced O_2^- production or vasoconstriction ($p>0.05$, **Figure 4.2c and d**).
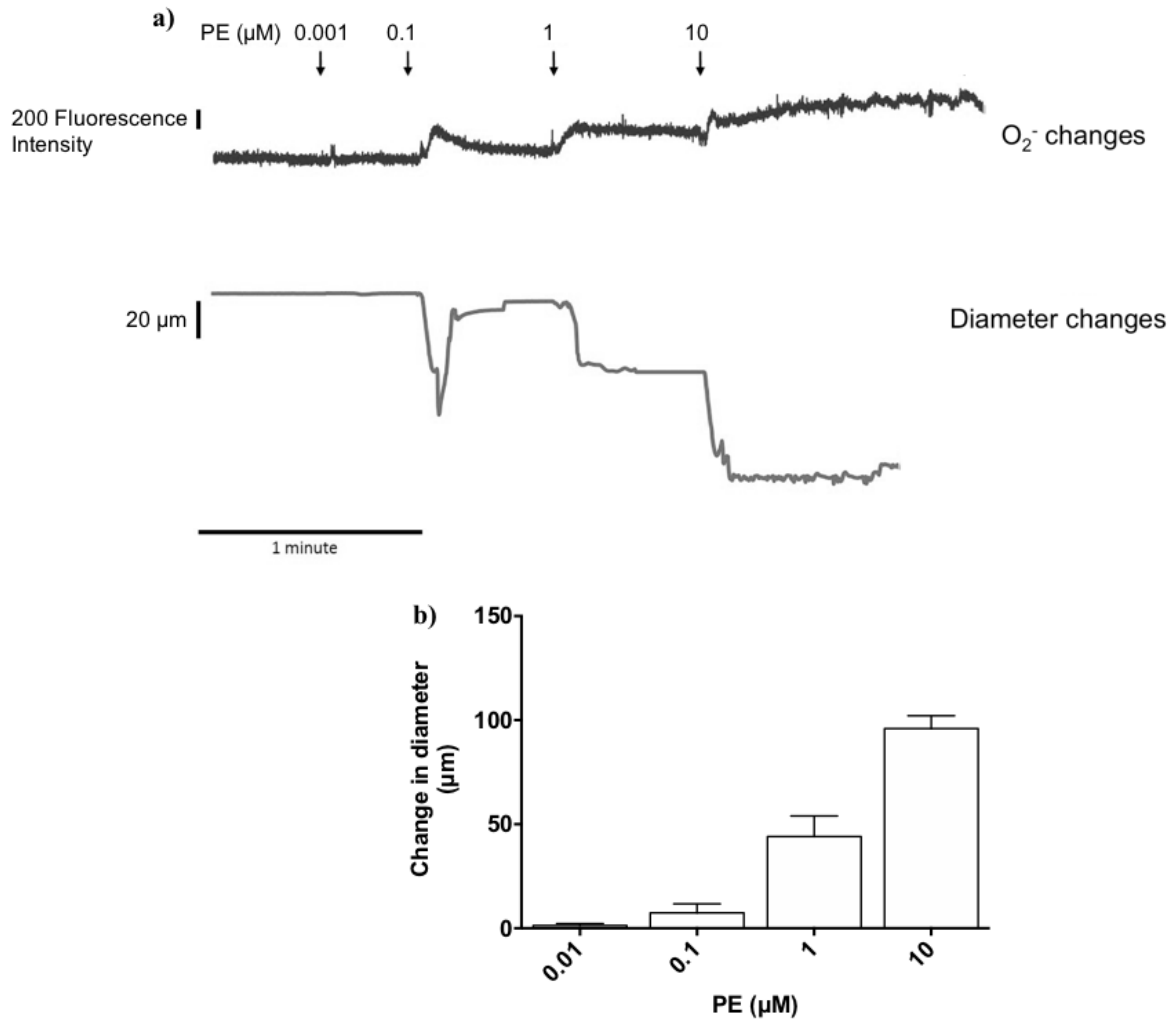
Figure 4.1: Characterization of phenylephrine-induced changes in diameter and O₂⁻ production in rat mesenteric arteries. a) Representative trace showing simultaneous recording of phenylephrine-induced O_2^- production and vasoconstriction in an endothelium-intact rat mesenteric resistance artery mounted in the pressure myograph. **b)** Mean changes in diameter in endothelium-intact rat mesenteric artery segments evoked by phenylephrine; n=6.
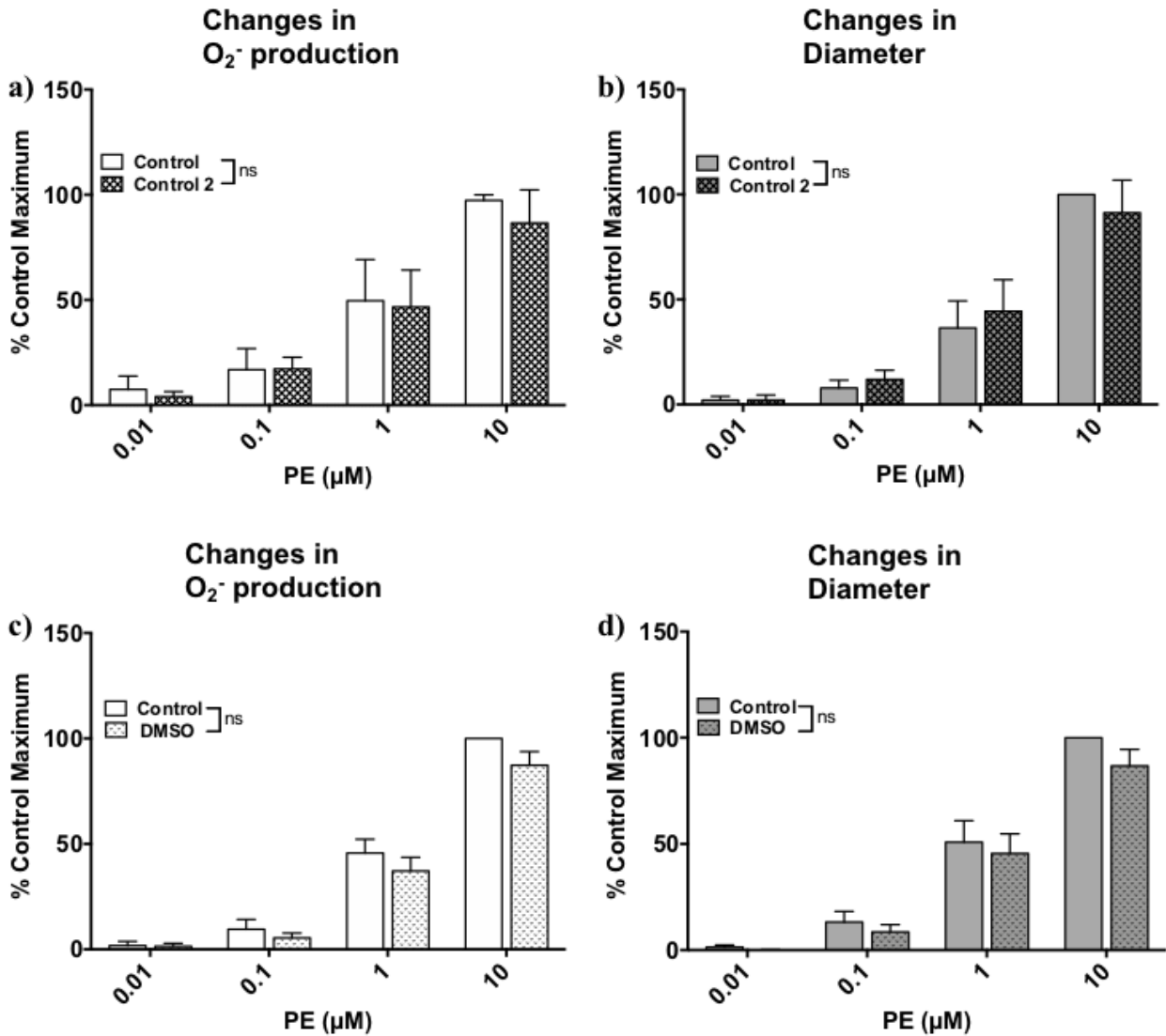
Figure 4.2: **Phenylephrine-induced O_2^- production and vasoconstriction is time-independent and unaffected by DMSO in rat mesenteric arteries.** Mean data showing phenylephrine-induced O_2^- production **a)** during two consecutive concentration-response curves or **c)** in the absence and presence of DMSO (1 in 500 dilution)) and phenylephrine-induced vasoconstriction **b)** during two consecutive concentration-response curves or **d)** in the absence and presence of DMSO (1 in 500 dilution) in endothelium-intact rat mesenteric artery segments. Values are presented as mean ± SEM, **a, b)** n=4 and **c, d)** n=5; two-way repeated-measures ANOVA.

Phenylephrine is a α_1-adrenoceptor agonist and so the α_1-adrenoceptor antagonist prazosin was used to demonstrate that the observed effects of phenylephrine on arterial diameter and O_2^- production were mediated by this receptor. In endothelium-intact arteries, prazosin (1 µM) abolished both phenylephrine-induced O_2^- production ($p<0.05$; **Figure 4.3a)** and vasoconstriction ($p<0.05$; **Figure 4.3b**).
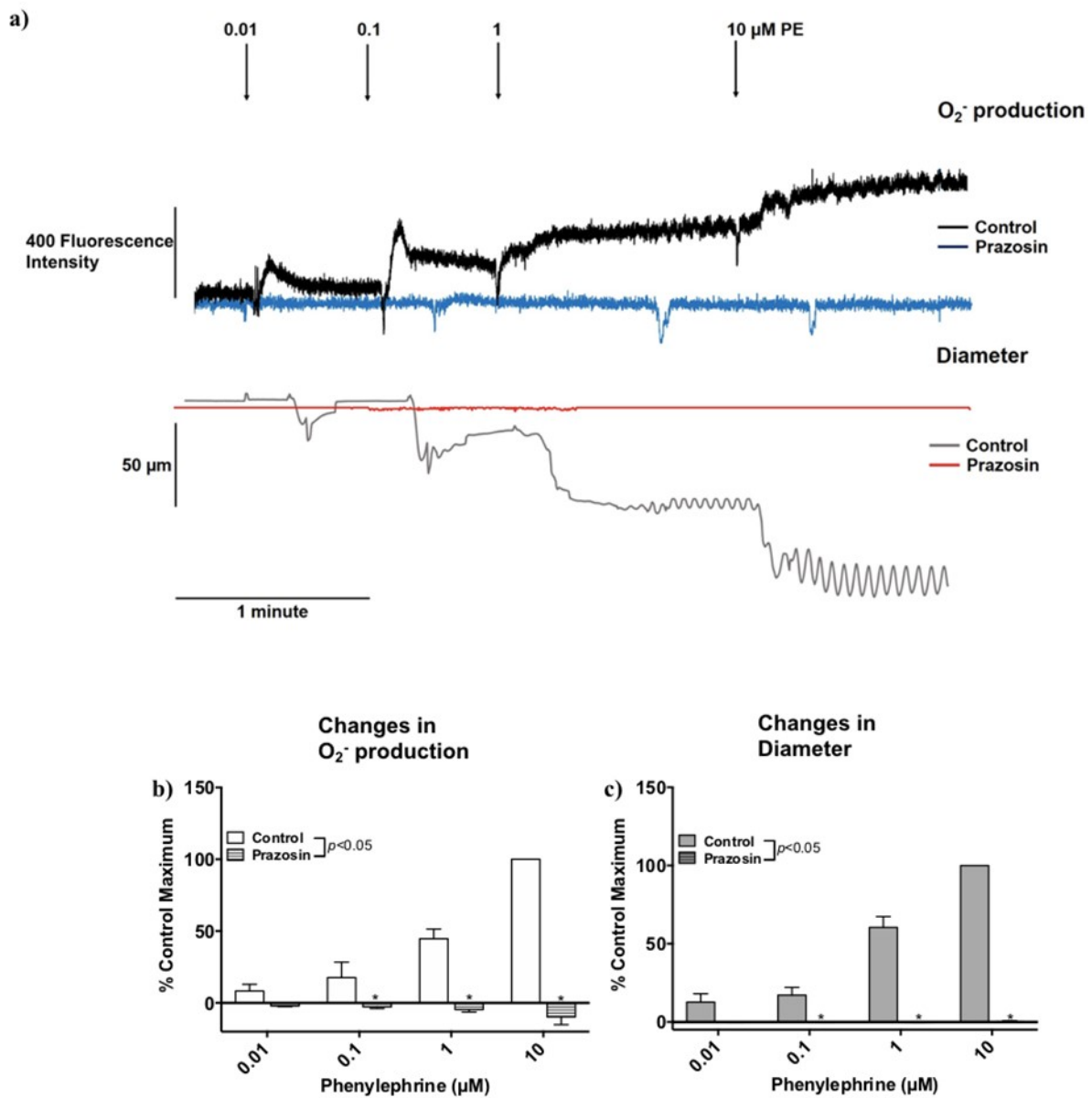
Figure 4.3: Antagonism of α₁-adrenoceptors abolishes phenylephrine-induced O₂⁻ production and vasoconstriction. a) Representative trace showing phenylephrine-induced O₂⁻ production and vasoconstriction in the absence and presence of prazosin (1 μM) in an endothelium-intact rat mesenteric artery segment. Mean data showing phenylephrine-induced **b)** O₂⁻ production and **c)** vasoconstriction in the absence and presence of prazosin (1 μM) in endothelium-intact rat mesenteric artery segments. Values are presented as mean ± SEM, n=4. * denotes $p<0.05$ from control; two-way repeated-measures ANOVA.

To demonstrate that modulation of phenylephrine-evoked increases in O₂⁻ levels can be detected by DHE fluorescence measurements, the effects of apocynin, a NADPH oxidase

inhibitor[541–543] and/or O_2^- scavenger[544], the O_2^- scavengers 1-oxyl-2,2,6,6-tetramethyl-4-hydroxypiperidine (tempol) and SOD, on responses to phenylephrine were investigated. Apocynin (20 μM) significantly reduced phenylephrine-evoked O_2^- production ($p<0.05$, **Figure 4.4a**), and vasoconstriction ($p<0.05$, **Figure 4.4b**). The O_2^- scavengers tempol (300 μM) and SOD (50 U/ml), each significantly reduced phenylephrine-induced O_2^- production ($p<0.05$, **Figure 4.5a** and **c**) but did not affect phenylephrine-induced vasoconstriction ($p>0.05$, **Figure 4.5b** and **d**).

The use of scavengers shows that phenylephrine-evoked changes in O_2^- levels can be detected in these experiments. However, although vasoconstriction to the α_1-adrenoceptor agonist phenylephrine, is accompanied by production of O_2^-, this radical may not be necessary for smooth muscle contraction as proposed previously[349].
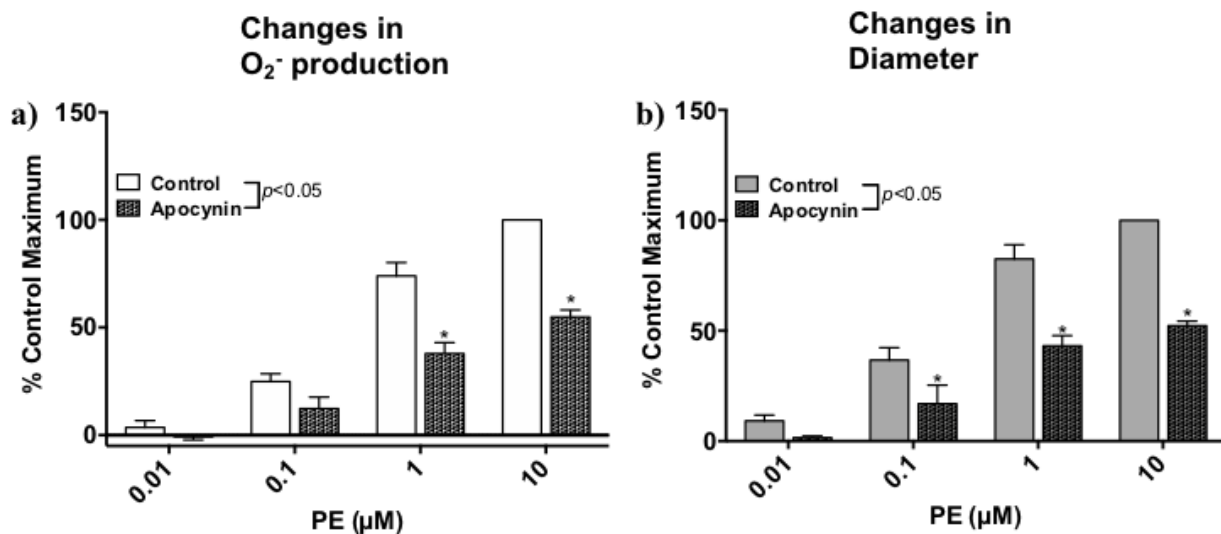
Figure 4.4: NADPH oxidase inhibition and/or a O_2^- scavenging significantly reduces phenylephrine-induced O_2^- production and vasoconstriction. Mean data showing phenylephrine-induced **a)** O_2^- production and **b)** vasoconstriction in the absence and presence of apocynin (20 μM) in endothelium-intact rat mesenteric artery segments. Values are presented as mean ± SEM. n=5. * denotes $p<0.05$ from control; two-way repeated-measures ANOVA.
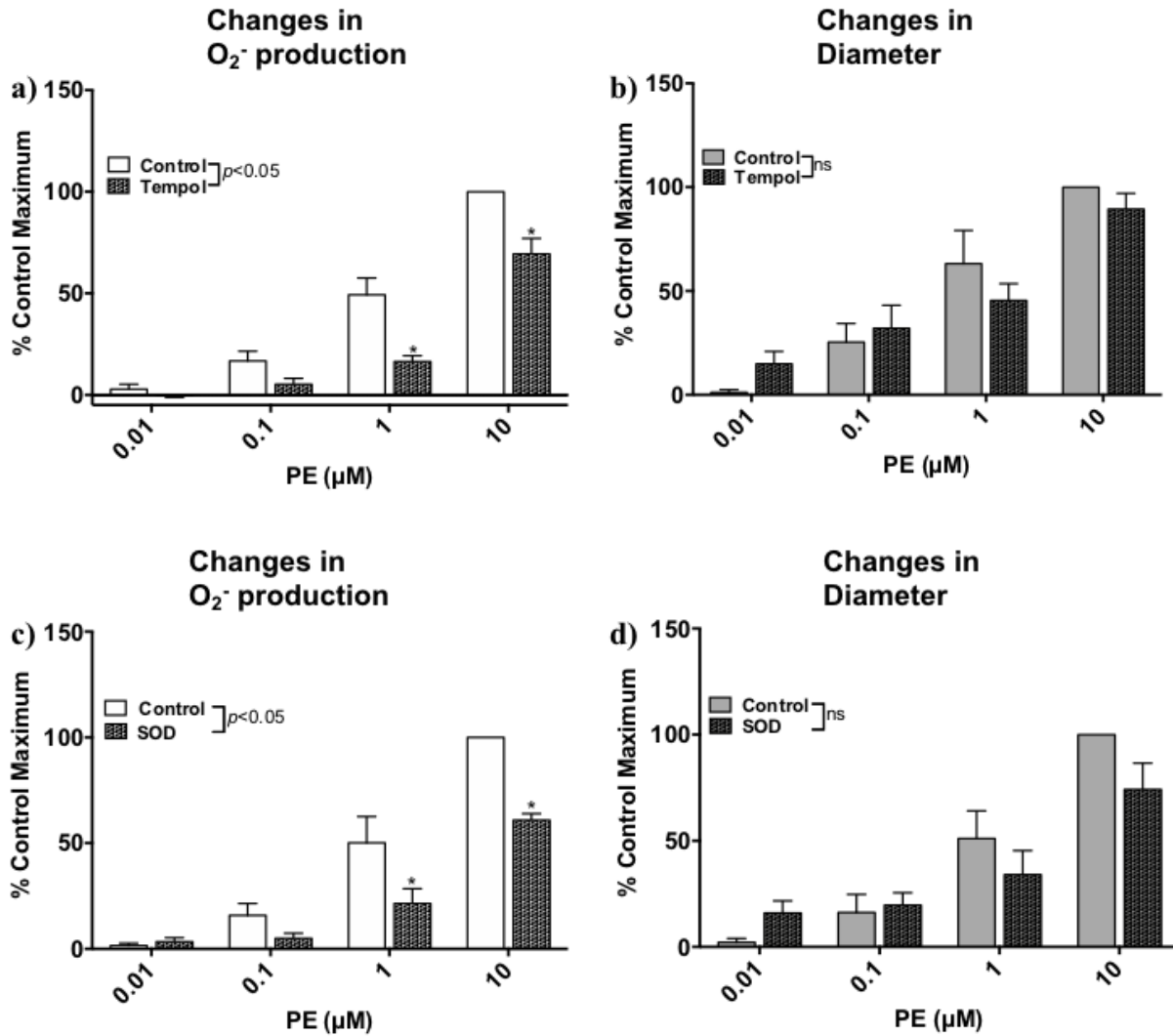
Figure 4.5: Tempol and SOD reduce phenylephrine-induced O_2^- production but not vasoconstriction. Mean data showing phenylephrine-induced O_2^- production in the absence and presence of **a)** tempol (300 μM) or **c)** SOD (50 U/ml) and phenylephrine-induced vasoconstriction in the absence and presence of **b)** tempol (300 μM) or **d)** SOD (50 U/ml) in endothelium-intact rat mesenteric artery segments. Values are presented as mean ± SEM, n=5. * denotes $p<0.05$ from control; two-way repeated-measures ANOVA.

4.3.2: Role of NO in phenylephrine-induced O_2^- production and vasoconstriction in mesenteric resistance arteries

The interaction between NO and O_2^- to form $ONOO^-$ reduces availability of both radicals[389]. Also, phenylephrine-evoked vasoconstriction in rat mesenteric arteries is modulated by the release of endothelium-derived NO[130,197]. Thus, a decrease in O_2^- levels may enhance NO

119

bioavailability and lead to reduced vasoconstrictor responses.

To determine if reduced NO production affects phenylephrine-induced O_2^- production and vasoconstriction, the NOS inhibitor L-NAME was applied. L-NAME (100 μM) did not affect phenylephrine-induced O_2^- production ($p > 0.05$, **Figure 4.6a**) but, as in previous work[197], did significantly enhance vasoconstriction to phenylephrine ($p < 0.05$, **Figure 4.6b**). These findings indicate that under these conditions, NOS is not a source of O_2^- and that the interaction between NO and O_2^- does not significantly contribute to regulation of phenylephrine-induced increases in O_2^-.
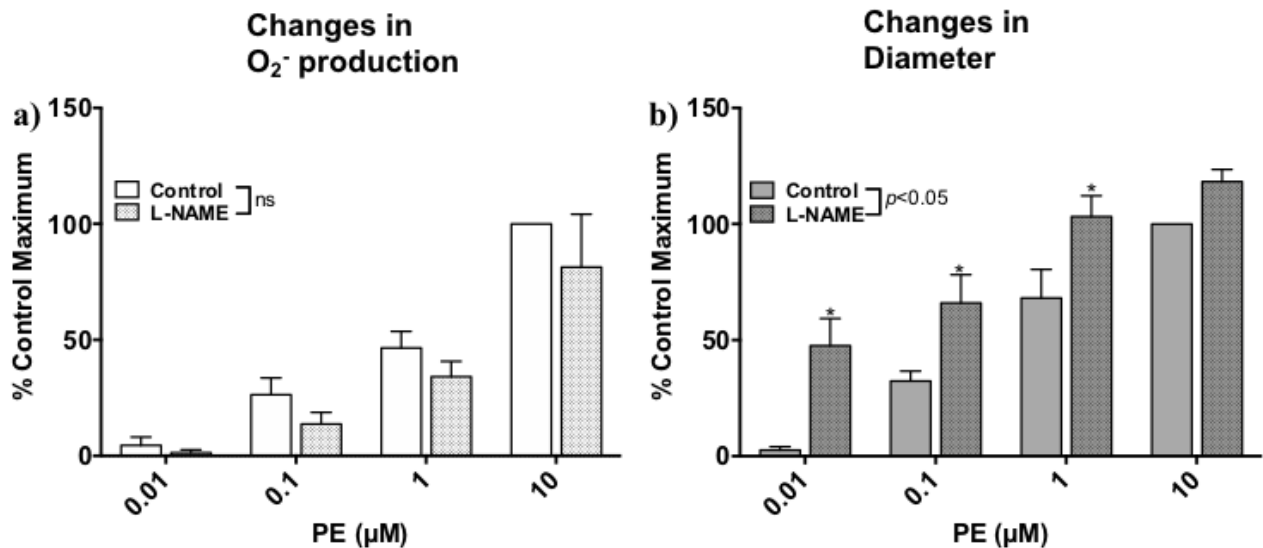
Figure 4.6: Inhibition of NOS does not affect phenylephrine-induced O_2^- production but significantly enhances phenylephrine-induced vasoconstriction. Mean data showing phenylephrine-induced **a)** O_2^- production and **b)** vasoconstriction in the absence and presence of L-NAME (100 μM) in endothelium-intact rat mesenteric artery segments. Values are presented as mean ± SEM, n=5. * denotes $p < 0.05$ from control; two-way repeated-measures ANOVA.

NADPH oxidase is the major source of O_2^{-}[351–356] in the vascular wall and its activity is regulated by membrane potential[126,367,386–388]. Thus, NADPH, an activator of NADPH oxidase[384],

was applied to determine if phenylephrine-evoked increases in O_2^- production could be enhanced. Unexpectedly, NADPH (100 μM) significantly reduced both phenylephrine-induced O_2^- production ($p<0.05$; **Figure 4.7a**) and vasoconstriction ($p<0.05$, **Figure 4.7b**). A possible reason for this finding is that NADPH is also a co-factor for NOS[545], and NADPH has been shown to stimulate NO production[384]. Thus, to determine if the effects of NADPH on phenylephrine-stimulated O_2^- production and vasoconstriction may be due to increased production of NO, the effect of NADPH was also examined in the presence of the NOS inhibitor, L-NAME.

As with NADPH alone, in the presence of NADPH and L-NAME (100 μM), phenylephrine-induced O_2^- production was significantly reduced ($p<0.05$, **Figure 4.7c**). However, whereas L-NAME alone enhanced phenylephrine-induced vasoconstriction and NADPH reduced it, in the presence of L-NAME and NADPH together, vasoconstriction was not different to controls ($p>0.05$, **Figure 4.7d**). These data indicate that NO does not appear to be involved in the NADPH-evoked reductions in O_2^- but may underlie the reduction in phenylephrine-induced vasoconstriction caused by this agent.
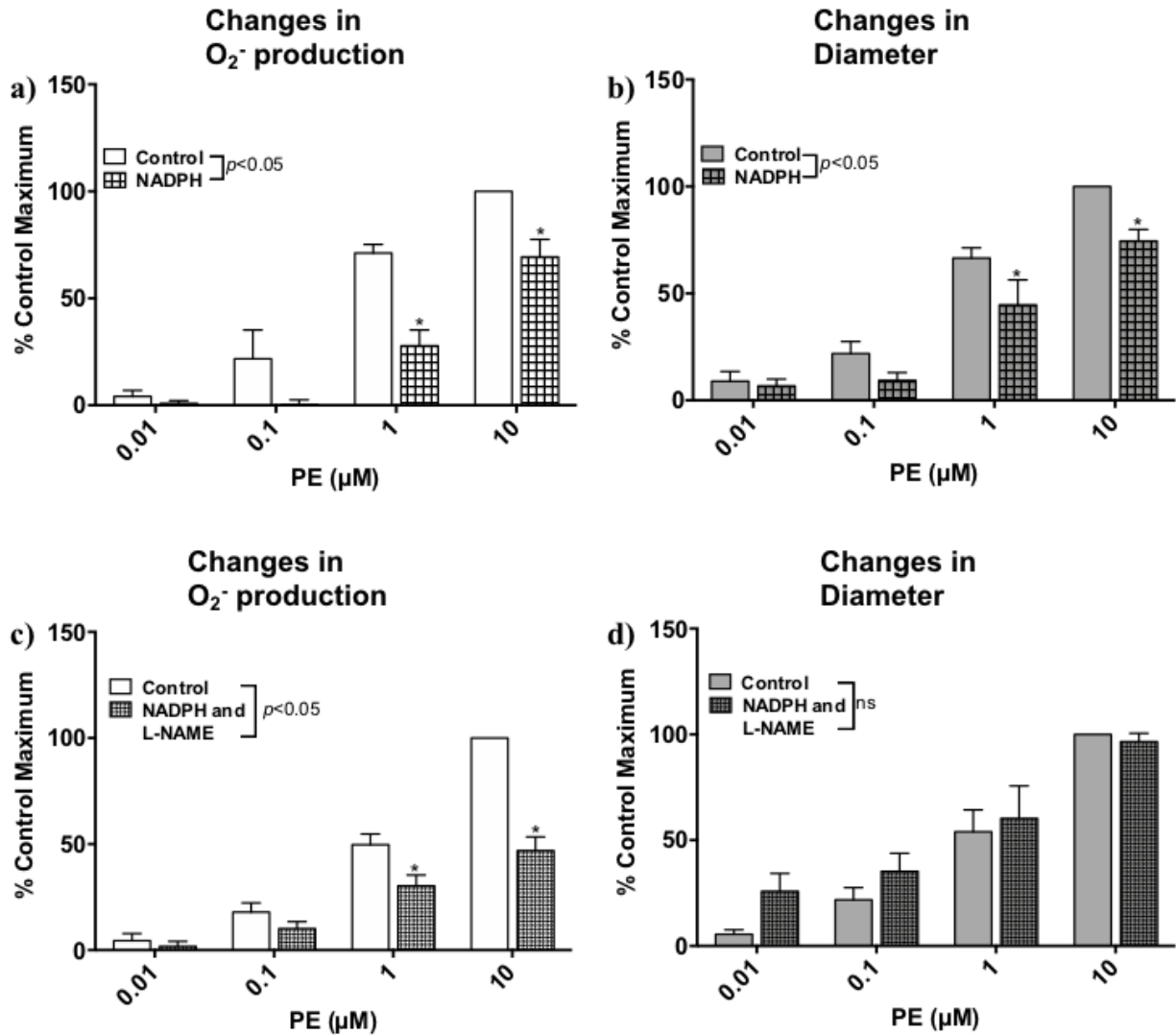
Figure 4.7: NADPH significantly reduces both phenylephrine-induced O_2^- production and vasoconstriction. Mean data showing phenylephrine-induced O_2^- production in the absence and presence of **a)** NADPH (100 μM) or **c)** NADPH (100 μM) with L-NAME (100 μM) and phenylephrine-induced vasoconstriction in the absence and presence of **b)** NADPH (100 μM) or **d)** NADPH (100 μM) with L-NAME (100 μM) in endothelium-intact rat mesenteric artery segments. Values are presented as mean ± SEM, n=5. * denotes $p<0.05$ from control; two-way repeated-measures ANOVA.

To further investigate if the observed effects of NADPH on vascular tone were mediated via a NO-dependent pathway, the effect of NADPH on nerve-evoked vasoconstriction in the perfused mesenteric vascular bed was investigated. The rationale for this approach was that, as

shown in **Chapter 2**, shear stress-induced inhibition of sympathetic vasoconstriction in the rat perfused mesenteric bed is mediated through the release of endothelium-derived NO. As shown in **Chapter 2**, L-NAME (100 µM) significantly enhanced nerve-evoked vasoconstriction at stimulation frequencies of 20 to 40 Hz ($p<0.05$, **Figure 4.8**). NADPH (100 µM) did not significantly affect nerve-evoked vasoconstriction ($p>0.05$, **Figure 4.8)** but in the presence of both L-NAME and NADPH, nerve-evoked responses were significantly reduced compared to L-NAME alone ($p<0.05$, **Figure 4.8**). This observation supports the notion that the actions of NADPH on arterial diameter may be mediated through increased bioavailability of NO.
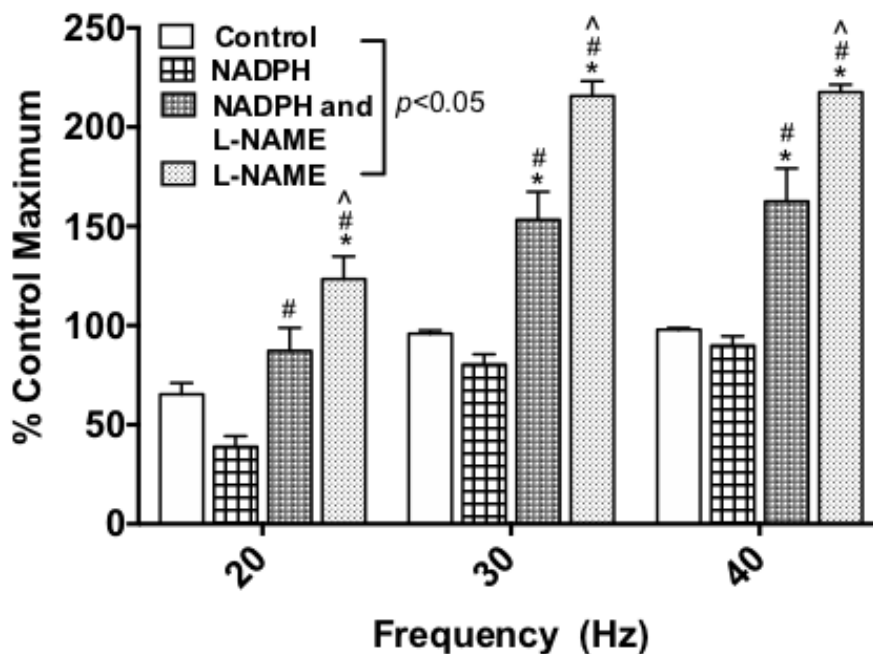
Figure 4.8: Enhancement of nerve-evoked vasoconstriction caused by L-NAME is attenuated by NADPH. Mean frequency-response relationships obtained from endothelium-intact perfused mesenteric beds in the absence and presence of NADPH (100 µM) without and with L-NAME (100 µM) and L-NAME (100 µM) alone. Values are presented as mean ± SEM, n=5. * denotes $p<0.05$ from control, # denotes $p<0.05$ from NADPH (100 µM) and ^ denotes $p<0.05$ from NADPH (100 µM) with L-NAME (100 µM); two-way repeated-measures ANOVA.

NADPH is also a rate limiting co-factor for glutathione reductase[408,411,415–417], the enzyme responsible for catalyzing the generation of glutathione from glutathione disulfide[408,411]. Glutathione is essential for regulation of ROS levels within cells; it scavenges free radicals, such as O_2^-, and through its thiol moiety reduces RNS, such as $ONOO^{-}$[407,408,410]. Thus, NADPH may increase the activity of glutathione reductase to enhance glutathione levels and subsequently, reduce O_2^-. To examine this hypothesis carmustine, a glutathione reductase inhibitor, was used.

Carmustine (50 μM) significantly enhanced basal O_2^- production over the course of its 30-minute incubation ($p<0.05$, **Figure 4.9**) in comparison to control, indicating that the glutathione pathway may actively regulate O_2^- levels in endothelium-intact rat mesenteric arteries. In the absence of carmustine, basal O_2^- production decreased, denoted by negative fluorescence intensity values. Thus, for these experiments, fluorescence intensity was measured before application of carmustine and after 30 minutes, and the difference was plotted to determine change in basal O_2^- production.

NADPH (100 μM) caused a significant reduction of basal O_2^- production ($p<0.05$, **Figure 4.9**). In the presence of carmustine and NADPH together, basal O_2^- was significantly greater than in the presence of NADPH alone ($p<0.05$, **Figure 4.9**) and so it is possible that the observed effects of NADPH on phenylephrine-induced O_2^- production may be due to activation of glutathione reductase.
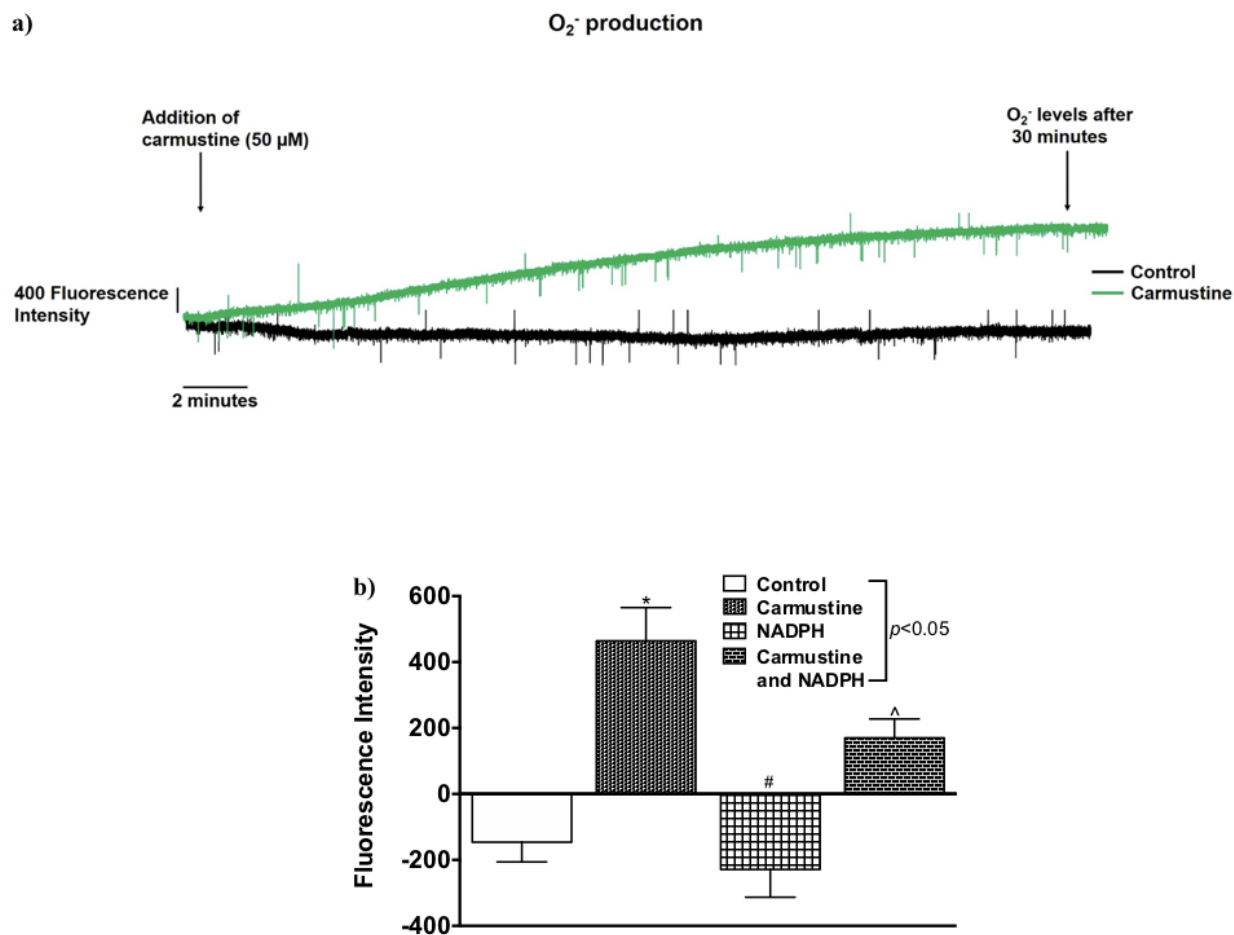
Figure 4.9: Vascular O_2^- levels are regulated by glutathione. a) Representative trace showing changes in basal O_2^- production in an endothelium-intact rat mesenteric artery segment in the absence and presence of carmustine (50 μM) incubated for 30 minutes. **b)** Mean data showing O_2^- production at the end of a period of 30 minutes in the absence and presence of carmustine (50 μM), NADPH (100 μM) and carmustine (50 μM) with NADPH (100 μM) in endothelium-intact rat mesenteric artery segments. Values are presented as mean ± SEM, n=5. * denotes $p<0.05$ from control, # denotes $p<0.05$ from carmustine (50 μM) and ^ denotes $p<0.05$ from NADPH (100 μM); one-way ANOVA.

4.3.3: Effect of inhibitors of SK_{Ca} and IK_{Ca} channels on phenylephrine-induced O_2^- production and vasoconstriction in mesenteric resistance arteries

To examine the role of endothelial SK_{Ca} and IK_{Ca} channels in phenylephrine-induced O_2^- production and vasoconstriction, experiments were conducted using apamin, a SK_{Ca} channel inhibitor, and NS 6180, an IK_{Ca} channel inhibitor.

125

Apamin (500 nM) did not affect either phenylephrine-induced O_2^- production or vasoconstriction ($p > 0.05$, **Figure 4.10a and b**). In contrast, NS 6180 (1 μM) significantly decreased phenylephrine-induced O_2^- production ($p < 0.05$, **Figure 4.10c**) and significantly increased phenylephrine-induced vasoconstriction ($p < 0.05$, **Figure 4.10d**). These effects of apamin and NS 6180 on phenylephrine-evoked vasoconstriction are in line with our previous work showing that IK_{Ca} but not SK_{Ca} channels mediate myoendothelial feedback to limit phenylephrine-evoked vasoconstriction in isolated mesenteric arteries[197]. The reason for the apparent inhibition of phenylephrine-evoked O_2^- production in the presence of NS6180 is unclear. However, during the 15 minute pre-incubation period, NS 6180 significantly enhanced basal O_2^- production in comparison to control ($p < 0.05$, **Figure 4.11**) in line with its ability to evoke endothelial depolarization[116,131].
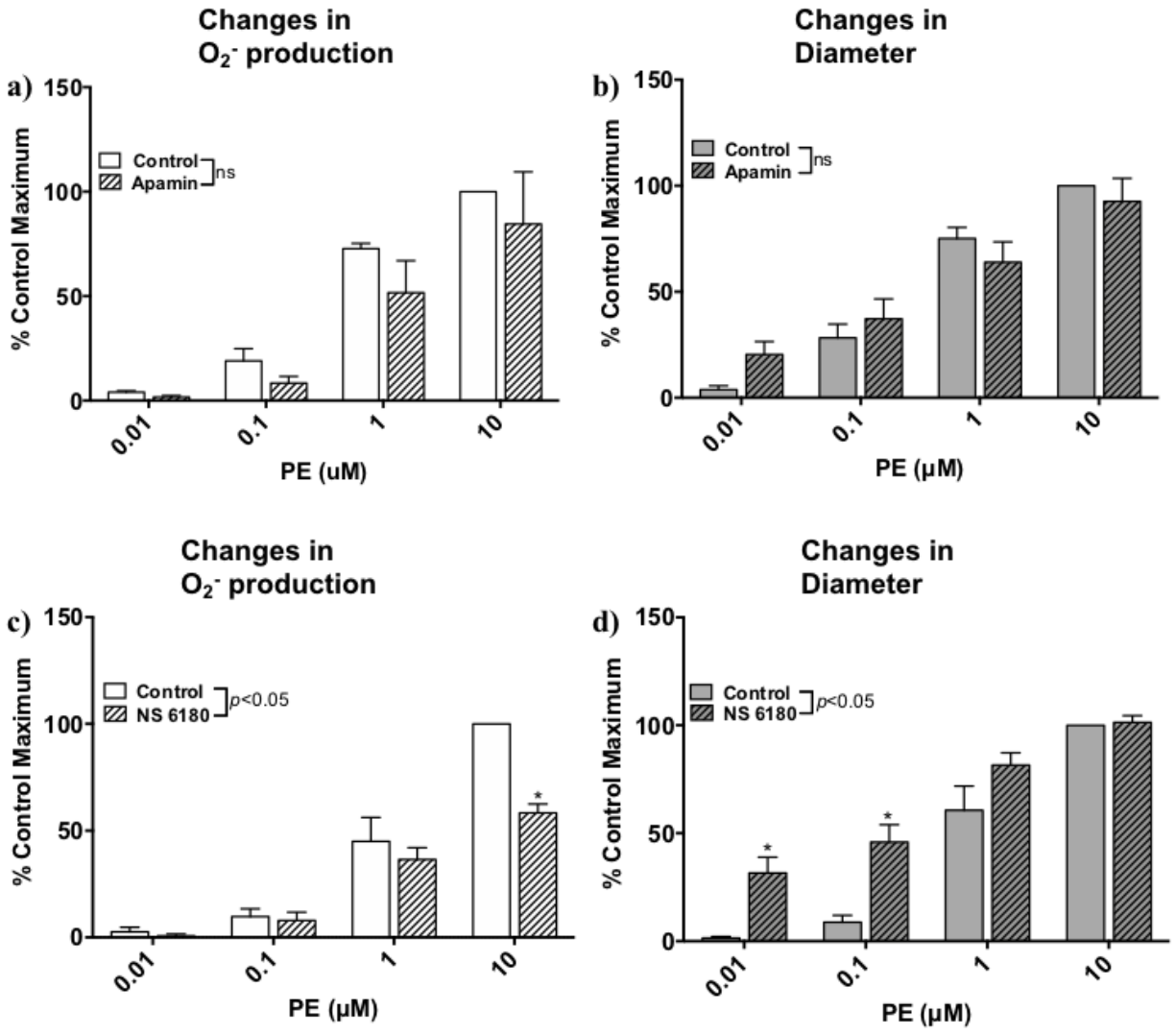
Figure 4.10: Inhibition of IK$_{Ca}$ but not SK$_{Ca}$ channels significantly reduces phenylephrine-induced O$_2^-$ production and enhances phenylephrine-induced vasoconstriction. Mean data showing phenylephrine-induced O$_2^-$ production in the absence and presence of **a)** apamin (500 nM) or **c)** NS 6180 (1 μM) and phenylephrine-induced vasoconstriction in the absence and presence of **b)** apamin (500 nM) or **d)** NS 6180 (1 μM) in endothelium-intact rat mesenteric artery segments. Values are presented as mean ± SEM, n=5. * denotes $p < 0.05$ from control; two-way repeated-measures ANOVA.
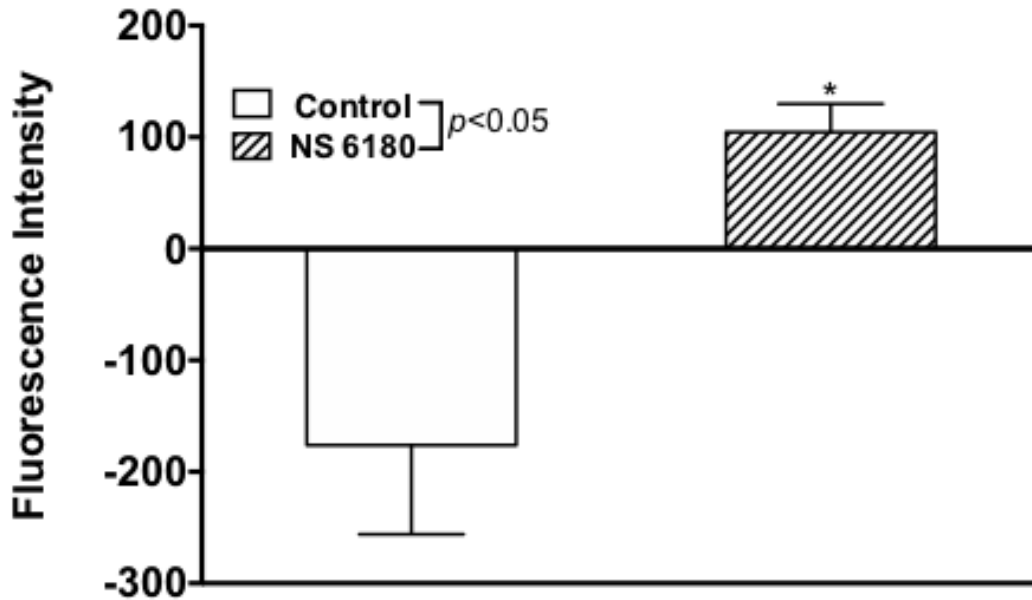
Figure 4.11: IK$_{Ca}$ channel inhibition significantly enhances basal O$_2^-$ production. Mean data showing basal O$_2^-$ production in the absence and presence of NS 6180 (1 µM) after 15 minutes of incubation in endothelium-intact rat mesenteric artery segments. Values are presented as mean ± SEM, n=5. * denotes $p < 0.05$ from control; unpaired t-test.

4.3.4: Effect of SK$_{Ca}$ and IK$_{Ca}$ channel activators on phenylephrine-induced changes in diameter and O$_2^-$ production in mesenteric resistance arteries

CyPPA[313,437] and SKA-31[121,124], activators of SK$_{Ca}$ and IK$_{Ca}$ channels respectively, were used to investigate whether K$_{Ca}$ channel-mediated hyperpolarization can modulate phenylephrine-evoked O$_2^-$ production and vasoconstriction in isolated mesenteric artery segments.

CyPPA (5 µM) significantly reduced phenylephrine-induced O$_2^-$ production ($p < 0.05$; **Figure 4.12a**) but had no effect on phenylephrine-induced vasoconstriction ($p > 0.05$, **Figure 4.12b**). The effect of CyPPA on phenylephrine-evoked O$_2^-$ levels was inhibited by apamin (500 nM); phenylephrine-induced O$_2^-$ production in the presence of CyPPA with apamin was not significantly different from control values ($p > 0.05$, **Figure 4.12c**). The ability of CyPPA to significantly reduce phenylephrine-induced O$_2^-$ production was not altered by inhibition of NOS

with L-NAME (100 µM; $p<0.05$; **Figure 4.13a**), indicating that it is unlikely to be accounted for

by increased production of NO.
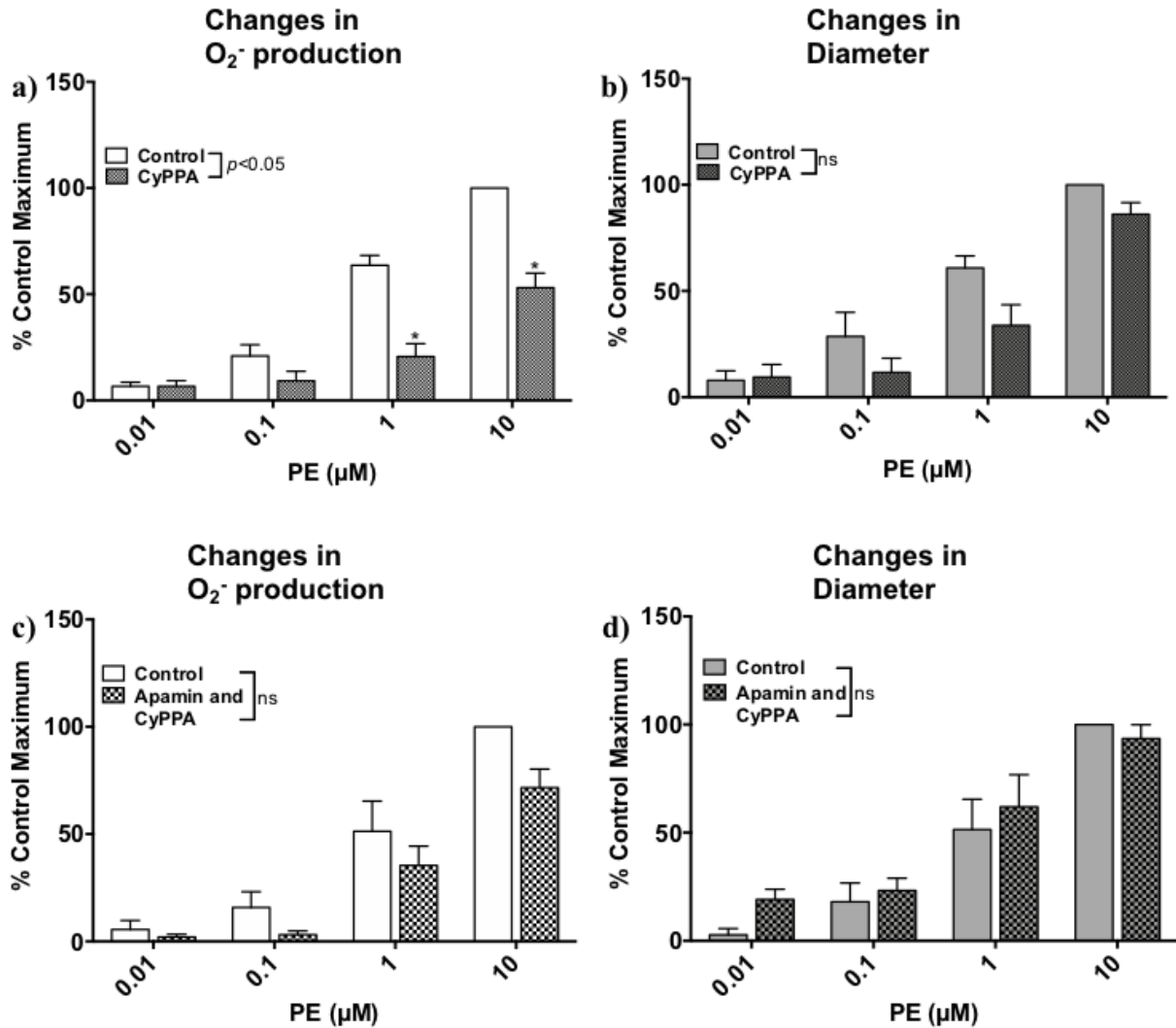
Figure 4.12: CyPPA inhibits phenylephrine-induced O_2^- production but not vasoconstriction. Mean data showing phenylephrine-induced O_2^- production in the absence and presence of **a)** CyPPA (5 µM) or **c)** CyPPA (5 µM) with apamin (500 nM) and phenylephrine-induced vasoconstriction in the absence and presence of **b)** CyPPA (5 µM) or **d)** CyPPA (5 µM) with apamin (500 nM) in endothelium-intact rat mesenteric artery segments. Values are presented as mean ± SEM, n=5. * denotes $p<0.05$ from control; two-way repeated-measures ANOVA.
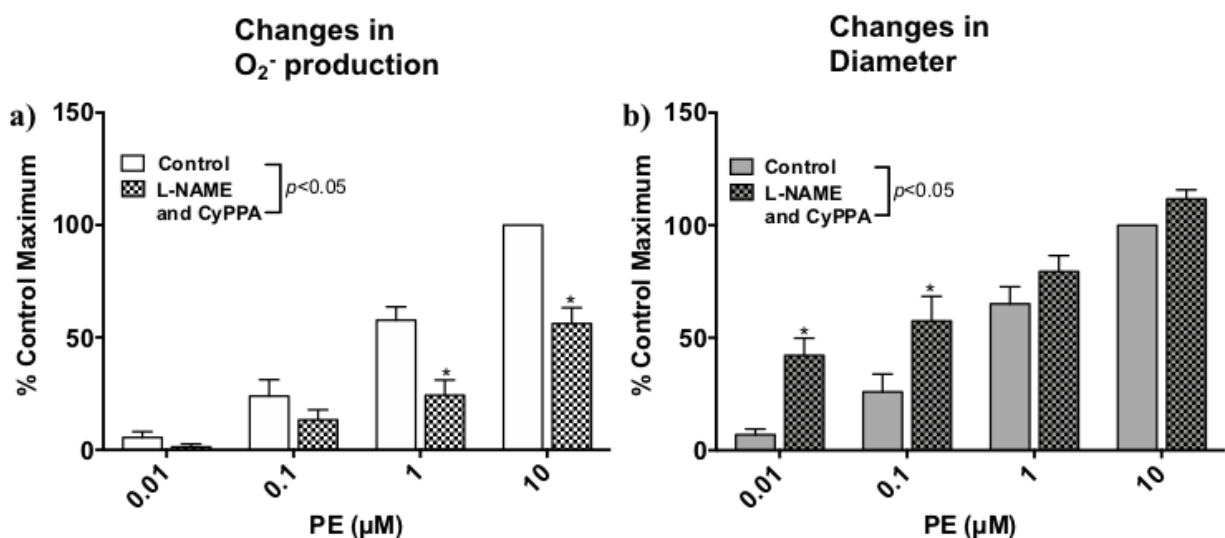
Figure 4.13: **CyPPA inhibition of phenylephrine-induced O$_2^-$ production is not prevented by NOS inhibition.** Mean data showing phenylephrine-induced **a)** O$_2^-$ production and **b)** vasoconstriction in the absence and presence of CyPPA (5 µM) with L-NAME (100 µM) in endothelium-intact rat mesenteric artery segments. Values are presented as mean ± SEM, n=6. * denotes $p<0.05$ from control; two-way repeated-measures ANOVA.

SKA-31 (1 µM) significantly reduced both phenylephrine-induced O$_2^-$ production ($p<0.05$) and vasoconstriction ($p<0.05$; **Figure 4.14a** and **b**). The IK$_{Ca}$ channel inhibitor NS 6180 (1 µM), prevented the effect of SKA-31 (1 µM) on phenylephrine-evoked vasoconstriction but did not block its effects on phenylephrine-induced O$_2^-$ production ($p<0.05$, **Figure 4.14c** and **d**) suggesting this effect may be independent of IK$_{Ca}$ channels. To investigate whether the effect was independent of the endothelium, the experiments were repeated in denuded mesenteric arteries.

In endothelium-denuded arteries, SKA-31 (1 µM) significantly reduced phenylephrine-induced O$_2^-$ levels ($p<0.05$, **Figure 4.15a**) but had no effect on phenylephrine-induced vasoconstriction ($p>0.05$, **Figure 4.15b**). As our lab has previously demonstrated that IK$_{Ca}$ channels are present only in endothelial cells of rat mesenteric arteries[197], the decrease in phenylephrine-induced O$_2^-$ production in endothelium-denuded arteries caused by SKA-31 is

likely through a mechanism other than increased activation of IK_{Ca} channels. One possible explanation for this observation is that SKA-31 is itself acting as a O_2^- scavenger and is therefore, still able to reduce phenylephrine-induced O_2^- production in the absence of IK_{Ca} channel activity and in endothelium-denuded arteries.

Block of NOS with L-NAME (100 μM) did not affect the ability of SKA-31 (1 μM) to reduce phenylephrine-induced O_2^- production ($p<0.05$, **Figure 4.16a**) but prevented its effects on phenylephrine-induced vasoconstriction ($p<0.05$, **Figure 4.16b**). Thus, like CyPPA, the reduction of phenylephrine-induced O_2^- production caused by SKA-31 is not through an increase in NO production to scavenge more O_2^-.
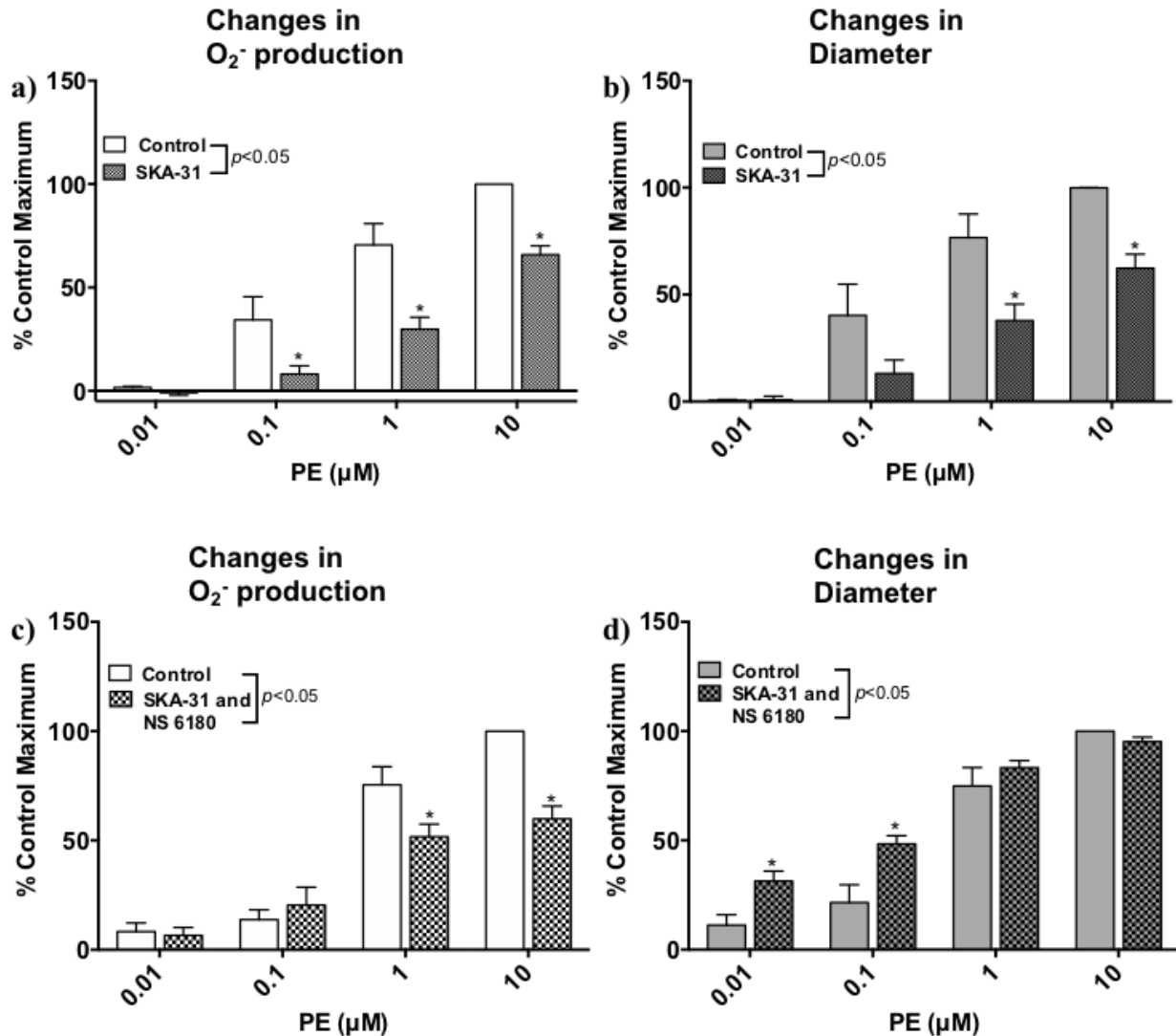
Figure 4.14: **SKA-31 significantly reduces phenylephrine-induced O_2^- production and vasoconstriction in endothelium-intact mesenteric arteries.** Mean data showing phenylephrine-induced O_2^- production in the absence and presence of **a)** SKA-31 (1 μM) or **c)** SKA-31 (1 μM) with NS 6180 (1 μM) and phenylephrine-induced vasoconstriction in the absence and presence of **b)** SKA-31 (1 μM) or **d)** SKA-31 (1 μM) with NS 6180 (1 μM) in endothelium-intact rat mesenteric artery segments. Values are presented as mean ± SEM, n=5. * denotes $p<0.05$ from control; two-way repeated-measures ANOVA.
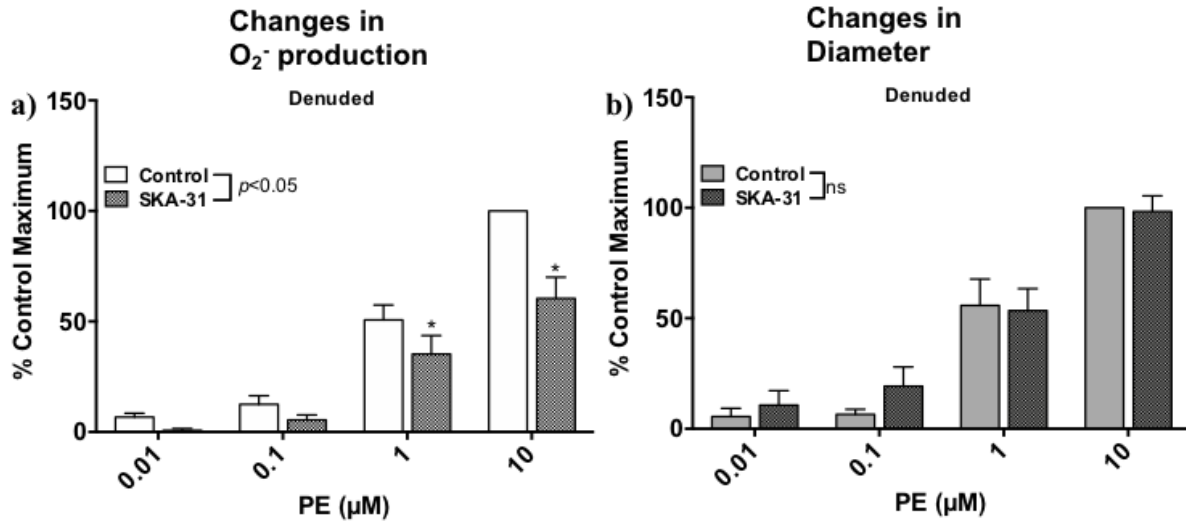
Figure 4.15: SKA-31 significantly reduces phenylephrine-induced O_2^- production in endothelium-denuded mesenteric arteries. Mean data showing phenylephrine-induced **a)** O_2^- production and **b)** vasoconstriction in the absence and presence of SKA-31 (1 μM) in endothelium-denuded rat mesenteric artery segments. Values are presented as mean ± SEM, n=7. * denotes $p<0.05$ from control; two-way repeated-measures ANOVA.
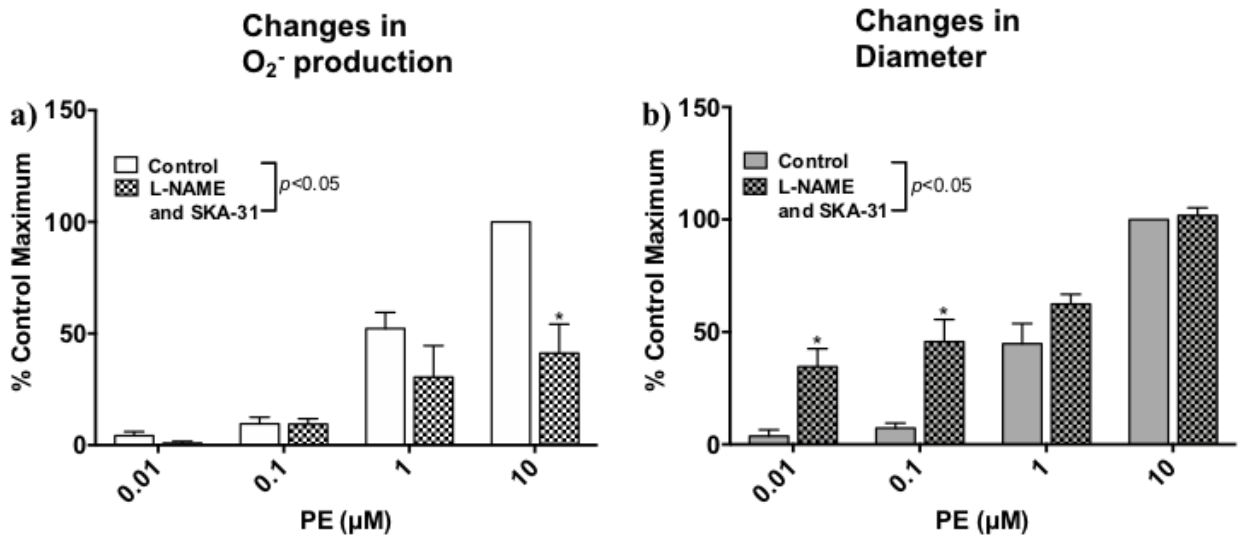
Figure 4.16: L-NAME inhibits the effect of SKA-31 on phenylephrine-induced vasoconstriction but not O_2^- production. Mean data showing phenylephrine-induced **a)** O_2^- production and **b)** vasoconstriction in the absence and presence of SKA-31 (1 μM) with L-NAME (100 μM) in endothelium-intact rat mesenteric artery segments. Values are presented as mean ± SEM, n=6. * denotes $p<0.05$ from control; two-way repeated-measures ANOVA.

4.3.5: Effect of modulators of smooth muscle BK_{Ca} channels on phenylephrine-induced changes in O_2^- production and vasoconstriction in mesenteric resistance arteries

To investigate if the observed effects of activators of endothelial SK_{Ca} and IK_{Ca} channel on O_2^- production are unique to those channels, phenylephrine-induced increases in O_2^- production and vasoconstriction were examined in the presence of iberiotoxin (IbTX) and N'-[3,5-Bis(trifluoromethyl)phenyl]-N-[4-bromo-2-(2H-tetrazol-5-yl-phenyl]thiourea (NS 11021), a selective inhibitor and activator of smooth muscle BK_{Ca} channels, respectively.

Depolarization of the smooth muscle membrane potential to phenylephrine[197,492] is limited by opening of BK_{Ca} channels, an effect which can be blocked by IbTX[94,97,99]. In line with this, IbTX (100 nM) significantly enhanced phenylephrine-induced vasoconstriction ($p<0.05$, **Figure 4.17b**) but had no effect on phenylephrine-induced O_2^- production ($p>0.05$, **Figure 4.17a**). Conversely, the BK_{Ca} channel opener NS 11021 (100 nM), significantly reduced phenylephrine-induced O_2^- production ($p<0.05$; **Figure 4.18a**) but had no effect on phenylephrine-induced vasoconstriction ($p>0.05$, **Figure 4.18b**). The effect of NS 11021 on phenylephrine-evoked O_2^- was prevented by IbTX ($p>0.05$, **Figure 4.18c**), and unlike in the presence of IbTX alone, phenylephrine-induced vasoconstriction was not different to controls in the presence of both agents ($p>0.05$, **Figure 4.18d**), indicating that NS11021 was able to prevent the actions of IbTX. These findings support the proposal that membrane hyperpolarization may regulate O_2^- production in mesenteric vessels and this is not an effect limited to opening of endothelial SK_{Ca} and IK_{Ca} channels.
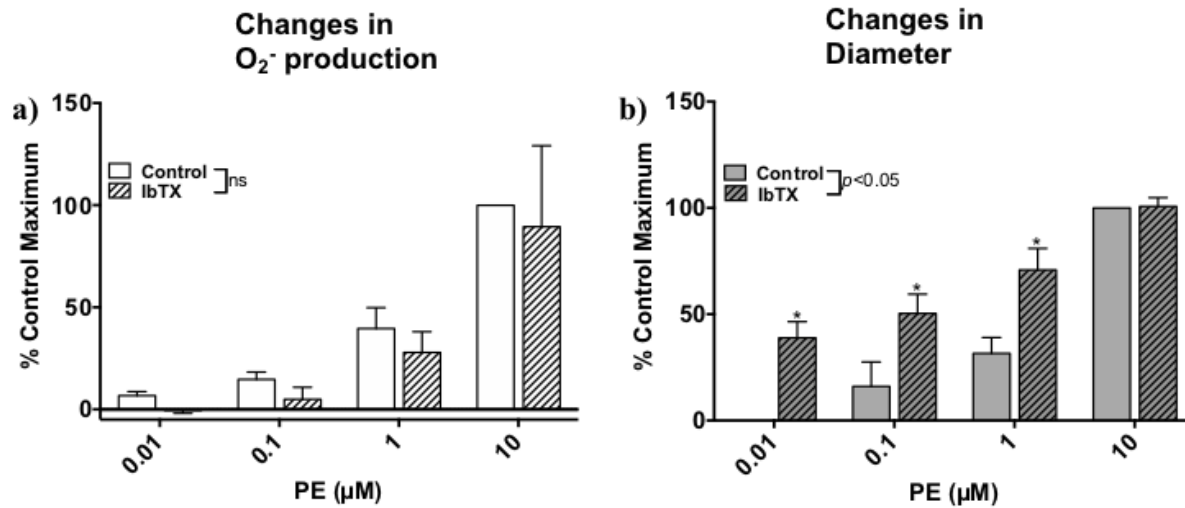
Figure 4.17: **BK_{Ca} channel inhibition significantly enhances phenylephrine-induced vasoconstriction.** Mean data showing phenylephrine-induced **a)** O_2^- production and **b)** vasoconstriction in the absence and presence of IbTX (100 nM) in endothelium-intact rat mesenteric artery segments. Values are presented as mean $\pm$ SEM, n=5. * denotes $p<0.05$ from control; two-way repeated-measures ANOVA.
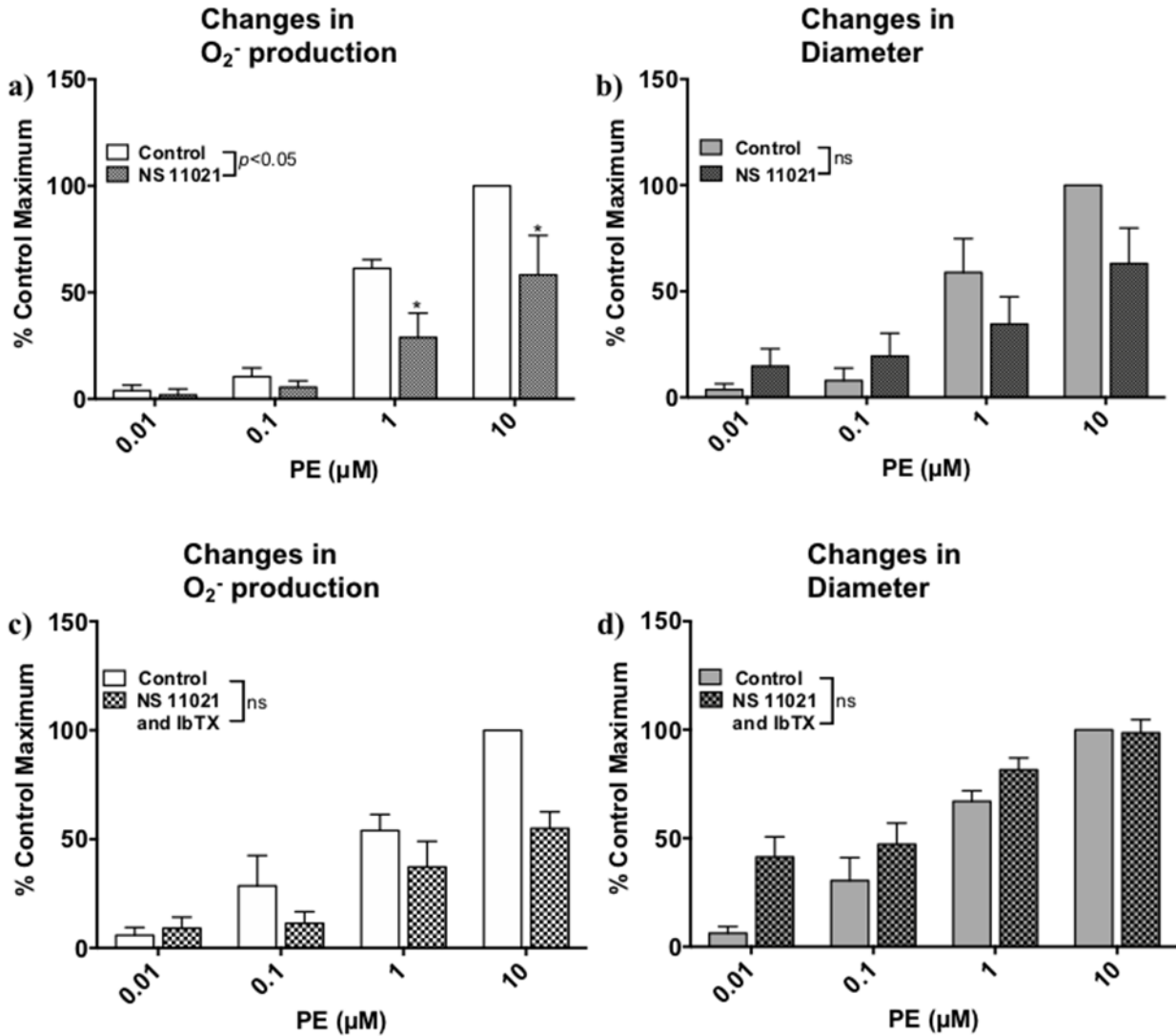
Figure 4.18: BK$_{Ca}$ channel activation significantly reduces phenylephrine-induced O$_2^-$ production. Mean data showing phenylephrine-induced O$_2^-$ production in the absence and presence of **a)** NS 11021 (100 nM) or **c)** NS 11021 (100 nM) with IbTX (100 nM) and phenylephrine-induced vasoconstriction in the absence and presence of **b)** NS 11021 (100 nM) or **d)** NS 11021 (100 nM) and IbTX (100 nM) in endothelium-intact rat mesenteric artery segments. Values are presented as mean ± SEM, n=5. * denotes $p < 0.05$ from control; two-way repeated-measures ANOVA.

4.4: Discussion

NO bioavailability within the vascular wall is determined by the balance between production by endothelial NOS and its interaction with O_2^-. Enhanced production of O_2^- leading to decreased bioavailability of endothelium-derived NO[518] appears to be a common mechanism underlying endothelial dysfunction associated with a wide range of risk factors for cardiovascular diseases, such as diabetes and atherosclerosis[268,328–336,546]. The data from the experiments described in this chapter demonstrate that small molecule activators of endothelial SK_{Ca} and IK_{Ca} channels can attenuate phenylephrine-induced O_2^- production in intact arteries. These data support my hypothesis that pharmacological activators of endothelial K_{Ca} channels can reduce vascular O_2^- production. It also supports the concept of endothelial cell membrane potential being a key determinant of vascular function and that activators of endothelial K_{Ca} channels may provide a novel therapeutic approach to reduce O_2^- in pathological states associated with endothelial dysfunction.

It is established that α_1-adrenoceptor-mediated vasoconstriction involves O_2^- production by both NADPH oxidase[347,348] and mitochondria[349] in rat mesenteric arteries[349], coronary myocytes[347] and tail arteries[348]. However, these data were obtained from experimental protocols in which O_2^- production was measured in flaccid tissues or fixed/frozen arteries, and so changes in O_2^- levels were not recorded in real time and arterial diameter was not assessed. Using arteries mounted in a pressure myograph in combination with a microscope fitted with a fluorescence attachment, I have demonstrated, for the first time, simultaneous phenylephrine-induced O_2^- production and vasoconstriction in isolated mesenteric arteries.

Using this approach, I have shown that phenylephrine evokes both O_2^- production and vasoconstriction in a concentration-dependent manner, that is reproducible over the time course of

the experiments and fully accounted for by activation of α_1-adrenoceptors. Tempol and SOD, scavengers of O_2^-, each significantly reduced phenylephrine-evoked increases in O_2^- but did not affect the accompanying vasoconstriction. These results are in contrast to a previous study in which α_1-adrenergic vasoconstriction in rat mesenteric arteries was proposed to be dependent on O_2^- generation and increased activity of matrix metalloproteinase enzymes[349]. However, in those experiments, scavenging of O_2^- production did not alter the peak phenylephrine-induced vasoconstriction though it did reduce the duration[349].

My experiments were conducted in endothelium-intact tissues as it was anticipated that scavenging of O_2^- by tempol or SOD would depress phenylephrine-induced vasoconstriction due to increased bioavailability of NO. The lack of effect of SOD and tempol on phenylephrine-evoked vasoconstriction could reflect the fact that although these agents did reduce O_2^- production, this may not be sufficient to significantly impact bioavailability of endothelium-derived NO and thus, arterial diameter. However, our lab has shown that endothelial modulation of phenylephrine-evoked vasoconstriction in rat isolated mesenteric arteries is due to both IK_{Ca} channel-mediated endothelium-dependent hyperpolarization and NO[130,197]. Thus, the lack of effect of a reduction in O_2^- levels on phenylephrine-induced vasoconstriction in these vessels may reflect the predominant role of activation of IK_{Ca} channels in endothelial modulation of smooth muscle contraction.

Alternatively, phenylephrine-induced O_2^- production enhances contractility via Ca^{2+} sensitization[66,67], through increasing RhoA activation and subsequently, phosphorylation of myosin phosphatase target subunit-1 and C-kinase potentiated protein phosphate-1 inhibitor; with these changes being observed after incubation with vasoconstrictors for 5 to 15 minutes[348,547,548]. As the phenylephrine dose response curve experiments in this thesis were 3 to 5 minutes in length, it is possible that the reduction in O_2^- production did not correlate to a diminished vasoconstriction

due to minimal involvement of Ca^{2+} sensitization as a result of the shorter experimental time frame. Thus, experiments where phenylephrine doses are incubated for longer periods of time will need to be carried out in order to examine the possibility that the duration of the phenylephrine-induced vasoconstriction is reduced in the presence of O_2^- scavengers.

In contrast to SOD and tempol, apocynin did reduce both phenylephrine-evoked increases in O_2^- and vasoconstriction. The reason for this is unclear but in addition to acting as a scavenger of O_2^-[544], apocynin is also an inhibitor of NADPH oxidase[541–543] and can scavenge H_2O_2[544], which has been shown to act as a vasoconstrictor[397–400] in isolated rat gracilis muscle arterioles[397] and mesenteric arteries[399]. Thus, scavenging of H_2O_2 by apocynin could contribute to the observed attenuation of phenylephrine-induced vasoconstriction observed with apocynin. Together, these data showed that there may be a complicated relationship between O_2^- levels and changes in arterial diameter such that significant reductions in O_2^- levels do not directly correlate to alterations in vasoconstrictor responses.

The interaction between NO and O_2^- to form $ONOO^-$ reduces availability of both radicals[389]. Also, phenylephrine-evoked vasoconstriction in rat mesenteric arteries is modulated by the endothelium, in part by the release of endothelium-derived NO[130,197]. Thus, the NOS inhibitor L-NAME was used to determine if reduced NO production can affect phenylephrine-induced O_2^- production and vasoconstriction in mesenteric arteries. It was expected that inhibition of NO synthesis would enhance O_2^- levels. But, although L-NAME significantly potentiated phenylephrine-induced vasoconstriction, it had no effect on O_2^- production. Thus, under my experimental conditions, NO does play a role in endothelial modulation of smooth muscle contractility but the interaction between NO and O_2^- may not contribute to regulation of O_2^- levels.

Further support for a separation between the effects of NO on smooth muscle contractility and on O_2^- levels is provided by experiments with NADPH. NADPH oxidase enzymes are one of the main sources of O_2^- production in the vasculature and I initially utilized NADPH in experiments with the idea that as an activator of NADPH oxidase[351–353,384,385], it would enhance phenylephrine-evoked increases in O_2^- levels in intact arteries. However, NADPH significantly reduced both phenylephrine-induced O_2^- production and vasoconstriction. NADPH is also a co-factor for NOS activity[384,545] and in the presence of L-NAME, the ability of NADPH to significantly reduce phenylephrine-induced O_2^- production was maintained but its effect on phenylephrine-induced vasoconstriction was lost. Similarly, in the perfused mesenteric bed, NADPH significantly reduced the enhancement of nerve-evoked vasoconstriction caused by block of NOS. Thus, it appears that although NADPH can enhance NO-mediated inhibition of smooth muscle contractility, this is independent of its ability to reduce O_2^- production.

As described in **Chapter 1**, NADPH is also a co-factor for glutathione reductase[408,411,415–417], an enzyme responsible for the reduction of glutathione disulfide to glutathione [408,411]. Glutathione is an antioxidant[408,411] and the major antioxidant mechanism within endothelial cells[412]. Glutathione is oxidized through interactions with ROS, such as $ONOO^-$, OH^-, O_2^- and H_2O_2, and two oxidized glutathione molecules form glutathione disulfide [408,411], which is converted back into two glutathione molecules through the actions of glutathione reductase. The balance between glutathione and glutathione disulfide is a determinant of the redox status of a cell[79].

Thus, to investigate the role of glutathione reductase in the effects of NADPH on phenylephrine-evoked O_2^- production and vasoconstriction, I used the glutathione reductase inhibitor, carmustine[408,411,549,550]. Interestingly, when applied alone, carmustine significantly enhanced basal O_2^- production, indicating that the glutathione pathway plays an active role in

regulating O_2^- in isolated rat mesenteric arteries. This the first description of such a role in intact arteries but is supported by a previous study in cultured bovine pulmonary artery endothelial cells[551]. Although NADPH had no effect on basal O_2^- production, the combination of NADPH and carmustine did significantly increase O_2^- levels, indicating NADPH may be mediating its effects on phenylephrine-induced O_2^- production by increasing the activity of glutathione reductase. This action would raise glutathione levels to increase the capability for scavenging of O_2^-.

As described earlier, NADPH oxidase, a major source of O_2^- in the vascular wall, is a voltage-sensitive enzyme which generates O_2^- by transferring electrons from cytosolic NADPH to extracellular O_2[126,367,368,371,372,374,386–388,529]. As previous work has shown that the activity of NADPH oxidase can be enhanced by membrane depolarization, it was anticipated that inhibition of endothelial IK_{Ca} channels would enhance both phenylephrine-induced O_2^- production and vasoconstriction in isolated arteries. IK_{Ca} channels mediate myoendothelial feedback, the mechanism by which endothelial cells limit agonist-evoked smooth muscle contraction, and our lab has shown that block of these channels causes both endothelial membrane potential depolarization and enhancement of phenylephrine-evoked smooth muscle membrane potential depolarization and constriction[130,197]. In this study, inhibition of IK_{Ca} channels by NS 6180 did indeed significantly enhance phenylephrine-induced vasoconstriction but unexpectedly, it reduced phenylephrine-induced O_2^- production. The reason for this is unclear but during the incubation period, prior to addition of phenylephrine, NS 6180 did cause a significant increase in production of O_2^-, supporting the notion that depolarization of the endothelial cell membrane potential by inhibition of IK_{Ca} channels increases basal O_2^- production in isolated arteries. In contrast, apamin, a selective inhibitor of SK_{Ca} channels, had no effect on either phenylephrine-induced O_2^- production or vasoconstriction. This is in agreement with previous reports from our lab and others

that SK_{Ca} channels do not play a functional role in regulating endothelial membrane potential or diameter in these vessels; block of SK_{Ca} channels by apamin does not cause endothelial depolarization[483] and does not enhance vasoconstriction[130].

To test the hypothesis that small molecule openers of SK_{Ca} and IK_{Ca} channels can limit phenylephrine-induced O_2^- production, I utilized the SK_{Ca} channel activator CyPPA[313,437], and IK_{Ca} channel activator SKA-31[121,124]. Both CyPPA and SKA-31 significantly reduced phenylephrine-induced O_2^- production, but whereas SKA-31 significantly limited phenylephrine-induced vasoconstriction, CyPPA had no effect, again demonstrating a dissociation between changes in O_2^- levels and arterial diameter. The ability of CyPPA and SKA-31 to reduce O_2^- levels supports my hypothesis, as well as previous reports, that hyperpolarization of the endothelial membrane potential can lead to a decrease in vascular O_2^- production[126,367,386–388].

Evidence that NADPH oxidase activity is regulated by membrane potential via the co-factor Rac1[367] has come from studies of rat aortic endothelial cells maintained under ischemic conditions[387] and human umbilical endothelial cells under normal conditions[367]. In these cells, membrane hyperpolarization reduced O_2^- production[388] and depolarization stimulated O_2^- production[386]. Additionally, in the rat perfused mesenteric bed, inhibition of SK_{Ca} and/or IK_{Ca} channels, led to enhanced O_2^- production via NADPH oxidase and increased perfusion pressure due to a reduction in NO levels[126]. However, my data provides the first evidence that activation of both SK_{Ca} and IK_{Ca} channels decreases O_2^- production in isolated resistance arteries. Block of NOS with L-NAME did not affect the ability of CyPPA or SKA-31 to limit phenylephrine-induced O_2^- production but abolished the effect of SKA-31 on phenylephrine-induced vasoconstriction, again, indicating a disconnect between O_2^- levels and the effects of NO on smooth muscle contractility.

The ability of CyPPA to reduce phenylephrine-evoked O_2^- production was prevented by the SK_{Ca} channel inhibitor apamin, supporting the hypothesis that it is modulated by endothelial membrane potential. However, the reduction in O_2^- production observed with SKA-31 was not prevented by NS6180, an inhibitor of IK_{Ca} channels, despite the fact that the effect of SKA-31 on vasoconstriction was inhibited by this agent. This finding may indicate that whereas the ability of CyPPA to limit O_2^- production is linked to SK_{Ca} channel activity, SKA-31 may be able to reduce O_2^- levels independently of IK_{Ca} channels. My observations that SKA-31 was able to also reduce phenylephrine-evoked increases in O_2^- levels but not arterial diameter in endothelium-denuded arteries supports this proposal, since these channels are not located on vascular smooth muscle cells[197]. The possibly that SKA-31 can directly scavenge O_2- requires further investigation.

In **Chapters 2** and **3**, I showed that both SKA-31 and CyPPA can inhibit phenylephrine-evoked increase in tone in mesenteric arteries mounted under isometric conditions. However, in arteries mounted under constant pressure, SKA-31 significantly inhibits phenylephrine-evoked vasoconstriction but CyPPA does not. The reason for this difference is unclear. Previous studies have described differences in agonist-evoked responses between arteries mounted in the two systems but not in terms of endothelial modulation[552,553]. As described earlier, SK_{Ca} and IK_{Ca} channels do show differential localization within endothelial cells[118,122,125,130,151,197]. CyPPA[313,437] and SKA-31[121,124] act to increase the sensitivity of the channels to Ca^{2+} and so differences in the ability of these agents to modulate phenylephrine-evoked vasoconstriction may reflect differences in endothelial Ca^{2+} signalling under the two experimental conditions. In support of this proposal, intraluminal pressure has been shown to influence the frequency of endothelial Ca^{2+} events linked to activation of IK_{Ca} but not SK_{Ca} channels in rat cremaster arterioles[554].

SK_{Ca} and IK_{Ca} channels are localized on endothelial cells and opening of these channels leads to membrane hyperpolarization which can spread to surrounding smooth muscle cells. Therefore, to investigate whether changes in smooth muscle membrane potential can regulate O_2^- production in intact arteries, I utilized a selective inhibitor and activator of BK_{Ca} channels, which are located on the vascular smooth muscle but not endothelial cells[76,106–108]. Inhibition of BK_{Ca} channels with IbTX significantly enhanced phenylephrine-induced vasoconstriction but did not affect phenylephrine-induced O_2^- production. This effect on vasoconstriction was anticipated, as BK_{Ca} channel activity plays a crucial role in limiting vasoconstriction[27,29,76,79–92,106,107]. The lack of effect of IbTX on O_2^- production was unexpected. Phenylephrine-evoked vasoconstriction of rat mesenteric arteries is due, at least in part, to depolarization of the smooth muscle cell membrane potential leading to entry of Ca^{2+} through L-type VOCCs[197,492] and this depolarization may be responsible for the accompanying increase in O_2^- production as opening of BK_{Ca} channels with NS 11021 did reduce phenylephrine-induced O_2^- production. Although the role of smooth muscle depolarization in vasoconstriction to α_1-adrenoceptor agonists is well established[118,123,555], previous studies have not considered its role in acute phenylephrine-evoked production of O_2^{-}[348,349] and further work is required to investigate this possibility.

The application of DHE for real-time measurements of O_2^- production in intact arteries is novel but does have some limitations. DHE can be oxidized by other ROS/RNS or by cytochrome *c* to produce ethidium, which emits at a similar wavelength as EOH bound to DNA (DHE oxidized by O_2^{-})[349,535–540]. EOH has an optimal excitation/emission spectrum of 490/590 nm[540] while ethidium has an optimal excitation/emission spectrum of 360/590 nm[556]. The filters used in this recording system excite at 535 nm and capture emission at 610 nm, giving minimal excitation of ethidium and so it is unlikely that production of ethidium is being measured under these

experimental conditions. In comparison to other fluorescent probes for O_2^- detection, such as lucigenin, DHE does not produce O_2^- directly[538,539]. Additionally, although DHE fluorescence cannot be used alone to quantify O_2^-, it is very useful for measuring changes in O_2^- production[538,557], as it is used for in this chapter. In light of these limitations, two further techniques (see **Chapter 5**) have been used to provide support for the use of DHE: histological analysis of fixed arteries and UPLC of DHE-derived oxidation products (the latter regarded as "the most unequivocal and quantitative detection of intracellular O_2^-"[538]).

Furthermore, it is possible that the reduction in fluorescence intensity observed in the absence of altered constriction could be the result of dye quenching by the pharmacological reagents thus, further experiments will need to be performed in order to investigate this possibility. And finally, while there was a disconnect between changes in O_2^- and changes in vasoconstriction (such as, L-NAME significantly enhancing phenylephrine-induced vasoconstriction but not O_2^- production), it is possible that movement of the vessel as a result of constriction could be contributing to the changes in fluorescence intensity. Therefore, further experiments will be performed to examine this possibility.

In conclusion, the data included in this chapter support my hypothesis that activators of K_{Ca} channels can significantly reduce phenylephrine-induced O_2^- production, this was not linked to changes in endothelial modulation of vasoconstriction in mesenteric arteries. These data also support the proposal that endothelial K_{Ca} channels may be a potential novel target for the prevention and treatment of cardiovascular diseases associated with increased production of O_2^- [268,328–336].

Chapter 5: Activators of SK_{Ca} and IK_{Ca} channels limit O_2^- production in isolated arteries

5.1: Introduction

In **Chapter 4**, I used DHE for real time measurements of changes in O_2^- levels in intact mesenteric arteries. This is in contrast to previous studies in which vascular O_2^- measurements have been determined in fixed/frozen tissues[347–349,558–560].

Recent studies have shown that the reaction product of DHE and O_2^- is EOH and not ethidium, as had been previously thought[535]. Ethidium is formed from the reaction of DHE with ROS other than O_2^-, RNS and cytochrome *c*, and EOH does not arise from the action of other intracellular oxidants[535]. Thus, quantitation of EOH can be considered as being tantamount to detecting the presence of O_2^- itself[539].

In this chapter, I conducted histological analysis of fixed arteries stained with DHE, to provide support for the functional data collected in the previous chapter. I also carried out UPLC analysis of the DHE oxidation products ethidium and EOH to demonstrate that DHE fluorescence provides a measure of O_2^- levels in the vascular wall rather than other ROS/ RNS.

5.2: Methods and materials

See **Appendix: Drugs and chemicals** for a list of the drugs and chemicals used.

5.2.1: Histological analysis of mesenteric arteries stained with DHE

5.2.1.1: Tissue preparation. Vessels were prepared for histological analysis by following the methods outlined by Hao et al[349]. Briefly, sections of second or third order mesenteric artery (4-5 mm in length) were cleaned of adhering connective tissue and individually placed in 1 ml of Krebs buffer in a 1.5 ml tube (Eppendorf, Germany). Stock solutions of DHE (10 mM) were made fresh in a darkened room[349,535,536] and all protocol steps described were also carried out in a darkened room. Each vessel was incubated with DHE (10 μM) for 30 minutes at 37ºC during which time

one of the following agents was added 10 minutes prior to the end of the DHE incubation period: SOD-PEG (25 U/ml), CyPPA (5 μM) or SKA-31 (1 μM). In each experiment, one tube was incubated with DHE alone to act as a control. At the end of the incubation period with DHE, phenylephrine (10 μM) was added to all tubes and incubated at 37°C for 45 minutes. Tissues were then washed in cold Krebs buffer and individually placed upright in small plastic containers full of optimal cutting temperature compound (Scientific Gardena), flash frozen in liquid nitrogen and placed in a -80°C freezer until cryo-sectioned onto microscope slides (by Ms Lynette Edler, HistoCore, Alberta Diabetes Institute, University of Alberta). The slides were stored in a -20°C freezer until stained with 1 in 1000 dilution of 4′,6-Diamidino-2-phenylindole dihydrochloride (DAPI) in 90% glycerol and cover slips (22x60 mm, thickness #1, Fisher Scientific, USA) placed on the slides. Slides were then stored flat in containers at 4°C.

5.2.1.2: Imaging. Histological analysis was carried out using an upright digital imaging microscope (Zeiss Imager Z1, power supply Zeiss 231) attached to a fluorescent lamp (X-cite 120 LED boost, Excelitas Technologies) and camera (Cooke Sensi Cam). For visualization of DAPI, samples were excited at wavelengths between 353-377 nm and emission was captured at 395 nm and above. For visualization of EOH bound to DNA[349,535,536] (the DHE oxidation product formed when DHE reacts with O_2^-), excitation was at 450-490 nm and emission was captured at 500-550 nm.

Metamorph (Universal Imaging, Downington, PA) was used for analysis of images; the DAPI fluorescent images were over-laid with the EOH fluorescent images and the EOH fluorescence within each nucleus was calculated, totalled and averaged per image. The average fluorescent intensity per image was then compared between treatment groups. Expressing EOH fluorescent intensity per nucleus normalized the responses to allow comparison between different

vessels and minimized interference from the internal elastic lamina. Adobe Photoshop (Adobe, San Jose, CA, USA) was used to add colour to the example images.

5.2.2: Quantification of DHE-derived oxidation products from aortic samples by UPLC

Due to the small size of mesenteric arteries, UPLC was used to quantify DHE-derived oxidation products[349,535,536,540,561] in aortic tissue by following the UPLC protocol for quantitation of EOH described by Lebed et.al.[562] Aortic tissues were prepared for analysis by UPLC by following the protocol described by Fernandes et.al.[561] The aorta was cleaned of connective tissue and fat and placed in iced cold phosphate buffered saline. The thoracic aorta was cut into 8-12 pieces and 2-3 pieces placed into each pre-weighed tube and weighed to determine tissue weight. Tissues were washed twice with ice cold phosphate buffered saline before 0.5 ml of phosphate buffered saline /diethylenetriaminepentaacetic acid was added to each tube. 2.5 μl of DHE, from a freshly made 10 mM DHE stock solution, was added to each tube in a darkened room. SOD-PEG (25 U/ml), CyPPA (5 μM) or SKA-31 (1 μM) was added 15 minutes prior to the addition of DHE and tubes were then incubated for 30 minutes at 37°C. After incubation, and still in the dark, vessels were washed twice with ice cold phosphate buffered saline before being flash frozen in a mortar full of liquid nitrogen and ground with a pestle. The ground vessel powder was transferred from the mortar into new tubes with 0.5 ml of acetonitrile and wrapped in aluminum foil.

The tubes containing ground vessel and acetonitrile were sonicated for 3 x 10 seconds in a darkened room and then centrifuged at 4°C *18,000 x g* for 15 minutes. The supernatant was removed, placed into separate tubes and wrapped in aluminum foil. The supernatant was evaporated off using a stream of N_2 until a pink pellet formed. All tubes were then wrapped in aluminum foil and stored in a -80°C freezer until the pink pellets were prepared for UPLC analysis (by Mr. Ken Strynadka, UPLC Analytical Core, Cardiovascular Research Centre).

The pink pellets were re-suspended in 100 μl phosphate buffered saline/diethylenetriaminepentaacetic acid and 5 μl of each sample was injected into a Waters Acquity UPLC System (H Class) consisting of a binary solvent manager, sample manager, column manager and fluorescence detector. The column used was a Zorbax SB-Phenyl column (250 mm, 4.6 mm, 5 μm) equilibrated with a mobile phase of 35% acetonitrile and 65% water, both containing a 0.1% (v/v) of trifluoroacetic acid. Ethidium and EOH were separated using a gradient from 35% to 55% in 5 min at a flow rate of 2 mlmin^{-1}. The fluorescence excitation was set at 470 nm and the emission was measured at 595 nm. The limit of quantitation for ethidium and EOH using this method was 0.4 μM, close to previously reported values[562].

All data were acquired and analyzed by means of Waters Empower 3 software. 2-EOH was purchased from Noxygen Science Transfer and Diagnostic GmBbH (Germany). All chemicals and solvents were of analytical grade. All solutions were prepared in ultrapure milliQ water (Millipore MilliQ, Germany) and filtered over a 0.22 μm filter (Millipore, Bedford, USA). Analysis was done with the operator blinded to sample identity. Data was expressed as the ratio of area under the curve per mg of initial sample weight (AUC/mg) as in previous studies[562].

5.2.3: Statistics

All data are expressed as mean ± SEM, *n* rats used and ordinary one-way ANOVA followed by a Tukey's multiple comparison post-hoc test was performed. *p*<0.05 was considered statistically significant in all cases.

5.3: Results

5.3.1: Histological analysis of mesenteric arteries stained with DHE

Representative images of DAPI and DHE stained sections of rat mesenteric arteries treated with phenylephrine (10 μM) plus CyPPA (5 μM), SKA-31 (1 μM) or SOD (25 U/ml) are shown in **Figure 5.1**.

CyPPA (5 μM), SKA-31 (1 μM) and SOD-PEG (25 U/ml) each significantly decreased DHE fluorescence intensity in comparison to control tissues incubated with phenylephrine (10 μM) ($p<0.05$, **Figure 5.2**).
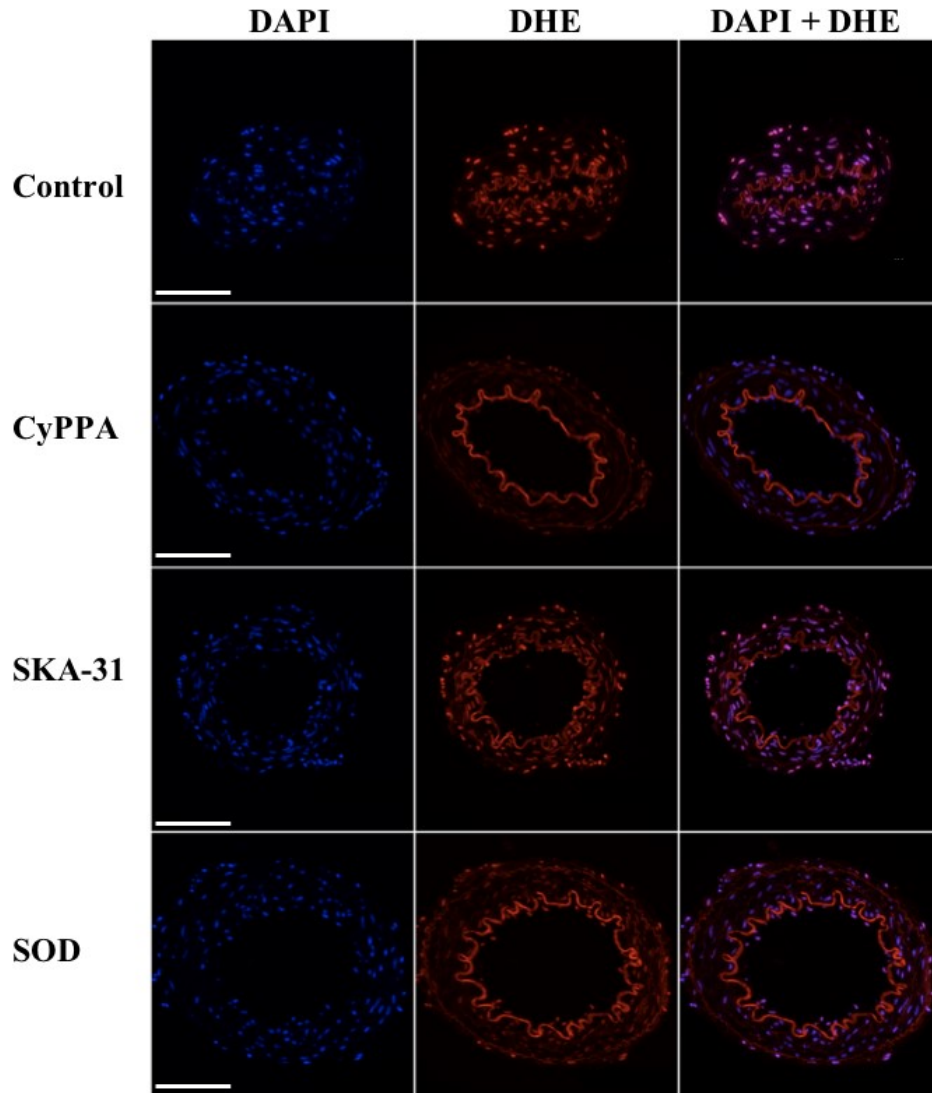
Figure 5.1: Representative images of DAPI and DHE stained sections of rat mesenteric artery. Arteries were treated with phenylephrine (10 µM) plus CyPPA (5 µM), SKA-31 (1 µM) or SOD-PEG (25 U/ml); bar equals 100 µm.
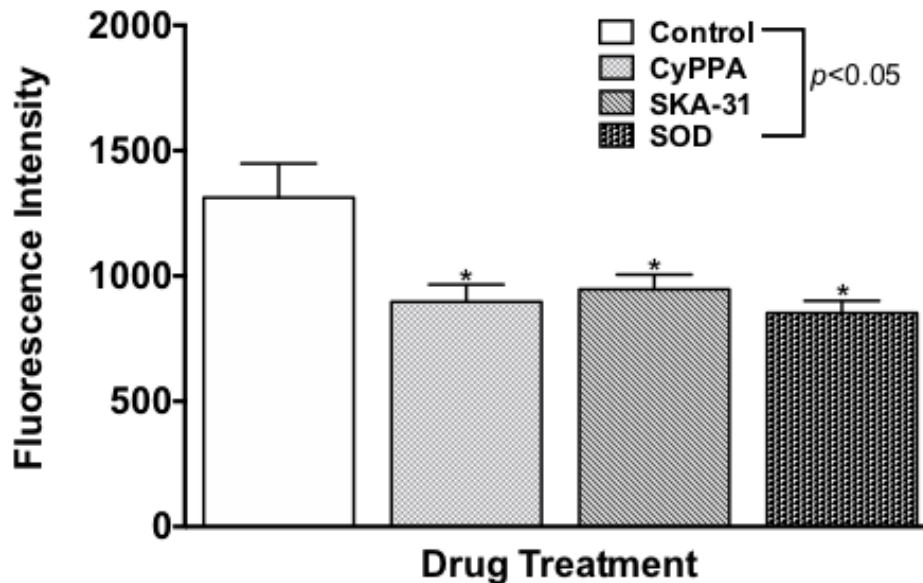
Figure 5.2: CyPPA, SKA-31 and SOD each significantly reduce phenylephrine-induced O_2^- levels in rat mesenteric arteries as measured by DHE fluorescence. Mean data showing the phenylephrine (10 µM) -induced O_2^- levels in the absence and presence of CyPPA (5 µM), SKA-31 (1 µM) or SOD (25 U/ml). Values are presented as a mean ± SEM, n=5. * denotes $p<0.05$ from control; one-way ANOVA.

5.3.2: Quantification of DHE-derived oxidation products from aortic samples by UPLC

CyPPA (5 µM), SKA-31 (1 µM) and SOD (25 U/ml) each significantly reduced EOH levels in isolated aortic samples as compared to controls ($p<0.05$, **Figure 5.3a**) but did not significantly affect levels of ethidium ($p>0.05$, **Figure 5.3b**)
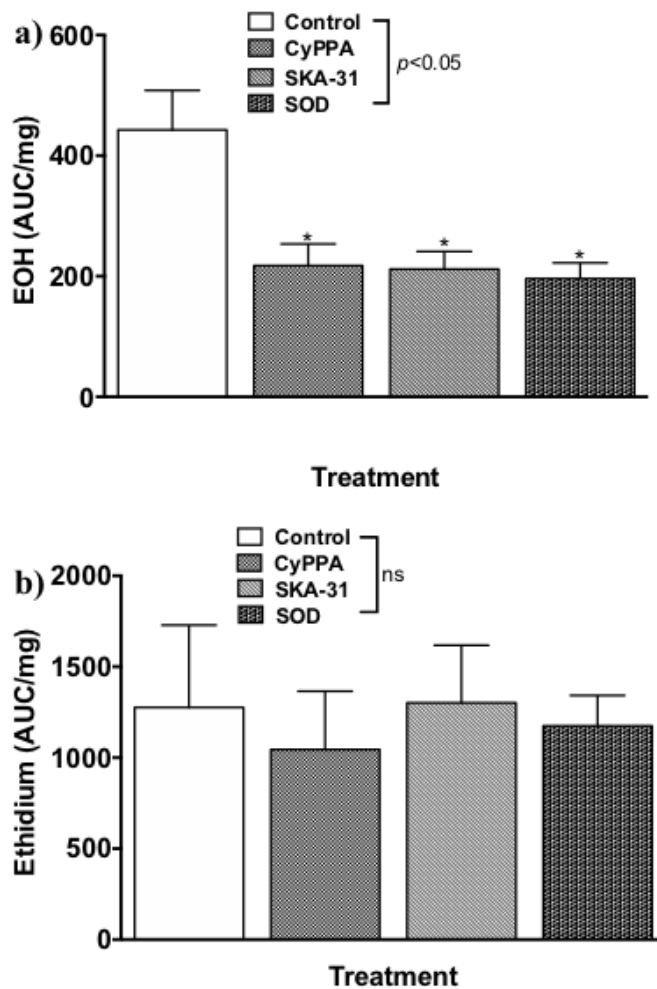
Figure 5.3: **CyPPA, SKA-31 and SOD each significantly reduced EOH but not ethidium in rat mesenteric arteries.** **a)** Mean data showing the amount of EOH (AUC/mg) in the absence and presence of CyPPA (5 µM), SKA-31 (1 µM) and SOD (25 U/ml). Values are presented as mean ± SEM, n=6. * denotes $p<0.05$ from control; one-way ANOVA. **b)** Mean data showing the amount of ethidium (AUC/mg) in the absence and presence of CyPPA (5 µM), SKA-31 (1 µM) and SOD (25 U/ml). Values are presented as mean ± SEM, n=6; one-way ANOVA.

5.4: Discussion

DHE is an O_2^- sensitive dye that has been used to detect O_2^- in a variety of biological samples, cells and tissues[349,535–540]. DHE is oxidized by O_2^- to form EOH which binds to DNA and fluoresces with optimal excitation/emission of 490/590 nm[540]. While the formation of EOH is specific to DHE oxidation by O_2^-, DHE can also be oxidized by other ROS/RNS, such as H_2O_2

and ONOO⁻, and cytochrome *c*, to form ethidium[349,535–540]. Ethidium has an optimal excitation/emission spectrum of 360/590 nm[556] thus, there is overlap between the excitation/emission spectrums for both DHE-derived oxidation products. However, through the use of specific filters to selectively excite/emit for EOH, DHE can be used as a means to selectively detect O_2^- in tissues[538,540,562]. I performed histological analysis on fixed mesenteric arteries stained with DHE to provide support for the functional data collected in the previous chapter. I also carried out UPLC analysis of the DHE oxidation products ethidium and EOH to demonstrate that DHE fluorescence provides a measure of O_2^- levels in the vascular wall rather than other ROS/ RNS.

Histological analysis of fixed mesenteric arteries stained with DHE in the absence and presence of the phenylephrine plus the SK_{Ca} channel activator CyPPA[313,437], the IK_{Ca} channel activator SKA-31[121,124] and SOD, demonstrated that these agents significantly reduced DHE fluorescence. The microscope used for this analysis permitted excitation/emission in the narrow ranges of 450-490/500-550 nm, optimal for detection of EOH[540] over ethidium (optimal excitation of 360 nm[556]). Thus, it is likely that the bulk of the fluorescent intensity captured was due to EOH.

By using UPLC analysis of DHE-derived oxidation products, I have demonstrated that CyPPA, SKA-31 and SOD each significantly reduced the amount of EOH levels in aortic samples without altering levels of ethidium. Ethidium is formed by oxidation of DHE by other ROS/RNS, such as ONOO⁻ and H_2O_2, and cytochrome *c*[349,535–540]. Thus, these findings give confidence that with the use of DHE in functional studies, I am measuring changes in EOH, and not ethidium, thus, reflecting changes in the production of O_2^-.

The transient lifetime of O_2^- means that there is little likelihood that any molecular probe will react with the total amount of O_2^- generated. This unavoidable underestimation implies that measurement of O_2^- levels through the use of DHE and quantitation of EOH can be viewed only

as, at best, a semi-quantitative method for assessing O_2^- concentrations. Also, as in **Chapter 4**, the source of O_2^- was not investigated in these experiments. My hypothesis is that membrane potential hyperpolarization may reduce O_2^- production and the data supports this proposal. However, K_{Ca} channels have been identified on the inner mitochondrial membrane in cardiac myocytes[137,138] and neurons[139–143,152–156] and the possibility that these channels are present in vascular smooth muscle and endothelial cell mitochondria, and thus, play a role in O_2^- generation in the vascular wall, cannot be ruled out.

In conclusion, activators of either SK_{Ca} or IK_{Ca} channels in rat mesenteric arteries or aorta significantly reduced the levels of fluorescence intensity and EOH, but not ethidium, as determined through the use of histological analysis and UPLC analysis of DHE-derived oxidation products, respectively, in a similar manner to the O_2^- scavenger, SOD. These findings indicate that the use of DHE fluorescence is an appropriate method to assess changes in O_2^- levels in arteries and support the methodology used in the experiments described in **Chapter 4**.

Chapter 6: General discussion and future directions

6.1: General discussion

Maintenance of adequate blood supply to tissues and organs requires co-ordination of the activity of nerves, endothelial and smooth muscle cells. Chemical mediators and changes in shear stress act on the endothelium to release diffusible relaxing and contracting factors and evoke electrical coupling with underlying smooth muscle cells. Conversely, stimulation of smooth muscle cells by neurotransmitters and increases in intravascular pressure leads to flux of second messengers to endothelial cells to elicit feedback to limit smooth muscle contraction. Endothelial dysfunction is associated with the risk factors for, and development of cardiovascular diseases, and is characterized by an increase in O_2^- production[116,268,328–336]. O_2^- interacts with NO to produce $ONOO^-$ at a rate three times faster than O_2^- undergoes dismutation by SOD[389,390]. Thus, increased O_2^- is associated with both reduced availability of NO and increased formation of $ONOO^-$ leading to enhanced vasoconstriction, augmented platelet adhesion and aggregation, vascular smooth muscle cell proliferation and diminished angiogenesis[298,328,406].

Endothelium-dependent modulation of smooth muscle contractility is initiated by a rise in Ca^{2+} levels within endothelial cells leading to activation of NOS and opening of K_{Ca} channels[80,84,85,100,116–131,148–151,197,202–205]. NOS converts L-arginine to NO[213,258–262] which relaxes smooth muscle cells via stimulation of soluble guanylyl cyclase to increase cyclic guanosine monophosphate[286] and activate protein kinase G-mediated phosphorylation of numerous target proteins[167,168,287,288]. Opening of endothelial K_{Ca} channels causes hyperpolarization of the endothelial cell membrane potential which spreads to surrounding smooth muscle cells to limit contraction by reducing the open probability VOCCs[80,84,85,100,116–131,148–151,197,202].

NO and spread of hyperpolarization have long being regarded as parallel pathways for endothelium-dependent vasodilation and the gold-standard test for responses mediated by hyperpolarization has been the demonstration that blockers of SK_{Ca} and IK_{Ca} channels inhibit endothelium-dependent relaxation in the presence of a NOS inhibitor, such as L-NAME[80,84,85,100,116–131,148–151,197,202–205]. However, two completely independent pathways for relaxation is counter to effective signal integration required for effective fine tuning of changes in arterial diameter in response to multiple stimuli, such as release of neurotransmitter from sympathetic nerves and increases in shear stress due to vasoconstriction. Several lines of evidence support a link between NO bioavailability and K_{Ca} channel activity. For example, in rat basilar and superior mesenteric arteries, agonist-evoked NO production and NO-mediated relaxations can be inhibited by blockers of endothelial K_{Ca} channels[203,418] and small molecule activators of endothelial K_{Ca} channels can evoke NO-mediated relaxation in rat mesenteric and porcine retinal arteries[437,481]. Also, studies in cultured endothelial cells have shown that O_2^- production by voltage-sensitive NADPH oxidase is reduced by membrane hyperpolarization[387,529] which may lead to increased bioavailability of NO.

Our lab and others have demonstrated that in small arteries, endothelial K_{Ca} channels show a differential distribution within endothelial cells with SK_{Ca} channels located on the luminal endothelial membrane and IK_{Ca} channels localized to MEGJs on the abluminal side[118,122,125,130,132,133,151,197]. This distribution supports the proposal that SK_{Ca} and IK_{Ca} channels may play different roles in endothelium-dependent modulation of arterial diameter. This proposal is borne out by reports that in cultured endothelial cells, increases in shear stress are linked to activation of SK_{Ca} channels[206,318,421–424], and our demonstration that in rat isolated mesenteric and basilar arteries, stimulation of smooth muscle cells by α_1-adrenoceptor agonists leads to flux of

IP$_3$ from smooth muscle to endothelial cells to elicit localized increases in Ca^{2+} that activates IK$_{Ca}$ channels located at MEGJs and production of NO to limit vasoconstriction, a mechanism termed myoendothelial feedback[197].

In this thesis, I have further explored the relationship between endothelial SK$_{Ca}$ and IK$_{Ca}$ channels and NO in regulating resistance artery diameter. *In vivo*, sympathetic nerve activity is the primary regulator of resistance artery diameter, and therefore, contributes to peripheral vascular resistance[434,435], with the endothelium playing a key role in limiting the vasoconstriction caused by neurotransmitters released from perivascular sympathetic nerves. Vasoconstriction increases shear stress, the frictional force exerted by flow of blood across the surface of endothelial cells, and sensing of these increases in shear stress plays an important role in regulating tissue perfusion[198–201]. However, despite its obvious physiological importance, the mechanisms underlying shear stress-induced increases in arterial diameter and thus, blood flow, are still a topic of debate. Data from *in vitro*, *in vivo* and clinical studies have demonstrated an important role for NO in acute responses to increases in shear stress and also support the contribution of endothelial hyperpolarization mediated by opening of SK$_{Ca}$ channels[132,133,206,220,241–248,318,421–433]. However, whether release of NO and activation of SK$_{Ca}$ channels are distinct pathways or two facets of the same mechanism is still unclear.

Therefore, in **Chapter 2**, I used the rat mesenteric bed perfused at a constant luminal flow so that vasoconstriction leads to increases in shear stress, to explore the functional link between NO and SK$_{Ca}$ channel activity modulation of sympathetic vasoconstriction. I found that shear stress-induced inhibition of nerve-evoked vasoconstriction is mediated by both NO and SK$_{Ca}$ channels. I also showed that CyPPA, a small molecule activator of SK$_{Ca}$ channels that increases the channels sensitivity to Ca^{2+} [313,437], can enhance the response to shear stress in this preparation

via a mechanism dependent on endothelium-derived NO. These findings support the notion that activators of SK_{Ca} channels may have therapeutic potential in enhancing shear stress-induced NO bioavailability in pathological states where there is a loss of shear stress-induced dilation[420]. Furthermore, as this enhancement occurred at a concentration of CyPPA that caused minimal direct vasorelaxation, activators of SK_{Ca} channels may provide a means to maintain coupling between physiological stimuli and changes in blood flow and avoid reflex increases in heart rate and blood pressure caused by direct vasodilators.

These experiments also revealed that voltage-independent mechanisms of smooth muscle contraction are a major contributor to nerve-evoked vasoconstriction in the rat mesenteric bed. Depolarization-mediated smooth muscle contraction is limited by opening of smooth muscle voltage-gated K^+ channels and BK_{Ca} channels, both of which hyperpolarize the membrane potential[26–29,76,448,449] to limit contraction. In contrast, contraction of smooth muscle by voltage-independent processes does not engage a similar "braking" mechanism. Therefore, the reliance of nerve-evoked vasoconstriction on voltage-independent processes may allow for a greater range of response than would be possible if depolarization was the only active mechanism.

As described above, in contrast to SK_{Ca} channels, IK_{Ca} channels are localized to MEGJs on the abluminal side of endothelial cells[118,122,125,130,132,133,151,197], a position that allows them to mediate myoendothelial feedback, the mechanisms by which agonists acting on smooth muscle cells can activate inhibitory endothelial pathways to limit contraction. This model arose from experiments utilizing the application of α_1-adrenoceptor agonists but its contribution to endothelial modulation of sympathetic nerve activity, a major stimulus for vasoconstriction *in vivo,* has not been investigated. The reliance of myoendothelial feedback on IK_{Ca} channels, provides the opportunity to use selective inhibitors of these channels to dissect out the contribution of the two

pathways to functional vascular responses and so in **Chapter 3**, I explored the role of the IK_{Ca} channel-mediated myoendothelial feedback pathway in limiting sympathetic vasoconstriction in the perfused mesenteric bed.

Using this approach, I found that in contrast to SK_{Ca} channels, endothelial IK_{Ca} channels do not appear to play a functional role in modulating nerve-evoked vasoconstriction in the perfused mesenteric bed. However, using SKA-31, an activator of IK_{Ca} channels, I identified a role for neuronal IK_{Ca} channels in limiting vasoconstriction via inhibition of noradrenaline release. IK_{Ca} channels have previously been localized on specific neurons in rat, mouse, guinea-pig and human enteric nervous systems[152–156] where they mediate the slow after-hyperpolarization following an action potential but this is the first report of IK_{Ca} channels on perivascular sympathetic nerves. The lack of effect of IK_{Ca} channel blockers on sympathetic vasoconstriction suggests that IK_{Ca} channels may not play a role in regulating noradrenaline release under normal conditions but targeting of IK_{Ca} channels could provide a new approach to reducing vasoconstriction in conditions associated with increased sympathetic drive, such as hypertension[174,499,500].

As described in **Chapter 1**, endothelial dysfunction associated with risk factors for cardiovascular diseases is characterized by increased production of O_2^- and decreased NO bioavailability[268,328–336]. Attempts to reduce O_2^- levels through use of dietary anti-oxidants such as vitamins B, C and E have been unsuccessful[337–342] and there is the need to identify new approaches to reduce O_2^- generation. In disease models, reduced NO bioavailability has been associated with upregulation of expression and activity of NADPH oxidase[332–336,383,528], a voltage-sensitive enzyme which generates O_2^- by transferring electrons from cytosolic NADPH to extracellular O_2[126,367,368,371,372,374,386–388,529]. In isolated endothelial cells, drugs which open K_{ATP} channels attenuate both membrane depolarization and O_2^- production, indicating that endothelial cell

membrane potential can regulate O_2^- production[387,529]. Our lab has previously shown that endothelial depolarization inhibits agonist-evoked, NO-mediated relaxation of rat basilar arteries, an effect that was overcome by the K_{ATP} channel opener, pinacidil[418], and we, and others, have demonstrated depolarization of the endothelial membrane potential in tail[530] and mesenteric arteries[531–533] from rat models of endothelial dysfunction. Therefore, in **Chapter 4,** I explored the relationship between endothelial K_{Ca} channels, O_2^- production and diameter in intact mesenteric arteries mounted in a pressure myograph coupled to a fluorescence detection system (IonOptix) for simultaneous measurement of changes in arterial diameter and O_2^- production using DHE.

   With this new approach, I found that small molecule activators of endothelial SK_{Ca} and IK_{Ca} channels, as well as scavengers of O_2^-, can attenuate phenylephrine-induced O_2^- production in intact arteries but this is not associated with potentiation of NO-mediated inhibition of vasoconstriction. I chose to use this bioassay approach to assess NO bioavailability as although it is not quantitative, it has the advantage over commercially available NO-sensitive electrodes or fluorescent dyes in that it is functionally and clinically relevant because it shows whether or not changes in NO bioavailability are sufficient to affect NO-mediated modulation of vasoconstriction. The observed disconnect between changes in levels of O_2^- and changes in arterial diameter in my experiments may indicate that under the acute conditions of my experiments, the changes in O_2^- are not sufficient to significantly impact availability of endothelium-derived NO to mediate relaxation. However, it could also be a reflection of the predominant role of hyperpolarization in endothelial modulation of smooth muscle contraction in small mesenteric arteries, masking the impact of enhanced NO bioavailability on vasoconstriction. Thus, for future studies, the use of larger arteries in which NO plays a more dominant role should be considered, together with investigation of the effects of K_{Ca} channel activators on the longer-term consequences of increases

in O_2^- levels, such as damage to proteins caused by $ONOO^-$.

Simultaneous recording of arterial diameter and changes O_2^- levels using DHE in isolated arteries is a new approach. Thus, in **Chapter 5**, I conducted histological analysis of fixed arteries stained with DHE and UPLC analysis of the DHE oxidation products, ethidium and EOH, to demonstrate that DHE fluorescence provides a measure of O_2^- levels in the vascular wall rather than other ROS/RNS. Using these approaches, I demonstrated that activators of K_{Ca} channels significantly reduced the levels of fluorescence intensity, and of EOH, but not ethidium, in a similar manner to the O_2^- scavenger, SOD. These findings confirm that the use of DHE fluorescence is an appropriate method to assess changes in O_2^- levels in arteries and support the methodology used in the experiments described in **Chapter 4**.

In conclusion, traditionally, release of NO and opening of K_{Ca} channels have been regarded as distinct endothelium-dependent pathways for modulation of resistance artery diameter. This thesis presents several lines of evidence to support the proposal that the integrated activity of K_{Ca} channels, and NO provide a stimulus- and context -dependent mechanism to fine tune arterial diameter and maintain appropriate levels of tissue perfusion. Together, these data support my hypothesis that pharmacological activators of endothelial K_{Ca} channels can reduce vascular O_2^- production and may provide a novel therapeutic approach to reducing O_2^- in pathological states associated with endothelial dysfunction

6.2: Future directions

The data presented in this thesis opens up a number of potential avenues for future research such as:

Exploration of the source of O_2^- regulated by openers of K_{Ca} channels. NADPH oxidase is a voltage-sensitive enzyme and so its activity can be modulated by cell membrane potential. The

possibility that other sources of O_2^-, such as xanthine oxidase, may be modulated by changes in membrane potential remains to be explored.

SK_{Ca} channels identified on the inner mitochondrial membrane in both neurons and cardiac myocytes have been identified as a potential target for new approaches to the treatment of conditions associated with increased production of O_2^-, such as cerebral and cardiac ischemia, as well as endoplasmic reticulum stress and oxidative cell death[137–143,152–156,563,564]. Cell surface expression of SK_{Ca} channels has been identified in endothelial cells, but whether they are present on mitochondria on endothelial and/or smooth muscle cells has yet to be investigated.

Investigation of the ability of activators of SK_{Ca} and IK_{Ca} to reduce O_2^- availability in models of endothelial dysfunction and transgenic animals. Our lab has shown that acute exposure of isolated arteries from diabetic rats to K_{Ca} channel activators can enhance NO-mediated endothelium-dependent relaxation. Application of the methodology to simultaneously measure arterial diameter and changes in O_2^- levels to isolated arteries from animal models of disease, and potentially patients, will allow for investigation of the ability of K_{Ca} channel activators to reduce O_2^- production and reduce other deleterious consequences of O_2^- generation (such as increased formation of $ONOO^-$ producing detrimental effects on many proteins and lipids) in the setting of disease.

The use of arteries from mice lacking endothelial SK_{Ca} and IK_{Ca} channels would allow for investigation of the role of these channels in regulation of O_2^- levels and be useful in confirming the selectivity of K_{Ca} channel activators.

References:

1. Grundy D. Principles and standards for reporting animal experiments. *Exp Physiol*. 2015;100(7):755-758.
2. WHO|Cardiovascular diseases (CVDs). *WHO*. 2017:http://www.who.int/cardiovascular_diseases/en/.
3. Schiffrin EL. The endothelium of resistance arteries: physiology and role in hypertension. *Prostaglandins, Leukot Essent Fat Acids*. 1996;54(1):17-25.
4. Somlyo AP, Himpens B. Cell calcium and its regulation in smooth muscle. *FASEB J*. 1989;3(11):2266-2276.
5. Filo RS, Bohr DF, Ruegg JC. Glycerinated skeletal and smooth muscle: calcium and magnesium dependence. *Science*. 1965;147(3665):1581-1583.
6. Allen BG, Walsh MP. The biochemical basis of the regulation of smooth-muscle contraction. *Trends Biochem Sci*. 1994;19(9):362-368.
7. Ghosh D, Syed AU, Prada MP, Nystoriak MA, Santana LF, Nieves-Cintrón M, Navedo MF. Calcium Channels in Vascular Smooth Muscle. *Adv Pharmacol*. 2017;78:49-87.
8. McDaniel SS, Platoshyn O, Wang J, Yu Y, Sweeney M, Krick S, Rubin LJ, Yuan JX. Capacitative Ca(2+) entry in agonist-induced pulmonary vasoconstriction. *Am J Physiol Lung Cell Mol Physiol*. 2001;280(5):L870-L870.
9. Kamm KE, Stull JT. Dedicated myosin light chain kinases with diverse cellular functions. *J Biol Chem*. 2001;276(7):4527-4530.
10. Hasegawa Y, Morita F. Role of 17-kDa essential light chain isoforms of aorta smooth muscle myosin. *J Biochem*. 1992;111(6):804-809.
11. Kim HR, Appel S, Vetterkind S, Gangopadhyay SS, Morgan KG. Smooth muscle signalling pathways in health and disease. *J Cell Mol Med*. 2008;12(6a):2165-2180.
12. Saddouk FZ, Ginnan R, Singer HA. Ca2+/calmodulin-dependent protein kinase II in vascular smooth muscle. *Adv Pharmacol*. 2017;78:171-202.
13. Walsh MP. The Ayerst Award Lecture 1990. Calcium-dependent mechanisms of regulation of smooth muscle contraction. *Biochem Cell Biol*. 1991;69(12):771-800.
14. Kuo IY, Ehrlich BE. Signaling in Muscle Contraction. *Cold Spring Harb Perspect Biol*. 2015;7(2):a006023.
15. Brozovich F V., Nicholson CJ, Degen C V., Gao YZ, Aggarwal M, Morgan KG. Mechanisms of vascular smooth muscle contraction and the basis for pharmacologic treatment of smooth muscle disorders. *Pharmacol Rev*. 2016;68(2):476-532.
16. Kim J-H, Lee L-K, Lee W-D, Lee J-U, Kim -Young, Kim -Hyun, Choi B-R, Yang S-M, Jeon H-J, Lee T-H, Kwak T-Y, Kim B, Kim J. A Review of Signal Transduction in Mechanisms of Smooth Muscle Contraction and Its Relevance for Specialized Physical Therapy. *J Phys Ther Sci*. 2013;25:129-141.
17. Tribe RM, Borin ML, Blaustein MP. Functionally and spatially distinct Ca2+ stores are revealed in cultured vascular smooth muscle cells (sarcoplasmic reticulum/thaplgarn/caffeine/fura-2/chlortetracycline). *Physiology*. 1994;91:5908-5912.
18. Bian J, Ghosh TK, Wang J-C, Gill DL. Identification of intracellular calcium pools selective modification by thapsigargin. 1991;266(14):8801-8806.
19. Chueh SH, Gill DL. Inositol 1,4,5-trisphosphate and guanine nucleotides activate calcium release from endoplasmic reticulum via distinct mechanisms. *J Biol Chem*. 1986;261(30):13883-13886.
20. Baró I, Eisner DA. The effects of thapsigargin on [Ca2+]i in isolated rat mesenteric artery

vascular smooth muscle cells. *Pflogers Arch Eur J Physiol*. 1992;420(1):115-117.

21. Knot HJ, Standen NB, Nelson MT. Ryanodine receptors regulate arterial diameter and wall [Ca2+] in cerebral arteries of rat via Ca2+-dependent K+ channels. *J Physiol*. 1998;508((Pt 1)):211-221.

22. Kamishima T, McCarron JG. Regulation of the cytosolic Ca2+ concentration by Ca2+ stores in single smooth muscle cells from rat cerebral arteries. *J Physiol*. 1997;501 (Pt 3):497-508.

23. Marks AR. Calcium channels expressed in vascular smooth muscle. *Circulation*. 1992;86(6 Suppl):III61-III67.

24. Berridge MJ. Smooth muscle cell calcium activation mechanisms. *J Physiol*. 2008;586(21):5047-5061.

25. Amberg GC, Navedo MF. Calcium Dynamics in Vascular Smooth Muscle. *Microcirculation*. 2013;20(4):281-289.

26. Nelson MT, Cheng H, Rubart M, Santana LF, Bonev AD, Knot HJ, Lederer WJ. Relaxation of arterial smooth muscle by calcium sparks. *Science*. 1995;270(5236):633-637.

27. Pérez GJ, Bonev AD, Nelson MT. Micromolar Ca(2+) from sparks activates Ca(2+)-sensitive K(+) channels in rat cerebral artery smooth muscle. *Am J Physiol Cell Physiol*. 2001;281(6):C1769-C1775.

28. Lamont C, Wier WG. Different roles of ryanodine receptors and inositol (1,4,5)-trisphosphate receptors in adrenergically stimulated contractions of small arteries. *Am J Physiol Heart Circ Physiol*. 2004;287(2):H617-H625.

29. Krishnamoorthy G, Sonkusare SK, Heppner TJ, Nelson MT. Opposing roles of smooth muscle BK channels and ryanodine receptors in the regulation of nerve-evoked constriction of mesenteric resistance arteries. *Am J Physiol Heart Circ Physiol*. 2014;306(7):H981-H988.

30. Ji G, Feldman ME, Greene KS, Sorrentino V, Xin H-B, Kotlikoff MI. RYR2 proteins contribute to the formation of Ca(2+) sparks in smooth muscle. *J Gen Physiol*. 2004;123(4):377-386.

31. Jaggar JH, Porter VA, Lederer WJ, Nelson MT. Calcium sparks in smooth muscle. *Am J Physiol Cell Physiol*. 2000;278(2):C235-C256.

32. Jaggar JH. Intravascular pressure regulates local and global Ca(2+) signaling in cerebral artery smooth muscle cells. *Am J Physiol Cell Physiol*. 2001;281(2):C439-C448.

33. Bonev AD, Jaggar JH, Rubart M, Nelson MT. Activators of protein kinase C decrease Ca2+ spark frequency in smooth muscle cells from cerebral arteries. *Am J Physiol*. 1997;273(6 Pt 1):C2090-C2095.

34. Jaggar JH, Wellman GC, Heppner TJ, Porter VA, Perez GJ, Gollasch M, Kleppisch T, Rubart M, Stevenson AS, Lederer WJ, Knot HJ, Bonev AD, Nelson MT. Ca2+ channels, ryanodine receptors and Ca(2+)-activated K+ channels: a functional unit for regulating arterial tone. *Acta Physiol Scand*. 1998;164(4):577-587.

35. Liou J, Kim ML, Heo W Do, Jones JT, Myers JW, Ferrell JE, Meyer T. STIM is a Ca2+ sensor essential for Ca2+-store-depletion-triggered Ca2+ influx. *Curr Biol*. 2005;15(13):1235-1241.

36. Trebak M. STIM/Orai signalling complexes in vascular smooth muscle. *J Physiol*. 2012;590(17):4201-4208.

37. Zeng W, Yuan JP, Kim MS, Choi YJ, Huang GN, Worley PF, Muallem S. STIM1 Gates

TRPC Channels, but Not Orai1, by Electrostatic Interaction. *Mol Cell*. 2008;32(3):439-448.

38. Beech DJ. Integration of transient receptor potential canonical channels with lipids. *Acta Physiol*. 2012;204(2):227-237.

39. Catterall WA. Voltage-Gated Calcium Channels. *Cold Spring Harb Perspect Biol*. 2011;3(8):a003947.

40. Tanabe T, Takeshima H, Mikami A, Flockerzi V, Takahashi H, Kangawa K, Kojima M, Matsuo H, Hirose T, Numa S. Primary structure of the receptor for calcium channel blockers from skeletal muscle. *Nature*. 1987;328(6128):313-318.

41. Gurnett CA, Waard M De, Campbell KP. Dual Function of the Voltage-Dependent Ca2+ Channel α2δ Subunit in Current Stimulation and Subunit Interaction. *Neuron*. 1996;16(2):431-440.

42. Jay SD, Ellis SB, McCue AF, Williams ME, Vedvick TS, Harpold MM, Campbell KP. Primary structure of the gamma subunit of the DHP-sensitive calcium channel from skeletal muscle. *Science*. 1990;248(4954):490-492.

43. Ruth P, Röhrkasten A, Biel M, Bosse E, Regulla S, Meyer HE FVH. Primary structure of the beta subunit of the DHP-sensitive calcium channel from skeletal muscle. *Science (80-)*. 1989;245(4922):1115-1118.

44. Liu H, De Waard M, Scott VE, Gurnett CA, Lennon VA, Campbell KP. Identification of three subunits of the high affinity omega-conotoxin MVIIC-sensitive Ca2+ channel. *J Biol Chem*. 1996;271(23):13804-13810.

45. Letts VA, Frankel WN, Felix R, Biddlecome GH, Arikkath J, Mahaffey CL, Valenzuela A, Bartlett FS, Mori Y, Campbell KP. The mouse stargazer gene encodes a neuronal Ca2+-channel |[gamma]|subunit. *Nat Genet*. 1998;19(4):340-347.

46. Lacerda AE, Kim HS, Ruth P, Perez-Reyes E, Flockerzi V, Hofmann F, Birnbaumer L, Brown AM. Normalization of current kinetics by interaction between the α1and β subunits of the skeletal muscle dihydropyridine-sensitive Ca2+ channel. *Nature*. 1991;352(6335):527-530.

47. Catterall WA, Perez-Reyes E, Snutch TP, Striessnig J. International Union of Pharmacology. XLVIII. Nomenclature and structure-function relationships of voltage-gated calcium channels. *Pharmacol Rev*. 2005;57(4):411-425.

48. Benham CD, Hess P, Tsien RW. Two types of calcium channels in single smooth muscle cells from rabbit ear artery studied with whole-cell and single-channel recordings. *Circ Res*. 1987;61(4 Pt 2):I10-I16.

49. Loirand G, Pacaud P, Mironneau C, Mironneau J. Evidence for two distinct calcium channels in rat vascular smooth muscle cells in short-term primary culture. *Pfliigers Arch*. 1986;407:566-568.

50. Bean BP, Sturek M, Puga A, Hermsmeyer K. Calcium channels in muscle cells isolated from rat mesenteric arteries: modulation by dihydropyridine drugs. *Circ Res*. 1986;59(2):229-235.

51. Knot HJ, Nelson MT. Regulation of arterial diameter and wall [Ca2+] in cerebral arteries of rat by membrane potential and intravascular pressure. *J Physiol*. 1998;508(Pt 1):199-209.

52. Hwa JJ, Bevan JA. Stretch-dependent (myogenic) tone in rabbit ear resistance arteries. *Am J Physiol Circ Physiol*. 1986;250(1):H87-H95.

53. Lee SHW · CO. Role of PKC in the effects of α1-adrenergic stimulation on Ca2+

transients, contraction and Ca2+ current in guinea-pig ventricular myocytes. *Pflügers Arch – Eur J Physiol*. 1999;437:335–344.

54. Tseng GN, Boyden PA. Different effects of intracellular Ca and protein kinase C on cardiac T and L Ca currents. *Am J Physiol*. 1991;261(2 Pt 2):H364-H379.

55. Taguchi K, Ueda M, Kubo T. Effects of cAMP and cGMP on L-Type Calcium Channel Currents in Rat Mesenteric Artery Cells. *J Pharmacol*. 1997;74:179-186.

56. Ousterhout JM, Sperelakis N. Cyclic nucleotides depress action potentials in cultured aortic smooth muscle cells. *Eur J Pharmacol*. 1987;144:7-14.

57. Delpy E, Coste H, Gouville AC. Effects of cyclic GMP elevation on isoprenaline-induced increase in cyclic AMP and relaxation in rat aortic smooth muscle: role of phosphodiesterase 3. *Br J Pharmacol*. 1996;119(3):471-478.

58. Bkaily G, Sperelakis N. Injection of guanosine 5'-cyclic monophosphate into heart cells blocks calcium slow channels. *Am J Physiol*. 1985;248(5 Pt 2):H745-H749.

59. Wahler GM, Sperelakis N. Intracellular injection of cyclic GMP depresses cardiac slow action potentials. *J Cyclic Nucleotide Protein Phosphor Res*. 1985;10(1):83-95.

60. Brueggemann LI, Martin BL, Barakat J, Byron KL, Cribbs LL. Low voltage-activated calcium channels in vascular smooth muscle: T-type channels and AVP-stimulated calcium spiking. *Am J Physiol Heart Circ Physiol*. 2005;288(2):H923-H935.

61. Harraz OF, Abd El-Rahman RR, Bigdely-Shamloo K, Wilson SM, Brett SE, Romero M, Gonzales AL, Earley S, Vigmond EJ, Nygren A, Menon BK, Mufti RE, Watson T, Starreveld Y, Furstenhaupt T, Muellerleile PR, Kurjiaka DT, Kyle BD, Braun AP, Welsh DG. CaV3.2 Channels and the Induction of Negative Feedback in Cerebral Arteries. *Circ Res*. 2014;115(7):650-661.

62. Tsien RW, Lipscombe D, Madison D V, Bley KR, Fox AP. Multiple types of neuronal calcium channels and their selective modulation. *Trends Neurosci*. 1988;11(10):431-438.

63. Kuo IY, Ellis A, Seymour VAL, Sandow SL, Hill CE. Dihydropyridine-insensitive calcium currents contribute to function of small cerebral arteries. *J Cereb Blood Flow Metab*. 2010;30(6):1226-1239.

64. Abd El-Rahman RR, Harraz OF, Brett SE, Anfinogenova Y, Mufti RE, Goldman D, Welsh DG. Identification of L- and T-type Ca2+ channels in rat cerebral arteries: role in myogenic tone development. *Am J Physiol Heart Circ Physiol*. 2013;304(1):H58-H71.

65. Harraz OF, Visser F, Brett SE, Goldman D, Zechariah A, Hashad AM, Menon BK, Watson T, Starreveld Y, Welsh DG. CaV1.2/CaV3.x channels mediate divergent vasomotor responses in human cerebral arteries. *J Gen Physiol*. 2015;145(5):405-418.

66. Goulopoulou S, Webb RC. Symphony of vascular contraction: how smooth muscle cells lose harmony to signal increased vascular resistance in hypertension. *Hypertension*. 2014;63(3):e33-e39.

67. Somlyo AP, Somlyo A V. Ca2+ sensitivity of smooth muscle and nonmuscle myosin II: modulated by G proteins, kinases, and myosin phosphatase. *Physiol Rev*. 2003;83(4):1325-1358.

68. Wilson DP, Susnjar M, Kiss E, Sutherland C, Walsh MP. Thromboxane A2 -induced contraction of rat caudal arterial smooth muscle involves activation of Ca 2+ entry and Ca 2+ sensitization: Rho-associated kinase-mediated phosphorylation of MYPT1 at Thr-855, but not Thr-697. *Biochem J*. 2005;389(3):763-774.

69. Swärd K, Mita M, Wilson DP, Deng JT, Susnjar M, Walsh MP. The role of RhoA and Rho-associated kinase in vascular smooth muscle contraction. *Curr Hypertens Rep*.

2003;5(1):66-72.

70. Feng J, Ito M, Ichikawa K, Isaka N, Nishikawa M, Hartshorne DJ, Nakano T. Inhibitory phosphorylation site for Rho-associated kinase on smooth muscle myosin phosphatase. *J Biol Chem*. 1999;274(52):37385-37390.

71. Nihon Seikagakkai. M, Ohmori T, Suzuki M, Furuya K, Morita F. A Novel Protein Phosphatase-1 Inhibitory Protein Potentiated by Protein Kinase C. Isolation from Porcine Aorta Media and Characterization. *J Biochem*. 1995;118(6):1104-1107.

72. Walsh MP, Susnjar M, Deng J, Sutherland C, Kiss E, Wilson DP. Phosphorylation of the Protein Phosphatase Type 1 Inhibitor Protein CPI-17 by Protein Kinase C. *Protein Phosphatase Protoc*. 2007;365:209-223.

73. El-Yazbi AF, Abd-Elrahman KS. ROK and Arteriolar Myogenic Tone Generation: Molecular Evidence in Health and Disease. *Front Pharmacol*. 2017;8:87.

74. Nelson MT. Regulation of arterial tone by potassium channels. *Jpn J Pharmacol*. 1992;58(Suppl 2):238P-242P.

75. Nelson MT. Ca2+-activated potassium channels and ATP-sensitive potassium channels as modulators of vascular tone. *Trends Cardiovasc Med*. 1993;3(2):54-60.

76. Nelson MT, Quayle JM. Physiological roles and properties of potassium channels in arterial smooth muscle. *Am Physiol Soc*. 1995;268(4 Pt 1):C799-C822.

77. Nelson MT, Patlak JB, Worley JF, Standen NB. Calcium channels, potassium channels, and voltage dependence of arterial smooth muscle tone. *Am J Physiol Physiol*. 1990;259(1):C3-C18.

78. Jackson WF. Potassium Channels in Regulation of Vascular Smooth Muscle Contraction and Growth. In: *Advances in Pharmacology (San Diego, Calif.)*. Vol 78. ; 2017:89-144.

79. Lang RJ, Harvey JR, McPhee GJ, Klemm MF. Nitric oxide and thiol reagent modulation of Ca2+-activated K+ (BKCa) channels in myocytes of the guinea-pig taenia caeci. *J Physiol*. 2000;525(Pt 2):363-376.

80. Quignard JF, Félétou M, Edwards G, Duhault J, Weston AH, Vanhoutte PM. Role of endothelial cell hyperpolarization in EDHF-mediated responses in the guinea-pig carotid artery. *Br J Pharmacol*. 2000;129(6):1103-1112.

81. Catacuzzeno L, Pisconti DA, Harper AA, Petris A, Franciolini F. Characterization of the large-conductance Ca-activated K channel in myocytes of rat saphenous artery. *Pflugers Arch*. 2000;441(2-3):208-218.

82. Aldrich RW, Brenner R, Peréz GJ, Bonev AD, Eckman DM, Kosek JC, Wiler SW, Patterson AJ, Nelson MT. Vasoregulation by the beta1 subunit of the calcium-activated potassium channel. *Nature*. 2000;407(6806):870-876.

83. Suh EY, Yin MZ, Lin H, Zhang YH, Yoo HY, Kim SJ. Maxi-K channel (BK$_{Ca}$) activity veils the myogenic tone of mesenteric artery in rats. *Physiol Rep*. 2017;5(14):e13330.

84. Köhler R, Ruth P. Endothelial dysfunction and blood pressure alterations in K+-channel transgenic mice. *Pflügers Arch - Eur J Physiol*. 2010;459(6):969-976.

85. Adeagbo AS. 1-Ethyl-2-benzimidazolinone stimulates endothelial K(Ca) channels and nitric oxide formation in rat mesenteric vessels. *Eur J Pharmacol*. 1999;379(2-3):151-159.

86. Kun A, Matchkov V V, Stankevicius E, Nardi A, Hughes AD, Kirkeby HJ, Demnitz J, Simonsen U. NS11021, a novel opener of large-conductance Ca(2+)-activated K(+) channels, enhances erectile responses in rats. *Br J Pharmacol*. 2009;158(6):1465-1476.

87. Ohya S, Kuwata Y, Sakamoto K, Muraki K, Imaizumi Y. Cardioprotective effects of estradiol include the activation of large-conductance Ca(2+)-activated K(+) channels in

cardiac mitochondria. *Am J Physiol Heart Circ Physiol*. 2005;289(4):H1635-H1642.

88. Borchert GH, Hlaváčková M, Kolář F. Pharmacological activation of mitochondrial BK(Ca) channels protects isolated cardiomyocytes against simulated reperfusion-induced injury. *Exp Biol Med (Maywood)*. 2013;238(2):233-241.

89. Soltysinska E, Bentzen BH, Barthmes M, Hattel H, Thrush AB, Harper M-E, Qvortrup K, Larsen FJ, Schiffer TA, Losa-Reyna J, Straubinger J, Kniess A, Thomsen MB, Brüggemann A, Fenske S, Biel M, Ruth P, Wahl-Schott C, Boushel RC, Olesen S-P, Lukowski R. KCNMA1 encoded cardiac BK channels afford protection against ischemia-reperfusion injury. *PLoS One*. 2014;9(7):e103402.

90. Bentzen BH, Osadchii O, Jespersen T, Hansen RS, Olesen S-P, Grunnet M. Activation of big conductance Ca(2+)-activated K (+) channels (BK) protects the heart against ischemia-reperfusion injury. *Pflugers Arch*. 2009;457(5):979-988.

91. Tanaka Y, Meera P, Song M, Knaus HG, Toro L. Molecular constituents of maxi KCa channels in human coronary smooth muscle: predominant alpha + beta subunit complexes. *J Physiol*. 1997;502 (Pt 3):545-557.

92. Barrett JN, Magleby KL, Pallotta BS. Properties of single calcium-activated potassium channels in cultured rat muscle. *J Physiol*. 1982;331:211-230.

93. Horrigan FT, Cui J, Aldrich RW. Allosteric Voltage Gating of Potassium Channels I: Mslo ionic currents in the absence of Ca(2+). *J Gen Physiol*. 1999;114(2):277-304.

94. Pallotta BS, Magleby KL, Barrett JN. Single channel recordings of Ca2+-activated K+ currents in rat muscle cell culture. *Nature*. 1981;293(5832):471-474.

95. Knaussp H-G, Folandefl K, Garcia-Calvosii M, Garcia ML, Kaczorowskis GJ, Smith M, Swansonn R. Primary Sequence and Immunological Characterization of beta-subunit of High Conductance Ca2+-activated K+ Channel from Smooth Muscle. *J Biol Chem*. 1994;269(25):17274-17278.

96. Balderas E, Zhang J, Stefani E, Toro L. Mitochondrial BKCa channel. *Front Physiol*. 2015;6:104.

97. Schreiber M, Salkoff L. A novel calcium-sensing domain in the BK channel. *Biophys J*. 1997;73(3):1355-1363.

98. Hoshi T, Pantazis A, Olcese R. Transduction of voltage and Ca2+ signals by Slo1 BK channels. *Physiology*. 2013;28(3):172-189.

99. Marty A. Ca-dependent K channels with large unitary conductance in chromaffin cell membranes. *Nature*. 1981;291(5815):497-500.

100. Ishii TM, Silvia C, Hirschberg B, Bond CT, Adelman JP, Maylie J. A human intermediate conductance calcium-activated potassium channel. *Proc Natl Acad Sci U S A*. 1997;94(21):11651-11656.

101. Benham CD, Bolton TB, Lang RJ, Takewaki T. Calcium-activated potassium channels in single smooth muscle cells of rabbit jejunum and guinea-pig mesenteric artery. *J Physiol*. 1986;371(1):45-67.

102. Petkov G V, Bonev AD, Heppner TJ, Brenner R, Aldrich RW, Nelson MT. Beta1-subunit of the Ca2+-activated K+ channel regulates contractile activity of mouse urinary bladder smooth muscle. *J Physiol*. 2001;537(Pt 2):443-452.

103. Ledoux J, Werner ME, Brayden JE, Nelson MT, Matthias WE, Brayden JE, Nelson MT. Calcium-Activated Potassium Channels and the Regulation of Vascular Tone. *Physiology*. 2006;21(1):69-78.

104. McManus OB, Helms LM, Pallanck L, Ganetzky B, Swanson R, Leonard RJ. Functional

role of the beta subunit of high conductance calcium-activated potassium channels. *Neuron*. 1995;14(3):645-650.

105. Meera P, Wallner M, Jiang Z, Toro L. A calcium switch for the functional coupling between alpha (hslo) and beta subunits (KV,Ca beta) of maxi K channels. *FEBS Lett*. 1996;382(1-2):84-88.

106. Yang Y, Sohma Y, Nourian Z, Ella SR, Li M, Stupica A, Korthuis RJ, Davis MJ, Braun AP, Hill MA. Mechanisms underlying regional differences in the ca 2+ sensitivity of BK Ca current in arteriolar smooth muscle. *J Physiol*. 2013;591(5):1277-1293.

107. Yang Y, Murphy T V, Ella SR, Grayson TH, Haddock R, Hwang YT, Braun AP, Peichun G, Korthuis RJ, Davis MJ, Hill MA. Heterogeneity in function of small artery smooth muscle BKCa: involvement of the beta1-subunit. *J Physiol*. 2009;587(Pt 12):3025-3044.

108. Sandow SL, Grayson TH. Limits of isolation and culture: intact vascular endothelium and BKCa. *Am J Physiol Heart Circ Physiol*. 2009;297(1):H1-H7.

109. Castillo K, Contreras GF, Pupo A, Torres YP, Neely A, González C, Latorre R. Molecular mechanism underlying β1 regulation in voltage- and calcium-activated potassium (BK) channels. *Proc Natl Acad Sci U S A*. 2015;112(15):4809-4814.

110. Singh H, Lu R, Bopassa JC, Meredith AL, Stefani E, Toro L. MitoBK(Ca) is encoded by the Kcnma1 gene, and a splicing sequence defines its mitochondrial location. *Proc Natl Acad Sci U S A*. 2013;110(26):10836-10841.

111. Stowe DF, Aldakkak M, Camara AKS, Riess ML, Heinen A, Varadarajan SG, Jiang M-T. Cardiac mitochondrial preconditioning by Big Ca2+-sensitive K+ channel opening requires superoxide radical generation. *Am J Physiol Heart Circ Physiol*. 2006;290(1):H434-H440.

112. Aldakkak M, Stowe DF, Cheng Q, Kwok W-M, Camara AKS. Mitochondrial matrix K+ flux independent of large-conductance Ca2+-activated K+ channel opening. *Am J Physiol Cell Physiol*. 2010;298(3):C530-C541.

113. Xia X-M, Ding JP, Lingle CJ. Molecular Basis for the Inactivation of Ca 2+ -and Voltage-Dependent BK Channels in Adrenal Chromaffin Cells and Rat Insulinoma Tumor Cells. *J Neurosci*. 1999;19(13):5255-5264.

114. Yan X-H, Guo X-Y, Jiao F-Y, Liu X, Liu Y. Activation of large-conductance Ca(2+)-activated K(+) channels inhibits glutamate-induced oxidative stress through attenuating ER stress and mitochondrial dysfunction. *Neurochem Int*. 2015;90:28-35.

115. Kerbiriou-Nabias D, Arachiche A, Dachary-Prigent J. Phosphatidylserine exposure and calcium-activated potassium efflux in platelets. *Br J Haematol*. 2011;155(2):268-270.

116. Kerr PM, Tam R, Narang D, Potts K, Mcmillan D, Mcmillan K, Plane F. Endothelial calcium-activated potassium channels as therapeutic targets to enhance availability of nitric oxide. *Can J Physiol Pharmacol*. 2012;90(6):739-752.

117. Burnham MP, Bychkov R, Félétou M, Richards GR, Vanhoutte PM, Weston AH, Edwards G. Characterization of an apamin-sensitive small-conductance Ca(2+)-activated K(+) channel in porcine coronary artery endothelium: relevance to EDHF. *Br J Pharmacol*. 2002;135(5):1133-1143.

118. Dora KA, Gallagher NT, Mcneish A, Garland CJ. Modulation of Endothelial Cell K Ca 3.1 Channels During Endothelium-Derived Hyperpolarizing Factor Signaling in Mesenteric Resistance Arteries. *Circ Res*. 2008;102(10):1247-1255.

119. Marchenko SM, Sage S 0. Calcium-activated potassium channels in the endothelium of intact rat aorta. *J Physiol*. 1996;492(1):53-60.

120. Chen MX, Gorman SA, Benson B, Singh K, Hieble JP, Michel MC, Tate SN, Trezise DJ. Small and intermediate conductance Ca 2+ -activated K + channels confer distinctive patterns of distribution in human tissues and differential cellular localisation in the colon and corpus cavernosum. *Naunyn Schmiedebergs Arch Pharmacol*. 2004;369(6):602-615.

121. Sankaranarayanan A, Raman G, Busch C, Schultz T, Zimin PI, Hoyer J, Köhler R, Wulff H. Naphtho[1,2-d]thiazol-2-ylamine (SKA-31), a new activator of KCa2 and KCa3.1 potassium channels, potentiates the endothelium-derived hyperpolarizing factor response and lowers blood pressure. *Mol Pharmacol*. 2009;75(2):281-295.

122. Absi M, Burnham MP, Weston AH, Harno E, Rogers M, Edwards G. Effects of methyl β-cyclodextrin on EDHF responses in pig and rat arteries; association between SKCa channels and caveolin-rich domains. *Br J Pharmacol*. 2009;151(3):332-340.

123. Crane GJ, Garland CJ. Thromboxane receptor stimulation associated with loss of SK Ca activity and reduced EDHF responses in the rat isolated mesenteric artery. *Br J Pharmacol*. 2004;142(1):43-50.

124. Damkjaer M, Nielsen G, Bodendiek S, Staehr M, Gramsbergen J-B, de Wit C, Jensen BL, Simonsen U, Bie P, Wulff H, Köhler R. Pharmacological activation of KCa3.1/KCa2.3 channels produces endothelial hyperpolarization and lowers blood pressure in conscious dogs. *Br J Pharmacol*. 2012;165(1):223-234.

125. Sandow SL, Neylon CB, Chen MX, Garland CJ. Spatial separation of endothelial small- and intermediate-conductance calcium-activated potassium channels (KCa) and connexins: possible relationship to vasodilator function? *J Anat*. 2006;209(5):689-698.

126. Gaete PS, Lillo MA, Ardiles NM, Pérez FR, Figueroa XF. Ca2+-activated K+ channels of small and intermediate conductance control eNOS activation through NAD(P)H oxidase. *Free Radic Biol Med*. 2012;52(5):860-870.

127. Taylor MS, Bonev AD, Gross TP, Eckman DM, Brayden JE, Bond CT, Adelman JP, Nelson MT. Altered Expression of Small-Conductance Ca2+-Activated K+ (SK3) Channels Modulates Arterial Tone and Blood Pressure. *Circ Res*. 2003;93(2):124-131.

128. Sheng J, Ella S, Davis MJ, Hill MA, Braun AP. Openers of SKCa and IKCa channels enhance agonist-evoked endothelial nitric oxide synthesis and arteriolar vasodilation. *FASEB J*. 2009;23(4):1138-1145.

129. Doughty JM, Plane F, Langton PD. Charybdotoxin and apamin block EDHF in rat mesenteric artery if selectively applied to the endothelium. *Am J Physiol*. 1999;276(3 Pt 2):H1107-H1112.

130. Wei R, Lunn SE, Tam R, Gust SL, Classen B, Kerr PM, Plane F. Vasoconstrictor stimulus determines the functional contribution of myoendothelial feedback to mesenteric arterial tone. *J Physiol*. 2018;596(7):1181-1197.

131. Sheng J-Z, Braun AP. Small-and intermediate-conductance Ca 2+ -activated K+ channels directly control agonist-evoked nitric oxide synthesis in human vascular endothelial cells. *Am J Physiol Cell Physiol*. 2007;293(1):458-467.

132. Goedicke-Fritz S, Kaistha A, Kacik M, Markert S, Hofmeister A, Busch C, Bänfer S, Jacob R, Grgic I, Hoyer J. Evidence for functional and dynamic microcompartmentation of Cav-1/TRPV4/K(Ca) in caveolae of endothelial cells. *Eur J Cell Biol*. 2015;94(7-9):391-400.

133. Lu T, Wang X-L, Chai Q, Sun X, Sieck GC, Katusic ZS, Lee H-C. Role of the endothelial caveolae microdomain in shear stress-mediated coronary vasorelaxation. *J Biol Chem*. 2017;292(46):19013-19023.

134. Li N, Timofeyev V, Tuteja D, Xu D, Lu L, Zhang Q, Zhang Z, Singapuri A, Albert TR, Rajagopal A V, Bond CT, Periasamy M, Adelman J, Chiamvimonvat N. Ablation of a Ca2+-activated K+ channel (SK2 channel) results in action potential prolongation in atrial myocytes and atrial fibrillation. *J Physiol*. 2009;587(Pt 5):1087-1100.

135. Mizukami K, Yokoshiki H, Mitsuyama H, Watanabe M, Tenma T, Takada S, Tsutsui H. Small-conductance Ca2+-activated K+ current is upregulated via the phosphorylation of CaMKII in cardiac hypertrophy from spontaneously hypertensive rats. *Am J Physiol Heart Circ Physiol*. 2015;309(6):H1066-H1074.

136. Tuteja D, Xu D, Timofeyev V, Lu L, Sharma D, Zhang Z, Xu Y, Nie L, Vázquez AE, Young JN, Glatter KA, Chiamvimonvat N. Differential expression of small-conductance Ca2+-activated K+ channels SK1, SK2, and SK3 in mouse atrial and ventricular myocytes. *Am J Physiol Heart Circ Physiol*. 2005;289(6):H2714-H2723.

137. Yun Kim T, Terentyeva R, Roder KHF, Li W, Liu M, Greener I, Hamilton S, Polina I, Murphy KR, Clements RT, Dudley SC, Koren G, Choi B-R, Terentyev D. SK Channel Enhancers Attenuate Ca 2+ -Dependent Arrhythmia in Hypertrophic Hearts by Regulating Mito-ROS-Dependent Oxidation and Activity of RyR. *Cardiovasc Res*. 2017;113(3):343-353.

138. Stowe DF, Gadicherla AK, Zhou Y, Aldakkak M, Cheng Q, Kwok W-M, Jiang MT, Heisner JS, Yang M, Camara AKS. Protection against cardiac injury by small Ca(2+)-sensitive K(+) channels identified in guinea pig cardiac inner mitochondrial membrane. *Biochim Biophys Acta*. 2013;1828(2):427-442.

139. Köhler M, Hirschberg B, Bond CT, Kinzie JM, Marrion N V, Maylie J, Adelman JP. Small-conductance, calcium-activated potassium channels from mammalian brain. *Science*. 1996;273(5282):1709-1714.

140. Xia XM, Fakler B, Rivard A, Wayman G, Johnson-Pais T, Keen JE, Ishii T, Hirschberg B, Bond CT, Lutsenko S, Maylie J, Adelman JP. Mechanism of calcium gating in small-conductance calcium-activated potassium channels. *Nature*. 1998;395(6701):503-507.

141. Herrik KF, Redrobe JP, Holst D, Hougaard C, Sandager-Nielsen K, Nielsen AN, Ji H, Holst NM, Rasmussen HB, Nielsen EØ, Strøbæk D, Shepard PD, Christophersen P. CyPPA, a Positive SK3/SK2 Modulator, Reduces Activity of Dopaminergic Neurons, Inhibits Dopamine Release, and Counteracts Hyperdopaminergic Behaviors Induced by Methylphenidate1. *Front Pharmacol*. 2012;3:11.

142. Bourque CW, Brown DA. Apamin and d-tubocurarine block the after-hyperpolarization of rat supraoptic neurosecretory neurons. *Neurosci Lett*. 1987;82(2):185-190.

143. Zhang L, Krnjević K. Apamin depresses selectively the after-hyperpolarization of cat spinal motoneurons. *Neurosci Lett*. 1987;74(1):58-62.

144. Richter M, Nickel C, Apel L, Kaas A, Dodel R, Culmsee C, Dolga AM. SK channel activation modulates mitochondrial respiration and attenuates neuronal HT-22 cell damage induced by H2O2. *Neurochem Int*. 2015;81:63-75.

145. Dolga AM, Netter MF, Perocchi F, Doti N, Meissner L, Tobaben S, Grohm J, Zischka H, Plesnila N, Decher N, Culmsee C. Mitochondrial small conductance SK2 channels prevent glutamate-induced oxytosis and mitochondrial dysfunction. *J Biol Chem*. 2013;288(15):10792-10804.

146. Schmidt E-M, Münzer P, Borst O, Kraemer BF, Schmid E, Urban B, Lindemann S, Ruth P, Gawaz M, Lang F. Ion channels in the regulation of platelet migration. *Biochem Biophys Res Commun*. 2011;415(1):54-60.

147. Krötz F, Hellwig N, Bürkle MA, Lehrer S, Riexinger T, Mannell H, Sohn H-Y, Klauss V, Pohl U. A sulfaphenazole-sensitive EDHF opposes platelet-endothelium interactions in vitro and in the hamster microcirculation in vivo. *Cardiovasc Res*. 2010;85(3):542-550.

148. Hasenau A-L, Nielsen G, Morisseau C, Hammock BD, Wulff H, Köhler R. Improvement of endothelium-dependent vasodilations by SKA-31 and SKA-20, activators of small- and intermediate-conductance Ca2+ -activated K+ -channels. *Acta physiol*. 2011;203(1):117-126.

149. Chen G, Cheung DW. Effect of K+-channel blockers on ACh-induced hyperpolarization and relaxation in mesenteric arteries. *Am Physiol Soc*. 1997;272(41):H2306-H2312.

150. Walker SD, Dora KA, Ings NT, Crane GJ, Garland CJ. Activation of endothelial cell IK(Ca) with 1-ethyl-2-benzimidazolinone evokes smooth muscle hyperpolarization in rat isolated mesenteric artery. *Br J Pharmacol*. 2001;134(7):1548-1554.

151. Ledoux J, Taylor MS, Bonev AD, Hannah RM, Solodushko V, Shui B, Tallini Y, Kotlikoff MI, Nelson MT. Functional architecture of inositol 1,4,5-trisphosphate signaling in restricted spaces of myoendothelial projections. *Proc Natl Acad Sci*. 2008;105(28):9627-9632.

152. Arnold SJ, Facer P, Yiangou Y, Chen MX, Plumpton C, Tate SN, Bountra C, Chan CLH, Williams NS, Anand P. Decreased potassium channel IK1 and its regulator neurotrophin-3 (NT-3) in inflamed human bowel. *Neuroreport*. 2003;14(2):191-195.

153. Vogalis F, Harvey JR, Neylon CB, Furness JB. Regulation of K+ channels underlying the slow afterhyperpolarization in enteric afterhyperpolarization-generating myenteric neurons: role of calcium and phosphorylation. *Clin Exp Pharmacol Physiol*. 2002;29(10):935-943.

154. Vogalis F, Harvey JR, Furness JB. TEA- and apamin-resistant K(Ca) channels in guinea-pig myenteric neurons: slow AHP channels. *J Physiol*. 2002;538(Pt 2):421-433.

155. Neylon CB, Nurgali K, Hunne B, Robbins HL, Moore S, Chen MX, Furness JB. Intermediate-conductance calcium-activated potassium channels in enteric neurones of the mouse: pharmacological, molecular and immunochemical evidence for their role in mediating the slow afterhyperpolarization. *J Neurochem*. 2004;90(6):1414-1422.

156. Furness JB, Robbins HL, Selmer I-S, Hunne B, Chen MX, Hicks GA, Moore S, Neylon CB. Expression of intermediate conductance potassium channel immunoreactivity in neurons and epithelial cells of the rat gastrointestinal tract. *Cell Tissue Res*. 2003;314(2):179-189.

157. Jensen BS, Odum N, Jorgensen NK, Christophersen P, Olesen SP. Inhibition of T cell proliferation by selective block of Ca(2+)-activated K(+) channels. *Proc Natl Acad Sci U S A*. 1999;96(19):10917-10921.

158. Hoffman JF, Joiner W, Nehrke K, Potapova O, Foye K, Wickrema A. The hSK4 (KCNN4) isoform is the Ca2+-activated K+ channel (Gardos channel) in human red blood cells. *Proc Natl Acad Sci*. 2003;100(12):7366-7371.

159. de Silva HA, Carver JG, Aronson JK. Pharmacological evidence of calcium-activated and voltage-gated potassium channels in human platelets. *Clin Sci (Lond)*. 1997;93(3):249-255.

160. Thompson-Vest N, Shimizu Y, Hunne B, Furness JB. The distribution of intermediate-conductance, calcium-activated, potassium (IK) channels in epithelial cells. *J Anat*. 2006;208(2):219-229.

161. Wang J, Morishima S, Okada Y. IK channels are involved in the regulatory volume

decrease in human epithelial cells. *Am J Physiol Physiol*. 2003;284(1):C77-C84.

162. Joiner WJ, Basavappa S, Vidyasagar S, Nehrke K, Krishnan S, Binder HJ, Boulpaep EL, Rajendran VM. Active K^+ secretion through multiple K_{Ca}-type channels and regulation by IK_{Ca} channels in rat proximal colon. *Am J Physiol Liver Physiol*. 2003;285(1):G185-G196.

163. Westcott EB, Jackson WF. Heterogeneous function of ryanodine receptors, but not IP3 receptors, in hamster cremaster muscle feed arteries and arterioles. *Am J Physiol Circ Physiol*. 2011;300(5):H1616-H1630.

164. Ko EA, Han J, Jung D, Park WS, Ko EA. Hirosi Kuriyama Award 2007 Memorial Review Physiological roles of K + channels in vascular smooth muscle cells. *J Smooth Muscle Res*. 2008;44(2):65-81.

165. Fukao M, Mason HS, Britton FC, Kenyon JL, Horowitz B, Keef KD. Cyclic GMP-dependent protein kinase activates cloned BKCa channels expressed in mammalian cells by direct phosphorylation at serine 1072. *J Biol Chem*. 1999;274(16):10927-10935.

166. Schlossmann J, Feil R, Hofmann F. Annals of Medicine Signaling through NO and cGMP-dependent protein kinases Signaling through NO and cGMP-dependent protein kinases. *Ann Med*. 2003;35:21-27.

167. Kyle BD, Hurst S, Swayze RD, Sheng J, Braun AP. Specific phosphorylation sites underlie the stimulation of a large conductance, Ca^{2+}-activated K^+ channel by cGMP-dependent protein kinase. *FASEB J*. 2013;27(5):2027-2038.

168. Kyle BD, Mishra RC, Braun AP. The augmentation of BK channel activity by nitric oxide signaling in rat cerebral arteries involves co-localized regulatory elements. *J Cereb Blood Flow Metab*. 2017;37(12):3759-3773.

169. Schubert R, Noack T, Serebryakov VN. Protein kinase C reduces the KCa current of rat tail artery smooth muscle cells. *Am J Physiol*. 1999;276(3):C648-C658.

170. Minami K, Fukuzawa K, Nakaya Y, Zeng XR, Inoue I. Mechanism of activation of the Ca(2+)-activated K+ channel by cyclic AMP in cultured porcine coronary artery smooth muscle cells. *Life Sci*. 1993;53(14):1129-1135.

171. Taguchi K, Kaneko K, Kubo T. Protein kinase C modulates Ca2+-activated K+ channels in cultured rat mesenteric artery smooth muscle cells. *Biol Pharm Bull*. 2000;23(12):1450-1454.

172. Barman SA, Zhu S, White RE. Protein kinase C inhibits BKCa channel activity in pulmonary arterial smooth muscle. *Am J Physiol - Lung Cell Mol Physiol*. 2003;286(1):L149-L155.

173. Köhler R, Wulff H, Eichler I, Kneifel M, Neumann D, Knorr A, Grgic I, Kämpfe D, Si H, Wibawa J, Real R, Borner K, Brakemeier S, Orzechowski H-D, Reusch H-P, Paul M, Chandy KG, Hoyer J. Blockade of the intermediate-conductance calcium-activated potassium channel as a new therapeutic strategy for restenosis. *Circulation*. 2003;108(9):1119-1125.

174. Westcott EB, Segal SS. Perivascular innervation: a multiplicity of roles in vasomotor control and myoendothelial signaling. *Microcirculation*. 2013;20(3):217-238.

175. Burnstock G, Iwayama T. Fine-structural Identification of Autonomic Nerves and their Relation to Smooth Muscle. *Prog Brain Res*. 1971;34:389-404.

176. Yokomizo A, Takatori S, Hashikawa-Hobara N, Goda M, Kawasaki H. Characterization of Perivascular Nerve Distribution in Rat Mesenteric Small Arteries. *Biol Pharm Bull*. 2015;38(11):1757-1764.

177. Tangsucharit P, Takatori S, Sun P, Zamami Y, Goda M, Pakdeechote P, Takayama F, Kawasaki H. Do cholinergic nerves innervating rat mesenteric arteries regulate vascular tone? *Am J Physiol Integr Comp Physiol*. 2012;303(11):R1147-R1156.

178. Ralevic V. P2X receptors in the cardiovascular system. *WIREs Membr Transp Signal*. 2012;1:663-674.

179. Hatanaka Y, Hobara N, Honghua J, Akiyama S, Nawa H, Kobayashi Y, Takayama F, Gomita Y, Kawasaki H. Neuronal nitric-oxide synthase inhibition facilitates adrenergic neurotransmission in rat mesenteric resistance arteries. *J Pharmacol Exp Ther*. 2006;316(2):490-497.

180. Förstermann U, Closs EI, Pollock JS, Nakane M, Schwarz P, Gath I, Kleinert H. Nitric oxide synthase isozymes. Characterization, purification, molecular cloning, and functions. *Hypertension*. 1994;23(6 Pt 2):1121-1131.

181. Falck B, Torp A. New Evidence for the Localization of Noradrenalin in the Adrenergic Nerve Terminals. *Pharmacology*. 1962;6(3):169-172.

182. Lundeberg JM, Terenius L, Hókfelt T, Martling CR, Tatemoto K, Mutt V, Polak J, Bloom S, Goldestein M. Neuropeptide Y (NPY)-like immunoreactivity in peripheral noradrenergic neurons and effects of NPY on sympathetic function. *Acta Physiol Scand*. 1982;116(4):477-480.

183. Hiromu Kawasaki, Koichiro Takasaki AS& KG. Calcitonin gene-related peptide acts as a novel vasodilator neurotransmitter in mesenteric resistance vessels of the rat. *Nature*. 1988;335:164-167.

184. J A Angus, A Broughton and MJM. Role of alpha-adrenoceptors in constrictor responses of rat, guinea-pig and rabbit small arteries to neural activation. *J Physiol*. 1988:403: 495–510.

185. Nilsson H, Goldstein J M, Nilsson O. Adrenergic innervation and neurogenic response in large and small arteries and veins from the rat. *Acta Physiol Scand*. 1986;126(1):121-133.

186. Dunn WR, Brock JA, Hardy TA. Electrochemical and electrophysiological characterization of neurotransmitter release from sympathetic nerves supplying rat mesenteric arteries. *Br J Pharmacol*. 1999;128(1):174-180.

187. Shatarat A, Dunn WR, Ralevic V. Raised tone reveals ATP as a sympathetic neurotransmitter in the porcine mesenteric arterial bed. *Purinergic Signal*. 2014;10(4):639-649.

188. Pakdeechote P, Rummery NM, Ralevic V, Dunn WR. Raised tone reveals purinergic-mediated responses to sympathetic nerve stimulation in the rat perfused mesenteric vascular bed. *Eur J Pharmacol*. 2007;563(1-3):180-186.

189. Mauban JR, Lamont C, Balke CW, Wier WG. Adrenergic stimulation of rat resistance arteries affects Ca(2+) sparks, Ca(2+) waves, and Ca(2+) oscillations. *Am J Physiol Heart Circ Physiol*. 2001;280(5):H2399-H2405.

190. Villalba N, Stankevicius E, Garcia-Sacristán A, Simonsen U, Prieto D. Contribution of both Ca2+ entry and Ca2+ sensitization to the α1-adrenergic vasoconstriction of rat penile small arteries. *Am J Physiol Circ Physiol*. 2007;292(2):H1157-H1169.

191. Evans RJ, Lewis C, Virginio C, Lundstrom K, Buell G, Surprenant A, North RA. Ionic permeability of, and divalent cation effects on, two ATP-gated cation channels (P2X receptors) expressed in mammalian cells. *J Physiol*. 1996;497((Pt 2)):413-422.

192. Evans RJ, Cunnane TC. Relative contributions of ATP and noradrenaline to the nerve evoked contraction of the rabbit jejunal artery. Dependence on stimulation parameters.

Naunyn Schmiedebergs Arch Pharmacol. 1992;345(4):424-430.

193. Chu DQ, Cox HM, Costa SKP, Herzog H, Brain SD. The ability of neuropeptide Y to mediate responses in the murine cutaneous microvasculature: an analysis of the contribution of Y1 and Y2 receptors. *Br J Pharmacol*. 2003;140(2):422-430.

194. Edvinsson L, Ekblad E, Håkanson R, Wahlestedt C. Neuropeptide Y potentiates the effect of various vasoconstrictor agents on rabbit blood vessels. *Br J Pharmacol*. 1984;83(2):519-525.

195. Furchgott RF, Zawadzki J V. The obligatory role of endothelial cells in the relaxation of arterial smooth muscle by acetylcholine. *Nature*. 1980;288(5789):373-376.

196. Sessa WC. Regulation of endothelial derived nitric oxide in health and disease. *Mem Inst Oswaldo Cruz*. 2005;100(Suppl 1):15-18.

197. Kerr PM, Wei R, Tam R, Sandow SL, Murphy TV, Ondrusova K, Lunn SE, Tran CHT, Welsh DG, Plane F. Activation of endothelial IKCa channels underlies NO-dependent myoendothelial feedback. *Vascul Pharmacol*. 2015;74:130-138.

198. Erkens R, Suvorava T, Kramer CM, Diederich LD, Kelm M, Cortese-Krott MM. Modulation of Local and Systemic Heterocellular Communication by Mechanical Forces: A Role of Endothelial Nitric Oxide Synthase. *Antioxid Redox Signal*. 2017;26(16):917-935.

199. Balligand J-L, Feron O, Dessy C. eNOS activation by physical forces: from short-term regulation of contraction to chronic remodeling of cardiovascular tissues. *Physiol Rev*. 2009;89(2):481-534.

200. Shen J, Luscinskas FW, Connolly A, Dewey CF, Gimbrone MA. Fluid shear stress modulates cytosolic free calcium in vascular endothelial cells. *Am J Physiol*. 1992;262(2 Pt 1):C384-C390.

201. Dewey CF, Bussolari SR, Gimbrone MA, Davies PF. The dynamic response of vascular endothelial cells to fluid shear stress. *J Biomech Eng*. 1981;103(3):177-185.

202. Bychkov R, Burnham MP, Richards GR, Edwards G, Weston AH, Félétou M, Vanhoutte PM. Characterization of a charybdotoxin-sensitive intermediate conductance Ca^{2+}-activated K^+ channel in porcine coronary endothelium: relevance to EDHF. *Br J Pharmacol*. 2002;137(8):1346-1354.

203. Stankevičius E, Lopez-Valverde V, Rivera L, Hughes AD, Mulvany MJ, Simonsen U. Combination of Ca^{2+}-activated K^+ channel blockers inhibits acetylcholine-evoked nitric oxide release in rat superior mesenteric artery. *Br J Pharmacol*. 2006;149(5):560-572.

204. Brahler S, Kaistha A, Schmidt VJ, Wolfle SE, Busch C, Kaistha BP, Kacik M, Hasenau A-L, Grgic I, Si H, Bond CT, Adelman JP, Wulff H, de Wit C, Hoyer J, Kohler R. Genetic Deficit of SK3 and IK1 Channels Disrupts the Endothelium-Derived Hyperpolarizing Factor Vasodilator Pathway and Causes Hypertension. *Circulation*. 2009;119(17):2323-2332.

205. Stankevičius E, Dalsgaard T, Kroigaard C, Beck L, Boedtkjer E, Misfeldt MW, Nielsen G, Schjorring O, Hughes A, Simonsen U. Opening of Small and Intermediate Calcium-Activated Potassium Channels Induces Relaxation Mainly Mediated by Nitric-Oxide Release in Large Arteries and Endothelium-Derived Hyperpolarizing Factor in Small Arteries from Rat. *J Pharmacol Exp Ther*. 2011;339(3):842-850.

206. Sun D, Huang A, Koller A, Kaley G. Endothelial KCa Channels Mediate Flow-Dependent Dilation of Arterioles of Skeletal Muscle and Mesentery. *Microvasc Res*. 2001;61(2):179-186.

207. Mayer B, Hemmens B. Biosynthesis and action of nitric oxide in mammalian cells. *Trends Biochem Sci*. 1997;22(12):477-481.

208. Plane F, Zwozdesky M, Wei R, Godin D, Kerr PM. Activation of Endothelial Calcium-Activated Potassium Channels Limits Nerve-Mediated Vasoconstriction in Resistance Arteries. *Can J Cardiol*. 2013;29(10):S228-S229.

209. Burnham MP, Bychkov R, Félétou M, Richards GR, Vanhoutte PM, Weston AH, Edwards G. Characterization of an apamin-sensitive small-conductance Ca 2+ -activated K + channel in porcine coronary artery endothelium: relevance to EDHF. *Br J Pharmacol*. 2002;135(5):1133-1143.

210. Schmidt HH, Pollock JS, Nakane M, Gorsky LD, Förstermann U, Murad F. Purification of a soluble isoform of guanylyl cyclase-activating-factor synthase. *Proc Natl Acad Sci U S A*. 1991;88(2):365-369.

211. Bredt DS, Snyder SH. Isolation of nitric oxide synthetase, a calmodulin-requiring enzyme. *Proc Natl Acad Sci U S A*. 1990;87(2):682-685.

212. Mitchell JA, Förstermann U, Warner TD, Pollock JS, Schmidt HH, Heller M, Murad F. Endothelial cells have a particulate enzyme system responsible for EDRF formation: measurement by vascular relaxation. *Biochem Biophys Res Commun*. 1991;176(3):1417-1423.

213. Förstermann U, Pollock JS, Schmidt HH, Heller M, Murad F. Calmodulin-dependent endothelium-derived relaxing factor/nitric oxide synthase activity is present in the particulate and cytosolic fractions of bovine aortic endothelial cells. *Proc Natl Acad Sci U S A*. 1991;88(5):1788-1792.

214. Bolz SS, de Wit C, Pohl U. Endothelium-derived hyperpolarizing factor but not NO reduces smooth muscle Ca2+ during acetylcholine-induced dilation of microvessels. *Br J Pharmacol*. 1999;128(1):124-134.

215. Uchida H, Tanaka Y, Ishii K, Nakayama K. L-type Ca2+ channels are not involved in coronary endothelial Ca2+ influx mechanism responsible for endothelium-dependent relaxation. *Res Commun Mol Pathol Pharmacol*. 1999;104(2):127-144.

216. Hirano K, Hirano M, Hanada A. Involvement of STIM1 in the proteinase-activated receptor 1-mediated Ca2+ influx in vascular endothelial cells. *J Cell Biochem*. 2009;108(2):499-507.

217. Abdullaev IF, Bisaillon JM, Potier M, Gonzalez JC, Motiani RK, Trebak M. Stim1 and Orai1 mediate CRAC currents and store-operated calcium entry important for endothelial cell proliferation. *Circ Res*. 2008;103(11):1289-1299.

218. Himmel HM, Whorton AR, Strauss HC. Intracellular calcium, currents, and stimulus-response coupling in endothelial cells. *Hypertension*. 1993;21(1):112-127.

219. Chen G, Suzuki H, Weston AH. Acetylcholine releases endothelium-derived hyperpolarizing factor and EDRF from rat blood vessels. *Br J Pharmacol*. 1988;95(4):1165-1174.

220. Zhang DX, Mendoza SA, Bubolz AH, Mizuno A, Ge Z-D, Li R, Warltier DC, Suzuki M, Gutterman DD. Transient receptor potential vanilloid type 4-deficient mice exhibit impaired endothelium-dependent relaxation induced by acetylcholine in vitro and in vivo. *Hypertension*. 2009;53(3):532-538.

221. Earley S, Pauyo T, Drapp R, Tavares MJ, Liedtke W, Brayden JE. TRPV4-dependent dilation of peripheral resistance arteries influences arterial pressure. *AJP Hear Circ Physiol*. 2009;297(3):H1096-H1102.

222. Kochukov MY, Balasubramanian A, Noel RC, Marrelli SP. Role of TRPC1 and TRPC3 Channels in Contraction and Relaxation of Mouse Thoracic Aorta. *J Vasc Res*. 2013;50:11-20.

223. Freichel M, Suh SH, Pfeifer A, Schweig U, Trost C, Weissgerber P, Biel M, Philipp S, Freise D, Droogmans G, Hofmann F, Flockerzi V, Nilius B. Lack of an endothelial store-operated Ca2+ current impairs agonist-dependent vasorelaxation in TRP4-/- mice. *Nat Cell Biol*. 2001;3(2):121-127.

224. Mendoza SA, Fang J, Gutterman DD, Wilcox DA, Bubolz AH, Li R, Suzuki M, Zhang DX. TRPV4-mediated endothelial Ca2+ influx and vasodilation in response to shear stress. *Am J Physiol Heart Circ Physiol*. 2010;298(2):H466-H476.

225. Wilson C, Lee MD, McCarron JG. Acetylcholine released by endothelial cells facilitates flow-mediated dilatation. *J Physiol*. 2016;594(24):7267-7307.

226. Zhang DX, Gutterman DD. Transient receptor potential channel activation and endothelium-dependent dilation in the systemic circulation. *J Cardiovasc Pharmacol*. 2011;57(2):133-139.

227. Hill-Eubanks DC, Gonzales AL, Sonkusare SK, Nelson MT. Vascular TRP channels: performing under pressure and going with the flow. *Physiology*. 2014;29(5):343-360.

228. Pedersen SF, Owsianik G, Nilius B. TRP channels: An overview. *Cell Calcium*. 2005;38(3-4):233-252.

229. Alonso-Carbajo L, Kecskes M, Jacobs G, Pironet A, Syam N, Talavera K, Vennekens R. Muscling in on TRP channels in vascular smooth muscle cells and cardiomyocytes. *Cell Calcium*. 2017;66:48-61.

230. Nilius B, Szallasi A. Transient receptor potential channels as drug targets: from the science of basic research to the art of medicine. *Pharmacol Rev*. 2014;66(3):676-814.

231. Yue Z, Xie J, Yu AS, Stock J, Du J, Yue L. Role of TRP channels in the cardiovascular system. *Am J Physiol Circ Physiol*. 2015;308(3):H157-H182.

232. Zimmermann K, Lennerz JK, Hein A, Link AS, Kaczmarek JS, Delling M, Uysal S, Pfeifer JD, Riccio A, Clapham DE. Transient receptor potential cation channel, subfamily C, member 5 (TRPC5) is a cold-transducer in the peripheral nervous system. *Proc Natl Acad Sci U S A*. 2011;108(44):18114-18119.

233. Nilius B. TRP channels in disease. *Biochim Biophys Acta*. 2007;1772(8):805-812.

234. Trebak M, St. J. Bird G, McKay RR, Birnbaumer L, Putney JW. Signaling Mechanism for Receptor-activated Canonical Transient Receptor Potential 3 (TRPC3) Channels. *J Biol Chem*. 2003;278(18):16244-16252.

235. Venkatachalam K, Zheng F, Gill DL. Regulation of Canonical Transient Receptor Potential (TRPC) Channel Function by Diacylglycerol and Protein Kinase C. *J Biol Chem*. 2003;278(31):29031-29040.

236. Hofmann T, Obukhov AG, Schaefer M, Harteneck C, Gudermann T, Schultz G. Direct activation of human TRPC6 and TRPC3 channels by diacylglycerol. *Nature*. 1999;397(6716):259-263.

237. Zurborg S, Yurgionas B, Jira JA, Caspani O, Heppenstall PA. Direct activation of the ion channel TRPA1 by Ca2+. *Nat Neurosci*. 2007;10(3):277-279.

238. Du J, Xie J, Yue L. Intracellular calcium activates TRPM2 and its alternative spliced isoforms. *Proc Natl Acad Sci U S A*. 2009;106(17):7239-7244.

239. Prawitt D, Monteilh-Zoller MK, Brixel L, Spangenberg C, Zabel B, Fleig A, Penner R. TRPM5 is a transient Ca2+-activated cation channel responding to rapid changes in

[Ca2+]i. *Proc Natl Acad Sci U S A*. 2003;100(25):15166-15171.

240. Launay P, Fleig A, Perraud AL, Scharenberg AM, Penner R, Kinet JP. TRPM4 is a Ca2+-activated nonselective cation channel mediating cell membrane depolarization. *Cell*. 2002;109(3):397-407.

241. Köhler R, Heyken W-T, Heinau P, Schubert R, Si H, Kacik M, Busch C, Grgic I, Maier T, Hoyer J. Evidence for a functional role of endothelial transient receptor potential V4 in shear stress-induced vasodilatation. *Arterioscler Thromb Vasc Biol*. 2006;26(7):1495-1502.

242. Gao X, Wu L, O'Neil RG. Temperature-modulated diversity of TRPV4 channel gating: activation by physical stresses and phorbol ester derivatives through protein kinase C-dependent and -independent pathways. *J Biol Chem*. 2003;278(29):27129-27137.

243. Hong K, Cope EL, DeLalio LJ, Marziano C, Isakson BE, Sonkusare SK. TRPV4 (Transient Receptor Potential Vanilloid 4) Channel-Dependent Negative Feedback Mechanism Regulates Gq Protein-Coupled Receptor-Induced Vasoconstriction. *Arterioscler Thromb Vasc Biol*. 2018;38(3):542-554.

244. Sonkusare SK, Bonev AD, Ledoux J, Liedtke W, Kotlikoff MI, Heppner TJ, Hill-Eubanks DC, Nelson MT. Elementary Ca2+ signals through endothelial TRPV4 channels regulate vascular function. *Science*. 2012;336(6081):597-601.

245. Pankey EA, Zsombok A, Lasker GF, Kadowitz PJ. Analysis of responses to the TRPV4 agonist GSK1016790A in the pulmonary vascular bed of the intact-chest rat. *Am J Physiol Heart Circ Physiol*. 2014;306(1):H33-H40.

246. Pankey EA, Kassan M, Choi S-K, Matrougui K, Nossaman BD, Hyman AL, Kadowitz PJ. Vasodilator responses to acetylcholine are not mediated by the activation of soluble guanylate cyclase or TRPV4 channels in the rat. *Am J Physiol Hear Circ Physiol*. 2014;306(11):H1495-H1506.

247. Hartmannsgruber V, Heyken W-T, Kacik M, Kaistha A, Grgic I, Harteneck C, Liedtke W, Hoyer J, Köhler R. Arterial response to shear stress critically depends on endothelial TRPV4 expression. *PLoS One*. 2007;2(9):e827.

248. Sukumaran S V., Singh TU, Parida S, Narasimha Reddy CEE, Thangamalai R, Kandasamy K, Singh V, Mishra SK. TRPV4 channel activation leads to endothelium-dependent relaxation mediated by nitric oxide and endothelium-derived hyperpolarizing factor in rat pulmonary artery. *Pharmacol Res*. 2013;78:18-27.

249. Kwan H-Y, Huang Y, Yao X. Protein kinase C can inhibit TRPC3 channels indirectly via stimulating protein kinase G. *J Cell Physiol*. 2006;207(2):315-321.

250. Liu C-L, Huang Y, Ngai C-Y, Leung Y-K, Yao X-Q. TRPC3 is involved in flow- and bradykinin-induced vasodilation in rat small mesenteric arteries. *Acta Pharmacol Sin*. 2006;27(8):981-990.

251. Xia C, Bao Z, Yue C, Sanborn BM, Liu M. Phosphorylation and regulation of G-protein-activated phospholipase C-beta 3 by cGMP-dependent protein kinases. *J Biol Chem*. 2001;276(23):19770-19777.

252. Lee SB, Shin SH, Hepler JR, Gilman AG, Rhee SG. Activation of phospholipase C-beta 2 mutants by G protein alpha q and beta gamma subunits. *J Biol Chem*. 1993;268(34):25952-25957.

253. Camps M, Carozzi A, Schnabel P, Scheer A, Parker PJ, Gierschik P. Isozyme-selective stimulation of phospholipase C-beta 2 by G protein beta gamma-subunits. *Nature*. 1992;360(6405):684-686.

254. Katz A, Wu D, Simon MI. Subunits beta gamma of heterotrimeric G protein activate beta 2 isoform of phospholipase C. *Nature*. 1992;360(6405):686-689.

255. Gaut ZN, Huggins CG. Effect of epinephrine on the metabolism of the inositol phosphatides in rat heart in vivo. *Nature*. 1966;212(5062):612-613.

256. Senadheera S, Kim Y, Grayson TH, Toemoe S, Kochukov MY, Abramowitz J, Housley GD, Bertrand RL, Chadha PS, Bertrand PP, Murphy T V, Tare M, Birnbaumer L, Marrelli SP, Sandow SL. Transient receptor potential canonical type 3 channels facilitate endothelium-derived hyperpolarization-mediated resistance artery vasodilator activity. *Cardiovasc Res*. 2012;95(4):439-447.

257. Kochukov MY, Balasubramanian A, Abramowitz J, Birnbaumer L, Marrelli SP. Activation of endothelial transient receptor potential C3 channel is required for small conductance calcium-activated potassium channel activation and sustained endothelial hyperpolarization and vasodilation of cerebral artery. *J Am Heart Assoc*. 2014;3(4):e000913.

258. Pollock JS, Förstermann U, Mitchell JA, Warner TD, Schmidt HH, Nakane M, Murad F. Purification and characterization of particulate endothelium-derived relaxing factor synthase from cultured and native bovine aortic endothelial cells. *Proc Natl Acad Sci U S A*. 1991;88(23):10480-10484.

259. Bredt DS, Hwang PM, Glatt CE, Lowenstein C, Reed RR, Snyder SH. Cloned and expressed nitric oxide synthase structurally resembles cytochrome P-450 reductase. *Nature*. 1991;351(6329):714-718.

260. Knowles RG, Palacios M, Palmer RMJ, Moncada S. Formation of nitric oxide from L-arginine in the central nervous system: A transduction mechanism for stimulation of the soluble guanylate cyclase. *Med Sci*. 1989;86:5159-5162.

261. Mccall TB, Boughton-Smith NK, Palmer RMJ, Whittle BJR, Moncada S. Synthesis of nitric oxide from L-arginine by neutrophils Release and interaction with superoxide anion. *Biochem J*. 1989;261:293-296.

262. Palmer RMJ, Ashton DS, Moncada S. Vascular endothelial cells synthesize nitric oxide from L-arginine. *Nature*. 1988;333(6174):664-666.

263. Ghosh DK, Stuehr DJ. Macrophage NO synthase: characterization of isolated oxygenase and reductase domains reveals a head-to-head subunit interaction. *Biochemistry*. 1995;34(3):801-807.

264. Richards MK, Marletta MA. Characterization of neuronal nitric oxide synthase and a C415H mutant, purified from a baculovirus overexpression system. *Biochemistry*. 1994;33(49):14723-14732.

265. McMillan K, Masters BS. Prokaryotic expression of the heme- and flavin-binding domains of rat neuronal nitric oxide synthase as distinct polypeptides: identification of the heme-binding proximal thiolate ligand as cysteine-415. *Biochemistry*. 1995;34(11):3686-3693.

266. Fisslthaler B, Dimmeler S, Hermann C, Busse R, Fleming I. Phosphorylation and activation of the endothelial nitric oxide synthase by fluid shear stress. *Acta Physiol Scand*. 2000;168(1):81-88.

267. Laursen JB, Somers M, Kurz S, McCann L, Warnholtz A, Freeman BA, Tarpey M, Fukai T, Harrison DG. Endothelial regulation of vasomotion in apoE-deficient mice: implications for interactions between peroxynitrite and tetrahydrobiopterin. *Circulation*. 2001;103(9):1282-1288.

268. Landmesser U, Dikalov S, Price SR, McCann L, Fukai T, Holland SM, Mitch WE, Harrison DG. Oxidation of tetrahydrobiopterin leads to uncoupling of endothelial cell nitric oxide synthase in hypertension. 2003;111(8):1201-1209.

269. Kuzkaya N, Weissmann N, Harrison DG, Dikalov S. Interactions of Peroxynitrite, Tetrahydrobiopterin, Ascorbic Acid, and Thiols. *J Biol Chem*. 2003;278(25):22546-22554.

270. Kohnen SL, Mouithys-Mickalad AA, Deby-Dupont GP, Deby CM, Lamy ML, Noels AF. Oxidation of tetrahydrobiopterin by peroxynitrite or oxoferryl species occurs by a radical pathway. *Free Radic Res*. 2001;35(6):709-721.

271. Vásquez-Vivar J, Kalyanaraman B, Martásek P, Hogg N, Masters BS, Karoui H, Tordo P, Pritchard KA. Superoxide generation by endothelial nitric oxide synthase: the influence of cofactors. *Proc Natl Acad Sci U S A*. 1998;95(16):9220-9225.

272. Hauschildt S, Lückhoff A, Mülsch A, Kohler J, Bessler W, Busse R. Induction and activity of NO synthase in bone-marrow-derived macrophages are independent of Ca2+. *Biochem J*. 1990;270(2):351-356.

273. Garthwaite J, Charles SL, Chess-Williams R. Endothelium-derived relaxing factor release on activation of NMDA receptors suggests role as intercellular messenger in the brain. *Nature*. 1988;336(6197):385-388.

274. Corson MA, James NL, Latta SE, Nerem RM, Berk BC, Harrison DG. Phosphorylation of endothelial nitric oxide synthase in response to fluid shear stress. *Circ Res*. 1996;79(5):984-991.

275. Hauschildt S, Bassenge E, Bessler W, Busse R, Mülsch A. L-arginine-dependent nitric oxide formation and nitrite release in bone marrow-derived macrophages stimulated with bacterial lipopeptide and lipopolysaccharide. *Immunology*. 1990;70(3):332-337.

276. Carnicer R, Crabtree MJ, Sivakumaran V, Casadei B, Kass DA. Nitric oxide synthases in heart failure. *Antioxid Redox Signal*. 2013;18(9):1078-1099.

277. Vanhoutte PM, Zhao Y, Xu A, Leung SWS. Thirty Years of Saying NO: Sources, Fate, Actions, and Misfortunes of the Endothelium-Derived Vasodilator Mediator. *Circ Res*. 2016;119(2):375-396.

278. Vanhoutte PM, Shimokawa H, Feletou M, Tang EHC. Endothelial dysfunction and vascular disease - a 30th anniversary update. *Acta Physiol*. 2017;219(1):22-96.

279. Abu-Soud HM, Yoho LL, Stuehr DJ. Calmodulin controls neuronal nitric-oxide synthase by a dual mechanism. Activation of intra- and interdomain electron transfer. *J Biol Chem*. 1994;269(51):32047-32050.

280. Gachhui R, Presta A, Bentley DF, Abu-Soud HM, McArthur R, Brudvig G, Ghosh DK, Stuehr DJ. Characterization of the reductase domain of rat neuronal nitric oxide synthase generated in the methylotrophic yeast Pichia pastoris. Calmodulin response is complete within the reductase domain itself. *J Biol Chem*. 1996;271(34):20594-20602.

281. Alderton WK, Cooper CE, Knowles RG. Nitric oxide synthases : structure, function and inhibition. *Biochem J*. 2001;357:593-615.

282. Ou J, Fontana JT, Ou Z, Jones DW, Ackerman AW, Oldham KT, Yu J, Sessa WC, Pritchard KA. Heat shock protein 90 and tyrosine kinase regulate eNOS NO· generation but not NO· bioactivity. *Am J Physiol - Hear Circ Physiol*. 2004;286(2):H561-H569.

283. Drab M, Verkade P, Elger M, Kasper M, Lohn M, Lauterbach B, Menne J, Lindschau C, Mende F, Luft FC, Schedl A, Haller H, Kurzchalia T V. Loss of caveolae, vascular dysfunction, and pulmonary defects in caveolin-1 gene-disrupted mice. *Science*.

2001;293(5539):2449-2452.

284. García-Cardeña G, Fan R, Shah V, Sorrentino R, Cirino G, Papapetropoulos A, Sessa WC. Dynamic activation of endothelial nitric oxide synthase by Hsp90. *Nature*. 1998;392(6678):821-824.

285. Sheng J-Z, Arshad F, Braun JE, Braun AP. Estrogen and the Ca^{2+}-mobilizing agonist ATP evoke acute NO synthesis via distinct pathways in an individual human vascular endothelium-derived cell. *Am J Physiol Physiol*. 2008;294(6):C1531-C1541.

286. Ignarro LJ, Buga GM, Wood KS, Byrns RE, Chaudhuri G. Endothelium-derived relaxing factor produced and released from artery and vein is nitric oxide. *Proc Natl Acad Sci U S A*. 1987;84(24):9265-9269.

287. Lincoln T, Dills W, Corbin J. Purification and subunit composition of guanosine 3':5'-monophosphate-dependent protein kinase from bovine lung. *J Biol Chem*. 1977;(252):4269-4275.

288. Wolfe L CJ, Francis S. Characterization of a novel isozyme of cGMP-dependent protein kinase from bovine aorta. *J Biol Chem*. (264):7734-7741.

289. Ruth P, Wang GX, Boekhoff I, May B, Pfeifer A, Penner R, Korth M, Breer H, Hofmann F. Transfected cGMP-dependent protein kinase suppresses calcium transients by inhibition of inositol 1,4,5-trisphosphate production. *Proc Natl Acad Sci U S A*. 1993;90(7):2623-2627.

290. Williams DL, Katz GM, Roy-Contancin L, Reuben JP. Guanosine 5'-monophosphate modulates gating of high-conductance Ca2+-activated K+ channels in vascular smooth muscle cells. *Proc Natl Acad Sci U S A*. 1988;85(23):9360-9364.

291. Robertson BE, Schubert R, Hescheler J, Nelson MT. cGMP-dependent protein kinase activates Ca-activated K channels in cerebral artery smooth muscle cells. *Am J Physiol*. 1993;265(1 Pt 1):C299-C303.

292. Brayden J, Nelson M. Regulation of arterial tone by activation of calcium-dependent potassium channels. *Science (80-)*. 1992;256(5056):532-535.

293. Gur S, Kadowitz PJ, Serefoglu EC, Hellstrom WJG. PDE5 inhibitor treatment options for urologic and non-urologic indications: 2012 update. *Curr Pharm Des*. 2012;18(34):5590-5606.

294. Pfeiffer S, Leopold E, Schmidt K, Brunner F, Mayer B. Inhibition of nitric oxide synthesis by N(G)-nitro-L-arginine methyl ester (L-NAME): Requirement for bioactivation to the free acid, N(G)-nitro-L-arginine. *Br J Pharmacol*. 1996;118(6):1433-1440.

295. Moore PK, Al-Swayeh OA, Chong NW, Evans RA, Gibson A. L-NG-nitro arginine (L-NOARG), a novel, L-arginine-reversible inhibitor of endothelium-dependent vasodilatation in vitro. *Br J Pharmacol*. 1990;99(2):408-412.

296. Gardiner SM, Compton AM, Bennett T, Palmer RM, Moncada S. Regional haemodynamic changes during oral ingestion of NG-monomethyl-L-arginine or NG-nitro-L-arginine methyl ester in conscious Brattleboro rats. *Br J Pharmacol*. 1990;101(1):10-12.

297. Gardiner SM, Kemp PA, Bennett T, Palmer RM, Moncada S. Nitric oxide synthase inhibitors cause sustained, but reversible, hypertension and hindquarters vasoconstriction in Brattleboro rats. *Eur J Pharmacol*. 1992;213(3):449-451.

298. Huang PL, Huang Z, Mashimo H, Bloch KD, Moskowitz MA, Bevan JA, Fishman MC. Hypertension in mice lacking the gene for endothelial nitric oxide synthase. *Nature*. 1995;377(6546):239-242.

299. Weston AH, Edwards G, Dora KA, Gardener MJ, Garland CJ. K+ is an endothelium-

derived hyperpolarizing factor in rat arteries. *Nature*. 1998;396(6708):269-272.

300. Si H, Heyken W-T, Wölfle SE, Tysiac M, Schubert R, Grgic I, Vilianovich L, Giebing G, Maier T, Gross V, Bader M, de Wit C, Hoyer J, Köhler R. Impaired endothelium-derived hyperpolarizing factor-mediated dilations and increased blood pressure in mice deficient of the intermediate-conductance Ca2+-activated K+ channel. *Circ Res*. 2006;99(5):537-544.

301. McGuire JJ, Ding H, Triggle CR. Endothelium-derived relaxing factors: a focus on endothelium-derived hyperpolarizing factor(s). *Can J Physiol Pharmacol*. 2001;79(6):443-470.

302. Bény J. Electrical coupling between smooth muscle cells and endothelial cells in pig coronary arteries. *Pflugers Arch*. 1997;433(3):364-367.

303. Busse R, Edwards G, Félétou M, Fleming I, Vanhoutte PM, Weston AH. EDHF: bringing the concepts together. *Trends Pharmacol Sci*. 2002;23(8):374-380.

304. Joiner WJ, Wang LY, Tang MD, Kaczmarek LK. hSK4, a member of a novel subfamily of calcium-activated potassium channels. *Proc Natl Acad Sci U S A*. 1997;94(20):11013-11018.

305. Maingret F, Coste B, Hao J, Giamarchi A, Allen D, Crest M, Litchfield DW, Adelman JP, Delmas P. Neurotransmitter Modulation of Small-Conductance Ca2+-Activated K+ Channels by Regulation of Ca2+ Gating. *Neuron*. 2008;59(3):439-449.

306. Bildl W, Strassmaier T, Thurm H, Andersen J, Eble S, Oliver D, Knipper M, Mann M, Schulte U, Adelman JP, Fakler B. Protein Kinase CK2 Is Coassembled with Small Conductance Ca. *Neuron*. 2004;43:847-858.

307. Sakai T. Acetylcholine induces Ca-dependent K currents in rabbit endothelial cells. *Jpn J Pharmacol*. 1990;53(2):235-246.

308. Nam Y-W, Orfali R, Liu T, Yu K, Cui M, Wulff H, Zhang M. Structural insights into the potency of SK channel positive modulators. *Sci Rep*. 2017;7(1):17178.

309. Weatherall KL, Seutin V, Liegeois J-F, Marrion N V. Crucial role of a shared extracellular loop in apamin sensitivity and maintenance of pore shape of small-conductance calcium-activated potassium (SK) channels. *Proc Natl Acad Sci*. 2011;108(45):18494-18499.

310. Lamy C, Goodchild SJ, Weatherall KL, Jane DE, Liégeois J-F, Seutin V, Marrion N V. Allosteric Block of KCa2 Channels by Apamin. *J Biol Chem*. 2010;285(35):27067-27077.

311. Strøbaek D, Brown D, Jenkins D, Chen Y-J, Coleman N, Ando Y, Chiu P, Jørgensen S, Demnitz J, Wulff H, Christophersen P. NS6180, a new KCa 3.1 channel inhibitor prevents T-cell activation and inflammation in a rat model of inflammatory bowel disease. *Br J Pharmacol*. 2013;168(2):432-444.

312. Nguyen HM, Singh V, Pressly B, Jenkins DP, Wulff H, Yarov-Yarovoy V. Structural Insights into the Atomistic Mechanisms of Action of Small Molecule Inhibitors Targeting the KCa3.1 Channel Pore. *Mol Pharmacol*. 2017;91(4):392-402.

313. Hougaard C, Eriksen BL, Jørgensen S, Johansen TH, Dyhring T, Madsen LS, Strøbaek D, Christophersen P. Selective positive modulation of the SK3 and SK2 subtypes of small conductance Ca2+-activated K+ channels. *Br J Pharmacol*. 2007;151(5):655-665.

314. Mishra RC, Wulff H, Hill MA, Braun AP. Inhibition of Myogenic Tone in Rat Cremaster and Cerebral Arteries by SKA-31, an Activator of Endothelial KCa2.3 and KCa3.1 Channels. *J Cardiovasc Pharmacol*. 2015;66(1):118-127.

315. Mishra RC, Wulff H, Cole WC, Braun AP. A pharmacologic activator of endothelial KCa channels enhances coronary flow in the hearts of type 2 diabetic rats. *J Mol Cell Cardiol*.

2014;72:364-373.

316. Radtke J, Schmidt K, Wulff H, Köhler R, de Wit C. Activation of KCa3.1 by SKA-31 induces arteriolar dilatation and lowers blood pressure in normo- and hypertensive connexin40-deficient mice. *Br J Pharmacol*. 2013;170(2):293-303.

317. Kerr PM, Tam R, Narang D, Potts K, McMillan D, McMillan K, Plane F. Endothelial calcium-activated potassium channels as therapeutic targets to enhance availability of nitric oxide. *Can J Physiol Pharmacol*. 2012;90(6):739-752.

318. Saliez J, Bouzin C, Rath G, Ghisdal P, Desjardins F, Rezzani R, Rodella LF, Vriens J, Nilius B, Feron O, Balligand J-L, Dessy C. Role of caveolar compartmentation in endothelium-derived hyperpolarizing factor-mediated relaxation: Ca2+ signals and gap junction function are regulated by caveolin in endothelial cells. *Circulation*. 2008;117(8):1065-1074.

319. Brähler S, Kaistha A, Schmidt VJ, Wölfle SE, Busch C, Kaistha BP, Kacik M, Hasenau A-L, Grgic I, Si H, Bond CT, Adelman JP, Wulff H, de Wit C, Hoyer J, Köhler R. Genetic deficit of SK3 and IK1 channels disrupts the endothelium-derived hyperpolarizing factor vasodilator pathway and causes hypertension. *Circulation*. 2009;119(17):2323-2332.

320. Bolton TB, Lang RJ, Takewaki T. Mechanisms of action of noradrenaline and carbachol on smooth muscle of guinea-pig anterior mesenteric artery. *J Physiol*. 1984;351:549-572.

321. Isakson BE. Localized expression of an Ins(1,4,5)P3 receptor at the myoendothelial junction selectively regulates heterocellular Ca2+ communication. *J Cell Sci*. 2008;121(21):3664-3673.

322. Biwer LA, Taddeo EP, Kenwood BM, Hoehn KL, Straub AC, Isakson BE. Two functionally distinct pools of eNOS in endothelium are facilitated by myoendothelial junction lipid composition. *Biochim Biophys Acta*. 2016;1861(7):671-679.

323. Qian X, Francis M, Köhler R, Solodushko V, Lin M, Taylor MS. Positive feedback regulation of agonist-stimulated endothelial Ca2+ dynamics by KCa3.1 channels in mouse mesenteric arteries. *Arterioscler Thromb Vasc Biol*. 2014;34(1):127-135.

324. Clapham DE. Calcium signaling. *Cell*. 2007;131(6):1047-1058.

325. Dora KA, Garland CJ. Linking Hyperpolarization to Endothelial Cell Calcium Events in Arterioles. *Microcirculation*. 2013;20(3):248-256.

326. Behringer EJ, Segal SS. Membrane potential governs calcium influx into microvascular endothelium: integral role for muscarinic receptor activation. *J Physiol J Physiol J Physiol*. 2015;593(20):4531-4548.

327. Vanhoutte PM. Endothelial control of vasomotor function: from health to coronary disease. *Circ J*. 2003;67(7):572-575.

328. Rudic RD, Shesely EG, Maeda N, Smithies O, Segal SS, Sessa WC. Direct evidence for the importance of endothelium-derived nitric oxide in vascular remodeling. *J Clin Invest*. 1998;101(4):731-736.

329. Berry C, Hamilton CA, Brosnan MJ, Magill FG, Berg GA, McMurray JJ V., Dominiczak AF. Investigation Into the Sources of Superoxide in Human Blood Vessels. *Circulation*. 2000;101(18):2206-2212.

330. Douglas G, Bendall JK, Crabtree MJ, Tatham AL, Carter EE, Hale AB, Channon KM. Endothelial-specific Nox2 overexpression increases vascular superoxide and macrophage recruitment in ApoE−/− mice. *Cardiovasc Res*. 2012;94(1):20-29.

331. Barry-Lane PA, Patterson C, van der Merwe M, Hu Z, Holland SM, Yeh ET, Runge MS. p47phox is required for atherosclerotic lesion progression in ApoE(-/-) mice. *J Clin Invest*.

2001;108(10):1513-1522.

332. Pagano PJ, Chanock SJ, Siwik DA, Colucci WS, Clark JK, Aranha AB, Tostes RC, Reudelhuber T, Touyz RM. Angiotensin II induces p67phox mRNA expression and NADPH oxidase superoxide generation in rabbit aortic adventitial fibroblasts. *Hypertension*. 1998;32(2):331-337.

333. Matsuno K, Yamada H, Iwata K, Jin D, Katsuyama M, Matsuki M, Takai S, Yamanishi K, Miyazaki M, Matsubara H, Yabe-Nishimura C. Nox1 is involved in angiotensin II-mediated hypertension: a study in Nox1-deficient mice. *Circulation*. 2005;112(17):2677-2685.

334. Gavazzi G, Banfi B, Deffert C, Fiette L, Schappi M, Herrmann F, Krause K-H. Decreased blood pressure in NOX1-deficient mice. *FEBS Lett*. 2006;580(2):497-504.

335. Laursen JB, Rajagopalan S, Galis Z, Tarpey M, Freeman BA, Harrison DG, Martin AS, Lyle A, Weber DS, Weiss D, Taylor WR, Schmidt HHHW, Owens GK, Lambeth JD, Griendling KK. Role of superoxide in angiotensin II-induced but not catecholamine-induced hypertension. *Circulation*. 1997;95(3):588-593.

336. Landmesser U, Cai H, Dikalov S, McCann L, Hwang J, Jo H, Holland SM, Harrison DG. Role of p47(phox) in vascular oxidative stress and hypertension caused by angiotensin II. *Hypertension*. 2002;40(4):511-515.

337. Albert CM, Cook NR, Gaziano JM, Zaharris E, MacFadyen J, Danielson E, Buring JE, Manson JE. Effect of Folic Acid and B Vitamins on Risk of Cardiovascular Events and Total Mortality Among Women at High Risk for Cardiovascular Disease. *JAMA*. 2008;299(17):2027-2036.

338. Cook NR, Albert CM, Gaziano JM, Zaharris E, MacFadyen J, Danielson E, Buring JE, Manson JE. A Randomized Factorial Trial of Vitamins C and E and Beta Carotene in the Secondary Prevention of Cardiovascular Events in Women. *Arch Intern Med*. 2007;167(15):1610-1618.

339. Song Y, Cook NR, Albert CM, Van Denburgh M, Manson JE. Effects of vitamins C and E and -carotene on the risk of type 2 diabetes in women at high risk of cardiovascular disease: a randomized controlled trial. *Am J Clin Nutr*. 2009;90(2):429-437.

340. Sesso HD, Buring JE, Christen WG, Kurth T, Belanger C, MacFadyen J, Bubes V, Manson JE, Glynn RJ, Gaziano JM. Vitamins E and C in the prevention of cardiovascular disease in men: the Physicians' Health Study II randomized controlled trial. *JAMA*. 2008;300(18):2123-2133.

341. Lonn E, Bosch J, Yusuf S, Sheridan P, Pogue J, Arnold JMO, Ross C, Arnold A, Sleight P, Probstfield J, Dagenais GR, HOPE and HOPE-TOO Trial Investigators. Effects of Long-term Vitamin E Supplementation on Cardiovascular Events and Cancer. *JAMA*. 2005;293(11):1338-1347.

342. Lee I-M, Cook NR, Gaziano JM, Gordon D, Ridker PM, Manson JE, Hennekens CH, Buring JE. Vitamin E in the primary prevention of cardiovascular disease and cancer: the Women's Health Study: a randomized controlled trial. *JAMA*. 2005;294(1):56-65.

343. Di Meo S, Reed TT, Venditti P, Victor VM. Role of ROS and RNS Sources in Physiological and Pathological Conditions. *Oxid Med Cell Longev*. 2016;2016(1245049).

344. Guzik TJ, West NEJ, Pillai R, Taggart DP, Channon KM. Nitric Oxide Modulates Superoxide Release and Peroxynitrite Formation in Human Blood Vessels. *Hypertension*. 2002;39(6).

345. Konior A, Schramm A, Czesnikiewicz-Guzik M, Guzik TJ. NADPH Oxidases in Vascular

Pathology. *Antioxid Redox Signal*. 2014;20(17):2794-2814.

346. Lassègue B, Sorescu D, Szöcs K, Yin Q, Akers M, Zhang Y, Grant SL, Lambeth JD, Griendling KK. Novel gp91(phox) homologues in vascular smooth muscle cells : nox1 mediates angiotensin II-induced superoxide formation and redox-sensitive signaling pathways. *Circ Res*. 2001;88(9):888-894.

347. Yamaguchi O, Kaneshiro T, Saitoh S-I, Ishibashi T, Maruyama Y, Takeishi Y. Regulation of coronary vascular tone via redox modulation in the alpha1 -adrenergic-angiotensin-endothelin axis of the myocardium. *Am J Physiol Hear Circ Physiol*. 2009;296:H226-H232.

348. Tsai M-H, Jiang M. Reactive oxygen species are involved in regulating α1-adrenoceptor-activated vascular smooth muscle contraction. *J Biomed Sci*. 2010;17(1):67.

349. Hao L, Nishimura T, Wo H, Fernandez-Patron C. Vascular responses to alpha1-adrenergic receptors in small rat mesenteric arteries depend on mitochondrial reactive oxygen species. *Arterioscler Thromb Vasc Biol*. 2006;26(4):819-825.

350. Sies H. Oxidative stress: oxidants and antioxidants. *Exp Physiol*. 1997;82(2):291-295.

351. Görlach A, Brandes RP, Nguyen K, Amidi M, Dehghani F, Busse R. A gp91phox Containing NADPH Oxidase Selectively Expressed in Endothelial Cells Is a Major Source of Oxygen Radical Generation in the Arterial Wall. *Circ Res*. 2000;87(1):26-32.

352. Barbacanne MA, Souchard JP, Darblade B, Iliou JP, Nepveu F, Pipy B, Bayard F, Arnal JF. Detection of superoxide anion released extracellularly by endothelial cells using cytochrome c reduction, ESR, fluorescence and lucigenin-enhanced chemiluminescence techniques. *Free Radic Biol Med*. 2000;29(5):388-396.

353. Souza HP, Laurindo FRM, Ziegelstein RC, Berlowitz CO, Zweier JL. Vascular NAD(P)H oxidase is distinct from the phagocytic enzyme and modulates vascular reactivity control. *Am J Physiol - Hear Circ Physiol*. 2001;280(2):H658-H667.

354. Sorescu D, Somers MJ, Lassègue B, Grant S, Harrison DG, Griendling KK. Electron spin resonance characterization of the NAD(P)H oxidase in vascular smooth muscle cells. *Free Radic Biol Med*. 2001;30(6):603-612.

355. Jones SA, O'Donnell VB, Wood JD, Broughton JP, Hughes EJ, Jones OT. Expression of phagocyte NADPH oxidase components in human endothelial cells. *Am J Physiol*. 1996;271(4 Pt 2):H1626-H1634.

356. Meyer JW, Holland JA, Ziegler LM, Chang MM, Beebe G, Schmitt ME. Identification of a functional leukocyte-type NADPH oxidase in human endothelial cells :a potential atherogenic source of reactive oxygen species. *Endothelium*. 1999;7(1):11-22.

357. McCord JM, McCord JM. Oxygen-derived free radicals in postischemic tissue injury. *N Engl J Med*. 1985;312(3):159-163.

358. McCord JM, Roy RS, Schaffer SW. Free radicals and myocardial ischemia. The role of xanthine oxidase. *Adv Myocardiol*. 1985;5:183-189.

359. Weisiger R, Fridovich I. Superoxide Dismutase: Organelle specificity. *J Biol Chem*. 1973;248(10):3582-3592.

360. Forman HJ, Kennedy JA. Role of superoxide radical in mitochondrial dehydrogenase reactions. *Biochem Biophys Res Commun*. 1974;60(3):1044-1050.

361. Loschen G, Azzi A, Richter C, Flohé L. Superoxide radicals as precursors of mitochondrial hydrogen peroxide. *FEBS Lett*. 1974;42(1):68-72.

362. Jensen PK. Antimycin-insensitive oxidation of succinate and reduced nicotinamide-adenine dinucleotide in electron-transport particles. I. pH dependency and hydrogen

peroxide formation. *Biochim Biophys Acta*. 1966;122(2):157-166.

363. Muller FL, Liu Y, Van Remmen H. Complex III releases superoxide to both sides of the inner mitochondrial membrane. *J Biol Chem*. 2004;279(47):49064-49073.

364. Cadenas E, Boveris A, Ragan CI, Stoppani AO. Production of superoxide radicals and hydrogen peroxide by NADH-ubiquinone reductase and ubiquinol-cytochrome c reductase from beef-heart mitochondria. *Arch Biochem Biophys*. 1977;180(2):248-257.

365. Fukai T, Ushio-Fukai M. Superoxide dismutases: role in redox signaling, vascular function, and diseases. *Antioxid Redox Signal*. 2011;15(6):1583-1606.

366. Schröder K, Zhang M, Benkhoff S, Mieth A, Pliquett R, Kosowski J, Kruse C, Luedike P, Michaelis UR, Weissmann N, Dimmeler S, Shah AM, Brandes RP. Nox4 is a protective reactive oxygen species generating vascular NADPH oxidase. *Circ Res*. 2012;110(9):1217-1225.

367. Sohn HY, Keller M, Gloe T, Morawietz H, Rueckschloss U, Pohl U. The small G-protein Rac mediates depolarization-induced superoxide formation in human endothelial cells. *J Biol Chem*. 2000;275(25):18745-18750.

368. Ago T, Kitazono T, Kuroda J, Kumai Y, Kamouchi M, Ooboshi H, Wakisaka M, Kawahara T, Rokutan K, Ibayashi S, Iida M. NAD(P)H Oxidases in Rat Basilar Arterial Endothelial Cells. *Stroke*. 2005;36(5):1040-1046.

369. Haurani MJ, Cifuentes ME, Shepard AD, Pagano PJ. Nox4 Oxidase Overexpression Specifically Decreases Endogenous Nox4 mRNA and Inhibits Angiotensin II–Induced Adventitial Myofibroblast Migration. *Hypertension*. 2008;52(1):143-149.

370. Lassègue B, Clempus RE. Vascular NAD(P)H oxidases: specific features, expression, and regulation. *Am J Physiol - Regul Integr Comp Physiol*. 2003;285(2):R277-R297.

371. Höhler B, Holzapfel B, Kummer W. NADPH oxidase subunits and superoxide production in porcine pulmonary artery endothelial cells. *Histochem Cell Biol*. 2000;114(1):29-37.

372. Usatyuk P V, Romer LH, He D, Parinandi NL, Kleinberg ME, Zhan S, Jacobson JR, Dudek SM, Pendyala S, Garcia JGN, Natarajan V. Regulation of hyperoxia-induced NADPH oxidase activation in human lung endothelial cells by the actin cytoskeleton and cortactin. *J Biol Chem*. 2007;282(32):23284-23295.

373. Félétou M, Vanhoutte PM. Endothelial dysfunction: a multifaceted disorder. *Am J Physiol Hear Circ Physiol*. 2006;291:985-1002.

374. Rueckschloss U, Galle J, Holtz J, Zerkowski H-R, Morawietz H. Induction of NAD(P)H Oxidase by Oxidized Low-Density Lipoprotein in Human Endothelial Cells. *Circulation*. 2001;104(15):1767-1772.

375. Lambeth JD. NOX enzymes and the biology of reactive oxygen. *Nat Rev Immunol*. 2004;4(3):181-189.

376. Dusting GJ, Selemidis S, Jiang F. Mechanisms for suppressing NADPH oxidase in the vascular wall. *Mem Inst Oswaldo Cruz*. 2005;100(Suppl 1):97-103.

377. Bedard K, Krause K-H. The NOX Family of ROS-Generating NADPH Oxidases: Physiology and Pathophysiology. *Physiol Rev*. 2007;87(1):245-313.

378. Lassègue B, Griendling KK, Lassegue B, Griendling KK. NADPH Oxidases: Functions and Pathologies in the Vasculature. *Arterioscler Thromb Vasc Biol*. 2010;30(4):653-661.

379. Royer-Pokora B, Kunkel LM, Monaco AP, Goff SC, Newburger PE, Baehner RL, Cole FS, Curnutte JT, Orkin SH. Cloning the gene for an inherited human disorder—chronic granulomatous disease—on the basis of its chromosomal location. *Nature*. 1986;322(6074):32-38.

380. Rossi F, Zatti M. Biochemical aspects of phagocytosis in polymorphonuclear leucocytes. NADH and NADPH oxidation by the granules of resting and phagocytizing cells. *Experientia*. 1964;20(1):21-23.

381. Ago T, Kitazono T, Ooboshi H, Iyama T, Han YH, Takada J, Wakisaka M, Ibayashi S, Utsumi H, Iida M. Nox4 as the Major Catalytic Component of an Endothelial NAD(P)H Oxidase. *Circulation*. 2004;109(2):227-233.

382. Buul JD Van, Fernandez-Borja M, Anthony EC, Hordijk PL. Expression and Localization of NOX2 and NOX4 in Primary Human Endothelial Cells. *Antioxid Redox Signal*. 2005;7(3-4):308-317.

383. Hilenski LL, Clempus RE, Quinn MT, Lambeth JD, Griendling KK. Distinct Subcellular Localizations of Nox1 and Nox4 in Vascular Smooth Muscle Cells. *Arterioscler Thromb Vasc Biol*. 2004;24(4):677-683.

384. Silverton SF, Mesaros S, Markham GD, Malinski T. Osteoclast radical interactions: NADPH causes pulsatile release of NO and stimulates superoxide production. *Endocrinology*. 1995;136(11):5244-5247.

385. Sullivan MN, Gonzales AL, Pires PW, Bruhl A, Leo MD, Li W, Oulidi A, Boop FA, Feng Y, Jaggar JH, Welsh DG, Earley S. Localized TRPA1 channel Ca2+ signals stimulated by reactive oxygen species promote cerebral artery dilation. *Sci Signal*. 2015;8(358):ra2.

386. Al-Mehdi AB, Zhao G, Dodia C, Tozawa K, Costa K, Muzykantov V, Ross C, Blecha F, Dinauer M, Fisher AB. Endothelial NADPH Oxidase as the Source of Oxidants in Lungs Exposed to Ischemia or High K+. *Circ Res*. 1998;83(7):730-737.

387. Matsuzaki I, Chatterjee S, Debolt K, Manevich Y, Zhang Q, Fisher AB. Membrane depolarization and NADPH oxidase activation in aortic endothelium during ischemia reflect altered mechanotransduction. *Am J Physiol Heart Circ Physiol*. 2005;288(1):H336-H343.

388. McCabe RD, Bakarich MA, Srivastava K, Young DB. Potassium inhibits free radical formation. *Hypertension*. 1994;24(1):77-82.

389. Huie RE, Padmaja S. The reaction of no with superoxide. *Free Radic Res Commun*. 1993;18(4):195-199.

390. Didion SP, Ryan MJ, Didion LA, Fegan PE, Sigmund CD, Faraci FM. Increased Superoxide and Vascular Dysfunction in CuZnSOD-Deficient Mice. *Circ Res*. 2002;91(10):938-944.

391. Mehta JL, Li D. Epinephrine upregulates superoxide dismutase in human coronary artery endothelial cells. *Free Radic Biol Med*. 2001;30(2):148-153.

392. Faraci FM, Didion SP. Vascular Protection. *Arterioscler Thromb Vasc Biol*. 2004;24(8).

393. Crapo JD, Oury T, Rabouille C, Slot JW, Chang LY. Copper,zinc superoxide dismutase is primarily a cytosolic protein in human cells. *Proc Natl Acad Sci U S A*. 1992;89(21):10405-10409.

394. Wambi-Kiéssé CO, Katusic ZS. Inhibition of copper/zinc superoxide dismutase impairs NO ·-mediated endothelium-dependent relaxations. *Am J Physiol - Hear Circ Physiol*. 1999;276(3 Pt 2):H1043-H1048.

395. Matoba T, Shimokawa H, Morikawa K, Kubota H, Kunihiro I, Urakami-Harasawa L, Mukai Y, Hirakawa Y, Akaike T, Takeshita A. Electron spin resonance detection of hydrogen peroxide as an endothelium-derived hyperpolarizing factor in porcine coronary microvessels. *Arterioscler Thromb Vasc Biol*. 2003;23(7):1224-1230.

396. Matoba T, Shimokawa H, Nakashima M, Hirakawa Y, Mukai Y, Hirano K, Kanaide H,

Takeshita A. Hydrogen peroxide is an endothelium-derived hyperpolarizing factor in mice. *J Clin Invest*. 2000;106(12):1521-1530.

397. Viktoria Csato, Attila Peto, Akos Koller, Istvan Eds, Attila Toth ZP. Hydrogen Peroxide Elicits Constriction of Skeletal Muscle Arterioles by Activating the Arachidonic Acid Pathway. Xu S-Z, ed. *PLoS One*. 2014;9(8):e103858.

398. Ardanaz N, Beierwaltes WH, Pagano PJ. Distinct hydrogen peroxide-induced constriction in multiple mouse arteries: potential influence of vascular polarization. *Pharmacol Rep*. 60(1):61-67.

399. Gao Y-J, Hirota S, Zhang D-W, Janssen LJ, Lee RMKW. Mechanisms of hydrogen-peroxide-induced biphasic response in rat mesenteric artery. *Br J Pharmacol*. 2003;138(6):1085-1092.

400. Yang Y, Shi W, Cui N, Wu Z, Jiang C. Oxidative stress inhibits vascular K(ATP) channels by S-glutathionylation. *J Biol Chem*. 2010;285(49):38641-38648.

401. Adachi T, Weisbrod RM, Pimentel DR, Ying J, Sharov VS, Schneich C, Cohen RA. S-Glutathiolation by peroxynitrite activates SERCA during arterial relaxation by nitric oxide. *Nat Med*. 2004;10(11):1200-1207.

402. W-u M, Pritchard KA, Kaminski PM, Fayngersh RP, Hintze TH, Wolin MS. Involvement of nitric oxide and nitrosothiols in relaxation of pulmonary arteries to peroxynitrite. *Am Physiol Soc*. 1994;266(5 Pt 2):H2108-13.

403. Francis SH, Busch JL, Corbin JD. cGMP-Dependent Protein Kinases and cGMP Phosphodiesterases in Nitric Oxide and cGMP Action. *Pharmacol Rev*. 2010;62(3):525-563.

404. J. E. Fisha and P.A. Marsden a B. Endothelial nitric oxide synthase: insight into cell-specific gene regulation in the vascular endothelium. *Cell Mol Life Sci*. 2006;63:144-162.

405. Lee PC, Salyapongse AN, Bragdon GA, Shears LL, Watkins SC, Edington HD, Billiar TR. Impaired wound healing and angiogenesis in eNOS-deficient mice. *Am J Physiol*. 1999;277(4 Pt 2):H1600-H1608.

406. Freedman JE, Sauter R, Battinelli EM, Ault K, Knowles C, Huang PL, Loscalzo J. Deficient platelet-derived nitric oxide and enhanced hemostasis in mice lacking the NOSIII gene. *Circ Res*. 1999;84(12):1416-1421.

407. Moellering D, McAndrew J, Patel RP, Cornwell T, Lincoln T, Cao X, Messina JL, Forman HJ, Jo H, Darley-Usmar VM. Nitric oxide-dependent induction of glutathione synthesis through increased expression of gamma-glutamylcysteine synthetase. *Arch Biochem Biophys*. 1998;358(1):74-82.

408. Luperchio S, Tamir S, Tannenbaum SR. NO-induced oxidative stress and glutathione metabolism in rodent and human cells. *Free Radic Biol Med*. 1996;21(4):513-519.

409. Hwang C, Sinskey AJ, Lodish HF. Oxidized redox state of glutathione in the endoplasmic reticulum. *Science (80-)*. 1992;257(5076):1496-1502.

410. Winterbourn CC, Metodiewa D. Reactivity of biologically important thiol compounds with superoxide and hydrogen peroxide. *Free Radic Biol Med*. 1999;27(3-4):322-328.

411. Tribble DL, Jones DP. Oxygen dependence of oxidative stress. Rate of NADPH supply for maintaining the GSH pool during hypoxia. *Biochem Pharmacol*. 1990;39(4):729-736.

412. Meister A. Selective modification of glutathione metabolism. *Science*. 1983;220(4596):472-477.

413. Ishikawa T, Esterbauer H, Sies H. Role of cardiac glutathione transferase and of the glutathione S-conjugate export system in biotransformation of 4-hydroxynonenal in the

heart. *J Biol Chem*. 1986;261(4):1576-1581.

414. Meister A. Glutathione, Ascorbate, and Cellular Protection. *Cancer Res*. 1994;54(7 Supplement):969s-1975s.

415. Ziegler DM. Role of the reversible oxidation-reduction of enzyme thiols-bisulfides in metabolic regulation. *Ann Rev Biochem*. 1985;54:305-329.

416. Schaedle M, Bassham2 JA. Chloroplast Glutathione Reductase1. *Plant Physiol*. 1977;59:1011-1012.

417. Woodin T, Segel I. Isolation and characterization of glutathione reductase from Penicillium chrysogenum. *Biochim Biophys Acta*. 1968;167(1):64-77.

418. Allen T, Iftinca M, Cole WC, Plane F. Smooth muscle membrane potential modulates endothelium-dependent relaxation of rat basilar artery via myo-endothelial gap junctions. *J Physiol*. 2002;545(Pt 3):975-986.

419. Ghiadoni L, Salvetti M, Muiesan ML, Taddei S. Evaluation of endothelial function by flow mediated dilation: methodological issues and clinical importance. *High Blood Press Cardiovasc Prev*. 2015;22(1):17-22.

420. Yeboah J, Crouse JR, Hsu F-C, Burke GL, Herrington DM. Brachial flow-mediated dilation predicts incident cardiovascular events in older adults: the Cardiovascular Health Study. *Circulation*. 2007;115(18):2390-2397.

421. Olesen SP, Clapham DE, Davies PF. Haemodynamic shear stress activates a K+ current in vascular endothelial cells. *Nature*. 1988;331(6152):168-170.

422. Macedo MP, Lautt WW. Shear-induced modulation by nitric oxide of sympathetic nerves in the superior mesenteric artery. *Can J Physiol Pharmacol*. 1996;74(6):692-700.

423. Macedo MP, Lautt WW. Shear-induced modulation of vasoconstriction in the hepatic artery and portal vein by nitric oxide. *Am J Physiol*. 1998;274(2 Pt 1):G253-G260.

424. Takamura Y, Shimokawa H, Zhao H, Igarashi H, Egashira K, Takeshita A. Important role of endothelium-derived hyperpolarizing factor in shear stress--induced endothelium-dependent relaxations in the rat mesenteric artery. *J Cardiovasc Pharmacol*. 1999;34(3):381-387.

425. Green DJ, Dawson EA, Groenewoud HMM, Jones H, Thijssen DHJ. Is Flow-Mediated Dilation Nitric Oxide Mediated?: A Meta-Analysis. *Hypertension*. 2014;63(2):376-382.

426. Markos F, Ruane O'Hora T, Noble MIM. What is the mechanism of flow-mediated arterial dilatation. *Clin Exp Pharmacol Physiol*. 2013;40(8):489-494.

427. Stoner L, Erickson ML, Young JM, Fryer S, Sabatier MJ, Faulkner J, Lambrick DM, McCully KK. There's more to flow-mediated dilation than nitric oxide. *J Atheroscler Thromb*. 2012;19(7):589-600.

428. Heiss C, Sievers RE, Amabile N, Momma TY, Chen Q, Natarajan S, Yeghiazarians Y, Springer ML. In vivo measurement of flow-mediated vasodilation in living rats using high-resolution ultrasound. *Am J Physiol Heart Circ Physiol*. 2008;294(2):H1086-H1093.

429. Bellien J, Thuillez C, Joannides R. Role of endothelium-derived hyperpolarizing factor in the regulation of radial artery basal diameter and endothelium-dependent dilatation in vivo. *Clin Exp Pharmacol Physiol*. 2008;35(4):494-497.

430. Bellien J, Iacob M, Gutierrez L, Isabelle M, Lahary A, Thuillez C, Joannides R. Crucial Role of NO and Endothelium-Derived Hyperpolarizing Factor in Human Sustained Conduit Artery Flow-Mediated Dilatation. *Hypertension*. 2006;48(6):1088-1094.

431. Gündüz F, Koçer G, Ulker S, Meiselman HJ, Başkurt OK, Sentürk UK. Exercise training enhances flow-mediated dilation in spontaneously hypertensive rats. *Physiol Res*.

2011;60(4):589-597.

432. Marziano C, Hong K, Cope EL, Kotlikoff MI, Isakson BE, Sonkusare SK. Nitric Oxide-Dependent Feedback Loop Regulates Transient Receptor Potential Vanilloid 4 (TRPV4) Channel Cooperativity and Endothelial Function in Small Pulmonary Arteries. *J Am Heart Assoc*. 2017;6(12):e007157.

433. He D, Pan Q, Chen Z, Sun C, Zhang P, Mao A, Zhu Y, Li H, Lu C, Xie M, Zhou Y, Shen D, Tang C, Yang Z, Jin J, Yao X, Nilius B, Ma X. Treatment of hypertension by increasing impaired endothelial TRPV4-KCa2.3 interaction. *EMBO Mol Med*. 2017;9(11):1491-1503.

434. Matheson PJ, Wilson MA, Garrison RN. Regulation of Intestinal Blood Flow. *J Surg Res*. 2000;93(1):182-196.

435. Fenger-Gron J, Mulvany MJ, Christensen KL. Mesenteric blood pressure profile of conscious, freely moving rats. *J Physiol*. 1995;488(Pt 3):753-760.

436. Kamiya A, Togawa T. Adaptive regulation of wall shear stress to flow change in the canine carotid artery. *Am J Physiol Circ Physiol*. 1980;239(1):H14-H21.

437. Dalsgaard T, Kroigaard C, Misfeldt M, Bek T, Simonsen U. Openers of small conductance calcium-activated potassium channels selectively enhance NO-mediated bradykinin vasodilatation in porcine retinal arterioles. *Br J Pharmacol*. 2010;160(6):1496-1508.

438. Narang D, Kerr PM, Lunn SE, Beaudry R, Sigurdson J, Lalies MD, Hudson AL, Light PE, Holt A, Plane F. Modulation of resistance artery tone by the trace amine β-phenylethylamine: Dual indirect sympathomimetic and α1-adrenoceptor blocking actions. *J Pharmacol Exp Ther*. 2014;351(1):164-171.

439. Yoshitake T, Kehr J, Yoshitake S, Fujino K, Nohta H, Yamaguchi M. Determination of serotonin, noradrenaline, dopamine and their metabolites in rat brain extracts and microdialysis samples by column liquid chromatography with fluorescence detection following derivatization with benzylamine and 1,2-diphenylethylenediamine. *J Chromatogr B Analyt Technol Biomed Life Sci*. 2004;807(2):177-183.

440. Wright CE, Angus JA. Effects of N-, P- and Q-type neuronal calcium channel antagonists on mammalian peripheral neurotransmission. *Br J Pharmacol*. 1996;119(1):49-56.

441. Mundiña-Weilenmann C, Vittone L, Rinaldi G, Said M, de Cingolani GC, Mattiazzi A. Endoplasmic reticulum contribution to the relaxant effect of cGMP- and cAMP-elevating agents in feline aorta. *Am J Physiol Heart Circ Physiol*. 2000;278(6):H1856-H1865.

442. Trepakova ES, Cohen RA, Bolotina VM. Nitric oxide inhibits capacitative cation influx in human platelets by promoting sarcoplasmic/endoplasmic reticulum Ca2+-ATPase-dependent refilling of Ca2+ stores. *Circ Res*. 1999;84(2):201-209.

443. Plane F, Garland CJ. Influence of contractile agonists on the mechanism of endothelium-dependent relaxation in rat isolated mesenteric artery. *Br J Pharmacol*. 1996;119(2):191-193.

444. Moosmang S1, Schulla V, Welling A, Feil R, Feil S, Wegener JW, Hofmann F KN. Dominant role of smooth muscle L-type calcium channel Cav1.2 for blood pressure regulation. *EMBO J*. 2003;22(22):6027-6034.

445. Tran CHT, Vigmond EJ, Plane F, Welsh DG. Mechanistic basis of differential conduction in skeletal muscle arteries. *J Physiol*. 2009;587(6):1301-1318.

446. Skärby T V, Högestätt ED. Differential effects of calcium antagonists and Bay K 8644 on contractile responses to exogenous noradrenaline and adrenergic nerve stimulation in the

rabbit ear artery. *Br J Pharmacol*. 1990;101(4):961-967.

447. Bulloch JM, MacDonald A, McGrath JC. Different sensitivities of rabbit isolated blood vessels exhibiting co-transmission to the slow calcium channel blocker, nifedipine. *Br J Pharmacol*. 1991;103(3):1685-1690.

448. Gelband CH, Hume JR. Ionic currents in single smooth muscle cells of the canine renal artery. *Circ Res*. 1992;71(4):745-758.

449. Bonnet P, Rusch NJ, Harder DR. Characterization of an outward K+ current in freshly dispersed cerebral arterial muscle cells. *Pflugers Arch*. 1991;418(3):292-296.

450. Hristovska A-M, Rasmussen LE, Hansen PBL, Nielsen SS, Nüsing RM, Narumiya S, Vanhoutte P, Skøtt O, Jensen BL. Prostaglandin E2 Induces Vascular Relaxation by E-Prostanoid 4 Receptor-Mediated Activation of Endothelial Nitric Oxide Synthase. *Hypertension*. 2007;50(3):525-530.

451. Ghisdal P, Morel N. Cellular target of voltage and calcium-dependent K(+) channel blockers involved in EDHF-mediated responses in rat superior mesenteric artery. *Br J Pharmacol*. 2001;134(5):1021-1028.

452. Furchgott RF, Carvalho MH, Khan MT, Matsunaga K. Evidence for endothelium-dependent vasodilation of resistance vessels by acetylcholine. *Blood Vessels*. 1987;24(3):145-149.

453. Qiu W-P, Hu Q, Paolocci N, Ziegelstein RC, Kass DA. Differential effects of pulsatile versus steady flow on coronary endothelial membrane potential. *Am J Physiol Heart Circ Physiol*. 2003;285(1):H341-H346.

454. Sinkler SY, Segal SS. Rapid versus slow ascending vasodilatation: intercellular conduction versus flow-mediated signalling with tetanic versus rhythmic muscle contractions. *J Physiol*. 2017;595(23):7149-7165.

455. Watanabe S, Yashiro Y, Mizuno R, Ohhashi T. Involvement of NO and EDHF in flow-induced vasodilation in isolated hamster cremasteric arterioles. *J Vasc Res*. 2005;42(2):137-147.

456. Huang A, Sun D, Koller A, Kaley G. Gender difference in flow-induced dilation and regulation of shear stress: role of estrogen and nitric oxide. *Am J Physiol*. 1998;275(5 Pt 2):R1571-R1577.

457. Mullen MJ, Kharbanda RK, Cross J, Donald AE, Taylor M, Vallance P, Deanfield JE, MacAllister RJ. Heterogenous nature of flow-mediated dilatation in human conduit arteries in vivo: relevance to endothelial dysfunction in hypercholesterolemia. *Circ Res*. 2001;88(2):145-151.

458. Joannides R, Haefeli WE, Linder L, Richard V, Bakkali EH, Thuillez C, Lüscher TF. Nitric oxide is responsible for flow-dependent dilatation of human peripheral conduit arteries in vivo. *Circulation*. 1995;91(5):1314-1319.

459. Celermajer DS, Sorensen KE, Gooch VM, Spiegelhalter DJ, Miller OI, Sullivan ID, Lloyd JK, Deanfield JE. Non-invasive detection of endothelial dysfunction in children and adults at risk of atherosclerosis. *Lancet (London, England)*. 1992;340(8828):1111-1115.

460. Bellien J, Iacob M, Eltchaninoff H, Bourkaib R, Thuillez C, Joannides R. AT1 receptor blockade prevents the decrease in conduit artery flow-mediated dilatation during NOS inhibition in humans. *Clin Sci (Lond)*. 2007;112(7):393-401.

461. Pyke K, Green DJ, Weisbrod C, Best M, Dembo L, O'Driscoll G, Tschakovsky M. Nitric oxide is not obligatory for radial artery flow-mediated dilation following release of 5 or 10 min distal occlusion. *Am J Physiol Circ Physiol*. 2010;298(1):H119-H126.

462. Taddei S, Versari D, Cipriano A, Ghiadoni L, Galetta F, Franzoni F, Magagna A, Virdis A, Salvetti A. Identification of a cytochrome P450 2C9-derived endothelium-derived hyperpolarizing factor in essential hypertensive patients. *J Am Coll Cardiol*. 2006;48(3):508-515.

463. Miura H, Bosnjak JJ, Ning G, Saito T, Miura M, Gutterman DD. Role for hydrogen peroxide in flow-induced dilation of human coronary arterioles. *Circ Res*. 2003;92(2):e31-e40.

464. Huang A, Wu Y, Sun D, Koller A, Kaley G. Effect of estrogen on flow-induced dilation in NO deficiency: role of prostaglandins and EDHF. *J Appl Physiol*. 2001;91(6):2561-2566.

465. Sun D, Huang A, Smith CJ, Stackpole CJ, Connetta JA, Shesely EG, Koller A, Kaley G. Enhanced release of prostaglandins contributes to flow-induced arteriolar dilation in eNOS knockout mice. *Circ Res*. 1999;85(3):288-293.

466. Kleinert H, Wallerath T, Euchenhofer C, Ihrig-Biedert I, Li H, Förstermann U. Estrogens increase transcription of the human endothelial NO synthase gene: analysis of the transcription factors involved. *Hypertension*. 1998;31(2):582-588.

467. Chambliss KL, Shaul PW. Estrogen Modulation of Endothelial Nitric Oxide Synthase. *Endocr Rev*. 2002;23(5):665-686.

468. Sorensen KE, Dorup I, Hermann AP, Mosekilde L. Combined hormone replacement therapy does not protect women against the age-related decline in endothelium-dependent vasomotor function. *Circulation*. 1998;97(13):1234-1238.

469. Parkington HC, Chow JAM, Evans RG, Coleman HA, Tare M. Role for endothelium-derived hyperpolarizing factor in vascular tone in rat mesenteric and hindlimb circulations in vivo. *J Physiol*. 2002;542(Pt 3):929-937.

470. Ralevic V. Endothelial nitric oxide modulates perivascular sensory neurotransmission in the rat isolated mesenteric arterial bed. *Br J Pharmacol*. 2002;137(1):19-28.

471. Nakane M, Klinghofer V, Kuk JE, Donnelly JL, Budzik GP, Pollock JS, Basha F, Carter GW. Novel potent and selective inhibitors of inducible nitric oxide synthase. *Mol Pharmacol*. 1995;47(4):831-834.

472. Tagaya E, Tamaoki J, Takemura H, Nagai A. Regulation of adrenergic nerve-mediated contraction of canine pulmonary artery by K+ channels. *Eur Respir J*. 1998;11(3):571-574.

473. Gokina NI, Bonev AD, Phillips J, Gokin AP, Veilleux K, Oppenheimer K, Goloman G. Impairment of IKCa channels contributes to uteroplacental endothelial dysfunction in rat diabetic pregnancy. *Am J Physiol Heart Circ Physiol*. 2015;309(4):H592-H604.

474. Church JE, Fulton D. Differences in eNOS activity because of subcellular localization are dictated by phosphorylation state rather than the local calcium environment. *J Biol Chem*. 2006;281(3):1477-1488.

475. Michel JB, Feron O, Sacksṭ D, Michel T. Reciprocal Regulation of Endothelial Nitric-oxide Synthase by Ca. *J Biol Chem*. 1997;272(25):15583-15586.

476. Feron O, Belhassen L, Kobzik L, Smith TW, Kelly RA, Michel T. Endothelial nitric oxide synthase targeting to caveolae. Specific interactions with caveolin isoforms in cardiac myocytes and endothelial cells. *J Biol Chem*. 1996;271(37):22810-22814.

477. Addison MP, Singh TU, Parida S, Choudhury S, Kasa JK, Sukumaran S V., Darzi SA, Kandasamy K, Singh V, Kumar D, Mishra SK. NO synthase inhibition attenuates EDHF-mediated relaxation induced by TRPV4 channel agonist GSK1016790A in the rat pulmonary artery: Role of TxA2. *Pharmacol Reports*. 2016;68(3):620-626.

478. Adams DJ, Barakeh J, Laskey R, Van Breemen C. Ion channels and regulation of intracellular calcium in vascular endothelial cells. *FASEB J*. 1989;3(12):2389-2400.

479. Lückhoff A, Busse R. Calcium influx into endothelial cells and formation of endothelium-derived relaxing factor is controlled by the membrane potential. *Pflugers Arch*. 1990;416(3):305-311.

480. Lückhoff A, Busse R. Activators of potassium channels enhance calcium influx into endothelial cells as a consequence of potassium currents. *Naunyn Schmiedebergs Arch Pharmacol*. 1990;342(1):94-99.

481. Brøndum E, Kold-Petersen H, Simonsen U, Aalkjaer C. NS309 restores EDHF-type relaxation in mesenteric small arteries from type 2 diabetic ZDF rats. *Br J Pharmacol*. 2010;159(1):154-165.

482. Marrelli SP, Eckmann MS, Hunte MS. Role of endothelial intermediate conductance KCa channels in cerebral EDHF-mediated dilations. *Am J Physiol Heart Circ Physiol*. 2003;285(4):H1590-H1599.

483. McSherry IN, Spitaler MM, Takano H, Dora KA. Endothelial cell Ca2+ increases are independent of membrane potential in pressurized rat mesenteric arteries. *Cell Calcium*. 2005;38(1):23-33.

484. Balut CM, Hamilton KL, Devor DC. Trafficking of intermediate (KCa3.1) and small (KCa2.x) conductance, Ca(2+)-activated K(+) channels: a novel target for medicinal chemistry efforts? *ChemMedChem*. 2012;7(10):1741-1755.

485. Feron O, Saldana F, Michel JB, Michel T. The endothelial nitric-oxide synthase-caveolin regulatory cycle. *J Biol Chem*. 1998;273(6):3125-3128.

486. Straub AC, Billaud M, Johnstone SR, Best AK, Yemen S, Dwyer ST, Looft-Wilson R, Lysiak JJ, Gaston B, Palmer L, Isakson BE. Compartmentalized connexin 43 s-nitrosylation/denitrosylation regulates heterocellular communication in the vessel wall. *Arterioscler Thromb Vasc Biol*. 2011;31(2):399-407.

487. Straub AC, Lohman AW, Billaud M, Johnstone SR, Dwyer ST, Lee MY, Bortz PS, Best AK, Columbus L, Gaston B, Isakson BE. Endothelial cell expression of haemoglobin α regulates nitric oxide signalling. *Nature*. 2012;491(7424):473-477.

488. Blough N V., Zafiriou OC. Reaction of superoxide with nitric oxide to form peroxonitrite in alkaline aqueous solution. *Inorg Chem*. 1985;24(22):3502-3504.

489. Ignarro LJ, Lippton H, Edwards JC, Baricos WH, Hyman AL, Kadowitz PJ GC. Mechanism of vascular smooth muscle relaxation by organic nitrates, nitrites, nitroprusside and nitric oxide: evidence for the involvement of S-nitrosothiols as active intermediates. *J Pharmacol Exp Ther*. 1981;218(3):739-749.

490. Standen NB, Quayle JM, Davies NW, Brayden JE, Huang Y, Nelson MT. Hyperpolarizing vasodilators activate ATP-sensitive K+ channels in arterial smooth muscle. *Science*. 1989;245(4914):177-180.

491. Kuo L, Chilian WM, Davis MJ. Coronary arteriolar myogenic response is independent of endothelium. *Circ Res*. 1990;66(3):860-866.

492. Tran CHT, Taylor MS, Plane F, Nagaraja S, Tsoukias NM, Solodushko V, Vigmond EJ, Furstenhaupt T, Brigdan M, Welsh DG. Endothelial Ca2+ wavelets and the induction of myoendothelial feedback. *Am J Physiol Cell Physiol*. 2012;302(8):C1226-C1242.

493. Nausch LWM, Bonev AD, Heppner TJ, Tallini Y, Kotlikoff MI, Nelson MT. Sympathetic nerve stimulation induces local endothelial Ca2+ signals to oppose vasoconstriction of mouse mesenteric arteries. *Am J Physiol Heart Circ Physiol*. 2012;302(3):H594-H5602.

494. Joyner MJ, Thomas GD. Having it both ways? Vasoconstriction in contracting muscles. *J Physiol*. 2003;550(2):333.

495. Remensnyder J, Mitchell J, Sarnoff S. Functional sympatholysis during muscular activity. Observations on influence of carotid sinus on oxygen uptake. *Circ Res*. 1962;11:370-380.

496. Dinenno FA, Joyner MJ. Combined NO and PG inhibition augments alpha-adrenergic vasoconstriction in contracting human skeletal muscle. *Am J Physiol Heart Circ Physiol*. 2004;287(6):H2576-H2584.

497. Hearon CM, Richards JC, Racine ML, Luckasen GJ, Larson DG, Joyner MJ, Dinenno FA. Sympatholytic effect of intravascular ATP is independent of nitric oxide, prostaglandins, Na+/K+-ATPase and KIRchannels in humans. *J Physiol*. 2017;595(15):5175-5190.

498. Molinoff PB, Axelrod J. Biochemistry of catecholamines. *Annu Rev Biochem*. 1971;40(1):465-500.

499. Grassi G, Mark A, Esler M. The Sympathetic Nervous System Alterations in Human Hypertension. *Circ Res*. 2015;116(6):976-990.

500. Wyss JM. The role of the sympathetic nervous system in hypertension. *Curr Opin Nephrol Hypertens*. 1993;2(2):265-273.

501. Chaston DJ, Haddock RE, Howitt L, Morton SK, Brown RD, Matthaei KI, Hill CE. Perturbation of chemical coupling by an endothelial Cx40 mutant attenuates endothelium-dependent vasodilation by KCa channels and elevates blood pressure in mice. *Pflugers Arch*. 2015;467(9):1997-2009.

502. Mishra RC, Belke D, Wulff H, Braun AP. SKA-31, a novel activator of SKCa and IKCa channels, increases coronary flow in male and female rat hearts. *Cardiovasc Res*. 2013;97(2):339-348.

503. Mishra RC, Mitchell JR, Gibbons-Kroeker C, Wulff H, Belenkie I, Tyberg J V., Braun AP. A pharmacologic activator of endothelial KCa channels increases systemic conductance and reduces arterial pressure in an anesthetized pig model. *Vascul Pharmacol*. 2016;79:24-31.

504. Neylon CB, Avdonin P V, Larsen MA, Bobik A. Rat aortic smooth muscle cells expressing charybdotoxin-sensitive potassium channels exhibit enhanced proliferative responses. *Clin Exp Pharmacol Physiol*. 1994;21(2):117-120.

505. Tharp DL, Wamhoff BR, Turk JR, Bowles DK, Limsuwan A, Sweeney M, Rubin LJ, Yuan JX. Upregulation of intermediate-conductance Ca2+-activated K+ channel (IKCa1) mediates phenotypic modulation of coronary smooth muscle. *Am J Physiol Heart Circ Physiol*. 2006;291(5):H2493-H2503.

506. Neylon CB, Lang RJ, Fu Y, Bobik A, Reinhart PH. Molecular cloning and characterization of the intermediate-conductance Ca(2+)-activated K(+) channel in vascular smooth muscle: relationship between K(Ca) channel diversity and smooth muscle cell function. *Circ Res*. 1999;85(4):e33-e43.

507. Cheong A, Bingham AJ, Li J, Kumar B, Sukumar P, Munsch C, Buckley NJ, Neylon CB, Porter KE, Beech DJ, Wood IC. Downregulated REST Transcription Factor Is a Switch Enabling Critical Potassium Channel Expression and Cell Proliferation. *Mol Cell*. 2005;20(1):45-52.

508. Beech DJ. Ion channel switching and activation in smooth-muscle cells of occlusive vascular diseases. *Biochem Soc Trans*. 2007;35(Pt 5):890-894.

509. Hayabuchi Y, Nakaya Y, Yasui S, Mawatari K, Mori K, Suzuki M, Kagami S. Angiotensin II activates intermediate-conductance Ca2+ -activated K+ channels in arterial

smooth muscle cells. *J Mol Cell Cardiol*. 2006;41(6):972-979.

510. Bi D, Toyama K, Lemaitre V, Takai J, Fan F, Jenkins DP, Wulff H, Gutterman DD, Park F, Miura H. The Intermediate Conductance Calcium-activated Potassium Channel KCa3.1 Regulates Vascular Smooth Muscle Cell Proliferation via Controlling Calcium-dependent Signaling. *J Biol Chem*. 2013;288(22):15843-15853.

511. Li F-F, He M-Z, Xie Y, Wu Y-Y, Yang M-T, Fan Y, Qiao F-Y, Deng D-R. Involvement of dysregulated IKCaand SKCachannels in preeclampsia. *Placenta*. 2017;58:9-16.

512. McNeish AJ, Sandow SL, Neylon CB, Chen MX, Dora KA, Garland CJ. Evidence for involvement of both IKCa and SKCa channels in hyperpolarizing responses of the rat middle cerebral artery. *Stroke*. 2006;37(5):1277-1282.

513. Mather S, Dora KA, Sandow SL, Winter P, Garland CJ. Rapid Endothelial Cell-Selective Loading of Connexin 40 Antibody Blocks Endothelium-Derived Hyperpolarizing Factor Dilation in Rat Small Mesenteric Arteries. *Circ Res*. 2005;97(4):399-407.

514. Sandow SL, Tare M, Coleman HA, Hill CE, Parkington HC. Involvement of myoendothelial gap junctions in the actions of endothelium-derived hyperpolarizing factor. *Circ Res*. 2002;90(10):1108-1113.

515. Robitaille R, Garcia ML, Kaczorowski GJ, Charlton MP. Functional colocalization of calcium and calcium-gated potassium channels in control of transmitter release. *Neuron*. 1993;11(4):645-655.

516. Wang X-C, Sun W-T, Fu J, Huang J-H, Yu C-M, Underwood MJ, He G-W, Yang Q. Impairment of Coronary Endothelial Function by Hypoxia-Reoxygenation Involves TRPC3 Inhibition-mediated KCaChannel Dysfunction: Implication in Ischemia-Reperfusion Injury. *Sci Rep*. 2017;7(1):5895.

517. Yang Q, Huang J-H, Yao X-Q, Underwood MJ, Yu C-M. Activation of canonical transient receptor potential channels preserves Ca2+ entry and endothelium-derived hyperpolarizing factor-mediated function in vitro in porcine coronary endothelial cells and coronary arteries under conditions of hyperkalemia. *J Thorac Cardiovasc Surg*. 2014;148(4):1665-1673.

518. De Vriese AS, Verbeuren TJ, Van de Voorde J, Lameire NH, Vanhoutte PM. Endothelial dysfunction in diabetes. *Br J Pharmacol*. 2000;130(5):963-974.

519. Triggle CR, Howarth A, Cheng ZJ, Ding H. Twenty-five years since the discovery of endothelium-derived relaxing factor (EDRF): does a dysfunctional endothelium contribute to the development of type 2 diabetes? *Can J Physiol Pharmacol*. 2005;83(8-9):681-700.

520. Ding H, Triggle CR. Endothelial dysfunction in diabetes: multiple targets for treatment. *Pflügers Arch - Eur J Physiol*. 2010;459(6):977-994.

521. Drummond GR, Selemidis S, Griendling KK, Sobey CG. Combating oxidative stress in vascular disease: NADPH oxidases as therapeutic targets. *Nat Rev Drug Discov*. 2011;10(6):453-471.

522. Mitani H, Egashira K, Ohashi N, Yoshikawa M, Niwa S, Nonomura K, Nakashima A, Kimura M. Preservation of endothelial function by the HMG-CoA reductase inhibitor fluvastatin through its lipid-lowering independent antioxidant properties in atherosclerotic rabbits. *Pharmacology*. 2003;68(3):121-130.

523. Takai S, Jin D, Ikeda H, Sakonjo H, Miyazaki M. Significance of angiotensin II receptor blockers with high affinity to angiotensin II type 1 receptors for vascular protection in rats. *Hypertens Res*. 2009;32(10):853-860.

524. Schramm A, Matusik P, Osmenda G, Guzik TJ. Targeting NADPH oxidases in vascular

pharmacology. *Vascul Pharmacol*. 2012;56(5-6):216-231.

525. Margaritis M, Channon KM, Antoniades C. Statins as regulators of redox state in the vascular endothelium: beyond lipid lowering. *Antioxid Redox Signal*. 2014;20(8):1198-1215.

526. Tousoulis D, Simopoulou C, Papageorgiou N, Oikonomou E, Hatzis G, Siasos G, Tsiamis E, Stefanadis C. Endothelial dysfunction in conduit arteries and in microcirculation. Novel therapeutic approaches. *Pharmacol Ther*. 2014;144(3):253-267.

527. Reriani MK, Dunlay SM, Gupta B, West CP, Rihal CS, Lerman LO, Lerman A. Effects of statins on coronary and peripheral endothelial function in humans: a systematic review and meta-analysis of randomized controlled trials. *Eur J Cardiovasc Prev Rehabil*. 2011;18(5):704-716.

528. Zalba G, Beaumont FJ, San José G, Fortuño A, Fortuño MA, Etayo JC, Díez J. Vascular NADH/NADPH oxidase is involved in enhanced superoxide production in spontaneously hypertensive rats. *Hypertension*. 2000;35(5):1055-1061.

529. Chatterjee S, Browning EA, Hong N, DeBolt K, Sorokina EM, Liu W, Birnbaum MJ, Fisher AB. Membrane depolarization is the trigger for PI3K/Akt activation and leads to the generation of ROS. *Am J Physiol Heart Circ Physiol*. 2012;302(1):H105-H114.

530. Cheung DW. Membrane potential of vascular smooth muscle and hypertension in spontaneously hypertensive rats. *Can J Physiol Pharmacol*. 1984;62(8):957-960.

531. Sunano S, Watanabe H, Tanaka S, Sekiguchi F, Shimamura K. Endothelium-derived relaxing, contracting and hyperpolarizing factors of mesenteric arteries of hypertensive and normotensive rats. *Br J Pharmacol*. 1999;126(3):709-716.

532. Friedman SM, Tanaka M. Increased sodium permeability and transport as primary events in the hypertensive response to deoxycorticosterone acetate (DOCA) in the rat. *J Hypertens*. 1987;5(3):341-345.

533. Plüger S, Faulhaber J, Fürstenau M, Löhn M, Waldschütz R, Gollasch M, Haller H, Luft FC, Ehmke H, Pongs O. Mice with disrupted BK channel beta1 subunit gene feature abnormal Ca(2+) spark/STOC coupling and elevated blood pressure. *Circ Res*. 2000;87(11):E53-E60.

534. Plane F, Walsh E, Cole W. Activation of endothelial Ca2+-activated potassium channels can improve endothelial function in basilar arteries from diabetic rats. *FASEB J*. 2007;21(6):A1231.

535. Zhao H, Kalivendi S, Zhang H, Joseph J, Nithipatikom K, Vsquez-Vivar J, Kalyanaraman B. Superoxide reacts with hydroethidine but forms a fluorescent product that is distinctly different from ethidium: potential implications in intracellular fluorescence detection of superoxide. *Free Radic Biol Med*. 2003;34(11):1359-1368.

536. Zhao H, Joseph J, Fales HM, Sokoloski EA, Levine RL, Vasquez-Vivar J, Kalyanaraman B. Detection and characterization of the product of hydroethidine and intracellular superoxide by HPLC and limitations of fluorescence. *Proc Natl Acad Sci U S A*. 2005;102(16):5727-5732.

537. Wojtala A, Bonora M, Malinska D, Pinton P, Duszynski J, Wieckowski MR. Methods to Monitor ROS Production by Fluorescence Microscopy and Fluorometry. *Concept Backgr Bioenerg Asp oncometabolism*. 2014;542:243-262.

538. Griendling KK, Touyz RM, Zweier JL, Dikalov S, Chilian W, Chen Y-R, Harrison DG, Bhatnagar A. Measurement of Reactive Oxygen Species, Reactive Nitrogen Species, and Redox-Dependent Signaling in the Cardiovascular System: A Scientific Statement From

the American Heart Association. *Circ Res*. 2016;119(5):e39-e75.

539. Dikalov S, Griendling KK, Harrison DG. Measurement of Reactive Oxygen Species in Cardiovascular Studies. *Hypertension*. 2007;49(4):717-727.

540. Fernandes DC, Wosniak J, Pescatore LA, Bertoline MA, Liberman M, Laurindo FRM, Santos CXC. Analysis of DHE-derived oxidation products by HPLC in the assessment of superoxide production and NADPH oxidase activity in vascular systems. *Am J Physiol Cell Physiol*. 2007;292(1):C413-C422.

541. Simons JM, Hart BA, Ip Vai Ching TR, Van Dijk H, Labadie RP. Metabolic activation of natural phenols into selective oxidative burst agonists by activated human neutrophils. *Free Radic Biol Med*. 1990;8(3):251-258.

542. Holland JA, O'Donnell RW, Chang MM, Johnson DK, Ziegler LM. Endothelial cell oxidant production: effect of NADPH oxidase inhibitors. *Endothelium*. 2000;7(2):109-119.

543. Johnson DK, Schillinger KJ, Kwait DM, Hughes C V, McNamara EJ, Ishmael F, O'Donnell RW, Chang M-M, Hogg MG, Dordick JS, Santhanam L, Ziegler LM, Holland JA. Inhibition of NADPH oxidase activation in endothelial cells by ortho-methoxy-substituted catechols. *Endothelium*. 2002;9(3):191-203.

544. Heumuller S, Wind S, Barbosa-Sicard E, Schmidt HHHW, Busse R, Schroder K, Brandes RP, Heumüller S, Wind S, Barbosa-Sicard E, Schmidt HHHW, Busse R, Schröder K, Brandes RP. Apocynin Is Not an Inhibitor of Vascular NADPH Oxidases but an Antioxidant. *Hypertension*. 2008;51(2):211-217.

545. Marletta MA, Hurshman AR, Rusche KM. Catalysis by nitric oxide synthase. *Curr Opin Chem Biol*. 1998;2(5):656-663.

546. Järhult SJ, Sundström J, Lind L. Brachial artery hyperemic blood flow velocities are related to carotid atherosclerosis. *clin physiol funct imaging*. 2009:1-6.

547. Jernigan NL, Walker BR, Resta TC. Reactive oxygen species mediate RhoA/Rho kinase-induced Ca2+ sensitization in pulmonary vascular smooth muscle following chronic hypoxia. *Am J Physiol - Lung Cell Mol Physiol*. 2008;295(3):L515-L529.

548. Jin L, Ying Z, Webb RC. Activation of Rho/Rho kinase signaling pathway by reactive oxygen species in rat aorta. *Am J Physiol Hear Circ Physiol*. 2004;287(4):H1495-H1500.

549. Babson JR, Reed DJ. Inactivation of glutathione reductase by 2-chloroethyl nitrosourea-derived isocyanates. *Biochem Biophys Res Commun*. 1978;83(2):754-762.

550. Frischer H, Ahmad T. Severe generalized glutathione reductase deficiency after antitumor chemotherapy with BCNU" [1,3-bis(chloroethyl)-1-nitrosourea]. *J Lab Clin Med*. 1977;89(5):1080-1091.

551. Elliott SJ, Schilling WP. Carmustine augments the effects of tert-butyl hydroperoxide on calcium signaling in cultured pulmonary artery endothelial cells. *J Biol Chem*. 1990;265(1):103-107.

552. Buus NH, VanBavel E, Mulvany MJ. Differences in sensitivity of rat mesenteric small arteries to agonists when studied as ring preparations or as cannulated preparations. *Br J Pharmacol*. 1994;112(2):579-587.

553. McCarron JG, Quayle JM, Halpern W, Nelson MT, Halpern I. Cromakalim and pinacidil dilate small mesenteric arteries but not small cerebral arteries. *Am Physiol Soc*. 1991;261(2 Pt 2):H287-H291.

554. Bagher P, Beleznai T, Kansui Y, Mitchell R, Garland CJ, Dora KA. Low intravascular pressure activates endothelial cell TRPV4 channels, local Ca2+ events, and IKCa

channels, reducing arteriolar tone. *Proc Natl Acad Sci U S A*. 2012;109(44):18174-18179.

555.   Crane GJ, Gallagher N, Dora KA, Garland CJ. Small- and intermediate-conductance calcium-activated K+ channels provide different facets of endothelium-dependent hyperpolarization in rat mesenteric artery. *J Physiol*. 2003;553(Pt 1):183-189.

556.   Boer GJ. A simplified microassay of DNA and RNA using ethidium bromide. *Anal Biochem*. 1975;65(1-2):225-231.

557.   Benov L, Sztejnberg L, Fridovich I. Critical evaluation of the use of hydroethidine as a measure of superoxide anion radical. *Free Radic Biol Med*. 1998;25(7):826-831.

558.   Freidja ML, Toutain B, Caillon A, Desquiret V, Lambert D, Loufrani L, Procaccio V, Henrion D. Blood Vessels Heme Oxygenase 1 Is Differentially Involved in Blood Flow–Dependent Arterial Remodeling Role of Inflammation, Oxidative Stress, and Nitric Oxide. *Hypertension*. 2011;58:225-231.

559.   Caliman IF, Lamas AZ, Dalpiaz PLM, Medeiros ARS, Abreu GR, Figueiredo SG, Gusmão LN, Andrade TU, Bissoli NS. Endothelial relaxation mechanisms and oxidative stress are restored by atorvastatin therapy in ovariectomized rats. *PLoS One*. 2013;8(11):e80892.

560.   Harrington LS, Lundberg MH, Waight M, Rozario A, Mitchell JA. Reduced endothelial dependent vasodilation in vessels from TLR4−/− mice is associated with increased superoxide generation. *Biochem Biophys Res Commun*. 2011;408(4):511-515.

561.   Fernandes DC, Gonçalves RC, Laurindo FRM. Measurement of Superoxide Production and NADPH Oxidase Activity by HPLC Analysis of Dihydroethidium Oxidation. In: Humana Press, New York, NY; 2017:233-249.

562.   Lebed PJ, Grisales JO, Keunchkarian S, Gotta J, Giambelluca M, Castells C. Rapid and sensitive gradient liquid chromatography method for the quantitation of 2-hydroxyethidium ion from neutrophils. *Anal Methods*. 2011;3(3):593-598.

563.   Tano J-Y, Gollasch M. Calcium-activated potassium channels in ischemia reperfusion: a brief update. *Front Physiol*. 2014;5:381.

564.   Honrath B, Krabbendam IE, Culmsee C, Dolga AM. Small conductance Ca2+-activated K+channels in the plasma membrane, mitochondria and the ER: Pharmacology and implications in neuronal diseases. *Neurochem Int*. 2017;109:13-23.

565.   Wessler I, Kirkpatrick CJ, Racké K. The cholinergic "pitfall": Acetylcholine, a universal cell molecule in biological systems, including humans. *Clin Exp Pharmacol Physiol*. 1999;26(3):198-205.

566.   Habermann E. Apamin. *Pharmacol Ther*. 1984;25(2):255-270.

567.   Galvez A, Gimenez-Gallego G, Reuben JP, Roy-Contancin L, Feigenbaum P, Kaczorowski GJ, Garcia ML. Purification and characterization of a unique, potent, peptidyl probe for the high conductance calcium-activated potassium channel from venom of the scorpion Buthus tamulus. *J Biol Chem*. 1990;265(19):11083-11090.

568.   Bradshaw CM, Pun RYK, Slater NT, Szabadi E. Comparison of the effects of methoxamine with those of noradrenaline and phenylephrine on single cerebral cortical neurones. *Br J Pharmac*. 1981;73:47-54.

569.   Stork AP, Cocks TM. Pharmacological reactivity of human epicardial coronary arteries: phasic and tonic responses to vasoconstrictor agents differentiated by nifedipine. *Br J Pharmacol*. 1994;113(4):1093-1098.

570.   Shen J-B, Jiang B, Pappano AJ. Comparison of L-type calcium channel blockade by nifedipine and/or cadmium in guinea pig ventricular myocytes. *J Pharmacol Exp Ther*.

2000;294(2):562-570.

571. Bentzen BH, Nardi A, Calloe K, Madsen LS, Olesen S-P, Grunnet M. The small molecule NS11021 is a potent and specific activator of Ca2+-activated big-conductance K+ channels. *Mol Pharmacol*. 2007;72(4):1033-1044.

572. Layne JJ, Nausch B, Olesen S-P, Nelson MT. BK channel activation by NS11021 decreases excitability and contractility of urinary bladder smooth muscle. *Am J Physiol Regul Integr Comp Physiol*. 2010;298(2):R378-R384.

573. Minneman KP, Theroux TL, Hollinger S, Han C, Esbenshade T a. Selectivity of agonists for cloned alpha 1-adrenergic receptor subtypes. *Mol Pharmacol*. 1994;46(5):929-936.

574. Garthwaite J, Southam E, Boulton CL, Nielsen EB, Schmidt K, Mayer B. Potent and selective inhibition of nitric oxide-sensitive guanylyl cyclase by 1H-[1,2,4]oxadiazolo[4,3-a]quinoxalin-1-one. *Mol Pharmacol*. 1995;48(2):184-188.

575. Salvemini D, Misko TP, Masferrer JL, Seibert K, Currie MG, Needleman P. Nitric oxide activates cyclooxygenase enzymes. *Pharmacology*. 1993;90:7240-7244.

576. Offer T, Russo A, Samuni A. The pro-oxidative activity of SOD and nitroxide SOD mimics. *FASEB J*. 2000;14(9):1215-1223.

577. Wulff H, Miller MJ, Hansel W, Grissmer S, Cahalan MD, Chandy KG. Design of a potent and selective inhibitor of the intermediate-conductance Ca2+-activated K+ channel, IKCa1: a potential immunosuppressant. *Proc Natl Acad Sci U S A*. 2000;97(14):8151-8156.

Appendix: Drugs and Chemicals

Table 1: The mechanism of action, solvent, stock concentration, experimental concentration and supplier of the drugs and chemicals used.

Name	Mechanism of Action	Solvent	Stock Concentration (M)	Concentration Used	Company
Acetylcholine	Muscarinic agonist[225,452,565]	Water	10^{-2}	3 μM	Sigma-Aldrich
Apamin	SK_{Ca} channel inhibitor[566]	Water	10^{-4}	50 and 500 nM	Tocris
Apocynin	NADPH oxidase inhibitor[541–543]and/or O^{2-} scavenger[544]	DMSO	10^{-2}	20 μM	Sigma-Aldrich
Carmustine	Glutathione reductase inhibitor[408,411,549,550]	Ethanol	10^{-2}	50 μM	Sigma-Aldrich
***N*-cyclohexyl-*N*-[2-(3,5-dimethyl-pyrazol-1-yl)-6-methyl-4-pyrimidinamine (CyPPA)**	SK_{Ca} channel positive modulator[313]	DMSO	10^{-2}	0.001-30 μM	Tocris
Dihydroethidium (DHE)	O^{2-} sensitive fluorescent probe[349,535,536]	DMSO	10^{-2}	10 μM	Caymen Chemical
Iberiotoxin (IbTX)	BK_{Ca} channel inhibitor[567]	Water	10^{-4}	100 nM	Tocris
N^G-nitro-L-arginine methyl ester hydrochloride (L-NAME)	NOS inhibitor[294,471]	Water	10^{-1}	100 μM	Sigma-Aldrich
Methoxamine	α_1-adrenoceptor agonist[568]	Water	10^{-1}	1 μM	Sigma-Aldrich

Nicotinamide-adenine-dinucleotide phosphate (NADPH)	Electron donor [385,471]	10 mg/ml $NaHCO_3$	10^{-2}	100 µM	Sigma-Aldrich
Nifedipine	L-type VOCC inhibitor [569,570]	DMSO	10^{-2}	1 and 10 µM	Sigma-Aldrich
4-[[3-(Trifluoromethyl)phenyl]methyl]-2H-1,4-benzothiazin-3(4H)-one (NS 6180)	IK_{Ca} channel inhibitor [311]	DMSO	10^{-2}	1 µM	Tocris
N'-[3,5-Bis(trifluoromethyl)phenyl]-N-[4-bromo-2-(2H-tetrazol-5-yl-phenyl]thiourea (NS 11021)	BK_{Ca} channel activator [571,572]	DMSO	10^{-2}	100 nM	Tocris
Phenylephrine	α_1-adrenoceptor agonist [568,573]	Water	10^{-2}, 10^{-3}, 10^{-4} and 10^{-5}	0.001- 100 µM	Sigma-Aldrich
Prazosin	α_1-adrenoceptor antagonist [184]	Water	10^{-2}	1 µM	Tocris
1H-[1,2,4]Oxadiazolo[4,3-a]quinoxalin-1-one (ODQ)	Soluble guanylyl cyclase inhibitor [574]	DMSO	10^{-2}	5 µM	Tocris
Naphtho[1,2-d]thiazol-2-ylamine (SKA-31)	IK_{Ca} channel positive modulator [121]	DMSO	10^{-2}	0.001-30 µM	Tocris
Sodium Nitroprusside	NO donor [575]	Water	10^{-2}	1 µM	Sigma-Aldrich

Superoxide Dismutase (SOD)	Catalyzes superoxide anion dismutation[540,576]	Krebs	N/A	10 units/ml	Sigma-Aldrich
Superoxide Dismutase-Polyethylene Glycol (SOD-PEG)	Catalyzes superoxide anion dismutation[538]	phosphate buffered saline	N/A	25 units/ml	Sigma-Aldrich
Tempol	Intracellular superoxide scavenger[576]	Water	10^{-1}	300	Tocris
1-[(2-Chlorophenyl)diphenylmethyl]-1H-pyrazole (TRAM-34)	IK$_{Ca}$ channel inhibitor[577]	DMSO	10^{-3}	1 μM	Tocris

*For each of these drugs control experiments were carried out using appropriate concentrations of DMSO